Spot the difference

Bossers, C.A.M.

2009

document version
Publisher's PDF, also known as Version of record

Spot the difference: microarray analysis of gene expression changes in Alzheimer's and Parkinson's Disease

The research described in this thesis was conducted at the Netherlands Institute for Neuroscience, an Institute of the Royal Netherlands Academy of Arts and Sciences, Amsterdam, The Netherlands. The research was financially supported by a collaboration between the Netherlands Institute for Neuroscience and Solvay Pharmaceuticals.

Leescommissie:

dr. P. Broqua
prof.dr. P. Heutink
dr. P.A.C. 't Hoen
prof.dr. H.P.H. Kremer
prof.dr. A.B. Smit
dr. G.C.M. Zondag

Publication of this thesis was financially supported by:
Solvay Pharmaceuticals
Eurogentec
Vrije Universiteit
Nederlands Instituut voor Neurowetenschappen

ISBN 978-94-90371-05-0
Book and cover design: Koen Bossers
Print: Off Page, Amsterdam

VRIJE UNIVERSITEIT

Spot the difference: microarray analysis of gene expression changes in Alzheimer's and Parkinson's Disease

ACADEMISCH PROEFSCHRIFT

ter verkrijging van de graad Doctor aan
de Vrije Universiteit Amsterdam,
op gezag van de rector magnificus
prof.dr. L.M. Bouter,
in het openbaar te verdedigen
ten overstaan van de promotiecommissie
van de faculteit der Aard- en Levenswetenschappen
op dinsdag 10 november 2009 om 10.45 uur
in het auditorium van de universiteit,
De Boelelaan 1105

door

Conrad Antonius Martinus Bossers

geboren te Nijmegen

promotoren: prof.dr. J. Verhaagen
prof.dr. D.F. Swaab
prof.dr. C.G. Kruse

Contents

CHAPTER 1

General introduction

Koen Bossers, Joost Verhaagen, Dick F. Swaab

1. Introduction

In a population that is growing older and older, it is difficult to underestimate the impact of age-related neurodegenerative disorders such as Parkinson's Disease (PD) and Alzheimer's Disease (AD). In particular, the absence of treatment options to effectively treat, or even slow down the progression of these disorders means that individuals diagnosed with AD or PD face a long and debilitating disease with an inevitably negative outcome. This introduction will first focus on the clinical and neuropathological characteristics of PD and AD. Subsequently, advances in the understanding of putative molecular mechanisms underlying neurodegenerative events, mostly based on studies of rare familial variants of PD and AD, will be discussed. As mentioned, effective treatment regimes remain conspicuously absent, despite enormous research efforts during the last two decades. Therefore, the final part of this introduction will focus on new research strategies that might help to provide insight in the biological mechanisms that contribute to AD- or PD-associated neurodegeneration.

2. Parkinson's Disease

Parkinson's Disease (PD) is a severe movement disorder which is neuropathologically characterized by a dramatic and selective loss of dopaminergic (DAergic) neurons in the substantia nigra (SN). The clinical symptoms usually only arise when ~60% of the SN DAergic neurons is lost, and the levels of DA in the putamen are decreased by as much as 80%. The disease course is progressive, and the incidence increases strongly with age: the overall incidence is 1:5000, which increases to ~1:800 at age 70 (reviewed in Dauer and Przedborski 2003). Early in the disease course, PD motor symptoms can be effectively treated with DA replacement therapies. However, this treatment is only symptomatic and does not halt disease progression. The molecular mechanisms underlying PD-associated neurodegeneration remain poorly understood.

2.1 Clinical features of PD

Clinically, PD manifests itself as a movement disorder characterized by, amongst others, resting tremors, rigidity, difficulties with voluntary movement and postural instability. The quality of life of a PD patient is most severely affected by the disturbances in voluntary movement. Patients often have problems initiating movements, and move more slowly (bradykinesia). Other notable movement disturbances include a stooped posture, decreased volume of speaking (hypophonia) and reduced degree of facial expression (hypomimia). Not surprisingly, PD patients develop difficulties in performing simple daily routines such as getting dressed and walking the dog. Furthermore, the combined effects of hypophonia, hypomimia and the fact that PD patients often take longer to reply to questions, can pose a serious hin-

drance to the patient's social life. Also, depression and social withdrawal are often observed in PD patients (Reijnders *et al.* 2008).

Apart from motor symptoms, PD patients are at greater risk for developing cognitive defects and dementia. It has been reported that around one-third of newly-diagnosed PD patients without dementia are cognitively impaired in areas such as executive function and working memory (Foltynie *et al.* 2004). This impairment may result from disruption of striatofrontal connections such as the mesocortical DAergic system. Indeed, executive function performance depends on DA levels (Lewis *et al.* 2005; Lange *et al.* 1995). Furthermore, ~30% of PD patients develop dementia (Aarsland *et al.* 2005). The strongest neuropathological correlate for this finding is a reduced cholinergic activity in the cortex, secondary to degeneration of the nucleus basalis of Meynert (Bosboom *et al.* 2004). The presence of Lewy Body (LB, discussed below) pathology in limbic and frontal areas might also contribute to symptoms of dementia in PD. However, AD-associated neuropathological alterations are frequently co-existent with LB pathology (Emre 2003). Thus, the exact neuropathological correlate with dementia in PD remains unclear.

2.2 Neuropathological features of PD

The main neuropathological hallmark of PD is the selective loss of DAergic neurons in the SN. This is accompanied by two specific types of intraneuronal proteinacious inclusions: spindle- or threadlike Lewy neurites (LN), and globular Lewy bodies (LB) near the nucleus. However, the SN is not the only brain area affected in PD. In fact, PD-associated lesions appear in a precisely defined order in different brain areas, and the SN is only affected after the appearance of PD lesions in other brain areas. In 2003, Braak et al published a method for staging the progression of PD (Braak *et al.* 2003). The first two stages are characterized by lesions in the dorsal IX/X motor nucleus and/or the intermediate reticular zone (stage 1), followed by lesions in the raphe nuclei, gigantocellular reticular nucleus and the coereulus/subcoereulus complex (stage 2). In stage 3, the SN, in particular the pars compacta, becomes affected. Cortical involvement only occurs in later stages: the first lesions appear in the mesocortex (stage 4), whereas pathology in the neocortex is only observed in stages 5 and 6.

Although the SN is not the area where PD-associated lesions first appear, it is the most significantly affected area. The overall loss of neuromelanin-positive DAergic neurons in end-stage PD is ~80% (Damier *et al.* 1999), resulting in a dramatic reduction of DA output via the nigrostriatal pathway to the target areas of the SN: the caudate nucleus and putamen. Especially the DAergic innervation of the caudate nucleus is severely reduced. The motor disturbances observed in PD arise from the loss of DA input into the striatum.

2.3 Treatment strategies for PD

As the main symptoms of PD arise from a reduced DA level in the striatum, it is not surprising that the main treatment strategy for PD is the replenishment of striatal DA levels (DA replacement therapy). Indeed, the motor symptoms in PD can be successfully treated by administering L-dihydroxyphenylalanine (L-dopa), the natural DA precursor. An alternative approach is to use dopamine agonists that directly stimulate the postsynaptic dopamine receptor. In the first few years after diagnosis, DA replacement therapies are effective in treating PD motor symptoms. However, due to L-dopa-induced overstimulation, most patients will develop motor fluctuations, which eventually become independent of L-dopa intake and cannot be controlled by additional medication such as COMT and/or MAO-B inhibitors (Sydow 2008). Subsequently, the patient's symptoms become very difficult to treat. In this case, deep brain stimulation using electric stimulation can be applied to reduce motor problems (Sydow 2008). A commonly used target is the subthalamic nucleus, as the firing pattern of this nucleus is affected in PD, leading to altered excitation patterns in the motor cortex (Hamani *et al.* 2004).

Unfortunately, all of the previously mentioned therapies are only aimed at alleviating the symptoms of PD, and do not halt or even slow down the progression of the disease. More recent strategies involve cell replacement therapies and gene therapies, although these methods are still in their infancy (reviewed in Korecka *et al.* 2007). As these methods are aimed at either replacing DAergic neurons by new neurons, or halting PD progression by preventing further neurodegeneration, these strategies have the potential to actually cure the disease as opposed to only treat symptoms.

2.4 Genetic forms of PD

Although ~90% of PD is of sporadic origin, several gene mutations have been discovered that cause rare, familial forms of PD, usually characterized by an early age of disease onset. Mutations in α-synuclein (SNCA) and leucine-rich repeat kinase 2 (LRRK2) are known to cause autosomal dominant forms of the disease, whereas mutations in parkin (PARK2), PINK1 (PARK6) and DJ-1 (PARK7) are involved in recessively inherited PD. On first sight, the genes that are mutated in familial PD are of diverse and unrelated function. However, extensive research efforts towards the molecular mechanisms underlying the parkinsonian phenotype associated with the mutated genes have revealed several common pathways that appear to be very important in PD pathogenesis.

SNCA

SNCA was the first gene to be discovered as mutated in familial PD (Polymeropoulos *et al.* 1997). Interestingly, the protein encoded by the SNCA gene is the major component of LB and LN pathology, both in sporadic and familial PD. Furthermore, as a single point mutation in the SNCA gene is sufficient to cause dominantly inherited PD, the SCNA gene appears to be very important in the pathogenesis of PD.

So far, 3 PD-causing point mutations have been identified in SNCA. Also, a triplication of the SCNA gene leads to familial PD, suggesting that the phenotype in carriers of SNCA point mutations is not due to a loss-of-function mutation; it is more likely that the point mutations make SNCA more prone to aggregate, or represent a gain-of-function mutation. Despite its early discovery as an important player in both sporadic and familial PD, the normal physiological function of SNCA remains elusive. SNCA is believed to play a role as a presynaptic protein involved in vesicle recycling and storage of neurotransmitters (Yavich *et al.* 2006; Yavich *et al.* 2004). As SNCA is a highly abundant protein throughout the brain, the intriguing question remains why SN DAergic neurons are selectively vulnerable to mutations in SCNA and alterations in SCNA expression levels.

LRRK2

In the recent years, the LRRK2 gene has received much attention in relation to PD. Several mutations have been described in this gene that cause autosomal dominant forms of PD, and different LRRK2 mutations can lead to quite different forms of neuropathology. For example, the first kindred reported to carry mutations in LRRK2 is characterized by parkinsonism without LB pathology (Funayama *et al.* 2002). Later studies in other kindreds showed PD with LB, tangle pathology or even ubiquitin-negative protein deposits (Zimprich *et al.* 2004). Interestingly, the role of LRRK2 mutations appears to play a role in sporadic forms of PD as well (Gilks *et al.* 2005). Indeed, it is estimated that around 1-7% of European sporadic PD patients carry mutations in LRRK2 (Thomas and Beal 2007). Unfortunately, the role of dardarin, the protein product of the LRRK2 gene, remains elusive. It has a complex domain structure, including at least two protein-protein interaction domains, a kinase domain and a GTPase domain. Two common mutations occur in the kinase domain, resulting in an increased kinase activity. Whether this increased activity is connected to the neuropathological alterations needs to be further investigated.

PINK1

Mutations in PINK1 are associated with autosomal recessive PD, and are relatively rare: they account for ~5% of early-onset PD cases (Klein *et al.* 2006; Bonifati *et al.* 2005). The PINK1 gene encodes a putative serine/threonine kinase, which contains an N-terminal mitochondrial localization signal. Indeed, the PINK1 protein colocalizes with mitochondria as determined by immunohistochemical stainings and fractionation studies in human brain tissue (Gandhi *et al.* 2006). Furthermore, PINK1 regulates the mitochondrial protease HtrA2 (Plun-Favreau *et al.* 2007), and in vitro studies have shown that wild-type PINK1 can prevent apoptosis by inhibiting mitochondrial cytochrome c release, a function that is lost in mutant PINK1 (Petit *et al.* 2005). Together, these data suggest an important role of PINK1 in mitochondrial functioning. Interestingly, a number of toxins causing parkinsonism specifically act on mitochondria (see section on toxin-induced forms of PD below), suggesting that mitochondrial involvement in PD is an important phenomenon.

Parkin and UCH-L1

UCH-L1 is a protein which cleaves attached ubiquitin molecules from proteins tagged to be degraded by the proteasome, so they can enter the proteasome. An I93M mutation has been found in some PD families, but the prevalence of this mutation is very rare (Lincoln *et al.* 1999). However, mutations in the parkin gene are a major cause of early-onset autosomal recessive PD (Kitada *et al.* 1998). Parkin encodes an E3 ubiquitin ligase, which attaches ubiquitin molecules to proteins destined for degradation by the proteasome. As protein aggregation in LBs and LNs, especially of the SNCA protein, is a common feature in PD, a loss-of-function mutation in parkin seems a plausible cause for PD. Next to its function in protein degradation, parkin also appears to have a neuroprotective role. For example, parkin can activate the neuroprotective IkappaB kinase/NFkappaB signaling cascade, a function that is lost in mutant parkin (Henn *et al.* 2007), and parkin rescues mitochondrial dysfunction in PINK1-KO flies (Clark *et al.* 2006; Park *et al.* 2006). The exact relation between parkin and PINK1 needs to be studied in greater detail, but a recent study provided evidence that parkin binds directly to PINK1 and upregulates PINK1 levels, and PINK1 reduces the solubility of parkin, inducing the formation of microtubule-dependent cytoplasmic aggresomes (Um *et al.* 2009).

DJ-1

Initially discovered in a Dutch and an Italian family, mutations in the DJ-1 gene cause autosomal recessive PD (Bonifati *et al.* 2003). The exact physiological role of DJ-1 is unknown, but several experimental findings are suggestive for potential roles in PD pathogenesis. DJ-1 appears to be protective against oxidative stress, possibly by scavenging reactive oxygen species (Taira *et al.* 2004). Furthermore, DJ-1 is involved in regulating the levels of tyrosine hydroxylase (Zhong *et al.* 2006), which suggests that DJ-1 serves an important function in the maintenance of DAergic neurons.

Thus, in general, genetic forms of PD seem to be mainly associated with alterations in protein degradation and aggregation (such as the ubiquitin-proteasome system), and abnormalities in mitochondrial function.

2.5 PD induced by toxins in humans and animal models

In the later 1970s and early 1980s, a group of young drug users rapidly developed parkinsonism. Analysis of the injected synthetic drug meperidine revealed that the PD symptoms could be attributed to 1-methyl-4-phenyl-1,2,5,6-tetrahydropyridine (MPTP), a by-product of the drug synthesis process (Davis *et al.* 1979; Langston *et al.* 1983). Interestingly, MPTP-induced parkinsonism has strong overlaps with idiopathic PD: a severe drop op DA levels in the striatum, selective loss of DAergic neurons in the SN and PD-like motor disturbances. However, MPTP does not fully recapitulate all important features found in sporadic PD. For example, the patients did not suffer from the characteristic LB pathology. The discovery of MPTP as a se-

lective DAergic neurotoxin allowed for the development of PD animal models (reviewed in Bove *et al.* 2005; Przedborski *et al.* 2001). In particular, the MPTP mouse model and the MPTP monkey model have evolved to invaluable tools to study the effect of MPTP and MPP+ on the DAergic system. Although the cardinal features (selective DAergic neurodegeneration and severe disturbances in movement) are closely reproduced by MPTP, both in mice, monkeys and humans, some aspects of PD remain conspicuously absent. In almost all models, there are no convincing reports of LB pathology due to MPTP intoxification and the locus coeruleus remains unaffected, whereas in PD this area is already affected before the onset of pathology in the SN (Braak *et al.* 2003). Only in one mouse model, where MPTP is administered in a chronic manner via infusion through an osmotic minipump, locus coeruleus pathology and LB-line inclusions can be observed (Fornai *et al.* 2005).

Since the discovery of the link between MPTP and PD, the molecular mechanisms by which MPTP causes DAergic neurodegeneration have been subject to extensive investigations. It is now known that not MPTP itself, but its metabolite MPP+ is the main toxic species for neurons. In the body, MPTP is metabolized by monoamine oxidases (MAO), especially MAO-B. Interestingly, SN DAergic neurons have low levels of MAO-B activity; the majority of MPP+ in the SN is generated and secreted by astrocytes (Di Monte *et al.* 1996). Secreted MPP+ then selectively binds to the dopamine transporter (DAT), and enters the neuron. SN DAergic neurons express higher levels of DAT than the VTA, and DAT expression levels are correlated with neurodegeneration in PD (reviewed in Storch *et al.* 2004). Thus, the expression pattern of DAT might underlie the differential vulnerability of SN DAergic neurons in MPTP-induced parkinsonism, a mechanism that might also translate to sporadic PD.

Intracellulary, the MPTP metabolite MPP+ interferes with the mitochondrial Complex I by inhibiting NADH-linked electron transport. This results in a severe reduction of pyruvate- and glutamate-mediated ATP synthesis. The finding that mitochondrial dysfunction is also present in sporadic PD (Schapira *et al.* 1989), and both PINK1 and DJ-1 appear to be involved in mitochondrial functioning (reviewed in Schapira 2008), are strongly suggestive for an important role of mitochondria in PD neurodegeneration. Indeed, other compounds that specifically inhibit Complex I are also able to induce a PD-like phenotype. For example, chronic infusion of rodents with the pesticide rotenone (a potent Complex I inhibitor) results in degeneration of the nigrostriatal system (Betarbet *et al.* 2000). Furthermore, rotenone infusion also leads to oxidation of DJ-1, and accumulation of α-synuclein into LB-like structures (reviewed in Betarbet *et al.* 2006). Another widely-used neurotoxin to model PD is 6-hydroxydopamine (6-OHDA). 6-OHDA has a high affinity for catecholaminergic transporters such as the DA transporter and the norepinephrine transporter, but does not readily cross the blood-brain barrier. Therefore, in order to use 6-OHDA as a neurotoxin in the nigrostriatal system, it has to be directly injected into the substantia nigra, the medial forebrain bundle or the striatum. After uptaken by neurons, 6-OHDA rapidly oxidizes, resulting in the formation of radical oxygen species (ROS), which eventually causes cell death. Interestingly, the

formation of ROS is also an important phenomenon in neurodegeneration induced by Complex I inhibition. After stereotactic injection into the SN, the majority of DAergic neurons dies within a few days (Bove *et al.* 2005). Gliosis is also a prominent feature, but there are no reports of LB-like inclusions after intoxification with 6-OHDA. When injected unilaterally, rodents exhibit a characteristic turning behavior. As this phenotype can be readily quantified, 6-OHDA models have been instrumental for determining the efficacy of a variety of potential treatment options for PD, ranging from new pharmacological compounds to gene therapy (Gasmi *et al.* 2007; Takano *et al.* 2007). However, as the neurotoxic effects of 6-OHDA are not restricted to DAergic neurons alone, but also affect glial cells, it is difficult to determine whether the observed phenotype (for example rotational behavior) is caused by disturbances in neuronal or glial function, or a combination of both. This has become more relevant in the light of current insights in the role of astrocytes in synaptic transmission (Agulhon *et al.* 2008).

Taken together, none of the toxin-based models fully recapitulate the neurodegenerative features as seen in PD. Most notably, LB formation is not clearly observed. It is also important to note that PD is a chronic and slowly progressing disorder. Chronic infusion of low levels of toxin is therefore closest to the disease process. Recent models that use minipumps to centrally deliver MPTP are promising developments in this respect (Alvarez-Fischer *et al.* 2008; Fornai *et al.* 2005).

2.6 Gene polymorphisms in sporadic PD

In addition to mutations leading to rare familial forms of PD, researchers have identified several DNA sequence polymorphisms, most notably singe nucleotide polymorphisms (SNPs), that appear to be associated with particular aspects of the disease process in sporadic PD, such as age of onset or risk of disease development. PD-associated SNPs have for example been identified in MAPT (Tobin *et al.* 2008; Martin *et al.* 2001), in PITX3 (Fuchs *et al.* 2007; Bergman *et al.* 2008) and in SCNA (Mizuta *et al.* 2006; Kobayashi *et al.* 2006; Winkler *et al.* 2007). Interestingly, PITX3 is involved in the development and survival of meso-diencephalic DAergic neurons (Smits *et al.* 2006; Smits and Smidt 2006), and SCNA is found in LBs and is mutated or triplicated in genetic forms of PD (discussed earlier in this chapter). Unfortunately, the reproducibility of a substantial number of reported SNPs proves to be problematic. For example, in 2005, a SNP in the SEMA5A gene was found to be significantly associated with PD in American Caucasians (Maraganore *et al.* 2005). This SNP could not be confirmed in two independent cohorts of Polish and Asian origin (Bialecka *et al.* 2006). A third study confirmed the SNP in SEMA5A in a Taiwanese cohort, but failed to find a significant association in a Finnish cohort (Clarimon *et al.* 2006). A recent report in a Chinese Han cohort failed to replicate the SEMA5A SNP, but found an association between SEMA5A haplotype and risk of PD (Ding *et al.* 2008). Conflicting results have also been found for the S18Y polymorphism in UCHL1 (Tan *et al.* 2006; Carmine *et al.* 2007; Zhang *et al.* 2008; Hutter *et al.* 2008; Ding *et al.* 2008). The lack of reproducibility might be explained by

differences between cohorts, especially race differences. More importantly, it also raises questions about the involvement of the affected genes in PD pathogenesis in the world-wide population. In other words, their contribution to PD appears to be rather limited. This is in agreement with twin studies showing low concordance in both monozygotic and dizygotic twins, although conflicting reports exist (reviewed in Warner and Schapira 2003).

Of special interest are genome-wide association studies which examine the association between hundreds of thousands SNPs and the condition of interest. As PD is most likely a multifactorial disorder, these genome-wide approaches have a high potential in finding sets of SNPs that combined have a strong impact on PD. Recently, a number of genome-wide association studies have been carried out on different cohorts of PD patients (examples include Elbaz *et al.* 2006; Li *et al.* 2008; Lesnick *et al.* 2007; Maraganore *et al.* 2005). Unfortunately, as with single SNP studies, replication of published findings remains an issue. We anticipate that future advantages in statistical analyses of these datasets will aid in determining solid associations between polymorphisms and sporadic PD.

2.7 Genome-wide gene expression studies in PD

The combined evidence from genetic and neurotoxic forms of PD has clearly provided much insight into the complex and multifactorial origin of PD. However, the approach of focusing on genetic and toxin-induced forms of PD also has some restrictions. Firstly, it has centered PD research efforts around the relatively confined set of molecules and molecular biological processes that are associated with the modes of action of these genes and toxins. Secondly, there are no animal models (either genetic or toxin-based) that sufficiently recapitulate the full spectrum of molecular biological, morphological and behavioral changes as observed in sporadic PD, suggesting that additional mechanisms might be very important in PD-associated neuropathology. Thirdly, as discussed above, recent genome-wide association studies have discovered pathways previously undiscovered in PD, which appear to play a significant role in the predisposition of developing PD. For example, a recent study by Lesnick et al revealed a significant interaction between SNPs in axon guidance-related genes and the risk for developing PD (Lesnick *et al.* 2007). These risk-modulating factors delineate unexpected new potential mechanisms that would have been missed by hypothesis-driven approaches. Thus, it is of the utmost importance to maintain an unbiased approach towards mechanisms underlying PD in order to identify new molecules and/or pathways that might be very important in PD pathogenesis.

Recently (roughly in parallel with genome-wide SNP screening tools), an unbiased approach has become feasible with the development of platforms for genome-wide gene expression measurements such as high-density oligonucleotide microarrays. These tools allow for the simultaneous measurements of transcript levels of virtually all genes on the human genome. Combined with advances in bioinformatics approaches to analyze the resulting datasets, microarray experiments can

provide a molecular fingerprint of dysregulated molecules and biological processes in PD, and thus allow for the unbiased analysis of transcriptome alterations associated with PD pathogenesis. Indeed, in the last few years, a limited number of gene expression studies have been performed on the postmortem human PD SN (Papapetropoulos and McCorquodale 2007). These studies range from relatively small experiments (*n*=7) confined to the SN only (Grunblatt *et al.* 2004), to large-scale experiments (*n*=23) in multiple brain regions (Papapetropoulos *et al.* 2006). Different microarray platforms and statistical methods to determine significantly regulated genes were employed, which confounds a direct comparison between the generated gene lists.

Perhaps hampered by these limitations, a very preliminary meta-analysis indeed failed to yield a set of genes that is reproducible detected across these studies (Papapetropoulos and McCorquodale 2007). Noteworthy is that none of the genes involved in genetic forms of PD were found to be differentially regulated between PD and control. On the other hand, several molecular biological systems such as mitochondria and the ubiquitin-proteasome system were reproducibly found to be altered across several studies. These processes are also affected in genetic and toxin-induced forms of PD, and thus appear to be intimately involved in PD-associated neuropathology. It is however important to note that a full-fledged meta-analysis on the raw gene expression datasets, as opposed to the gene lists as included in the different studies (which have been used in the meta-analysis mentioned above), is more likely to identify sets of genes that are reproducibly altered between the separate studies. When using raw datasets, differences in gene expression platforms, normalization algorithms and methods for detecting differential gene expression can be dealt with in a more robust manner. Unfortunately, not all datasets are publically available at this moment, which precludes a proper meta-analysis.

Although very valuable, the gene expression studies on the human PD SN above all suffer from the same limitation: the interpretation of the results is hampered by the fact that the majority of the SN DAergic neurons are lost during the course of the disease. This results in an altered tissue composition (the ratio neurons versus glial cells is severely decreased), which is a major confounder for the interpretation of the gene expression measurements. For example: does the 50% reduction of a neuron-specific transcript indeed represent a true downregulation, or is this just secondary to the extent of neuronal loss in the PD SN? An alternative approach would be to isolate single DAergic neurons by using laser capture microscopy techniques. However, these are technically challenging experiments: the process of laser dissection itself is detrimental to the RNA quality (which is already suboptimal in human postmortem tissue), and due to the limited amount of cells harvested, one or two rounds of RNA amplification are needed to obtain sufficient material for microarray hybridization. Nonetheless, these technical limitations will most likely be overcome in the future, and microarray profiling of laser-captured cells can be a valuable tool in the search for transcriptional alterations associated with PD neurodegeneration.

However, PD is not a disease of (DAergic) neurons alone: glial cells play an important role in disease initiation and progression. For example, activated microglia and astrocytes might contribute to the inflammation observed in affected areas of the PD SN (Teismann and Schulz 2004; Qian and Flood 2008). Furthermore, in MPTP models, MPTP is processed into MPP+ in astrocytes, released into the extracellular space, after which it is subsequently taken up by DAergic neurons. Also, the recently discovered role of axon guidance molecules suggests that cells other than DAergic neurons play a part in the predisposition for PD (Lesnick *et al.* 2007). Thus, it is important to approach the diseased SN as a whole to be able to fully grasp the combination of glial and neuronal transcriptional alterations that occur simultaneously in PD.

3 Alzheimer's Disease

Alzheimer's Disease (AD) is the most prevalent age-related neurodegenerative disease, and the most common form of dementia in developed countries. Currently, in the US alone, around 4 million individuals are estimated to suffer from this debilitating disease. The incidence of AD increases exponentially with age: around 5% of individuals over the age of 70 develop AD. This number increases dramatically to 25-45% of individuals over the age of 85 (reviewed in Sleegers and van Duijn 2001). Therefore, in an ageing society, AD poses an ever-increasing socio-economic burden on society. There are no effective treatments for AD, and despite enormous research efforts during the last two decades, the biological mechanisms that underlie AD remain unknown.

3.1 Clinical features and diagnosis of AD

Clinically, AD is characterized by a general decline in brain functions, most notably a loss of memory function. Other symptoms include inattention, disoriented behavior, alterations in personality, difficulties with speaking and comprehending, and impaired gait and movement (reviewed in Forstl and Kurz 1999). Disease severity in dementia can be monitored with the Global Deterioration Scale/Functional Assessment Staging (Auer and Reisberg 1997). In the earliest (pre-dementia) stages, mild impairment in acquiring and remembering new information and complex planning tasks can be observed. At this moment, there are no reliable methods that discriminate incipient AD and cognitive decline associated with normal aging. When the disease progresses into mild dementia, learning and memory deficits become more pronounced. Interestingly, recent declarative memory is most heavily affected, whereas old declarative memory remains relatively intact. Patients develop difficulties performing complex household chores such as preparing meals and financial administrative tasks. Deficits in orientation might interfere with driving skills. Furthermore, depressive symptoms are common in mild dementia. At this stage of the disease, the patient might need support to be able to live independently.

As the cognitive deficits increase to the point of moderate dementia, patients are no longer able to properly dress themselves or perform household duties. Due to the severe impairment in recent memory, the patient sometimes has the illusion to live in past episodes of his or her life. This, in combination with impairments in the recognition of familiar faces, might lead to illusional misidentification of people. Deficits in language skills manifest themselves as problems with word finding, speaking and reading. It becomes impossible for the patient to live independently: full-time care from a partner or other people from the patient's social network may postpone hospitalization. However, the caretaking of moderately demented individuals is emotionally and physically extremely challenging. In the final stage of AD, the severe dementia stage, severe deficits exist in practically all cognitive functions. Restlessness and wandering due to disturbances in the circadian rhythm, apathy and almost complete loss of language skills can be observed. Double incontinence, difficulties with chewing and swallowing and other motor are common. Eventually, patients become bedridden and die of complications, mostly pneumonia.

As the definitive diagnosis of AD can only be made after postmortem brain examination for AD-associated brain lesions (see below), a range of neuropsychological tests have been devised that serve as diagnostic tools to assess the probability of the diagnosis "AD" in a given individual. One of the most widely used method for assessing the cognitive status is the Mini Mental State Examination (MMSE) (Folstein *et al.* 1975). Although not specifically designed to diagnose AD and/or dementia, but rather general deficits in cognition, the MMSE test is the most widely used test for the diagnosis of dementia. It consists of a 30-point questionnaire assessing cognitive functions such as orientation, arithmetic and memory. Based upon the score, individuals can be ranked as cognitively normal (score of 27-30), mild dementia (20-26), moderate dementia (10-19) and severe dementia (score below 10). The MMSE questionnaire is also part of the more elaborate the Consortium to Establish a Registry for Alzheimer's Disease (CERAD) neuropsychological test, which comprises of a battery of tests including a verbal fluency test, the Boston Naming test and word recall tests (Morris *et al.* 1988). Other common tests employed to assess the severity of AD and dementia are the clock drawing test (Sunderland *et al.* 1989) and the Alzheimer Disease Assessment Scale-Cognitive (ADAS-Cog) test (Rosen *et al.* 1984).

3.2 Neuropathological features of AD

Macroscopically, AD is characterized by cortical atrophy (gyral shrinkage and widening of cortical sulci), hippocampal atrophy and ventricular enlargement. However, cortical atrophy and ventricular dilation can also be observed to some degree in age-matched normal individuals, and these observations are thus by themselves not sufficient for the diagnosis of AD: the additional presence of two types of specific microscopic lesions (extracellular senile plaques and intraneuronal tangles, described below) is required.

In 1907, Alois Alzheimer described the occurrence of intraneuronal dense fibrillary aggregates after microscopic examination of silver-stained sections of the brain of Auguste D, the first reported presenile case of what later became known as AD (Alzheimer *et al.* 1995). The majority of these so-called neurofibrillary tangles appear in the cytoplasm of otherwise morphologically normal appearing neurons. In brain areas with substantial numbers of neurofibrillary tangles, some extracellular tangles can also be found. These "ghost" tangles are presumably the remainder of intraneuronal tangles after a neuron has died. It took the scientific community almost 80 years to identify the microtubule-associated protein tau as the main component of neurofibrillary tangles (Grundke-Iqbal *et al.* 1986). Tau aggregates predominantly as hyperphosphorylated and abnormally paired helical tau filaments into fibrous deposits, which together make up neurofibrillary tangles (Goedert 1993).

In addition to neurofibrillary tangles, a second type of microscopic lesion characterizes AD: the senile plaque. This is an extracellular proteinacious aggregate mainly composed of the amyloid-beta (Aβ) protein. Aβ originates from the sequential cleavage of the amyloid precursor protein (APP), a process which is described in detail in the paragraph 3.6. Senile plaques, also called neuritic plaques, are large structures (~50 to 150 μm in diameter), with a dense Aβ-positive core. The senile plaque is further characterized by the presence of proteinacious inclusions (such as paired helical filaments) in neurites in direct proximity of the senile plaque. Therefore, these neuronal processes are called dystrophic neurites. Similar thick knickey fibers that are found throughout the grey matter are called neuropil threads (Braak *et al.* 1998). Interestingly, a related but critically different form of Aβ plaques, the diffuse plaque, is not a feature specific for AD, but is associated with normal aging (Roe *et al.* 2008). The diffuse plaque consists of Aβ deposits, but lacks the dense core and dystrophic neurites.

As a fourth cardinal microscopic finding, ultrastructural studies have shown that AD is associated with a decrease in synaptic density, up to a 40% loss of synapses in lamina II and V in the superior frontal cortex (reviewed in Scheff and Price 2006). It is very likely that a reduction in neuronal connectivity at least partially underlies the memory deficits as observed in AD.

3.3 Progression of AD-associated neuropathology

In 1991, Braak and Braak systematically studied the distribution of neurofibrillary changes (NFC) and senile plaques throughout the brains of 83 non-demented and demented individuals (Braak and Braak 1991). This study yielded two important findings: 1) neurofibrillary pathology correlates with cognitive decline, whereas plaque pathology has limited discriminatory power and 2) the occurrence of neurofibrillary tangles follows a specific distribution pattern throughout the brain during the course of AD. The latter finding allowed the authors to define a neuropathological staging system for the progression of AD. The Braak score for NFC discriminates between 6 disease stages. In Braak stages I and II, the only brain area significantly affected is the transentorhinal cortex, whereas the CA1 region of the hippocampus

might be mildly affected. Individuals in these Braak stages are cognitively normal. In stages III and IV, both the entorhinal and transentorhinal cortex are clearly affected, and the hippocampal involvement is mild to moderate. In these stages, the first tangles in the isocortical areas appear. The stages are associated with mild cognitive impairment. In the final two Braak stages, stages V and VI, the isocortex becomes heavily affected, and the patient is clinically demented.

The extent and distribution of plaque deposits during the course of AD is less well-defined, mainly due to a large interindividual variation in early stages of the disease. Low densities of amyloid plaques first appear in isocortical areas, mainly in basal areas of the frontal, occipital and temporal lobe (stage A). The second stage for amyloid plaques (stage B), is characterized by a medium density plaque load in virtually all association areas in the cortex. In this stage, the first amyloid plaques can be observed in the hippocampus. In stage C, the final stage for amyloid deposits, the plaque density in cortical areas is further increased, whereas the hippocampus remains only mildly affected. Interestingly, it is not uncommon to find individuals with substantial plaque pathology (for example, stage B) without any tangle pathology. On the other hand, substantial tangle pathology (e.g. stage IV) is almost always accompanied by moderate to severe plaque pathology (Braak and Braak 1991).

3.4 Genetics forms of Alzheimer's Disease

In the last two decades, several genetic mutations have been found that cause early-onset familial forms of AD. As will be discussed later in this introduction, these mutations all occur in genes that are directly involved in the production of Aβ, and thus appear to be intimately linked to senile plaque formation.

APP

After several years of conflicting data on the existence of a linkage between a region on chromosome 21 and an autosomal dominant form of AD, in 1991, a missense mutation (V717I) was discovered in the APP gene that segregated with AD in several families (Goate *et al.* 1991). The mutation was found in the region of the gene (exon 17) which encodes for the Aβ peptide (the main component of the senile plaque), and it was thus hypothesized that this mutation was directly causative for the early occurrence of AD-associated neuropathology as observed in these patients. At present, 29 different APP mutations have been discovered in 80 FAD families (from the Alzheimer Disease & Frontotemporal Dementia Mutation Database http://www.molgen.ua.ac.be/ADMutations). Interestingly, ~70% of these mutations is indeed found in exon 17, further strengthening the significance of Aβ in AD neuropathology. Adding to this, chromosome 21, and thus the APP gene, is triplicated in Down Syndrome (DS). DS patients almost invariably develop dementia at an early age, which is accompanied by senile plaques and neurofibrillary tangles. An attractive hypothesis is therefore that the increased gene dosage of APP is directly causative for the neuropathology in DS, although the potential effect of other genes on chromosome 21 should not be underestimated.

Presenilins

A few years after the discovery of the first mutation in the APP gene, a mutation in a previously undiscovered gene (AD3) was found in several FAD families (Sherrington *et al.* 1995). The same research group identified yet another gene on chromosome 1, bearing strong sequence similarities with AD3, harboring mutations in other kindreds with FAD (Rogaev *et al.* 1995). The former gene later became known as presenilin 1 (PSEN1), the latter presenilin 2 (PSEN2). Mutations in PSEN1 are the single most common cause for early-onset FAD: there are now 167 pathogenic PSEN1 mutations found in 367 families. Mutations in PSEN2 are far less common: only 10 mutations in 18 families have been found so far (http://www.molgen.ua.ac.be/ADMutations). Interestingly, the presenilins are directly involved in the generation of Aβ by proteolytic cleavage of APP. This is described in detail in paragraph 3.6.

Tau

As already mentioned, the tau protein is the major component in neurofibrillary tangle pathology. Tau is abundantly expressed in neurons in both the central and peripheral nervous system, and is selectively enriched in axons (Binder *et al.* 1985). Tau serves a role in the assembly of free tubulin into microtubules, and is expressed in at least 6 major isoforms by means of alternative splicing (Goedert *et al.* 1989). As mutations in APP lead to senile plaque pathology, it was hypothesized that mutations in the MAPT gene encoding for tau might be associated with AD. Indeed, some studies reported linkage between MAPT polymorphisms and AD (Conrad *et al.* 2002; Myers *et al.* 2005). However, the scientific community has not been successful in replicating these findings (Mukherjee *et al.* 2007). The significance of the reported linkages for AD pathogenesis therefore remains unclear. On the other hand, several mutations in MAPT are causative for frontotemporal dementia with parkinsonism linked to chromosome 17 (FTPD-17), a collection of tauopathies with diverse clinical and neuropathological manifestations. For example, tau mutations can lead to both progressive supranuclear palsy and corticobasal degeneration (reviewed in Goedert 2005). Importantly, the occurrence of neurofibrillary pathology in these disorders clearly demonstrates that alterations in tau might lead to neuropathological changes. As discussed, presently there is no convincing evidence that genetic alterations in MAPT contribute to AD neuropathology.

3.5 Genetic variations associated with sporadic AD

Mutations in APP and the presenilins cause classical mendelian inherited forms of early-onset FAD. However, these forms of AD only make up ~1% of the general AD population: the overwhelming majority is of sporadic origin. There are strong indications for a genetic component in sporadic AD, and extensive searches for gene polymorphisms that modify the risk of developing sporadic late-onset AD have been carried out. It turned out to be very difficult to reliably pinpoint genes that modulate AD susceptibility, but in 1993, Corder et al demonstrated that having one

or two copies of the apolipoprotein E ε4 allele increased the risk of developing AD in a dose-dependent manner (Corder *et al.* 1993). More recent targeted and genome-wide association studies provided evidence for additional genetic factors modulating the risk of developing AD. Unfortunately, independent replication of SNPs remains troublesome (similar issues with SNP replication in PD cohorts have been described earlier in this chapter). In 2007, a systematic meta-analysis has been performed on gene polymorphisms that have been reported in at least 3 cohorts (Bertram *et al.* 2007). Out of the 127 polymorphisms in 69 genes, 20 variants in 13 loci were found to be significantly associated with AD. Except for ApoE, all polymorphisms had a very moderate effect (odds ratios between 1.17-2.04 for risk variants, and 0.84-0.56 for protective variants). Thus, the apolipoprotein E (APOE) gene remains the only strong genetic risk factor for AD so far. APOE is the major apolipoprotein in the brain, and is important in cholesterol transport. APOE occurs in 3 isoforms: ε2, ε3 and ε4. Due to the presence of an arginine residue at position 112 (which is a cysteine in the other isoforms), the ε4 isoform adopts a so-called molten globule conformation. Interestingly, this causes a dramatic shift in the molecular properties of APOE, which is reflected (via unknown mechanisms) in differential effects of APOE isoforms on several cellular processes. For example, APOE ε3 is known to be involved in protection against neurodegeneration and tau phosphorylation. APOE ε4 on the other hand causes neurodegeneration and stimulates tau phosphorylation. A detailed description of the functional differences between the APOE isoforms and the possible implication for AD can be found in a review by Mahley et al (Mahley *et al.* 2006).

3.6 APP, Abeta and the presenilins: the amyloid cascade hypothesis

As mentioned earlier, APP and the two presenilins PSEN1 and PSEN2 are presently the only known genes in which mutations are the direct cause of a familial form of AD. APP is a single-pass transmembrane protein with a large extracellular domain and a small cytoplasmic tail. As mentioned earlier, the Aβ peptide is encoded by exon 17, and Aβ is part of the transmembrane region of APP. APP occurs in different splice forms, and undergoes major posttranslational modifications. These modifications consist of glycosylation, sulfation and most notably secretase-mediated proteolytic cleavage (reviewed in Selkoe 2000; Van Gassen and Annaert 2003, Figure 1). There are three different secretases: α-, β- and γ-secretase, which sequentially cleave APP. α-Secretase cleaves APP within the Aβ region to yield the α form of soluble APP (sAPPα) and a membrane-bound C83 fragment. APP-C83 is then further processed by γ-secretase, which results in the P3 peptide and the cytosolic APP intracellular domain (AICD). As α-secretase cleaves within the Aβ region, the formation of Aβ is precluded. This pathway is therefore called the non-amyloidogenic pathway. When APP is processed via the amyloidogenic pathway, it is first cleaved by β-secretase, yielding sAPPβ and the membrane-anchored APP-C99. Next, the C99 fragment is cut within the transmembrane region by the γ-secretase complex, which generates the Aβ peptide and the AICD. Interestingly, the presenilin protein

(either PSEN1 or PSEN2) is the catalytic subunit of the γ-secretase complex, and is thus directly responsible for the cleavage of APP into Aβ.

The γ-secretase complex can cleave C99 at two different positions (amino acid 711 or 713), which results in either an Aβ peptide of 40 amino acids (Aβ40) or 42 amino acids (Aβ42). Due to the two additional amino acids, the Aβ42 peptide aggregates more readily into senile plaques: the initial plaque deposits contain almost exclusively the Aβ42 form (Roher *et al.* 1993), and animal models which overexpress Aβ42 develop plaques, whereas mice overexpressing Aβ40 do not (McGowan *et al.* 2005). Therefore, any process that alters the ratio between Aβ40 and Aβ42 is likely to affect senile plaque formation. Strikingly, almost all mutations in the APP gene that cause FAD occur in close proximity to the Aβ region, and result in a shift towards the production of Aβ42 (see e.g. Cai *et al.* 1993; Hardy 1992). Furthermore, FAD-linked mutations in both PSEN1 and PSEN2 also result in a shift towards Aβ42 (Scheuner *et al.* 1996). Thus, there is a very clear causal link between mutations in APP, PSEN1 and PSEN2 on one side, and senile plaque formation on the other side. Based upon these obervations, the amyloid cascade hypothesis has been put forward, which states that Aβ is the initiating molecule in both sporadic and familial AD (Hardy and Higgins 1992; Selkoe 1991). Although it was originally thought that the extracellular plaque itself was the toxic species in AD, it is now believed that soluble monomeric or oligomeric forms of Aβ underlie the neuropathological alteration (Kirkitadze *et al.* 2002). After its formulation around 15 years ago, the amyloid

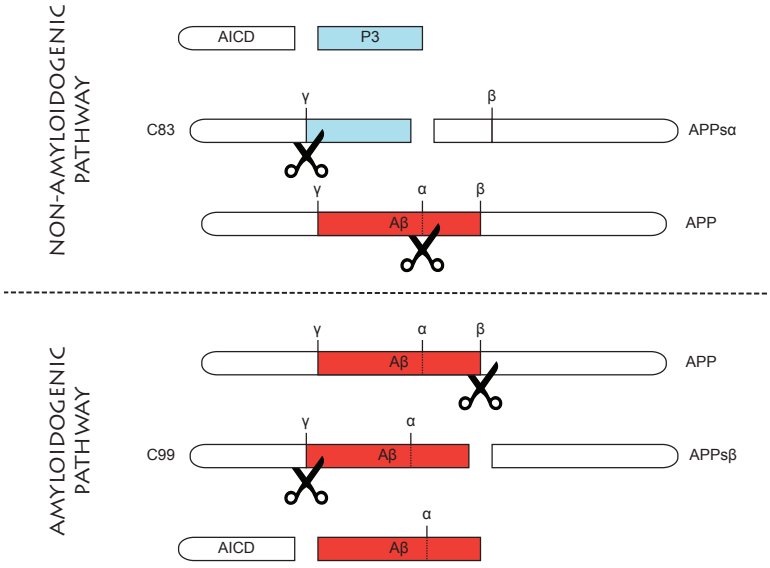

Figure 1 - Secretase-mediated APP processing. Only the amyloidogenic pathway leads to the formation of Aβ, the main component of senile plaques.

cascade hypothesis still remains the most prominent theory on the causal events leading to AD, also due to the lack of strong evidence supporting tau hyperphosphorylation and aggregation as an initiating event in AD pathogenesis.

3.7 Animal models in AD

The discovery of genes underlying familial forms of AD and FTDP-17 enabled the scientific community to develop a range of transgenic mouse models that mimic specific aspects of AD-associated neuropathological and cognitive alterations (reviewed in McGowan *et al.* 2006). Certainly not all of these animal models develop senile plaque- and/or NFC-like pathology. The most important mouse models will be briefly discussed here (an overview of these models can be found in Table 1).

The first mouse model that developed amyloid plaques was the PDAPP mouse, which overexpresses a transgene carrying the V717F mutation (the Indiana mutation) in APP (Games *et al.* 1995). In these mice, extensive plaque pathology can already be observed after 6 months. A year later, the Tg2576 model was introduced: this mouse line carries APP with the Swedish double mutation (K670M/N671L) (Hsiao *et al.* 1996). These mice are characterized by a progressive, age-related amyloid plaque buildup in combination with memory deficits. Interestingly, the plaques in both the PDAPP and Tg2576 mice are also surrounded by dystrophic neurites (Irizarry *et al.* 1997a; Irizarry *et al.* 1997b). Another widely use APP-based AD mouse model is TgCRND8, which harbors both the Swedish and Indiana mutation. This mouse model already develops plaques at 3 months of age, which coincides with the onset of cognitive defects (Chishti *et al.* 2001).

Mice transgenic for mutations in PSEN1 exhibit a selective elevation of Aβ42 levels, but this is not accompanied by plaque pathology (Duff *et al.* 1996). Crossing these mice with APP transgenic lines resulted in the PSAPP mouse models, which are characterized by a substantially faster buildup of plaque pathology than in the single APP lines themselves (Holcomb *et al.* 1998; Borchelt *et al.* 1996).

Tangle pathology can be observed in several mouse lines transgenic for mutant tau. Notable examples include the JNPL3 mouse model (first transgenic model for tau with the P301L mutation; substantial tangle pathology and neuron loss; Zhang *et al.* 2004), the tauV337M mouse line (tauV337M expressed at low levels under the PDGF promoter; mutation-specific tangle pathology independent of tau overexpression; Tanemura *et al.* 2001), and the rTg4510 mouse line (inducible expression of tau; tangle pathology, neuronal loss and cognitive defects from 2.5 months. Turning off tau expression improves cognition, but tangle pathology still builds up; Santacruz *et al.* 2005).

Interestingly, none of the above mouse models show both plaque and tangle pathology. In 2003, Oddo et al created a triple transgenic mouse model by co-injecting tauP301L and APPSWE into a PSEN1 knock-in background (Oddo *et al.* 2003). The resulting 3xTG-AD mouse progressively develops plaque pathology (onset around 6 months), which is followed by tangle pathology at 12 months of age. The first cognitive defects can be detected as early as 4 months. The order of appearance of

Reference	Line	Transgene(s)	Plaques	Tangles	Onset Pathology	Onset Cognitive Defects	Remarks
Games *et al.* 1995	PDAPP	APP-V717F	Yes	No	6 months	3 months	First mouse model developing AD-like amyloid plaques
Hsiao *et al.* 1996	Tg2576	APP-K670M/N671L	Yes	No	6 months	3 months	
Chisthi *et al.* 2001	TgCRND8	APP-KM670/671NL, V717F	Yes	No	3 months	3 months	
Duff *et al.* 1996	6.2 or 8.9	PSEN1-M146V or PSEN1-M146L	No	No	-	-	First lines that show PSEN-dependent enhanced Abeta42 levels, however no plaques develop
Borchelt *et al.* 1996	PSAPP	Tg2576 x PSEN1-M146L	Yes	No	10 weeks	Unclear	Mutations in PSEN accelerate Abeta aggregation
Lewis *et al.* 2000	JNPL3	MAPT-P301L	No	Yes	4.5 months	No robust changes	First mouse model developing tangles
Santacruz *et al.* 2005	rTg4510	MAPT-P301L	No	Yes	1 month	2.5 months	Inducible expression of MAPT (TET on/off system)
Oddo *et al.* 2003	3xTg-AD	APP-K670M/N671L, PSEN1-M146V, MAPT-P301L	Yes	Yes	6 months (plaques), 12 months (tangles)	4 months	First model developing both plaques and tangles

Table 1 - Overview of the main characteristics of the most important genetic mouse models for AD.

neuropathology in the 3xTG-AD mice resembles the human situation, where extensive plaque pathology can occur in the absence of neurofibrillary alterations (Braak and Braak 1991). Neuropathologically, the 3xTG-AD mouse is the closest match to the pathology observed in AD. It is however surprising that, where in human cases a single mutation in APP or presenilin is sufficient to cause both neuropathological alterations, a combination of 3 mutations is needed to achieve similar results in the mouse. The strong age component in AD might be one of the possible explanations for this; the process of aging is very difficult to model in rodents, and carriers in FAD families remain unaffected until they are middle-aged.

3.8 Gene expression studies in human postmortem AD brain

As mentioned above, due to the strong age component and its multifactorial origin, modeling AD using animal models remains a challenging task. High-throughput studies measuring transcript or protein levels in human brain material are therefore very important in capturing the complex nature of AD. A limited number of whole-genome gene expression experiments have been conducted on human postmortem AD brain material. In 2006, Reddy and McWeeney reviewed the 8 microarray studies on postmortem AD brains published until that time (Reddy and McWeeney 2006). All but one of these studies compared end-stage AD versus matched controls, and profiled different brain areas such as the hippocampus, amygdala and cingulate cortex. The last study that was discussed in the review by Reddy and McWeeney however took a more elaborate approach by distinguishing between incipient, moderate and severe AD, and comparing hippocampal gene expression profiles of these groups to controls (Blalock *et al.* 2004). Individuals were assigned to one of the four groups by means of MMSE score, and an elaborate gene selection algorithm was used to select genes that significantly correlated with MMSE, NFC measures or both. In this very elegant study, the authors were able to identify a set of genes that correlated with AD disease progression. There are however some drawbacks in their approach. First of all, the average Braak stage for NFC was II for the control subjects, and already V for the incipient AD group, which suggests that the selected samples did not span the full Braak stage range as the intermediate Braak stages were underrepresented. Furthermore, as the first NFC alterations already appear around Braak stage II in the hippocampus, the possibility for detecting transcriptional alterations that precede NFC formation (and thus are potentially causative) were very low. Thus, there is at present a lack of knowledge regarding transcriptional changes just before the onset of AD-associated neuropathology, and during the early-to-intermediate stages of disease progression.

CHAPTER 2

Scope and outline

Koen Bossers

Scope and outline

The general aim of this thesis is to gain insight in the complex molecular mechanisms underlying Parkinson's disease (PD) and Alzheimer's disease (AD), the two major age-related neurodegenerative disorders, by applying gene expression microarray technology to measure transcriptional alterations associated with PD and AD in human postmortem brain tissue. At present, the large majority of human brain studies of neurodegenerative diseases such as AD and PD focus on the comparison between end-stage disease cases versus matched controls, and is driven by rare, familial forms of AD and PD (see **Chapter 1**). In this respect, microarray technology (fundamentally characterized as an unbiased research tool) has huge potential for elucidating previously undiscovered transcriptional changes underlying sporadic AD and PD.

Neuropathological changes in diseased and healthy tissue can be quite pronounced, as illustrated by the concomitant massive loss of dopaminergic neurons and the occurrence of gliosis in the substantia nigra in PD. Changes in gene expression between disease and control patients may therefore contain important clues as to what causes the disease but may also be a transcriptional reflection of consequences of the disease process. Thus, one could raise the question whether the observed differences are representative of causative mechanisms, or are merely alterations secondary to the disease process. Furthermore, treatments counteracting deleterious processes in end-stage disease have little potential of preventing or curing the disease. We are particularly interested in early, possibly causative changes in neurodegenerative disorders. Therefore, a specific aim of this thesis is to identify early events in PD and AD pathogenesis, knowledge which eventually might lead to new therapeutic strategies such as the development of preventive or regenerative medicine.

Even in end stage PD, some parts of the substantia nigra are only moderately affected. For microarray studies, this fact can be exploited by selectively studying those parts of the PD SN that have a relatively normal neuronal density, thereby minimizing the confounding effect of loss of neurons on the gene expression profile. In **Chapter 3**, we describe a gene expression experiment on the PD substantia nigra, caudate nucleus and putamen based on such an approach. As we selectively measured gene expression patterns in dopaminergic neurons in PD before they degenerate, some of the transcriptional alterations found in this dataset are potentially causative to the pathogenesis as observed in PD, and can serve as new candidates for the development of treatments that halt or prevent PD-associated neurodegeneration. In the substantia nigra, next to downregulation of mitochondrial genes, genes involved in synaptic transmission and the ubiquitin-proteasome system, we observed changes in axon guidance cues, and a reduction in neurotrophic support. We hypothesize that these changes represent early processes that might have played a role in the neuronal demise of the degenerated parts of the PD substantia nigra.

For the microarray experiments described in Chapters 3 and 5, we have made use of the Agilent dual-color gene expression platform to measure gene expression levels. This platform is characterized by the simultaneous hybridization of two samples, labeled with different fluorescent dyes. The main outcome of such an experiment is, for every gene, a relative measure of expression between the two hybridized samples. This is very useful for the direct comparison between two conditions, such as control and PD substantia nigra. However, the comparison between multiple groups, which is the case for the AD study, is more difficult. In **Chapter 4**, we describe an improved method for the analysis of dual-color comparative gene expression experiments. This method is based on using the absolute expression levels from the two co-hybridized samples, which eliminates the limitations associated with dual-color designs. We show that for recent high-density dual-color array platforms, it is feasible to use intensity-based analysis models as opposed to the standard ratio-based methods. More importantly, our results indicate that intensity-based analysis yields more reproducible results, and we show that intensity-based analysis is more sensitive in the detection of differential gene expression. Using this method in the AD study (see Chapter 5) resulted in enhanced statistical power, and a more reliable list of regulated genes.

Chapter 5 describes a systematic search for changes in transcript levels during the progression of AD, using the Braak staging for neurofibrillary changes as an objective measure for the progression of AD-associated neuropathology throughout the brain. We examined genome-wide expression profiles of the prefrontal cortex (PFC). In this brain area, neurofibrillary changes only start to appear in Braak III, allowing for the possible detection of gene expression changes before, during and after the onset of AD neuropathology.

The main findings in this chapter are clusters of tightly co-regulated genes, that represent an early increase in neuronal activity, before the onset of neuropathology in the PFC. Subsequently, when the first plaques and tangles start to appear in the PFC, this initial increase in activity turns into a reduction in neuronal activity, coinciding with the clinical diagnosis of mild cognitive impairment. We hypothesize that this early activation represents a coping mechanism against increased soluble Aβ levels, as we observed several genes involved in APP and Aβ processing in these clusters. Furthermore, we observed evidence for the interaction of the ApoE gene with the expression levels of the genes involved in these clusters, suggesting an accelerating role for ApoE4 in AD disease progression, and a possible link between the increased Aβ levels and tau phosphorylation.

Gene expression studies in human postmortem brain tissue inherently suffer from substantial inter-individual variations. Thus, independent confirmation of differential gene expression is of particular importance in gene expression studies. Therefore, the results from our gene expression study were compared with a set of recent gene expression studies in postmortem AD brain tissue, in order to identify genes or gene groups most relevant to AD. The results of this meta-analysis can be

found in **Chapter 6**. Interestingly, we observed several reproducibly dysregulated genes involved in calcium homeostasis, mitochondrial function, cell cycle regulation, synaptic transmission, inflammation and cholesterol metabolism.

There is substantial evidence suggesting that sex steroids can mediate neuroprotection and neuronal survival in the CNS by regulating gene expression of neurotrophic factors and anti-inflammatory molecules. To investigate the possible interaction of alterations in sex steroids with AD, we describe in **Chapter 7** the expression of key enzymes involved in the synthesis and metabolism of sex steroids in the human PFC during the course of AD, using quantitative PCR and immunohistochemical methods. We provide evidence for increased levels of estrogens and allopregnanolone in end-stage AD, suggesting a neuroprotective response to AD-associated neurodegenerative events.

In **Chapter 8**, we discuss the results presented in the preceding chapters. Specifically, we elaborate on the role of ApoE polymorphisms in AD development and progression, and the (dis)similarities between aging and AD. For PD, the potential role of altered axon guidance cues in relation to the development of PD will be discussed. We propose and discuss experiments for the in silico, in vitro and in vivo characterization of genes detected in our studies. Finally, we will highlight potential confounding factors when working with post mortem tissue, and provide guidelines on how to minimize these factors.

CHAPTER 3

Analysis of gene expression in Parkinson's disease: possible involvement of neurotrophic support and axon guidance in dopaminergic cell death

Koen Bossers, Gideon Meerhoff, Rawien Balesar,
Jeroen van Dongen, Chris G. Kruse,
Dick F. Swaab, Joost Verhaagen

Brain Pathology 2009:19, 91-107

Abstract

Parkinson's Disease (PD) is a neurodegenerative disorder characterized by the progressive loss of dopaminergic neurons in the substantia nigra. We have studied alterations in gene expression in the substantia nigra, the caudate nucleus and putamen of 4 PD patients and 4 matched controls using custom designed Agilent microarrays. To gain insight into changes in gene expression during early stages of dopaminergic neurodegeneration we selectively investigated the relatively spared parts of the PD substantia nigra, and correlated gene expression changes with alterations in neuronal density. We identified changes in the expression of 287 transcripts in the substantia nigra, 16 transcripts in the caudate nucleus and 4 transcripts in the putamen. For selected transcripts, transcriptional alterations were confirmed with qPCR on a larger set of 7 PD cases and 7 matched controls. We detected concerted changes in functionally connected groups of genes. In the PD substantia nigra, we observed strong evidence for a reduction in neurotrophic support and alterations in axon guidance cues. As the changes occur in relatively spared parts of the PD substantia nigra, they suggest novel disease mechanisms involving neurotrophic support and axon guidance in early stages of cellular stress events, ultimately leading to dopaminergic cell death in PD.

Introduction

Parkinson's disease (PD) is, after Alzheimer's disease, the second most prevalent age-related neurodegenerative disorder, affecting approximately 1% of the population above the age of 65. The main clinical features of PD are resting tremor, rigidity, slowness of voluntary movement and postural instability (Dauer and Przedborski 2003; Moore *et al.* 2005). Neuropathologically, PD is characterized by the progressive loss of nigrostriatal dopaminergic (DAergic) neurons in the presence of two types of neuronal inclusion bodies: spindle- or threadlike Lewy neurites in cellular processes, and globular Lewy bodies in neuronal somata (Braak *et al.* 2003; Forno 1996). The loss of DAergic neurons in the substantia nigra pars compacta (SN) results in reduced dopamine (DA) levels in the striatum, which in turn causes the majority of the clinical symptoms of PD. Patients with severe neuronal loss in the SN show generally also pathology in the neocortex (Braak *et al.* 2003). Interestingly, the SN is affected in PD in a heterogeneous way. For example, DAergic neurons in calbindin-poor regions (the nigrosomes) of the SN are more prone to degenerate than neurons in the calbindin-rich nigral matrix (Damier *et al.* 1999). This suggests that interactions of DAergic neurons with their surroundings might be important in neuronal vulnerability in PD.

In the last decade, mutations in the SNCA, LRRK2, PARK2, PINK1 and DJ-1 genes have been found to cause inheritable forms of PD, with differences in age of onset and other specific clinical manifestations of the disease. Furthermore, association studies revealed several other genes which alter PD susceptibility such as

UCHL1 and NURR1 (Hardy *et al.* 2006). On first sight, the genes that are involved in PD are unrelated in function. For example, LRRK2 functions as a cytosolic kinase, PARK2 is an E3 ubiquitin ligase which tags ubiquitin molecules to proteins destined to be degraded by the proteasome, and DJ-1 is involved in signaling in response to oxidative stress (Hardy *et al.* 2006). The function of SNCA, although extensively studied, remains relatively unknown. It is likely to be involved in vesicle trafficking and synaptic transmission (Chandra *et al.* 2005). For SCNA, both a gene triplication and point mutations lead to familial PD (Polymeropoulos *et al.* 1997; Singleton *et al.* 2003). These alterations make SCNA more prone to aggregate, and SNCA is indeed a major component of Lewy bodies. Interestingly, UCHL1 and PARK2 are both involved in protein (de)-ubiquitination. Dysregulated protein aggregation therefore appears to be an important common factor in PD pathogenesis (Hol *et al.* 2005).

Apart from genetic mutations, toxins such as 1-Methyl-4-phenyl-1,2,3,6-tetrahydropyridine (MPTP), rotenone and 6OH-DA are known to induce Parkinson-like pathology (Bove *et al.* 2005). Induction of oxidative stress is a common mode of action of these neurotoxins. Mutations in DJ-1 and PINK1 are also associated with elevated levels of oxidative stress and/or mitochondrial dysfunction. Although discoveries of gene mutations in familial PD and the existence of specific neurotoxic substances inducing parkinsonian phenotypes have provided important insights into familial and sporadic PD, there are still many open questions regarding the specific molecular mechanisms underlying the sporadic form of PD. The etiology of sporadic PD is most likely multifactorial, and the heterogeneous vulnerability of SN DAergic neurons suggests involvement of the surrounding cellular environment. Also, in PD, the loss of presynaptic terminals in the striatum precedes the loss of neuronal cell bodies in the SN (Bernheimer *et al.* 1973). We therefore hypothesize that DAergic neurons are under the control of environmental cues in the SN as well as terminal areas. These environmental cues, together with factors intrinsic to DAergic neurons, make up the unique conditions in which SN DAergic neurons selectively degenerate in PD. To investigate these conditions, we have generated gene expression profiles of the caudate nucleus, putamen and SN of 4 clinically and neuropathologically well characterized PD patients and matched controls using custom designed high density microarrays, and validated genes possibly implicated in PD on a larger set of 7 PD patients and 7 matched controls.

Experimental procedures

Subjects

Postmortem human brain tissue was obtained from The Netherlands Brain Bank, Netherlands Institute for Neuroscience, Amsterdam (NBB). All material has been collected from donors from whom a written informed consent for a brain autopsy and the use of the material and clinical information for research purposes had been obtained by the NBB. All subjects were clinically diagnosed and treated PD pa-

tients, a diagnosis that was neuropathologically confirmed (N=7), or were controls without neurological or psychiatric disorders and without neuropathological alterations (N=8). All PD patients received DA replacement therapies during the course of their disease. Both PD patients and controls were neuropathologically systematically investigated as described earlier (van de Nes *et al.* 1998). The controls did not exceed a Braak pathology score for neurofibrillary tangles of 2 (Braak and Braak 1991). Care was taken to match subjects as closely as possible for age, sex, post mortem interval and brain pH (see Table 1). Since agonal state is one of the most important factors influencing RNA quality, and RNA expression profiles are correlated with brain pH (Tomita *et al.* 2004), samples with a cerebrospinal fluid pH below 6.3 were excluded. In addition we excluded patients who were treated with Prednisone at the time of death, unless stated otherwise. Only subjects from whom freshly frozen tissue samples of the caudate nucleus, putamen as well as SN were available, were included. There were no significant differences between PD and control groups for age, pH, RNA integrity, postmortem interval and brain weight (Mann-Whitney U test, Table 1).

Tissue dissection

For the caudate nucleus and putamen tissue samples, structures were identified macroscopically in the frozen tissue by the gross anatomical features and surrounding white matter. A cylindrical punch of 50-100 mg gray matter was obtained by a hollow dry-ice cooled drill, collected in prechilled 2 ml tubes and immediately put on dry ice. The SN tissue samples were first treated for 48 hours with RNAlater-ICE (Ambion, Austin, Texas) at -20°C to stabilize the RNA and to soften the tissue to enable dissection using scalpels. The area of interest was the least affected part of the SN of each PD patient, that was macroscopically defined by the presence of black pigmentation in the unstained tissue, which represents the neuromelanin in DAergic neurons. Although it was apparent that the SNs from PD patients lost the majority of its pigmentation, for all individuals, pigmented areas could easily be identified. Small portions of the pigmented areas (~10mg) were rapidly dissected out by hand on a dry-ice chilled metal plate, and transferred to prechilled 2 ml tubes and immediately put on dry ice. Dissected samples were stored at -80°C until use.

RNA isolation

Total RNA was extracted from all brain regions using a hybrid protocol of Trizol and Qiagen RNeasy Mini Kit RNA isolation methods. Briefly, samples were homogenized in Trizol (3ml per 100mg tissue; Life Technologies, Grand Island, New York). After phase separation by addition of chloroform, the aqueous phase was transferred to a new tube, and mixed with an equal amount of 70% EtOH. This mixture was then applied to an RNeasy Mini column (Qiagen, Valencia, California), and processed according to the RNeasy Mini Protocol for RNA Cleanup (version June 2001, from Step 3). RNA purity was determined using a NanoDrop ND-1000 spectrophotometer (Nanodrop Technologies, Wilmington, Delaware). RNA integrity was de-

Subject	Diagnosis	Sex	Age	PMI	pH	BW	RIN		Cause of Death
00-115	PD/DEM	m	70	9:05	6.33	1258	6.2		Pneumonia, septic shock
04-045	PD/DEM	m	71	6:58	6.55	1358	8.4	*	Pneumonia
00-139	PD/DEM	m	72	7:15	6.55	1546	6.7		Uremia
02-003	PD	f	75	5:00	6.52	1218	9.6	*	euthanasia
02-011	PD	f	79	5:45	6.37	1203	8.7	*	Myocard infarction
00-034	PD	m	86	8:30	6.52	1178	9.2	*	Unknown
02-064	PD	m	87	7:20	6.37	1166	7.4		Respiratory insufficiency
Mean±SD		5M/2F	77.1±7.1	7.1±1.3	6.5±0.1	1275±136	8.0±1.3		
98-126	CTRL	m	71	6:00	6.54	1385	8.8		Respiratory insufficiency
00-049	CTRL	m	78	6:55	6.42	1332	9.2	*	cardiac failure
97-144	CTRL	m	78	4:00	6.43	1160	9	*	Pulmonary carcinoma
00-142	CTRL	f	82	5:30	6.60	1280	9.2	*	Myocardial infarct
00-022	CTRL	f	83	7:45	6.52	1102	9.2	*	Acute myocard infarction
98-062	CTRL	m	85	4:35	6.95	1332	7.5		Respiratory insufficiency
99-046	CTRL	f	89	5:10	6.62	1168	9.5		Cardiac arrest
01-029	CTRL	f	90	5:25	6.58	1066	7.6		myocard infarction
Mean±SD		4M/4F	82±6.3	5.4±1.1	6.6±0.2	1228±119	8.8±0.8		
P-value			0.22	0.06	0.08	0.49	0.22		

Table 1 - Clinicopathological data of human postmortem samples. PD/DEM: Parkinson's Disease with dementia. PMI: post mortem interval (hours). BW: brain weight (grams). RIN: RNA integrity number. P-value: Kruskal-Wallis p-value.
** - samples used in microarray experiment.*

termined by the RNA Integrity Number (RIN) as measured on the Agilent 2100 bioanalyzer (Agilent Technologies, Palo Alto, California). The RIN values varied, ranging from 6.2 (moderately degraded) to 9.6 (intact RNA). Because RNA quality has strong effects on gene expression profiles, only samples with high RNA quality were selected for microarray experiments (4 PD patients and 4 controls, RIN > 8.3, see Table 1). RNA quality was sufficient for qPCR analysis for all samples under investigation.

Sample labeling and microarray hybridization

For microarray analysis, Agilent custom-made 22K 60-mer oligonucleotide arrays were used. Array probes were designed to contain all Homo Sapiens Unigene clusters consisting of at least one mRNA molecule (~15K probes) and ~7.5K probes for expressed sequence tags known to be expressed in the brain or eye. Array hybridization was performed according to the manufacturer's instructions. Briefly, equal amounts (500ng for caudate and putamen, 1µg for substantia nigra) of Cy3 and Cy5 labeled RNA were hydrolyzed for 30 minutes at 60°C in 1x fragmentation buffer (Agilent Technologies). The fragmented targets were hybridized to a microarray by incubating for 17 hours in 1x target solution (Agilent Technologies) at 60°C in a rotating hybridization chamber. Microarrays were washed in 6xSSPE/0.005% N-Lauroylsarcosine (Sigma-Aldrich, St Louis, Missouri) for 5 minutes at RT and 0.06xSSPE/0.005% N-Lauroylsarcosine for 1 minute at RT. Finally, microarray slides were washed in acetonitril (Sigma-Aldrich) for 30 seconds and dried in a nitrogen flow. Microarrays were scanned using an Agilent DNA Microarray Scanner at 5µm resolution and 100% PMT setting. Microarray scans were quantified using Agilent Feature Extraction Software (version 7.5.1).

Single gene analysis

Raw expression data generated by the Feature Extraction Software were imported into the R statistical processing environment (http://www.r-project.org), and analyzed using the LIMMA package in Bioconductor (http://www.bioconductor.org). Intra-array normalization was performed using the loess algorithm. The intensity distributions between arrays were normalized using the Aquantile scaling algorithm. For each brain area, significant genes were determined by fitting a linear model to the normalized ratios and determining the contrast between PD and controls. Uncorrected p-values were corrected for multiple testing using the Bonferroni correction algorithm. Genes with a corrected p-value < 0.05 were considered significant.

Gene group analysis

For analysis on a gene group level, probes on the microarray were annotated using the Gene Ontology database (GO) (Ashburner *et al.* 2000) and the Kyoto Encyclopedia of Genes and Genomes (KEGG) (Ogata *et al.* 1999). Briefly, Ensembl gene identifiers for the probe sequences were retrieved using the ProbeLynx probe annotation tool (Roche *et al.* 2004). GO annotation for the Ensembl identifiers was retrieved from the Ensembl Mart database using the Bioconductor biomaRt package. Out of the 21939 probes on the array, 10813 probes were annotated with one or more GO identifiers, for a total of 3941 unique GO identifiers. The KEGG annotation was retrieved from the Bioconductor KEGG package. 2663 probes were annotated with one ore more KEGG identifiers, for a total of 181 unique KEGG classes. A gene group was then defined as a group of probes with either the same GO or KEGG annotation. Only gene groups with 5 to 150 member genes were selected for subsequent analyses.

Significantly dysregulated gene groups were identified using the Functional Class Scoring approach as described in Pavlidis et al (Pavlidis *et al.* 2002). Briefly, for each gene group, a functional class score (FCS) was defined as the mean of the –log transformed uncorrected p-values of differential expression between PD and controls of the gene group members. In order to determine the background distribution of FCSs for each gene group, a random gene set of the same size as the gene group under investigation was chosen, and the FCS was calculated. This procedure was repeated 200.000 times to obtain the simulated background distribution. The FCS p-value was then defined as the fraction of simulated FCS scores that were higher than the actual FCS score for the gene group under investigation. The smallest possible p-value therefore was 5e-06. Groups with smaller p-values were set to 2.5e-06. FCS p-values were corrected for multiple testing with the Benjamini and Hochberg False Discovery Rate model. P-values < 0.05 were considered significant.

Reverse transcription and quantitative PCR

For the caudate nucleus and putamen, each sample was reversely transcribed using 500ng RNA, oligo dT primers and SuperScript II Reverse Transcriptase (Invitrogen, Carlsbad, California). 1/200 of the total cDNA yield was used for all quantification reactions. Due to lower yields, 250ng of SN RNA was used as input for the cDNA synthesis reaction, and 1/100 of the total cDNA yield was used for SN quantification reactions. Transcript quantifications were carried out on an ABI 7300 sequence detection system (Applied Biosystems, Foster City, California). Each reaction was performed with the appropriate amount of cDNA, 3pmol of forward and reverse primers and 10ul 2x SYBR green ready reaction mix (Applied Biosystems) in a total volume of 20µl. Forward and reverse primer sequences can be found in Table 2. To check for primer dimers, dissociation curves were generated for all wells. For between-sample normalization, genes were selected for each brain area that were not regulated between PD and control using expression stability measurements and geometric averaging of multiple internal reference genes (Vandesompele *et al.*

2002). Briefly, an initial selection of 10 genes was made based on the gene expression data and reference gene data from literature. The most stable genes between paradigms were selected, and for each sample a normalization factor was determined by geometric averaging of the expression values of these genes. For the SN, ACTB, MRPL24 and DHX16 were used for normalization purposes. For the caudate nucleus, ACTB, GAPDH, PRPSAP1 and UFM1 were used. For the putamen, ACTB, GAPDH, GOT2, DHX16 and FAM96B were used. Genes were selected for

Gene	Accession Number	Forward primer	Reverse primer
COMT	NM_000754	TCCTAAATGCAAAGCACACC	CAATCCAGTGTTGCAGTTCAG
DDC	NM_000790	GCAATCAATGTTCACGCAAC	AGGCATTTAGCCACATGACAA
NR4A2	NM_006186	ACTTGCATGCAGCAGCTTTT	AATTCAAAGTGCTCAGTTATTTCCA
SLC18A2	NM_003054	TCCAGTGACACAACTCATCCA	TGTTGGCAATCGACCATAAC
SNCA	NM_000345	CCTACACTCGGAATTCCCTGAA	GCCACTTAAGGAACCAGTGCAT
TH	NM_000360	GTGAGGTTGTGCTGCCTGT	CTTTTATTGTGACGGTGATTGG
GPRC5A	NM_003979	CTCTCATCTTGCACCCCAAC	GGAGACCATGCCCACTTACA
HS6ST3	AF339796	GAACTCATCAAAGGGCCAGA	GTCAAGGAGGTGGAAGACACA
MRPS25	NM_022497	TTTCTCACCCAGCCAACTTC	ACTTCCCCCTCATCTCCTTG
NETO2	NM_018092	CACATTCAGTGACAGCCCATT	AGGCCTCTCCCAAAGTGAAT
UNC13C	AK054981	TTGTGCTTTGTGAACAAGCTG	TCACCTCACTGGTCTGTGATTTC
DOK6	AK057795	GCCTCATCCAATGACACACA	CAGGAGGCAGAGGGTAATGA
PTS	NM_000317	ATTGCACAAAGCCCAGTTTC	TAGGCACTCCAGAGCACAATG
SDC2	J04621	GATTCCTGCCCCATCACTTAC	GGACACAGCGTGGCTTTAGA
SEMA5A	NM_003966	AGCCAGAGTGTCCTGTTCGT	ACATCCCAGCCACAGTAAGG
VIM	NM_003380	CTGGATTCACTCCCTCTGGTT	TCAAGGTCATCGTGATGCTG
AGTR1	NM_031850	CCAAAACAATGCCCGTAAGA	GGACCAGTGCAGCACCTTTA
LTF	NM_002343	CCCTCCTGTCAGCTGCATAAAG	TGGCCTGGATACACTGGATGG
RGMA	AL136826	TGGTTGTGTTTGCTCACGTT	CGGTGACACTCCACACAGGT
SLITRK5	AK024251	CCAAACCCAGTTGCATTTGTA	GCCCACAGGGATAAAGACATT
CAST1	AB002376	CCAGTGGGCATGTATTAGCC	AAATAAGGCGATCAGCACAA
CDK5	NM_004935	GGCACCTACGGAACTGTGTT	ACCCTCATCATCGTCATCCA
EN1	NM_001426	TGTCGGTCTGTCTGTTCTGC	TCTGTGGGGTCGTATTTCTCA
KCNJ6	NM_002240	CCCAGGTGAGCTGAAGACAA	GGTACTTTTGTACATGCTGGGTTT
EDG2	NM_001401	TGGAGCTCTTGCAATGGAAT	ACTTGCACCAAACCACACAA
ROBO2	AB046788	CAGTGCCGAGAGTATGTTCAGTT	TGGGTCAAACGTATTTTAGTTGG
CADPS	NM_003716	TGGATCCATCTTGCTTTTGC	TTGAGAAGCCACAGTTTTCCA
MAGEE1	AB046807	GGAAATCTTTCCATCTTGTTGC	GCTAGATTATTTTACTGGCGAATTT
TrkB.T1	NM_001007097	AACGCAAATCCTTGAGTTTCA	AAAAACAGGGCATGAGAATGA
MDH1	NM_005917	CTGATGGCAACTCCTATGGTG	GGAGACCTTCAACAAACTTCCA
TrkB.FL	NM_001018066.1;NM_001018065.1;NM_001018064.1;NM_006180.3	GGAGTAACACTCCATCTTCTTCG	TGGTGATGCCAAAGTACTGG
DYNC1I1	NM_004411	CTTCTCACTGAAGCTAACACAGTC	TTTTTGGTTTTATTGGCAACAC
HN1	NM_016185	GCACAACTTGAGCCTGACTGT	GGACAGAGAGAAACCTGTTCTTCA
PHLPP	AB011178	CCTTACTGCTGCCACAATCA	TCCATTTGTGCATTCTGCTT

Table 2 - qPCR primer sequences

qPCR validation in two ways: by random selection from the list of differentially expressed genes to technically validate the microarray data, and by selecting genes based upon their possible involvement in the dysregulated processes as determined by the gene group analysis. Genes of interest were quantified in the following manner. For each primer pair, relative amounts were calculated by means of the formula primer.eff^(Ct-minimal Ct). The resulting raw relative amounts were scaled using the normalization factor to yield corrected relative amounts. P-values between PD and control were calculated with the Mann-Whitney U test using the corrected relative amounts. P-values < 0.05 were considered significant.

Cell density measurements

In order to estimate the neuron density in the SN, for each of the 7 PD and 8 control subjects, five 6µm-thick sections were randomly taken from the formalin fixed, paraffin embedded mesencephalon contralateral to the frozen side that was used for the microarray and qPCR experiments. Sections were stained with hematoxylin-eosin. Pictures were taken using a Zeiss Axioskop microscope with Neofluar objectives (Carl Zeiss MicroImaging GmbH, Germany) and an EvolutionMP camera and Image Pro Plus (version 5, Media Cybernetics, Bethesda MD). Pictures were analyzed using a custom build macro in Image Pro Plus.

Two templates were constructed that represented 2x1mm or 1.5x1mm rectangles, which corresponded to the dimensions of dissected tissue samples used in the microarray and qPCR studies. For each section, the part on the SN that contained the highest density of neuromelanin was identified by eye at 2.5x magnification. A composite picture of this area was taken by combining 6 to 12 pictures at 2.5x magnification. In this composite picture, the area with the highest neuromelanin density was outlined, using the template best fitting this area. The outlined area was then divided into subsections by a macro for cell counting at 20x magnification. For each subsection, a picture at 20x magnification was made, and structures of interest were counted by visual identification. Two cell types were included in the counting experiment: large neuromelanin-positive neurons with a nucleolus, and large neuromelanin-negative neurons with a nucleolus. These two types of neurons were counted separately. To prevent double counting, only neurons containing a nucleolus were counted. This counting procedure, which was judged to be the best for the thin (6µm) section used (Bao *et al.* 2005; Huitinga *et al.* 2000), is based upon the principle that nucleoli can be considered as hard particles that will not be sectioned by a microtome knife but, instead, are pushed either in or out of the paraffin when hit by the knife (Cammermeyer 1967). No nuclei with double nucleoli were observed. The nucleoli could be easily identified at 20x magnification. When in doubt, identification was made using a 40x objective. The estimated densities of the two neuronal types per cubic millimeter were calculated by dividing the number of identified structures by the measured area, and by correcting for section thickness. The final density per subject was defined as the average density of the 5 sections. As the quantification of neuronal structures based on counting nucleoli might not

be related to the actual neuronal number in a one to one fashion, we expressed all counts as percentages of the average count of all structures in the control subjects (Popken and Farel 1997). P-values between PD and control were calculated with the Mann-Whitney U test. P-values < 0.05 were considered significant.

Results

Clustering of gene expression profiles

In order to identify differences in gene expression between PD and controls, we performed microarray experiments on the SN, caudate nucleus and putamen of 4 PD patients and 4 matched controls. First, a hierarchical cluster analysis was applied to the microarray dataset in order to detect possible outliers (Figure 1). Only genes with consistently high expression levels throughout all subjects and brain areas were used (intensity > 256 for all measurements, 6952 genes in total), to reduce the possible confounding effects of genes with low signal-to-noise ratios. The largest differences in expression were found between brain areas: the SN samples cluster apart from the caudate nucleus and putamen. Within the SN cluster, there was also full separation between PD and control samples, indicating substantial differences in gene expression. Unexpectedly, one control SN sample (sample ID 00-022, or CTRL2) clustered apart from all samples. A comparison of the expression pattern of CTRL2 with the average expression pattern of all other SN samples (both PD and control) revealed a strong decrease in neuron-specific transcripts in CTRL2 (data not shown). For example, SYT13 levels were only at 5% of combined PD and control levels. Similar low levels were found for, amongst others, NEFH (5%), MAP2 (18%) and NSE (20%). In contrast, several white matter-related genes were overexpressed in CTRL2. These transcripts included VIM (1132% of combined PD and control levels), PMP22 (1392%) and FN1 (373%). We therefore concluded that the sample analyzed from the CTRL2 SN consisted of a different tissue type, and discarded the sample from further analysis.

Detection of transcriptional alterations in the SN, caudate nucleus and putamen in PD

For each area of interest, the microarray data sets were analyzed to detect transcriptional alterations between PD and control. In the SN, 287 genes out of the 21939 genes on the array were significantly changed in PD. The majority of the significant genes (240) was downregulated in PD, whereas 47 genes were upregulated. Expression changes in the target areas of the nigrostriatal pathway were less pronounced. In the caudate nucleus, 16 genes were found to be differentially expressed (6 genes upregulated in PD, 10 genes downregulated). In the putamen, we found 2 genes significantly upregulated in PD, and 2 downregulated genes (see Table 3).

To validate the transcriptional alterations observed on the microarray, and to extrapolate the observed expression changes to the general PD population, we performed qPCR experiments on an extended set of 7 PD patients and 7 matched con-

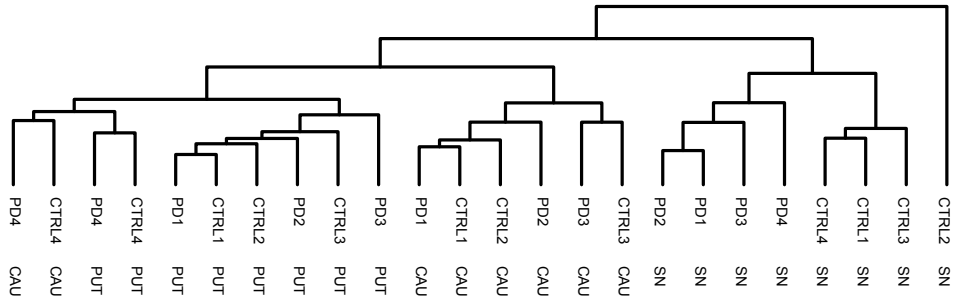

Figure 1 - Hierarchical clustering analysis on array probes with a background corrected intensity > 256 for all measurements (6952 genes in total). Note the aberrant position of CTRL2 SN. CAU - caudate nucleus. PUT - putamen.

trols (Figure 2). We were able to verify the direction of regulation of all transcripts investigated. Importantly, we detected significant differences between PD and controls for 26 out of the 34 genes under investigation ($p < 0.05$), with a further 3 genes nearing significance ($p<0.1$). Also, qPCR and microarray fold changes exhibited a very strong linear correlation ($r^2=0.86$, $p=2.67e\text{-}15$, Figure 3). This suggests that the observed alterations in the microarray experiment are indeed of relevance in a larger PD population.

Furthermore, several of the observed changes in SN gene expression corroborated earlier observations in PD. The most significantly downregulated gene in our SN dataset, GBE1, was also found to be significantly downregulated in the study performed by Grunblatt et al (Grunblatt *et al.* 2004). Other examples of transcriptional alterations that were in agreement with earlier findings in PD include SYT1, TRIM36, MDH1, NSF, SASH1, ALDH1A1, DSCR1L1 and SNX10 (Grunblatt *et al.* 2004; Miller *et al.* 2006; Zhang *et al.* 2005). Furthermore, we report transcriptional downregulation of both SNCA and NURR1, which are well known for their roles in familial PD. It is also noteworthy that in the studies of Miller et al, and Moran et al, the number of downregulated genes in the PD SN by far surpasses that of upregulated genes, an observation we corroborated (Miller *et al.* 2006; Moran *et al.* 2006).

We have also identified dysregulations in transcription levels of several genes previously not implicated in PD, which might have a role as new players in PD neurodegeneration. The most pronounced changes are described below.

Altered expression of genes involved in neurotrophin signaling

A substantial number of genes involved in neurotrophin signaling are transcriptionally altered in the PD SN. A reduction to 36% of control of RIT2 levels, a specific

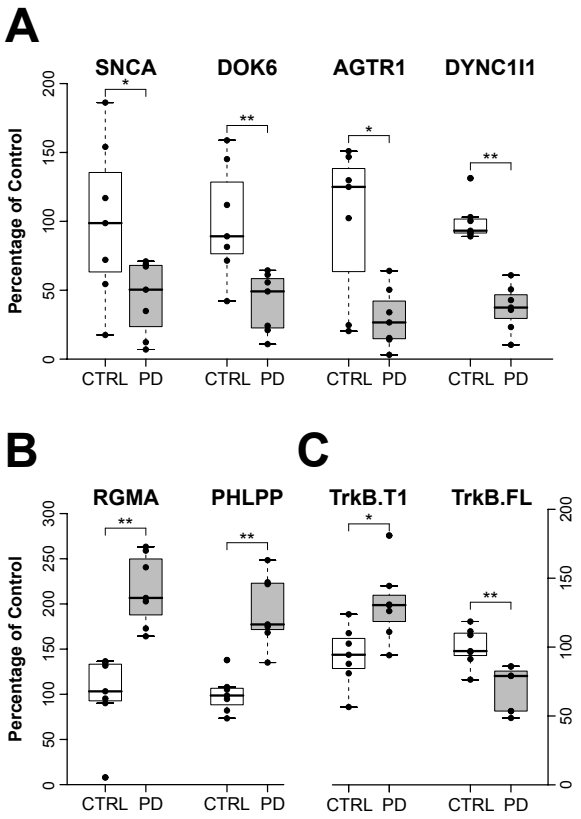

*Figure 2 - Selection of expression changes observed in the PD SN, as determined by qPCR on 7 PD patients and 7 controls. For each gene, the average of control measurements was set to 100%. All alterations are similar to those observed in the microarray experiment. A) downregulated transcripts in PD. B) upregulated transcripts in PD. C) Alterations in truncated (T1) and full length (FL) forms of TrkB. Note the shift in the ratio TrkB.T1/TrkB.FL in PD. P-values determined by the Mann-Whitney U test. ** p-value < 0.01, * p-value < 0.05.*

regulator of neurotrophin signaling (Shi *et al.* 2005), was detected. Transcript levels of MAGEE1, possibly involved in neurotrophin signaling via the p75 neurotrophin receptor (Albrecht and Froehner 2004), showed a similar decrease. The expression of NDN was reduced to 38% of normal levels in PD SN. NDN facilitates TrkA signaling to promote neuronal survival (Kuwako *et al.* 2005). Also, we observed a significant downregulation of DOK6, involved in the GDNF signaling pathway (Crowder *et al.* 2004). DLK1, which is known to be regulated by GDNF (Christophersen *et al.* 2007), also exhibited a severe decline in expression (22% of normal levels). Interestingly, the expression of PHLPP was increased. PHLPP is known to decrease intracellular neurotrophin signaling by dephosphorylating Akt (Gao *et al.* 2005). We also observed elevated transcript levels of a truncated form of TrkB (TrkB-T1), the

Table 3 - List of all significant expression changes in the PD substantia nigra, caudate nucleus and putamen, as determined by microarray analysis. DE: differential expression, as fraction of control levels. p-value: Bonferroni-adjusted p-value.

Systematic Name	GeneName	Description	DE	Pval
Downregulated genes - Substantia Nigra				
NM_000158	GBE1	Glucan (1,4-alpha-), branching enzyme 1 (glycogen branching enzyme, Andersen disease, glycogen storage disease type IV)	0.18	0.000
NM_033495	KLHL13	Kelch-like 13 (Drosophila)	0.24	0.000
AL117636		MRNA; cDNA DKFZp434H205 (from clone DKFZp434H205)	0.34	0.000
NM_004411	DYNC1I1	Dynein, cytoplasmic 1, intermediate chain 1	0.26	0.000
NM_002863	PYGL	Phosphorylase, glycogen; liver (Hers disease, glycogen storage disease type VI)	0.26	0.000
AB002376	CAST1	CAZ-associated structural protein	0.28	0.000
NM_000345	SNCA	Synuclein, alpha (non A4 component of amyloid precursor)	0.27	0.000
NM_002928	RGS16	Regulator of G-protein signalling 16	0.22	0.000
AB014731	DENR	Density-regulated protein	0.41	0.000
NM_018092	NETO2	Neuropilin (NRP) and tolloid (TLL)-like 2	0.46	0.000
NM_014332	SMPX	Small muscle protein, X-linked	0.31	0.000
NM_006670	TPBG	Trophoblast glycoprotein	0.18	0.000
NM_017999	RNF31	Ring finger protein 31	0.32	0.000
NM_006350	FST	Follistatin	0.17	0.000
BF035258	AKAP12	A kinase (PRKA) anchor protein (gravin) 12	0.39	0.000
AW974789	TTMA	Two transmembrane domain family member A	0.47	0.000
AF428101	DACH2	Dachshund homolog 2 (Drosophila)	0.35	0.001
NM_018700	TRIM36	Tripartite motif-containing 36	0.30	0.001
AK024251	SLITRK5	SLIT and NTRK-like family, member 5	0.46	0.001
NM_005639	SYT1	Synaptotagmin I	0.23	0.001
AB020710	EHBP1	EH domain binding protein 1	0.49	0.001
H06068		yl72g10.s1 Soares infant brain 1NIB Homo sapiens cDNA clone IMAGE:43489 3-, mRNA sequence	0.46	0.001
AF225987	SCN3A	Sodium channel, voltage-gated, type III, alpha	0.47	0.001
AL390172		Homo sapiens genomic DNA; cDNA DKFZp547I204 (from clone DKFZp547I204)	0.35	0.001
AK055427	DGKH	Diacylglycerol kinase, eta	0.31	0.001
NM_022726	ELOVL4	Elongation of very long chain fatty acids (FEN1/Elo2, SUR4/Elo3, yeast)-like 4	0.46	0.001
NM_006186	NR4A2	Nuclear receptor subfamily 4, group A, member 2	0.20	0.001
NM_031850	AGTR1	Angiotensin II receptor, type 1	0.07	0.001

NM_014309	RPL41	Ribosomal protein L41	0.38	0.001
R42166		yf99d08.s1 Soares infant brain 1NIB Homo sapiens cDNA clone IMAGE:30780 3-, mRNA sequence	0.25	0.001
NM_012189	CABYR	Calcium binding tyrosine-(Y)-phosphorylation regulated (fibrousheathin 2)	0.49	0.001
NM_006113	VAV3	Vav 3 oncogene	0.34	0.001
NM_014905	GLS	Glutaminase	0.43	0.001
J04621	SDC2	Syndecan 2 (heparan sulfate proteoglycan 1, cell surface-associated, fibroglycan)	0.37	0.001
AF070623	LOC138046	Hypothetical protein LOC138046	0.38	0.001
NM_004796	NRXN3	Neurexin 3	0.49	0.001
AK025615	BCAT1	Branched chain aminotransferase 1, cytosolic	0.31	0.002
NM_003979	GPRC5A	G protein-coupled receptor, family C, group 5, member A	0.30	0.002
AF339796	HS6ST3	Heparan sulfate 6-O-sulfotransferase 3	0.48	0.002
AL137498	SCN2A2	Sodium channel, voltage-gated, type II, alpha 2	0.45	0.002
NM_000809	GABRA4	Gamma-aminobutyric acid (GABA) A receptor, alpha 4	0.29	0.002
AW294729		Transcribed locus, moderately similar to NP_509344.1 HIStone family member (his-71) [Caenorhabditis elegans]	0.55	0.002
NM_003138	SRPK2	Homo sapiens SFRS protein kinase 2 (SRPK2), transcript variant 2, mRNA	0.53	0.002
AF397397	OLFM3	Olfactomedin 3	0.31	0.002
NM_005100	AKAP12	A kinase (PRKA) anchor protein (gravin) 12	0.43	0.002
AB046788	ROBO2	Roundabout, axon guidance receptor, homolog 2 (Drosophila)	0.32	0.002
AV707343		V707343 ADB Homo sapiens cDNA clone ADBBSH02 5-, mRNA sequence	0.25	0.002
BC004869	C6orf168	Chromosome 6 open reading frame 168	0.44	0.002
NM_021159	RAP1GDS1	RAP1, GTP-GDP dissociation stimulator 1	0.47	0.002
AI208142	DKFZ-P434L187	DKFZP434L187 protein	0.28	0.003
NM_014841	SNAP91	Synaptosomal-associated protein, 91kDa homolog (mouse)	0.45	0.003
AI363461		qy58d08.x1 NCI_CGAP_Brn23 Homo sapiens cDNA clone IMAGE:2016207 3- similar to gb:X15822 CYTOCHROME C OXIDASE POLYPEPTIDE VIIA-LIVER PRECURSOR (HUMAN);, mRNA sequence	0.51	0.003
AB011131	PCLO	Piccolo (presynaptic cytomatrix protein)	0.40	0.003
NM_000689	ALDH1A1	Aldehyde dehydrogenase 1 family, member A1	0.18	0.003
AB046854	MAGI3	Membrane associated guanylate kinase, WW and PDZ domain containing 3	0.49	0.003
AB046807	MAGEE1	Melanoma antigen family E, 1	0.40	0.003
AB020663	DMXL2	Dmx-like 2	0.47	0.003
AK054939	ST8SIA3	ST8 alpha-N-acetyl-neuraminide alpha-2,8-sialyltransferase 3	0.52	0.003
NM_016529	ATP8A2	ATPase, aminophospholipid transporter-like, Class I, type 8A, member 2	0.34	0.003
AL041224	AP1GBP1	AP1 gamma subunit binding protein 1	0.48	0.004
NM_022497	MRPS25	Mitochondrial ribosomal protein S25	0.51	0.004
NM_052953	LRRC3B	Leucine rich repeat containing 3B	0.39	0.004
NM_014970	KIFAP3	Kinesin-associated protein 3	0.45	0.004
AK054981	UNC13C	Unc-13 homolog C (C. elegans)	0.28	0.004

Systematic Name	GeneName	Description	DE	Pval
NM_003836	DLK1	Delta-like 1 homolog (Drosophila)	0.22	0.004
NM_019035	PCDH18	Protocadherin 18	0.54	0.005
NM_014278	HSPA4L	Heat shock 70kDa protein 4-like	0.48	0.005
NM_002866	RAB3A	RAB3A, member RAS oncogene family	0.46	0.005
NM_003385	VSNL1	Visinin-like 1	0.29	0.005
NM_018686	CMAS	Cytidine monophosphate N-acetylneuraminic acid synthetase	0.40	0.005
NM_016185	HN1	Hematological and neurological expressed 1	0.49	0.005
AI815915		au43d12.x1 Schneider fetal brain 00004 Homo sapiens cDNA clone IMAGE:2517527 3- similar to gb:X51956_rna1 GAMMA ENOLASE (HUMAN);, mRNA sequence	0.37	0.005
NM_001635	AMPH	Amphiphysin (Stiff-Man syndrome with breast cancer 128kDa autoantigen)	0.33	0.005
NM_004085	TIMM8A	Translocase of inner mitochondrial membrane 8 homolog A (yeast)	0.54	0.005
NM_031469	SH3BGRL2	SH3 domain binding glutamic acid-rich protein like 2	0.52	0.005
NM_018057	SLC6A15	Solute carrier family 6, member 15	0.41	0.005
NM_022912	REEP1	Receptor accessory protein 1	0.32	0.006
NM_014176	UBE2T	Ubiquitin-conjugating enzyme E2T (putative)	0.40	0.006
NM_000276	OCRL	Oculocerebrorenal syndrome of Lowe	0.52	0.006
AL512695	CD226	CD226 molecule	0.44	0.006
AI590401		ts10a11.x1 NCI_CGAP_Pan1 Homo sapiens cDNA clone IMAGE:2228156 3-, mRNA sequence	0.52	0.006
NM_000860	HPGD	Hydroxyprostaglandin dehydrogenase 15-(NAD)	0.29	0.006
AK057795	DOK6	Docking protein 6	0.26	0.006
NM_032873	STS-1	Cbl-interacting protein Sts-1	0.38	0.006
NM_005917	MDH1	Malate dehydrogenase 1, NAD (soluble)	0.40	0.006
BC010549	UBE2F	Ubiquitin-conjugating enzyme E2F (putative)	0.48	0.007
AK056217	FLJ44635	TPT1-like protein	0.46	0.007
NM_002930	RIT2	Ras-like without CAAX 2	0.36	0.007
NM_015294	TRIM37	Tripartite motif-containing 37	0.55	0.007
NM_032320	BTBD10	BTB (POZ) domain containing 10	0.49	0.007
NM_006178	NSF	N-ethylmaleimide-sensitive factor	0.49	0.007
NM_000194	HPRT1	Hypoxanthine phosphoribosyltransferase 1 (Lesch-Nyhan syndrome)	0.37	0.007
NM_002736	PRKAR2B	Protein kinase, cAMP-dependent, regulatory, type II, beta	0.35	0.007
D31886	RAB3GAP1	RAB3 GTPase activating protein subunit 1 (catalytic)	0.59	0.008
NM_021032	FGF12	Fibroblast growth factor 12	0.35	0.008
NM_016141	DYNC1LI1	Dynein, cytoplasmic 1, light intermediate chain 1	0.50	0.008
NM_000317	PTS	6-pyruvoyltetrahydropterin synthase	0.56	0.008
AL109678	LOC390616	Similar to RIKEN cDNA B230218L05 gene	0.35	0.008
NM_014906	PPM1E	Protein phosphatase 1E (PP2C domain containing)	0.36	0.008

AB020689	TBC1D9	TBC1 domain family, member 9	0.40	0.008
NM_002252	KCNS3	Potassium voltage-gated channel, delayed-rectifier, subfamily S, member 3	0.32	0.008
NM_016129	COPS4	COP9 constitutive photomorphogenic homolog subunit 4 (Arabidopsis)	0.48	0.008
AB033049	ANKRD50	Ankyrin repeat domain 50	0.48	0.009
AK055362	KCNMA1	Potassium large conductance calcium-activated channel, subfamily M, alpha member 1	0.53	0.010
AK057753	RGS8	Regulator of G-protein signalling 8	0.41	0.010
BI966682	PGM2L1	Phosphoglucomutase 2-like 1	0.29	0.010
AK054689	NAP1L5	Nucleosome assembly protein 1-like 5	0.36	0.011
NM_005713	COL4A3BP	Collagen, type IV, alpha 3 (Goodpasture antigen) binding protein	0.59	0.011
NM_003020	SCG5	Secretogranin V (7B2 protein)	0.48	0.011
BG704055		602687195F1 NIH_MGC_95 Homo sapiens cDNA clone IMAGE:4819775 5-, mRNA sequence	0.48	0.011
AK023042	LASS6	LAG1 longevity assurance homolog 6 (S. cerevisiae)	0.34	0.012
AK055065	UNC13A	Unc-13 homolog A (C. elegans)	0.44	0.012
NM_006159	NELL2	NEL-like 2 (chicken)	0.30	0.012
NM_002623	PFDN4	Prefoldin subunit 4	0.53	0.012
NM_020180	BRUNOL4	Bruno-like 4, RNA binding protein (Drosophila)	0.41	0.012
AK026786	PRMT8	Protein arginine methyltransferase 8	0.37	0.012
NM_003350	UBE2V2	Ubiquitin-conjugating enzyme E2 variant 2	0.50	0.012
NM_001445	FABP6	Fatty acid binding protein 6, ileal (gastrotropin)	0.41	0.012
NM_006936	SUMO3	SMT3 suppressor of mif two 3 homolog 3 (S. cerevisiae)	0.58	0.013
AL110139	LOC400451	Hypothetical gene supported by AK075564; BC060873	0.51	0.013
AK022817	NAPB	N-ethylmaleimide-sensitive factor attachment protein, beta	0.38	0.013
NM_021963	NAP1L2	Nucleosome assembly protein 1-like 2	0.46	0.013
NM_021083	XK	X-linked Kx blood group (McLeod syndrome)	0.48	0.013
NM_032594	INSM2	Insulinoma-associated 2	0.40	0.013
NM_014848	SV2B	Synaptic vesicle glycoprotein 2B	0.30	0.013
NM_002752	MAPK9	Mitogen-activated protein kinase 9	0.51	0.013
AB007877	HSPA12A	Heat shock 70kDa protein 12A	0.41	0.014
NM_017691	LRRC49	Leucine rich repeat containing 49	0.50	0.014
NM_000291	PGK1	Phosphoglycerate kinase 1	0.52	0.014
NM_020386	HRASLS	HRAS-like suppressor	0.51	0.014
NM_018159	NUDT11	Nudix (nucleoside diphosphate linked moiety X)-type motif 11	0.52	0.014
AB018345	KIAA0802	KIAA0802	0.39	0.015
NM_006803	AP3M2	Adaptor-related protein complex 3, mu 2 subunit	0.54	0.015
NM_022131	CLSTN2	Calsyntenin 2	0.52	0.015
NM_018000	DSU	Dilute suppressor	0.62	0.016
NM_015509	NECAP1	NECAP endocytosis associated 1	0.41	0.016
AK057055	RPL41	Ribosomal protein L41	0.51	0.016

Systematic Name	GeneName	Description	DE	Pval
NM_003010	MAP2K4	Mitogen-activated protein kinase kinase 4	0.51	0.017
NM_001686	ATP5B	ATP synthase, H+ transporting, mitochondrial F1 complex, beta polypeptide	0.60	0.017
AI200874	RIMS1	Regulating synaptic membrane exocytosis 1	0.31	0.018
NM_004280	EEF1E1	Eukaryotic translation elongation factor 1 epsilon 1	0.55	0.018
NM_020685	C3orf14	Chromosome 3 open reading frame 14	0.54	0.018
AK027572	KCTD6	Potassium channel tetramerisation domain containing 6	0.59	0.018
NM_001151	SLC25A4	Solute carrier family 25 (mitochondrial carrier; adenine nucleotide translocator), member 4	0.52	0.018
BC010282	LRPPRC	Leucine-rich PPR-motif containing	0.58	0.018
NM_003812	ADAM23	ADAM metallopeptidase domain 23	0.41	0.018
NM_002830	PTPN4	Protein tyrosine phosphatase, non-receptor type 4 (megakaryocyte)	0.53	0.018
NM_000259	MYO5A	Myosin VA (heavy polypeptide 12, myoxin)	0.44	0.019
NM_032814	TMEM118	Transmembrane protein 118	0.53	0.020
NM_018640	LMO3	LIM domain only 3 (rhombotin-like 2)	0.41	0.020
NM_018215	FLJ10781	Hypothetical protein FLJ10781	0.53	0.020
AL442092	LRRN3	Leucine rich repeat neuronal 3	0.55	0.021
NM_004993	ATXN3	Ataxin 3	0.56	0.021
NM_005822	DSCR1L1	Down syndrome critical region gene 1-like 1	0.37	0.021
AK025203	FAM102B	Family with sequence similarity 102, member B	0.41	0.021
BF438028		7q66b07.x1 NCI_CGAP_Lu24 Homo sapiens cDNA clone IMAGE:3703237 3-, mRNA sequence	0.63	0.021
NM_003081	SNAP25	Synaptosomal-associated protein, 25kDa	0.40	0.021
NM_005688	ABCC5	ATP-binding cassette, sub-family C (CFTR/MRP), member 5	0.61	0.021
NM_002816	PSMD12	Proteasome (prosome, macropain) 26S subunit, non-ATPase, 12	0.55	0.021
NM_003951	SLC25A14	Solute carrier family 25 (mitochondrial carrier, brain), member 14	0.58	0.021
NM_017784	OSBPL10	Oxysterol binding protein-like 10	0.34	0.022
NM_004586	RPS6KA3	Ribosomal protein S6 kinase, 90kDa, polypeptide 3	0.55	0.022
NM_004742	MAGI1	Membrane associated guanylate kinase, WW and PDZ domain containing 1	0.45	0.022
NM_005875	EIF1B	Eukaryotic translation initiation factor 1B	0.54	0.022
NM_005872	BCAS2	Breast carcinoma amplified sequence 2	0.55	0.023
NM_021637	TMEM35	Transmembrane protein 35	0.42	0.023
NM_033027	AXUD1	AXIN1 up-regulated 1	0.58	0.023
NM_021928	SPCS3	Signal peptidase complex subunit 3 homolog (S. cerevisiae)	0.59	0.024
BG196607		RST15833 Athersys RAGE Library Homo sapiens cDNA, mRNA sequence	0.53	0.024
AL096752	RAB3GAP1	RAB3 GTPase activating protein subunit 1 (catalytic)	0.62	0.024
AF400502	SNRPN	Small nuclear ribonucleoprotein polypeptide N	0.55	0.025
AK057555	PRKCB1	Protein kinase C, beta 1	0.55	0.025
NM_021980	OPTN	Optineurin	0.51	0.025

NM_015941	ATP6V1H	ATPase, H+ transporting, lysosomal 50/57kDa, V1 subunit H	0.56	0.025
NM_014961	RUFY3	RUN and FYVE domain containing 3	0.61	0.026
NM_003716	CADPS	Ca2+-dependent secretion activator	0.34	0.026
NM_003866	INPP4B	Inositol polyphosphate-4-phosphatase, type II, 105kDa	0.30	0.027
NM_031940	TM2D2	TM2 domain containing 2	0.53	0.027
NM_005151	USP14	Ubiquitin specific peptidase 14 (tRNA-guanine transglycosylase)	0.59	0.027
NM_023037	FRY	Furry homolog (Drosophila)	0.63	0.027
NM_002222	ITPR1	Inositol 1,4,5-triphosphate receptor, type 1	0.46	0.028
NM_017938	FAM70A	Family with sequence similarity 70, member A	0.32	0.029
NM_007275	TUSC2	Tumor suppressor candidate 2	0.59	0.029
NM_004496	FOXA1	Forkhead box A1	0.18	0.029
R45986		yg48e01.s1 Soares infant brain 1NIB Homo sapiens cDNA clone IMAGE:35586 3- similar to contains TAR1 repetitive element ;, mRNA sequence	0.31	0.029
NM_001936	DPP6	Dipeptidyl-peptidase 6	0.62	0.029
AF217190	DHX36	DEAH (Asp-Glu-Ala-His) box polypeptide 36	0.58	0.029
NM_015946	PELO	Pelota homolog (Drosophila)	0.62	0.031
NM_004046	ATP5A1	ATP synthase, H+ transporting, mitochondrial F1 complex, alpha subunit 1, cardiac muscle	0.53	0.031
NM_014175	MRPL15	Mitochondrial ribosomal protein L15	0.57	0.031
NM_032798		Homo sapiens hypothetical protein FLJ14503 (FLJ14503), mRNA.	0.30	0.031
NM_032804	C10orf22	Chromosome 10 open reading frame 22	0.61	0.031
AF056085	GABBR2	Gamma-aminobutyric acid (GABA) B receptor, 2	0.52	0.032
NM_003054	SLC18A2	Solute carrier family 18 (vesicular monoamine), member 2	0.16	0.033
NM_006561	CUGBP2	CUG triplet repeat, RNA binding protein 2	0.62	0.033
NM_000169	GLA	Galactosidase, alpha	0.47	0.034
AF090100	AAK1	AP2 associated kinase 1	0.43	0.034
AB058696	NAG6	Hypothetical protein DKFZp434G156	0.40	0.034
NM_022151	MOAP1	Modulator of apoptosis 1	0.38	0.035
BC013033	RAB3C	RAB3C, member RAS oncogene family	0.31	0.035
AB007896	PREPL	Prolyl endopeptidase-like	0.59	0.035
NM_003165	STXBP1	Syntaxin binding protein 1	0.44	0.035
NM_016656	RRAGB	Ras-related GTP binding B	0.51	0.036
NM_032568	GABA-RAPL3	Homo sapiens GABA(A) receptors associated protein like 3 (GABARAPL3), mRNA.	0.50	0.036
NM_002590	PCDH8	Protocadherin 8	0.19	0.037
NM_001313	CRMP1	Collapsin response mediator protein 1	0.60	0.037
AK056563	C1orf71	Chromosome 1 open reading frame 71	0.48	0.037
NM_031412	GABA-RAPL1	GABA(A) receptor-associated protein like 1	0.50	0.037

Systematic Name	GeneName	Description	DE	Pval
NM_025108	C16orf59	Chromosome 16 open reading frame 59	0.54	0.037
NM_004255	COX5A	Cytochrome c oxidase subunit Va	0.62	0.038
NM_012395	PFTK1	PFTAIRE protein kinase 1	0.36	0.038
AF288395	NMNAT2	Nicotinamide nucleotide adenylyltransferase 2	0.30	0.038
NM_014912	CPEB3	Cytoplasmic polyadenylation element binding protein 3	0.67	0.038
NM_014747	RIMS3	Regulating synaptic membrane exocytosis 3	0.57	0.039
NM_006918	SC5DL	Sterol-C5-desaturase (ERG3 delta-5-desaturase homolog, fungal)-like	0.63	0.040
AI498582		tn02e02.x1 NCI_CGAP_Brn25 Homo sapiens cDNA clone IMAGE:2166458 3-, mRNA sequence	0.59	0.041
BC001867		Homo sapiens cDNA clone IMAGE:3536204	0.55	0.041
AL136712	DNM3	Dynamin 3	0.55	0.041
NM_021800	DNAJC12	DnaJ (Hsp40) homolog, subfamily C, member 12	0.55	0.042
BC013576	GPRASP2	G protein-coupled receptor associated sorting protein 2	0.52	0.043
NM_002079	GOT1	Glutamic-oxaloacetic transaminase 1, soluble (aspartate aminotransferase 1)	0.48	0.043
NM_016183	C1orf33	Chromosome 1 open reading frame 33	0.59	0.043
NM_006839	IMMT	Inner membrane protein, mitochondrial (mitofilin)	0.55	0.043
AJ010230	RFPL1S	Ret finger protein-like 1 antisense	0.55	0.043
NM_014677	RIMS2	Regulating synaptic membrane exocytosis 2	0.55	0.043
NM_018477	ACTR10	Actin-related protein 10 homolog (S. cerevisiae)	0.46	0.043
NM_001863	COX6B1	Cytochrome c oxidase subunit Vib polypeptide 1 (ubiquitous)	0.63	0.044
NM_031468	CALN1	Calneuron 1	0.33	0.045
NM_021074	NDUFV2	NADH dehydrogenase (ubiquinone) flavoprotein 2, 24kDa	0.59	0.045
NM_006359	SLC9A6	Solute carrier family 9 (sodium/hydrogen exchanger), member 6	0.60	0.045
NM_013322	SNX10	Sorting nexin 10	0.44	0.045
NM_002847	PTPRN2	Protein tyrosine phosphatase, receptor type, N polypeptide 2	0.55	0.046
AL355687		EST from clone 24355, full insert	0.25	0.046
NM_012347	FBXO9	F-box protein 9	0.54	0.048
AK054565	TCP11L1	T-complex 11 (mouse) like 1	0.66	0.048
NM_001172	ARG2	Arginase, type II	0.47	0.049
NM_006818	MLLT11	Myeloid/lymphoid or mixed-lineage leukemia (trithorax homolog, Drosophila); translocated to, 11	0.38	0.049
AK054998	PLEKHB2	Pleckstrin homology domain containing, family B (evectins) member 2	0.54	0.049
AL133688		DKFZp761K1110_s1 761 (synonym: hamy2) Homo sapiens cDNA clone DKFZp761K1110 3-, mRNA sequence	0.52	0.049
NM_017933	FLJ20701	Hypothetical protein FLJ20701	0.46	0.050
Upregulated genes - Substantia Nigra				
BC013923	SOX2	SRY (sex determining region Y)-box 2	1.86	0.001
BI823317		603041226F1 NIH_MGC_115 Homo sapiens cDNA clone IMAGE:5182015 5-, mRNA sequence	2.18	0.001

NM_018276	SSH3	Slingshot homolog 3 (Drosophila)	1.66	0.002
NM_002343	LTF	Lactotransferrin	4.56	0.005
NM_003380	VIM	Vimentin	2.22	0.006
AB011178	PHLPP	PH domain and leucine rich repeat protein phosphatase	1.90	0.006
NM_001401	EDG2	Endothelial differentiation, lysophosphatidic acid G-protein-coupled receptor, 2	2.06	0.007
AK056822	LOC400960	Hypothetical gene supported by BC040598	1.71	0.008
NM_018494	LRDD	Leucine-rich repeats and death domain containing	2.00	0.009
NM_003244	TGIF	TGFB-induced factor (TALE family homeobox)	1.96	0.011
NM_002823	PTMA	Prothymosin, alpha (gene sequence 28)	1.80	0.011
AL136826	RGMA	RGM domain family, member A	1.97	0.012
NM_032161		Homo sapiens KIAA1870 protein (KIAA1870), mRNA.	1.89	0.013
NM_002053	GBP1	Guanylate binding protein 1, interferon-inducible, 67kDa	2.62	0.015
NM_002609	PDGFRB	Platelet-derived growth factor receptor, beta polypeptide	1.64	0.015
AB046774	C17orf27	Chromosome 17 open reading frame 27	1.96	0.015
AV723140		AV723140 HTB Homo sapiens cDNA clone HTBAAA04 5-, mRNA sequence	1.74	0.015
NM_000346	SOX9	SRY (sex determining region Y)-box 9 (campomelic dysplasia, autosomal sex-reversal)	1.72	0.015
NM_001227	CASP7	Caspase 7, apoptosis-related cysteine peptidase	1.91	0.017
AK025495	SASH1	SAM and SH3 domain containing 1	1.77	0.020
NM_004642	CDK2AP1	CDK2-associated protein 1	1.61	0.020
AB014555	HIP1R	Huntingtin interacting protein 1 related	1.66	0.021
NM_021200	PLEKHB1	Pleckstrin homology domain containing, family B (evectins) member 1	1.80	0.022
NM_018181	ZNF532	Zinc finger protein 532	1.69	0.023
NM_002774	KLK6	Kallikrein 6 (neurosin, zyme)	1.60	0.027
NM_012304	FBXL7	F-box and leucine-rich repeat protein 7	1.68	0.027
NM_002026	FN1	Fibronectin 1	1.86	0.030
NM_021198	CTDSP1	CTD (carboxy-terminal domain, RNA polymerase II, polypeptide A) small phosphatase 1	1.77	0.030
AK056809	LRRC58	Leucine rich repeat containing 58	1.64	0.031
BC004287		Homo sapiens, clone IMAGE:3618365, mRNA	1.94	0.032
NM_024516	MVP	Major vault protein	1.67	0.033
NM_005938	MLLT7	Myeloid/lymphoid or mixed-lineage leukemia (trithorax homolog, Drosophila); translocated to, 7	1.82	0.033
NM_000067	CA2	Carbonic anhydrase II	2.26	0.033
NM_021242	MID1IP1	MID1 interacting protein 1 (gastrulation specific G12-like (zebrafish))	1.86	0.034
NM_002562	P2RX7	Purinergic receptor P2X, ligand-gated ion channel, 7	1.90	0.034
NM_005979	S100A13	S100 calcium binding protein A13	1.69	0.035
AK023424	FLJ27365	FLJ27365 protein	1.65	0.037
AB058716		Homo sapiens mRNA for KIAA1813 protein, partial cds	1.68	0.039
AB020676	WWC1	WW, C2 and coiled-coil domain containing 1	1.69	0.040
NM_024513	FYCO1	FYVE and coiled-coil domain containing 1	1.56	0.041

Systematic Name	GeneName	Description	DE	Pval
NM_002070	GNAI2	Guanine nucleotide binding protein (G protein), alpha inhibiting activity polypeptide 2	1.49	0.042
AK027091		CDNA: FLJ23438 fis, clone HRC13275	1.85	0.042
NM_004723	ARHGEF2	Rho/rac guanine nucleotide exchange factor (GEF) 2	1.77	0.047
NM_013974	DDAH2	Dimethylarginine dimethylaminohydrolase 2	1.69	0.048
NM_002859	PXN	Paxillin	1.72	0.048
BI754846		603026815F1 NIH_MGC_114 Homo sapiens cDNA clone IMAGE:5197250 5-, mRNA sequence	2.34	0.048
NM_017707	DDEFL1	Development and differentiation enhancing factor-like 1	1.64	0.048
Downregulated genes - Caudate Nucleus				
NM_001888	CRYM	Crystallin, mu	0.43	0.025
NM_006211	PENK	Proenkephalin	0.45	0.038
NM_030615	KIF25	Kinesin family member 25	0.56	0.016
NM_016454	TMEM85	Transmembrane protein 85	0.61	0.006
NM_006680	ME3	Malic enzyme 3, NADP(+)-dependent, mitochondrial	0.62	0.020
NM_000783	CYP26A1	Cytochrome P450, family 26, subfamily A, polypeptide 1	0.64	0.024
AL538117	CXADR	Coxsackie virus and adenovirus receptor	0.65	0.024
NM_015417	C20orf28	Chromosome 20 open reading frame 28	0.68	0.031
NM_004087	DLG1	Discs, large homolog 1 (Drosophila)	0.70	0.048
NM_021252	RAB18	RAB18, member RAS oncogene family	0.71	0.038
Upregulated genes - Caudate Nucleus				
AL136693	CYBRD1	Cytochrome b reductase 1	1.39	0.031
NM_003243	TGFBR3	Transforming growth factor, beta receptor III (betaglycan, 300kDa)	1.47	0.011
NM_005413	SIX3	Sine oculis homeobox homolog 3 (Drosophila)	1.52	0.013
NM_005859	PURA	Purine-rich element binding protein A	1.54	0.041
AK026152	CTSH	Cathepsin H	1.64	0.005
NM_002343	LTF	Lactotransferrin	2.57	0.000
Downregulated genes - Putamen				
BF381899	GNPDA2	Glucosamine-6-phosphate deaminase 2	0.52	0.000
AC016696		Homo sapiens BAC clone RP11-130P22 from 2, complete sequence.	0.71	0.003
Upregulated genes - Putamen				
NM_015556	SIPA1L1	Signal-induced proliferation-associated 1 like 1	1.28	0.009
NM_001124	ADM	Adrenomedullin	1.80	0.027

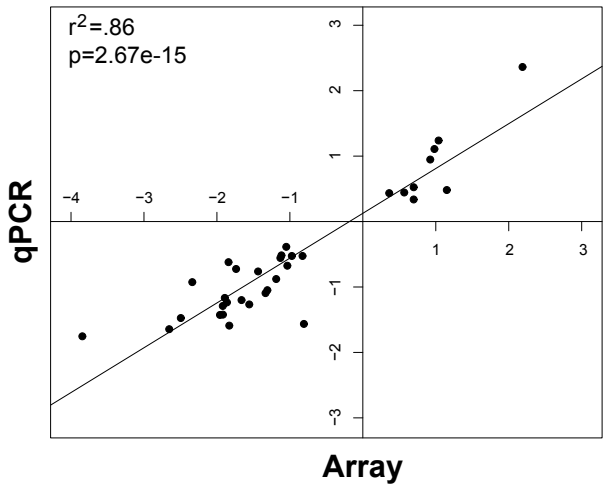

Figure 3 - Correlation between microarray and qPCR fold changes for all 34 transcripts investigated by qPCR in the SN. The line represents the least squares fitted curve through the data points. Fold changes are given as log2(PD/control).

receptor for BDNF. TrkB-T1 lacks the intracellular kinase domain, and is therefore unable to induce the intracellular BDNF signaling cascade. Interestingly, the splice variants encoding for the full length versions of TrkB were significantly reduced in PD, as determined by qPCR (see Figure 2).

Changes in genes encoding axon guidance cues

The expression levels of several genes implicated in axon guidance are changed in the PD SN. The repulsive guidance protein RGMA was upregulated to 197% of control levels. Furthermore, transcript levels of ROBO2, the receptor for Slit2, were significantly reduced. The expression of NETO2 and SLITRK5 were both decreased in the PD SN. Although there is little knowledge on the cellular function of these proteins, their domain structure is suggestive for a role in axon guidance in development. SDC2, a heparan sulfate proteoglycan possibly involved in regulating the function of some axon guidance molecules, was downregulated in the PD SN. Finally, although not significantly changed, a subset of patients showed elevated levels of the axon guidance molecule Sema5A (data not shown).

Other gene changes in PD SN, caudate nucleus and putamen

One of the most strongly upregulated genes in the PD SN was the gene coding for the iron-binding protein lactotransferrin (LTF), a finding which was replicated in the caudate nucleus. Other noteworthy gene changes in the PD SN include AGTR1, VMAT2, ALDH1A1, DSCR1L1 and PTS. In the PD caudate nucleus, in addition to

the upregulation of LTF, CYBRD1, involved in iron homeostasis, was also modestly upregulated. Furthermore, we observed expression changes in the mitochondrial enzyme ME3, and PENK. In the PD putamen, the most significantly changed gene was GNPDA2. Furthermore, a strong increase in transcriptional levels of adrenomedullin was detected.

Identification of dysregulated gene groups in the PD caudate, putamen and SN

One of the main advantages of global gene expression profiling is the ability to detect concerted changes in functionally related groups of genes. We applied an unbiased functional class scoring (FCS) approach to identify those GO or KEGG classes that were significantly dysregulated in PD. Also, the average expression change for each gene group was calculated to assess its overall directional change in transcript levels. The FCS calculations identified 75 GO classes and 29 KEGG classes as being differentially expressed in the SN between PD and control. 8 KEGG classes and one GO class were found to be changed in the putamen, and for the caudate nucleus no statistically significant differences were observed (Table 4).

Alterations in gene groups involved in synaptic transmission in the PD SN

Many gene groups related to synaptic transmission are compromised in the PD SN. For example, the average transcriptional activity of the 17 genes annotated as "Synaptosome" (GO:0019717) was reduced to 66% of control levels. Similar changes were detected for, amongst others, the classes "Synapse" (GO:0045202), "Long-term potentiation" (hsa04720) and "Long-term depression" (hsa04730). The average reduction of gene expression in synaptic transmission-related gene groups in PD was 15%. Although this seems a relatively mild change in expression levels, one should take into account that affected gene groups contain both changed and unchanged genes: the range of transcriptional changes runs up to a 77% reduction (SYT1). Related to lowered synaptic transmission in the SN, a dysregulation of "Gap junction" (hsa04540) was detected in the putamen.

Reduction of gene groups involved in oxidative phosphorylation in PD SN and putamen

We observed a strong reduction in transcriptional levels of gene groups involved in oxidative phosphorylation and ATP synthesis in the PD SN. This was reflected, amongst others, by the dowregulation of the KEGG classes "Oxidative phosphorylation" (hsa00190) and "ATP synthesis" (hsa00193), and the GO classes "ATP synthesis coupled proton transport" (GO:0015986) and "NADH dehydrogenase activity" (GO:0003954). Average transcript levels for these gene groups were reduced to ~70% of control. Interestingly, we also detected a reduction of the KEGG gene groups "Oxidative phosphorylation" and "ATP synthesis" in the putamen (~90% of

control levels). Additionally, a number of GO classes involved in oxidative phosphorylation showed a downward trend in the putamen ($p < .08$, data not shown).

Downregulation of ubiquitin-proteasome gene groups in PD SN

The ubiquitin-proteasome system (UPS) is dysregulated in PD. We observed a downregulation of the classes "Proteasome" (hsa03050), "Unfolded protein binding" (GO:0051082), "Proteasome core complex (sensu Eukaryota)" (GO:0005839), "proteasome regulatory particle (sensu Eukaryota)" (GO:0005838) and "Ubiquitin-dependent protein catabolism" (GO:0006511). Average transcript levels for these groups were reduced by 15%.

Alterations in gene groups encoding for proteins involved in cytoskeletal structure and microtubule-based transport in PD SN

Noteworthy is the dysregulation of gene groups involved in cytoskeletal structure and microtubule-based transport in the PD SN. Some groups were downregulated, such as "Microtubule-based movement" (GO:0007018), whereas we observed an increased average expression of transcripts belonging to "Cytoskeletal protein binding" (GO:0008092). Possibly related to this, the gene groups "Axon guidance" (hsa04360) and "Growth cone" (GO:0030426) were also changed in the PD SN.

Other gene group changes in PD

A transcriptional upregulation (average expression increase of ~10% over control levels) in the PD SN was found for extracellular matrix protein groups such as "Collagen binding" (GO:0005518) and "ECM-receptor interaction" (hsa04512). In the putamen, a similar increase was found for the group "Extracellular matrix structural constituent" (GO:0005201). Finally, we report expression changes in the gene groups "Parkinson's disease" (hsa05020), "Alzheimer's disease" (hsa05010) and "Neurodegenerative Disorders" (hsa01510) in the SN of PD patients.

Cell density measurements

The most typical and striking neuropathological feature of PD is the loss of neuromelanin-positive neurons from the SN. It is estimated that around 80% of the DAergic neurons in the SN are lost in the end stages of PD (Sulzer 2007). We and others found that DAergic neurons that are still present in end-stage PD tend to appear in clusters (Damier *et al.* 1999). We performed cell countings in order to estimate neuronal densities in the relatively spared parts of the PD SN, and in the control SN, on tissue sections of contralateral SN of the 7 PD subjects and 8 controls used in the qPCR and microarray experiments. We distinguished large neuromelanin-positive neuronal profiles and large neuromelanin-negative neuronal profiles. The number of small neuromelanin-negative structures was negligible. We observed a significant decrease of 51% in neuromelanin-positive profiles in the PD SN (Mann-Whitney U test, $p=0.015$) relative to control. Surprisingly, we measured

Table 4 - Gene groups identified by functional class scoring as significantly different (FDR-corrected p-value < 0.05) between PD and control, based on the microarray data. ClassSize: the number of genes with a particular GO or KEGG annotation on the array. Fold change: the mean fold change of all group members, as fraction of control levels. SN: substantia nigra. PUT: putamen.

Identifier	Description	p-value	classSize	Fold Change	Brain Area
Synaptic Transmission					
hsa04540	Gap junction	0.000	71	0.92	SN
GO:0019717	synaptosome	0.000	17	0.66	SN
GO:0007264	small GTPase mediated signal transduction	0.000	149	0.94	SN
GO:0045211	postsynaptic membrane	0.001	60	0.83	SN
GO:0007268	synaptic transmission	0.002	146	0.92	SN
GO:0005216	ion channel activity	0.002	96	0.94	SN
GO:0045202	synapse	0.002	34	0.80	SN
hsa04530	Tight junction	0.003	75	1.00	SN
GO:0008021	synaptic vesicle	0.015	33	0.79	SN
hsa04540	Gap junction	0.018	70	0.99	PUT
GO:0006887	exocytosis	0.025	31	0.81	SN
GO:0001518	voltage-gated sodium channel complex	0.025	9	0.85	SN
GO:0015075	ion transporter activity	0.029	9	1.01	SN
GO:0004890	GABA-A receptor activity	0.030	16	0.76	SN
GO:0009966	regulation of signal transduction	0.030	12	0.87	SN
GO:0005248	voltage-gated sodium channel activity	0.030	12	0.95	SN
GO:0030426	growth cone	0.032	8	0.73	SN
GO:0006814	sodium ion transport	0.032	70	0.92	SN
GO:0008503	benzodiazepine receptor activity	0.033	6	0.59	SN
GO:0005234	glutamate-gated ion channel activity	0.034	22	0.89	SN
GO:0030424	axon	0.035	8	0.76	SN
GO:0006904	vesicle docking during exocytosis	0.037	16	0.84	SN
GO:0030594	neurotransmitter receptor activity	0.039	19	0.77	SN
GO:0008308	voltage-gated ion-selective channel activity	0.044	7	0.73	SN

GO:0006836	neurotransmitter transport	0.044	28	0.80	SN
hsa04070	Phosphatidylinositol signaling system	0.046	71	0.95	SN
GO:0017137	Rab interactor activity	0.049	15	0.86	SN
Energy Synthesis					
hsa00193	ATP synthesis	0.000	26	0.70	SN
hsa00190	Oxidative phosphorylation	0.000	79	0.75	SN
GO:0046961	hydrogen-transporting ATPase activity, rotational mechanism	0.000	30	0.74	SN
GO:0046933	hydrogen-transporting ATP synthase activity, rotational mechanism	0.000	29	0.75	SN
GO:0015986	ATP synthesis coupled proton transport	0.000	31	0.75	SN
GO:0016469	proton-transporting two-sector ATPase complex	0.000	29	0.75	SN
hsa00190	Oxidative phosphorylation	0.000	79	0.91	PUT
GO:0015992	proton transport	0.001	37	0.79	SN
GO:0003954	NADH dehydrogenase activity	0.004	30	0.79	SN
GO:0008137	NADH dehydrogenase (ubiquinone) activity	0.004	30	0.79	SN
GO:0005743	mitochondrial inner membrane	0.004	58	0.86	SN
GO:0005753	proton-transporting ATP synthase complex (sensu Eukaryota)	0.009	7	0.68	SN
GO:0019866	inner membrane	0.016	27	0.80	SN
GO:0042623	ATPase activity, coupled	0.025	16	0.90	SN
GO:0004129	cytochrome-c oxidase activity	0.030	17	0.79	SN
hsa00193	ATP synthesis	0.034	26	0.90	PUT
GO:0006120	mitochondrial electron transport, NADH to ubiquinone	0.049	19	0.81	SN
Cytoskeleton					
GO:0005874	microtubule	0.000	117	0.91	SN
hsa04810	Regulation of actin cytoskeleton	0.003	144	1.02	SN
GO:0007018	microtubule-based movement	0.018	52	0.86	SN
GO:0003774	motor activity	0.030	64	0.99	SN
GO:0000776	kinetochore	0.032	15	0.79	SN
GO:0008092	cytoskeletal protein binding	0.032	35	1.08	SN
GO:0005875	microtubule associated complex	0.041	46	0.93	SN
GO:0000146	microfilament motor activity	0.044	11	1.03	SN
GO:0030048	actin filament-based movement	0.049	13	0.96	SN

Identifier	Description	p-value	classSize	Fold Change	Brain Area
Metabolism					
GO:0006096	glycolysis	0.000	35	0.82	SN
hsa00710	Carbon fixation	0.009	18	0.74	SN
hsa00020	Citrate cycle (TCA cycle)	0.009	14	0.90	SN
hsa00260	Glycine, serine and threonine metabolism	0.011	33	1.05	SN
hsa00564	Glycerophospholipid metabolism	0.015	56	0.95	SN
hsa00740	Riboflavin metabolism	0.018	11	0.88	SN
hsa00330	Arginine and proline metabolism	0.023	40	1.01	PUT
hsa00220	Urea cycle and metabolism of amino groups	0.034	15	1.01	PUT
hsa00620	Pyruvate metabolism	0.038	35	0.86	SN
hsa00720	Reductive carboxylate cycle (CO2 fixation)	0.038	7	0.89	SN
hsa00910	Nitrogen metabolism	0.041	18	0.99	PUT
hsa00340	Histidine metabolism	0.042	35	0.94	SN
hsa00480	Glutathione metabolism	0.042	18	0.97	SN
hsa00410	beta-Alanine metabolism	0.043	20	0.98	SN
hsa00650	Butanoate metabolism	0.046	39	0.96	SN
hsa00271	Methionine metabolism	0.046	14	1.02	SN
hsa00251	Glutamate metabolism	0.048	24	0.91	SN
Extracellular Matrix					
hsa04512	ECM-receptor interaction	0.001	59	1.19	SN
hsa04510	Focal adhesion	0.003	143	1.09	SN
GO:0005518	collagen binding	0.006	11	1.16	SN
hsa04514	Cell adhesion molecules (CAMs)	0.012	84	1.10	SN
hsa04510	Focal adhesion	0.018	137	1.01	PUT
GO:0007160	cell-matrix adhesion	0.018	48	1.12	SN
GO:0005201	extracellular matrix structural constituent	0.022	52	1.07	PUT
Neurodegeneration					
hsa05010	Alzheimer's disease	0.009	15	0.93	SN
hsa01510	Neurodegenerative Disorders	0.010	26	0.89	SN
hsa05020	Parkinson's disease	0.019	14	0.77	SN

hsa05040	Huntington's disease	0.046	18	1.06	SN
Ubiquitin-proteasome system					
hsa03050	Proteasome	0.000	20	0.73	SN
GO:0051082	unfolded protein binding	0.006	114	0.90	SN
GO:0005839	proteasome core complex (sensu Eukaryota)	0.015	13	0.84	SN
GO:0005838	proteasome regulatory particle (sensu Eukaryota)	0.032	7	0.78	SN
GO:0006511	ubiquitin-dependent protein catabolism	0.039	98	0.96	SN
Other					
GO:0005829	cytosol	0.000	134	0.89	SN
GO:0043234	protein complex	0.000	30	0.74	SN
GO:0007417	central nervous system development	0.000	68	0.95	SN
GO:0005516	calmodulin binding	0.000	110	1.00	SN
GO:0003924	GTPase activity	0.000	124	0.89	SN
hsa04020	Calcium signaling pathway	0.001	129	0.97	SN
hsa05110	Cholera - Infection	0.002	35	0.85	SN
GO:0007517	muscle development	0.002	96	1.05	SN
GO:0004618	phosphoglycerate kinase activity	0.002	6	0.89	SN
GO:0051301	cell division	0.006	115	1.01	SN
GO:0005386	carrier activity	0.007	9	0.84	SN
GO:0004721	phosphoprotein phosphatase activity	0.009	37	0.99	SN
GO:0004298	threonine endopeptidase activity	0.009	14	0.82	SN
GO:0030145	manganese ion binding	0.009	84	0.99	SN
GO:0045786	negative regulation of cell cycle	0.016	65	1.07	SN
GO:0004252	serine-type endopeptidase activity	0.016	12	1.00	SN
GO:0051258	protein polymerization	0.017	16	0.68	SN
hsa04110	Cell cycle	0.018	82	1.01	SN
GO:0004553	hydrolase activity, hydrolyzing O-glycosyl compounds	0.025	8	0.72	SN
GO:0030529	ribonucleoprotein complex	0.025	64	1.02	SN
GO:0007420	brain development	0.027	31	0.96	SN
GO:0016310	phosphorylation	0.030	10	0.84	SN
GO:0003705	RNA polymerase II transcription factor activity, enhancer binding	0.033	11	1.05	PUT
hsa00280	Valine, leucine and isoleucine degradation	0.034	36	0.99	PUT

Identifier	Description	p-value	classSize	Fold Change	Brain Area
GO:0008020	G-protein coupled photoreceptor activity	0.044	6	0.80	SN
GO:0006821	chloride transport	0.044	32	0.93	SN
GO:0004176	ATP-dependent peptidase activity	0.045	7	0.71	SN
hsa00770	Pantothenate and CoA biosynthesis	0.046	17	0.95	SN
hsa00290	Valine, leucine and isoleucine biosynthesis	0.046	9	0.90	SN
hsa04910	Insulin signaling pathway	0.046	97	0.94	SN
hsa00960	Alkaloid biosynthesis II	0.050	14	1.06	SN

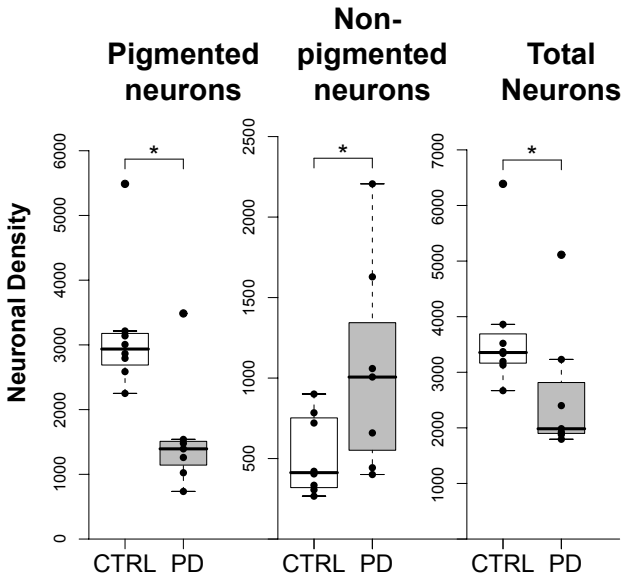

*Figure 4 - Estimated neuronal densities relative to the average total densities of control, of large neurons in the relatively spared parts of the PD SN that were used in the present study (n=7), and control SN (n=8). A distinction was made between neuromelanin-positive (pigmented) and neuromelanin-negative (non-pigmented) neurons. Note the relative increase in neuromelanin-negative neurons in PD, and the rather mild decrease in total neuronal density in the for the present study sampled areas of the PD SN. * Mann-Whitney U test p-value < 0.05.*

a relative increase of 104% in PD neuromelanin-negative neurons (Mann-Whitney U test, p=0.049). Overall, the relative total neuronal density was estimated to be decreased by 29% in PD as compared to control (Mann-Whitney U test, p=0.037) (Figure 4).

Discussion

To our knowledge, this is the first study to examine global changes in gene expression in relatively spared areas of the PD SN. Cell counting experiment enabled us to relate the microarray data to the degree of neuronal loss. We observed a moderate decrease in total neuronal density of 29% in the sampled part of the PD SN. Subpopulations of the SN are differentially vulnerable in PD. For example, the lateral and dorsal parts of the SN show a 21% and 57% loss of DAergic neurons respectively, whereas the pars compacta is more severely affected, with a decrease of 86% (Damier *et al.* 1999). Although differentially affected, all areas of the PD SN do exhibit cell loss during disease progression. Thus, gene expression measurements from less affected parts of the PD SN might provide insight in the molecular biological

processes leading to neuronal degeneration in PD. Transcriptional alterations that occur before massive neuronal demise has taken place might represent early, causative molecular changes instead of events that are the consequence of the disease process. The observed 51% decrease in neuromelanin-positive neurons in the SN in combination with a 104% increase in neuromelanin-negative neurons shows that many neurons are still present but are in the process of losing their neuromelanin content, which also explains the presence of extracellular neuromelanin granules in the PD neuropil. The observed decrease (29%) in total neuronal density in the PD SN is a confounding factor for the interpretation of gene expression data. The downregulation of a neuron-specific transcript by 29% might be explained fully by the loss of neurons. It is thus noteworthy that all of the 240 genes significantly downregulated in the PD SN are reduced by more than 29%, and 149 genes by more than 50%. Moreover, the downregulation of the neuron-specific transcript NURR1 by 82%, when correcting for the los of neurons, still translates to a 58% reduction per neuron. Therefore, the observed changes in gene expression are possibly relevant for PD pathogenesis and cannot simply be explained by a loss of DAergic neurons. In apparent contrast, the average downregulation for the most significantly altered gene groups in our study usually does not exceed 29%. However, the mean expression of each gene group is calculated by averaging the expression values for all group members. Therefore, transcripts that are not altered in PD contribute to the gene group expression value, effectively underestimating the "true" transcriptional downregulation for the changed group members. For example, NURR1 is decreased by 82%, whereas the total decrease of the gene group "Neurodegenerative disorders" (hsa01510) is 18%. We cannot exclude the possibility that changes in the expression of some genes in particular gene groups are due to the loss of DAergic neurons, and do not represent PD-specific transcriptional alterations in DAergic neurons. However, the observation of significant changes in multiple members of a specific gene group provides strong evidence for alterations in the processes in which these genes function.

Whole-tissue expression studies possibly provide insights into disease mechanisms that would have been missed in a study on DAergic neurons alone. For example, in PD animal models, reactive astrocytes have an essential role in the trophic support of DAergic neurons, by secreting neurotrophic factors such as GDNF and NGF(Nakagawa and Schwartz 2004; Nakagawa *et al.* 2005), and metabolizing potentially harmful extracellular DA by expression of MAOB and COMT. Interestingly, we observed a 50% increase in COMT expression in the PD SN. PD-induced death of DAergic neurons should therefore be regarded as a disease of the entire SN, not only of the neurons.

It must be noted that we cannot exclude the possible confounding influence of DA replacement therapies on the observed transcriptional alterations between PD and control, both on the level of the striatum and the SN. This is, however, a limitation that is likely to be present in all studies comparing gene and protein expression between the PD and control brain.

Gene group changes in the PD SN

We detected significant alterations in several gene groups, notably involved in oxidative phosphorylation, synaptic transmission, microtubular dynamics and microtubular-based transport, and the UPS. The reduced levels of transcripts involved in synaptic transmission and ATP synthesis, combined with lowered expression levels of individual genes involved in DA transmission such as VMAT2 and TH, all point to a functionally compromised tissue. This corroborates the idea that the SN in PD is unable to provide sufficient levels of DA to the striatum. Adding to that, the reduced capacity of targeted protein degradation might underlie the formation of Lewy bodies and Lewy neurites (Hol *et al.* 2005; Olanow and McNaught 2006). Thus, the observed alterations in specific gene groups are consistent with the neuropathological manifestations of PD.

Several of the observed gene group changes are in line with current literature on PD. Mitochondrial dysfunction has long been implicated in PD neuropathology. Two other gene expression studies on the PD SN report reductions in ATP synthesis (Grunblatt *et al.* 2004; Zhang *et al.* 2005). In the prefrontal cortex of PD patients, mitochondrial complex I subunits are oxidatively damaged and functionally impaired (Keeney *et al.* 2006). Together with findings on mitochondrial complex I inhibition by rotenone and MPTP, and mutations in genes linked to oxidative phosphorylation, including DJ-1 and PINK1, there is strong evidence for mitochondrial involvement in PD pathogenesis. Importantly, as we selectively investigated spared parts of the SN, mitochondrial alterations appear to play a role in the relatively early stages of DAergic neurodegeneration.

The severe reductions in synaptic transmission corroborates the microarray studies of Grunblatt et al, and Miller et al (Miller *et al.* 2006), but now in an area of the SN where a significant number of DAergic neurons has survived. This makes it likely that synaptic transmission is decreased in SN neurons that are still present. Also, SNCA, reduced in the PD SN in our study and in a study by Kingsbury et al as determined by in situ hybridization (Kingsbury *et al.* 2004), is thought to play a role in neurotransmission (Larsen *et al.* 2006). It was recently shown that presynaptic aggregates of SNCA cause neurodegeneration in dementia with Lewy bodies (Kramer and Schulz-Schaeffer 2007). One explanation of the observed reduction might be that the surviving neurons in PD express lower levels of SNCA, making them less vulnerable to SNCA-induced neurotoxicity.

Finally, the occurrence of protein aggregates suggests involvement of protein degradation pathways in PD neuropathology. We indeed observed reduced levels of transcripts of the UPS in surviving areas of the SN PD. Earlier studies also have shown alterations in proteasomal function within DAergic neurons in the SN in the endstage of PD (McNaught *et al.* 2003). Duke et al reported on an overall loss of genes encoding for UPS proteins, which was correlated with expression of mitochondrial gene groups (Duke *et al.* 2006). In that and our own study, UCHL1 was found to be significantly decreased. UCHL1 is responsible for converting polyubiquitin chains into monomeric ubiquitin molecules. When UCHL1 levels are reduced,

the available pool of ubiquitin might become too small to meet the demand for UPS-mediated protein degradation. Indeed, reduced UPS activity leads to a familial form of PD, and mice expressing the mutant form of UCHL1 show DAergic neuron loss (Wintermeyer *et al.* 2000; Setsuie *et al.* 2007).

In addition to UCHL1, several of the observed significant single gene changes are in agreement with previous reports. Examples of these genes include GBE1, SYT1, VMAT2, DSCR1L1 and ALDH1A1 (Grunblatt *et al.* 2004; Miller *et al.* 2006; Zhang *et al.* 2005). There are striking similarities between the single gene and gene group alterations found in this study, literature on sporadic and familial end stage PD, and PD animal model systems. These studies have however not specifically targeted the spared parts of the PD SN. We therefore suggest that the observed alterations are already implicated before massive neuronal loss.

It is noteworthy to address the potential regulation of genes known to be involved in familial PD. Apart from the previously mentioned alterations in SCNA and UCHL1 levels, other genes implicated in familial PD could not be shown to be changed in expression: the expression of PARK2 was too low to be reliably measured, DJ-1 is reduced by 30% (but this reduction is not statistically significant), PINK1 is not regulated, and a probe for LRRK2 was not present on the array (data not shown). Based on this experiment, it is difficult to draw definitive conclusions on the involvement of the aforementioned genes in sporadic PD, however other genome-wide expression studies do not report changes in the expression level of these genes either (Grunblatt *et al.* 2004; Miller *et al.* 2006; Zhang *et al.* 2005). This does not imply that the biological pathways in which familial PD genes play a role are not important in sporadic PD. For example, aggregation of aberrant proteins is a key feature of sporadic PD (Hol *et al.* 2005), and UCHL1 and PARK2 are both involved in protein (de)-ubiquitination.

Reduction of neurotrophic support and microtubular alterations in PD

We identified a number of novel single gene changes that are possibly involved in PD pathogenesis. Several genes implicated in neurotrophic support display altered expression. Neurotrophic factors, including BDNF, are reduced in PD, and the role of neurotrophic factors in animal models for PD has been studied extensively (reviewed in Dawbarn and Allen 2003; Kirik *et al.* 2004; Smidt and Burbach 2007). GDNF is an important factor in the development and survival of mesencephalic DAergic neurons, and protects DAergic neurons against MPTP-induced neurotoxic stress (Cheng *et al.* 1998; Kramer *et al.* 2007). We observed reductions in the expression of RIT2, DLK1, NDN, MAGEE1 and DOK6, all involved in neurotrophic signaling (Shi *et al.* 2005; Christophersen *et al.* 2007; Kuwako *et al.* 2005; Kurita *et al.* 2006; Crowder *et al.* 2004; Kramer *et al.* 2007). DLK1 is strongly coupled to both TH expression and neurotrophic signaling. Silencing of DLK1 causes a reduction in TH and VMAT2 expression (Bauer *et al.* 2005), and influences the GDNF pathway by a reduction in Ret expression (Christophersen *et al.* 2007). Furthermore, we ob-

served an increase in transcript levels of PHLPP, an inhibitor of Trk signaling by dephosphorylating Akt (Gao *et al.* 2005). Interestingly, both NDN and MAGEE1 are located in the chromosomal region deleted in Prader-Willi syndrome, and mouse models with a deleted paternal copy of the NDN gene show increased apoptosis in NGF-dependent neurons (Kuwako *et al.* 2005). It might therefore be of interest to study the SN in the aging Prader-Willi population.

Altered expression of TrkB isoforms is further evidence for a decrease in neurotrophic support in the PD SN. TrkB-T1, the truncated isoform of the TrkB receptor, functions as a dominant-negative receptor variant. Interestingly, haploinsufficiency for TrkB and TrkC results in cell loss and accumulation of SNCA in the SN of aged mice (Bohlen und *et al.* 2005), and increased levels of TrkB-T1 expression are known to be associated with neuronal atrophy and death (Dorsey *et al.* 2006; de Wit *et al.* 2006). We observed a shift in the ratio TrkB-T1/TrkB towards more TrkB-T1.

Adding to alterations in neurotrophic support, we also observed transcriptional evidence for changes in the endocytosis of activated receptors. AMPH, DNM3, NECAP-1 and AAK1 are all downregulated, and serve important roles in regulating endocytosis either by interacting with AP-2 (AAK1 and NECAP-1) (Ricotta *et al.* 2002; Ritter *et al.* 2007), by coupling the PSD to the endocytic zone (DNM3) (Lu *et al.* 2007) or by sensing and inducing membrane curvature (AMPH) (Habermann 2004). Interestingly, HIP1R is known to prolong the half-life of growth factor receptors after endocytosis (Hyun *et al.* 2004), and is increased in expression. STS-1, a gene that negatively regulates the endocytosis of receptor tyrosine kinases, is downregulated in PD (Raguz *et al.* 2007). The regulation of STS-1 and HIP1R might thus represent a coping mechanism of neurons suffering from reduced neurotrophic support in this disorder. Another transcriptional alteration potentially affecting neurotrophic signaling, is the severe decrease of DYNC1I1, a component of the dynein motor complex responsible for retrograde transport of activated Trk receptors (Bhattacharyya *et al.* 2002). Altered expression levels of several gene groups involved in microtubule-based transport may point to a more general impairment of axoplasmic transport. These simultaneous alterations in transcripts encoding for proteins involved in neurotrophic support and signaling, all suggest decreased levels of neurotrophic signaling, possibly directly underlying DAergic neuronal degeneration and death in PD.

Alterations in the expression of genes encoding repulsive axon guidance and outgrowth cues in the PD SN

We observed transcriptional evidence for the involvement of axon guidance molecules in SN PD neuropathology. The role of axon guidance cues in the development of the nervous system has been long appreciated, but recently they are also believed to be functionally relevant in the adult nervous system. Axon guidance cues might play a role in synaptic plasticity and neurodegeneration (de Wit and Verhaagen 2003; Mann *et al.* 2007). Increased expression of the chemorepulsive

protein Sema3A or the neurite outgrowth inhibitor Nogo-A promotes denervation in a model for amyotrophic lateral sclerosis (De Winter *et al.* 2006; Jokic *et al.* 2006), and Sema3A is increased in the cerebellum in schizophrenia (Eastwood *et al.* 2003). In the PD SN, we observed a twofold increase in RGMA expression. RGMA is a membrane-bound glycoprotein implicated in axon guidance and neural tube closure during development (Niederkofler *et al.* 2004). After human brain injury RGMA expression is enhanced (Schwab *et al.* 2005). We also observed changes in the expression of SDC2, a member of the heparan sulphate proteoglycan (HSPG) family of extracellular matrix proteins. Some axon guidance molecules bind to HSPGs, and this modulates their repulsive properties. When the axon guidance protein Sema5A binds to the HSPG SDC3, it acts as an axon attractant, and when Sema5A is bound to chondroitin sulphate proteoglycans, it converts to a chemorepulsive protein (Kantor *et al.* 2004). Thus, the decreased expression of SDC2 might suggest a shift to a more repulsive character of the extracellular matrix. This effect is possibly aggravated by the upregulation of Sema5A in a subset of patients (data not shown). An association between Sema5A polymorphisms and PD has been reported, although studies trying to replicate this in different populations were not successful (Maraganore *et al.* 2005; Bialecka *et al.* 2006; Clarimon *et al.* 2006).The 68% decrease of ROBO2 expression also suggests a change in axon guidance cue signaling in PD. ROBO2 is the receptor for Slit2, which regulates the outgrowth of developing midbrain DAergic neurons via the ROBO receptors(Lin *et al.* 2005). Also noteworthy are the reductions in SLITRK5 and NETO2, which are thought to play a role in axon guidance and outgrowth.

Taken together, transcriptional alterations of multiple genes involved in axon guidance and neurite outgrowth suggest an altered and possibly more chemorepulsive environment around DAergic neurons. Indeed, a recent SNP analysis of axon guidance pathways also implicated these pathways in PD (Lesnick *et al.* 2007). Changes in chemorepulsive signaling might contribute to the loss of synaptic contacts between DAergic neurons, ultimately leading to DAergic cell loss.

Expression changes in the caudate nucleus and putamen

We did not observe large alterations in gene expression in the putamen and caudate nucleus, which may result from the very stringent Bonferroni multiple testing correction method applied (to eliminate potential false positives), and/or the DA replacement therapies that all PD patients received during the disease course. We detected several noteworthy changes in gene expression that are apparently not prevented by the DA replacement therapies. Remarkable is the increase of LTF expression in the PD caudate nucleus and SN. LTF is not only involved in iron homeostasis, but also has cell growth and differentiation properties (Ward *et al.* 2005). The neuromelanin in SN DAergic neurons contains high levels of iron. Together with the observation that surviving neurons might lose their neuromelanin, the upregulation of LTF is indicative for increased cytosolic and synaptic iron levels. Indeed, increased iron levels are observed in surviving neurons in the PD SN, and

raise oxidative stress levels in SN DAergic neurons (Oakley *et al.* 2007; Zecca *et al.* 2004). Furthermore, in our study, CYBRD1, mutated in some iron overload disorders (Zaahl *et al.* 2005), is also upregulated in the caudate nucleus. Thus, increased iron loads in the striatum and SN might contribute to PD-associated neurodegeneration.

Complex interactions between multiple insults underlie SN DAergic neurons degeneration

Our microarray data point to the impairment in neurotrophic signaling pathways and retrograde transport in PD pathogenesis and to the involvement of molecules regulating axon guidance and neurite outgrowth. These changes might interact with deleterious processes already recognized to be involved in the etiology of sporadic PD, including mitochondrial dysfunction, reduction of synaptic transmission and impairment of the UPS. Importantly, genes encoding for proteins involved in these processes were also found to be affected in our study. In a recent review, a multiple hit hypothesis for SN DAergic degeneration was proposed, in which neuronal death only occurs after several cellular processes have been compromised (Sulzer 2007).

We hypothesize that complex interactions between altered processes such as loss of neurotrophic support and mitochondrial dysfunction together constitute the unique conditions in which SN DAergic neurons are prone to degenerate in PD. It is important to note that our study does not provide insight in the exact sequence of events ultimately leading to SN DA neuronal demise in PD. We propose the following model. Impairment of several neurotrophic support pathways reduces the viability of DAergic neurons. In conjuction, alterations in expression of axon guidance cues exert a negative influence on the synapses of SN DAergic neurons. As synaptic transmission is dependent on viable synaptic contacts, changes in neurotrophic support and axon guidance cue signaling negatively affect DA transmission to the striatum. The reduction of neurotrophic support is aggravated by the disturbance of microtubule-based transport, which impairs the retrograde transport of activated Trk receptors, necessary for neurotrophic signaling. In parallel, mitochondrial dysfunction leads to lower levels of available ATP. As SN DAergic neurons are metabolically more active than their VTA counterparts (Greene *et al.* 2005), the greater energy demands might make SN DAergic neurons more vulnerable to metabolic insults. Furthermore, as UPS-mediated protein degradation is ATP-dependent, a reduction in oxidative phosphorylation likely negatively affects the cell's capacity to break down proteins, with proteinacious inclusions as a result. The observation that some surviving neurons lose their neuromelanin content, possibly leads to increased iron contents in the SN and, via the nigrostriatal pathway, in the striatum. This increased iron load raises oxidative stress levels. Finally, the severe reduction of VMAT2 levels causes insufficient packaging of DA in DA vesicles, effectively increasing cytosolic DA concentrations, which also induces oxidative stress. Taken together, this model describes a complex interaction between seemingly unrelated, but most likely intimately related intra- and extracellular events, which together lead to selective DAergic vulnerability in PD.

The purpose of this study was to identify genes and gene classes that may be functionally linked to PD neurodegeneration. We have not as yet demonstrated the biological significance of the presented alterations: our observations are predictive of the role of specific molecules and pathways in the process of PD neurodegeneration. Therefore the challenge for the future lies in the translation of the current findings to functional studies in cellular and animal models of PD.

Funding

Royal Dutch Academy of Sciences, Innovation Fund; Solvay Pharmaceuticals.

Acknowledgements

The authors like to thank Anke Essing for technical support, and the Netherlands Brain Bank (Head: Inge Huitinga) for providing excellent human brain material and support. The authors also would like to acknowledge the valuable discussion on the work described in this paper with Pieter Houba and Claudia Thaete (Solvay Pharmaceuticals), Peter Burbach, Marten Smidt and Jeroen Pasterkamp (Rudolf Magnus Institute for Neuroscience, Utrecht), Guus Smit (Vrije Universiteit, Amsterdam) and Asia Korecka and Elly Hol (Netherlands Institute for Neuroscience, Amsterdam).

CHAPTER 4

Intensity-based analysis of dual-color gene expression data as an alternative to ratio-based analysis to enhance reproducibility

Koen Bossers, Bauke Ylstra, Ruud H. Brakenhoff,
Serge J. Smeets, Joost Verhaagen, Mark A. van de Wiel

Submitted

Abstract

Ratio-based analysis is the current standard for the analysis of dual-color microarray data. Indeed, this method provides a powerful means to account for potential technical variations such as differences in background signal, spot size and spot concentration. However, current high density dual-color array platforms are of very high quality, and inter-array variance has become much less pronounced. We therefore raised the question whether it is feasible to use an intensity-based analysis rather than ratio-based analysis of dual-color microarray datasets. Furthermore, we compared performance of both ratio- and intensity-based analyses in terms of reproducibility and sensitivity for differential gene expression.

By analyzing three distinct and technically replicated datasets with either ratio- or intensity-based models, we determined that, when applied to the same dataset, intensity-based analysis of dual-color gene expression experiments yields 1) more reproducible results, and 2) is more sensitive in the detection of differentially expressed genes. These effects were most pronounced in experiments with large biological variation and complex hybridization designs. Furthermore, a power analysis revealed that for direct two-group comparisons above a certain sample size, ratio-based models have higher power, although the difference with intensity-based models is very small.

Intensity-based analysis of dual-color datasets results in more reproducible results and increased sensitivity in the detection of differential gene expression that the analysis of the same dataset with ratio-based analysis. Complex dual-color setups such as interwoven loop designs benefit most from ignoring the array factor.

Introduction

During the last decade, microarray technology has evolved into an indispensable tool for high-throughput gene expression studies. For example, microarrays are now routinely applied to identify differentially expressed genes between paired sample series, classify tumors in prognostic groups, and identify transcriptional alterations during development (Bossers *et al.* 2008; Blalock *et al.* 2004; White *et al.* 1999). Two main types of commercial high density microarray platforms have emerged: one-color oligonucleotide platforms such as Affymetrix and Illumina, and dual-color oligonucleotide platforms such as Agilent and Nimblegen. Dual-color gene expression platforms are very efficient in directly comparing two conditions, by hybridizing the two conditions together on the same array. This greatly reduces the possible confounding effects of inter-array variability and local array effects.

The outcome of comparative microarray experiments is a ranked list of significant genes, possibly involved in the process under investigation. The resulting gene list then serves as a starting point for further investigations, such as constructing new hypotheses, or the in vitro characterization of putatively identified genes. Due to their dimensionality (few observations, many variables), microarray experiments

suffer from high rates of false positive and negative findings (Blalock *et al.* 2005). Thus, the issue of reproducibility is of utmost importance in array experiments.

Analysis of variance (ANOVA) is a widely used tool to analyze and rank genes in both one- and dual-color comparative gene expression experiments (Kerr and Churchill 2001). The ANOVA model incorporates factors such as treatment, tissue and age to estimate the effect of interest per gene. For dual-color arrays specifically, an array effect is included in the model to determine the technical noise introduced by any between-array differences. Accounting for such an array effect in the analysis of dual-color arrays was initially necessary due to the relatively poor quality of array platforms: researchers were confronted with different levels of background signals across arrays, and the process of spotting cDNAs yielded probes with different shapes and probe concentrations. The latest generations of commercial dual-color platforms however use synthesized oligonucleotide probes instead of cDNA probes, and are of much higher and consistent quality and concentration. Subsequently, the variance introduced by the array effect has become much less pronounced (Patterson *et al.* 2006). We recently reported that using the Agilent arrayCGH platform or other CGH array platforms, the separate channels of these dual channel arrays are interchangeable, avoiding redundant hybridizations of the same reference material in every experiment (Buffart *et al.* 2008). We therefore raised the question whether the results obtained by separately analyzing intensities from co-hybridized gene expression array samples are more reproducible than results based on classical ratio-based analysis. As an added benefit, an intensity-based analysis approach allows for pairwise comparison between any samples.

We have performed a set of experiments to determine whether the intensity-based analysis of dual-color arrays is more reproducible than the conventional ratio-based analysis. Two independent datasets were used: a human keratinocyte cell line dataset, and a dataset based on human brain tissue. By selecting these datasets, we were able to study the performance of the ratio- and intensity-based models in two distinct situations: no biological variation (cell line dataset) versus substantial biological variation (brain dataset).

For both the intensity-based and ratio-based analysis, we estimated the reproducibility and sensitivity in the detection of differential gene expression by analyzing technical replicates. Technical replicates, consisting of two non-overlapping sets of microarrays, were used rather than biological replicates, as our focus is on inclusion or exclusion of the array factor, which is a technical factor. Furthermore, we used a model selection algorithm to determine whether either intensity or ratio based analysis was most suitable for each dataset.

Our results indicate that intensity-based analysis outperforms the standard ratio-based analysis of the same dataset. Intensity-based results are more reproducible, and increase the sensitivity of detecting regulated genes. Our results also indicate that differences between ratio- and intensity-based results become smaller in large datasets with simple designs, suggesting that more complex designs such as factorial and loop designs benefit most from our approach.

Methods

Human keratinocyte cell line dataset

The cell line sample set consisted of two immortalized cell lines (cell lines 10 and 19) derived from a single primary keratinocyte culture. The two cell lines were subjected to four different treatments (treatments T1, T2, T3 and T4). After RNA isolation and labeling (labeling performed with Agilent Low RNA Input Fluorescent Linear Amplification Kit, Agilent Technologies), equal amounts (1µg) of Cy3-CTP and Cy5-CTP labeled samples were hybridized to Agilent 4x44K Whole Human Genome arrays (Agilent Technologies, Part Number G4112F), according to the manufacturer's instructions. The hybridization set-up on the 4x44K array was chosen in such a way that for each cell line, both Cy3- and Cy5-labeled samples for all treatments were hybridized on a single slide (containing 4 arrays). The entire experiment was technically replicated. The hybridization setup can be found in Figure 1.

Microarrays were scanned using the Agilent DNA Microarray Scanner (Agilent Technologies, Part Number G2505B), and scans were quantified using the Agilent Feature Extraction software (version 8.5.1). Raw expression data generated by the Feature Extraction software were imported into the R statistical environment using the LIMMA package (Smyth and Speed 2003) in Bioconductor (http://www.bioconductor.org). No background correction was performed, as overall background levels were very low. The intensity distributions within and between arrays were normalized using the quantile scaling algorithm (Bolstad *et al.* 2003) in LIMMA. After normalization, the separate intensity channels were extracted from the ratio measurements. The log2-transformed intensity measurements were used in all following analyses. The microarray data have been deposited in the Gene Express Omnibus (GEO) database (see section Additional Files).

MAQC dataset

Microarray hybridization data were extracted from the Gene Expression Omnibus (GEO accession number GSE5350, file MAQC_AGL_123_60TXTs.zip, series “C”: arrays AGL_3_C1.txt, AGL_3_C2.txt, AGL_3_C3.txt, AGL_3_C4.txt and AGL_3_C5.txt , series “D”: AGL_3_D1.txt, AGL_3_D2.txt, AGL_3_D3.txt, AGL_3_D4.txt and AGL_3_D5.txt). This dataset consists of 10 technical replications of a hybridization of Stratagene Universal Human Reference RNA (Cy3 in series “C”, Cy5 in series “D”) and Ambion Human Brain Reference RNA (Cy3 in series “D”, Cy5 in series “C”) as described in (Patterson *et al.* 2006). Microarray normalization procedures were performed as described for the cell line experiment. Power curves were computed from the non-central t-distribution.

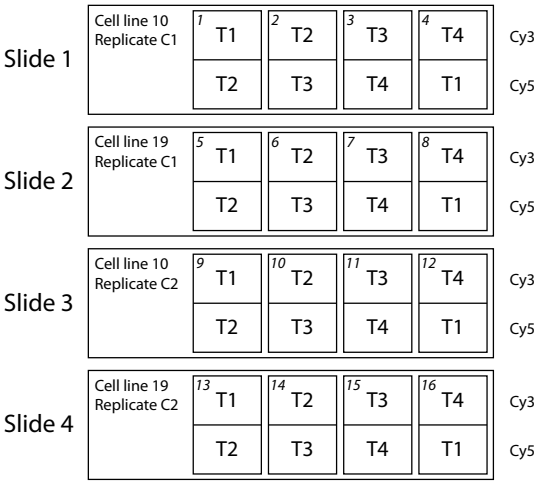

Figure 1 – Hybdridization setup cell line experiment. DN = P53DN mutant, SH= shRNA, MI=MIR372, E6=HPV16 E6. The array numbers are given in the top left corner of each array.

Human brain dataset

Fresh-frozen human brain tissue samples were obtained from the Netherlands Brain Bank, Amsterdam (NBB). Written informed consent for a brain autopsy and the use of the material and clinical information for research purposes was obtained by the NBB from the donor or next of kin. Gray matter was isolated from the prefrontal cortex of 49 individuals (matched for age, sex, postmortem interval and brain pH) with increasing levels of AD-related neuropathology, as defined by the Braak staging for neurofibrillary tangles (Braak and Braak 1991). For each of the 7 Braak stages, 7 individuals were included. Tissue dissection was performed using a cryostat. For each sample, between 20 and 30 sections of 50µm were cut. Grey matter areas were identified by eye and dissected out using pre-chilled scalpels. Tissue yields were typically around 50mg. Total RNA was isolated using a combination of Trizol-based and RNeasy Mini Kit RNA isolation methods. Briefly, samples were homogenized in ice-cold Trizol (Life Technologies, Grand Island, New York, 3ml Trizol per 100mg tissue). After phase separation by addition of chloroform, the aqueous phase was mixed with an equal volume of 70% RNAse-free ethanol. Samples were then applied to an RNeasy Mini column (Qiagen, Valencia, California), and processed according to the RNeasy Mini Protocol for RNA Cleanup. Overall, the isolated RNA was of high integrity (average RNA integrity number of of 8.3, range 6.5-9.6, as determined by Agilent 2100 Bioanalyzer analysis).

After RNA isolation, for each sample, two 500ng aliquots of RNA were linearly amplified and fluorescently labeled with either Cy3-CTP or Cy5-CTP (Perkin Elmer) with the Agilent Low RNA Input Fluorescent Linear Amplification Kit (Agilent Technologies). The most efficient hybridization scheme was calculated with the

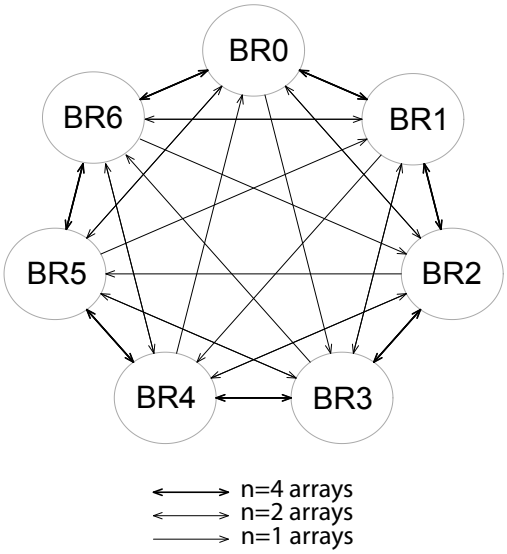

Figure 2 - Hybdridization setup brain experiment. BR = Braak stage.

od function of the SMIDA package (version 0.1) in R. The resulting hybridization setup can be found in Figure 2. Equal amounts (1µg) of Cy3-CTP and Cy5-CTP labeled samples were hybridized to Agilent 44K Whole Human Genome arrays (Part Number G4112A) according to manufacturer's instructions. Microarray scanning, feature extraction and normalization procedures were performed as described for the cell line experiment. The full set of normalized expression values is publicly available at http://www.vumc.nl/braindataset and as supplementary information to this manuscript (see section Additional Files).

Clustering and ANOVA models

Clustering of the intensity channels was performed using complete linkage hierarchical clustering. Only probes for which the average log2-transformed intensity (A, as derived from the separate Cy3 or Cy5 channels) was above A=7 were included. As this procedure removes data from all arrays for a particular probe, the sample sizes are the same for each probe in the final dataset. For the cell-line data, p-values for differential expression between treatments were generated as follows. First, the entire data set was split into two biologically identical parts by simply distinguishing the technical replicates A and B (Figure 1). The split resulted in cell line data sets C1 and C2. Next, two types of ANOVA models were used per array element. Model 1 represents the ratio-based analysis:

$$Y_{ijk} = \mu + \tau_i + \eta_j + \alpha_{k(j)} + \varepsilon_{ijk} \quad (1)$$

Here, μ captures the average gene intensity, τ_i is the treatment specific effect, η_j is the cell line (10 or 19) effect, $\alpha_{k(j)}$ is the array effect, and ε_{ijk} is the error component. Dye effects have not been incorporated, because the design was balanced for dyes and the data were normalized to remove dye-specific bias. Model 2 lacks the factor $\alpha_{k(j)}$ and hence represents the intensity-based model. The treatment effect is the factor of biological interest, to which an F-test was applied to compute p-values. This resulted in four lists of p-values: ratio-based and intensity-based p-values for technical replicate C1, and ratio-based and intensity-based p-values for technical replicate C2.

A similar approach was taken for the human brain data. Each patient was hybridized twice. The resulting set of arrays was split in such a manner that each patient was represented exactly once in both data sets (brain datasets B1 and B2). It is noteworthy that the obtained datasets are indeed technical replicates, but not on the level of the experimental design, as is the case for cell line datasets C1 and C2. The cell line effect η_j was dropped from the model, and the treatment effect τ_i now represented the Braak stage. The F-test was performed on the Braak stage factor. Again, two ANOVA models were used: the ratio model which included the array effect $\alpha_{k(j)}$, and the intensity model without array effect. Consequently, four lists of p-values were generated: ratio-based and intensity-based p-values for dataset B1, and ratio-based and intensity-based p-values for dataset B2.

We did not apply any multiple testing corrections for our purpose, since a criterion like False Discovery Rate (FDR) might distort the comparison between the models somewhat. Also, since both splits contain an equal numbers of samples, sample size 'bias' is absent.

Comparison ratio and intensity data, reproducibility calculations and model selection

For the cell line dataset, direct ratio measurements between co-hybridized sample pairs were compared with in silico reconstructed ratios of the two intensity measurements of the same sample pair, as measured on separate arrays, and against different samples. For example, in dataset C1, the directly measured ratios between samples T1 and T2 on array 1, were compared with the reconstructed ratios between T1 on array 4, and T2 on array 2 (Figure 1). To eliminate possible confounding effects of noise introduced by genes expressed at very low levels, only genes with an average log-transformed intensity levels greater than 7 were used. To compare the overlap between gene rankings based on the ratio and intensity models, genes were ordered by p-value and assigned to bins containing 1,000 genes. The fraction of overlap then was defined as the amount of genes ranked in the same bin by both models, divided by the size of the bin.

Both for the cell line datasets C1 and C2, and the human brain datasets B1 and B2, reproducibility between the replicated datasets was determined as follows. First, the correlation between sets of p-values was calculated using Spearman's rho. Second, to assess the proportion of genes with similar ranks between replicates, genes

were ordered by p-value. For bins of increasing size (10 to 1,000 genes, by increments of 10 genes), the proportion of overlap was defined as the fraction of genes, occurring in both sets. Third, Bayesian information criterion (BIC) model selection was used to score the ratio- and intensity-based linear models for each array feature. Information criterion methods, which aim to determine which set of model parameters the data support best, penalize models with more unknown parameters in order to select a model with a lower generalization error and hence more reproducible results (Hastie *et al.* 2001). The preferred model was defined by the model with the lowest BIC value. BIC calculations were performed using the nlme package in R.

Results

Intensity-based analysis yields comparable results to ratio-based analysis, but is more sensitive in detecting differential gene expression

To determine the feasibility of intensity-based analysis of dual-color arrays, we performed a microarray experiment in which the effects of 4 different treatments (T1, T2, T3 and T4) were investigated using two keratinocyte-derived cell lines by measuring transcript levels on Agilent 4x44K Whole Human Genome arrays. The entire experiment was technically replicated (experiment C1 and C2).

One of the prerequisites of intensity-based analysis of dual-color arrays is that co-hybridized samples do not influence gene expression measurements in the opposite channels. In other words, the intensity distribution of sample X should be independent of the co-hybridized sample. A hierarchical cluster analysis of the individual intensities of all arrays showed that cell line-treatment combinations invariably clustered together (Figure 3). This indeed suggests that intensities do not

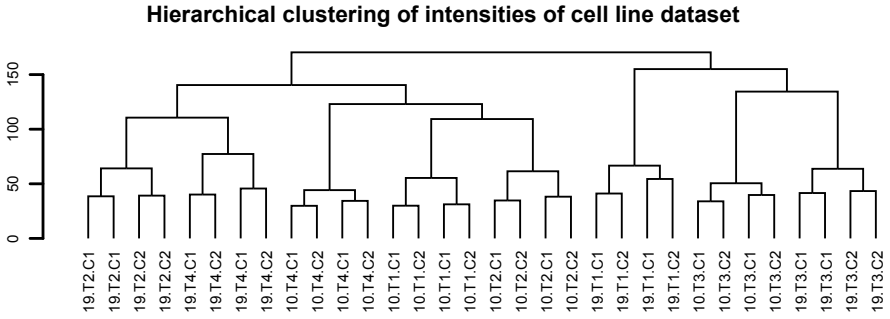

Figure 3 – Intensities of the same sample measured on separate arrays are highly correlated. Hierarchical clustering of log2-transformed single channel intensities of the complete cell line experiment. Only genes with an average intensity A > 7 were used. dentical cell line-treatment combinations always cluster together, regardless of the co-hybridized sample. Sample naming = [cell line].[treatment].[duplicate set]

seem to be influenced by the co-hybridized sample or array used, as the array effect appears to be smaller than the treatment effect.

To further investigate the magnitude of array-specific effects we compared the relative effect sizes of the array and treatment effects as defined by the ANOVA model. This analysis revealed that, apart from the noise component introduced by genes that are not differentially expressed between treatments, the treatment effect is much larger than the array effect (Figure 4A). Consequently, we expected the in silico reconstructed ratios between two samples that were not co-hybridized, to be very similar to the directly measured ratios between those samples. We indeed observed a strong linear correlation between the directly measured ratios, and the in silico reconstructed ratios based on separate hybridizations (average correlation 0.78, range 0.47-0.88, data not shown).

To investigate whether these findings translate to other datasets as well, we analyzed a publicly available dataset in which two commercially available samples were hybridized 10 times on Agilent dual-color microarrays (data obtained from the MAQC dataset; Patterson *et al.* 2006). We selected this experiment specifically, because treatment and array effects are not partially confounded (as is the case in the cell line dataset), and biological variance is absent. We observed a very strong

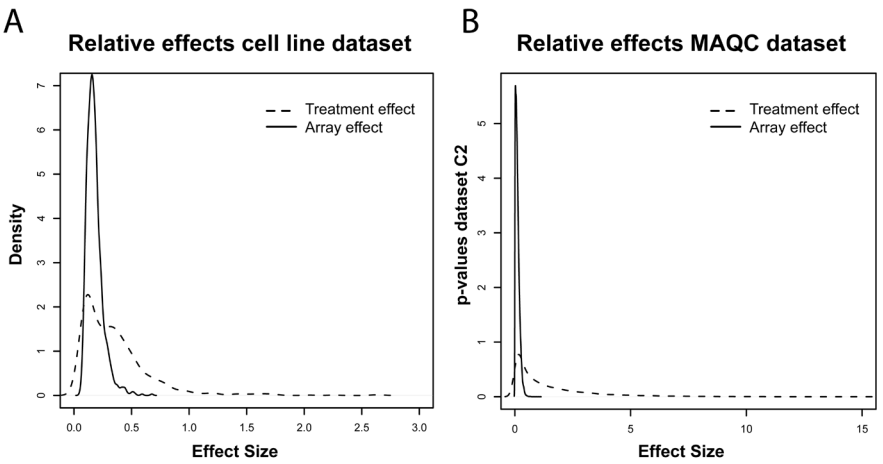

Figure 4 – Comparison between the relative sizes of the array and treatment effects, derived from the ANOVA model. Panel A: cell line dataset. Panel B: MAQC dataset. Dashed line: smoothed histogram over all genes for treatment effect size (absolute value of M-value), averaged over all treatment comparisons. Solid line: smoothed histogram over all genes for average array effect size (absolute value of M-value). Note that both the treatment and array effects still include an unavoidable noise component, hence one expects a partial overlap in the histograms because of genes that do not show a differential effect between treatments. Still there is a clear proportion of genes for which the mean treatment effect is much larger than the array effect size.

linear correlation between real and in silico reconstructed ratios (data not shown), and the ANOVA-derived array effect was very small compared to the treatment effect (Figure 4B).

Ultimately, the reliable detection of differential gene expression between treatments is the main interest of the cell line experiment. We therefore, for the cell line dataset, compared the ranking of genes by p-values generated with two different ANOVA models: one including the array effect (the ratio analysis), and one without the array effect (the intensity analysis). We observed a substantial overlap of 64% (replicate dataset C1) and 66% (replicate dataset C2) between the ratio- and intensity-based lists of the 1,000 most significant genes, suggesting that the intensity-based model yields similar results as the ratio-based model (Figure 5). Furthermore, when using the p-value of the 1,000th most significant gene in the ratio dataset as a cutoff for the intensity dataset, 89% (dataset C1) and 92% (dataset C2) of the 1,000 genes selected by the ratio model were also present in the set of intensity-selected genes. Interestingly, the p-values generated by the intensity model are smaller than those generated by the ratio model, indicating that the intensity model is more sensitive in detecting differential gene expression.

Intensity-based results reproduce better than ratio-based results

The detection of regulated genes should be reproducible; between two technically replicated experiments, one expects to find highly similar sets of differentially expressed genes. To assess the reproducibility of the ratio and intensity models, we separately calculated p-values for both technical replicate datasets C1 and C2 of the cell line experiment. We observed a strong correlation (r=0.75) between p-values generated by the ratio model for the two datasets (Figure 6A). However, the correlation between the p-values generated by the intensity model was even more pronounced (r=0.82, Figure 6B). Next, we compared, for increasing numbers of genes, the overlap between the highest ranked genes within the replicate datasets, based on p-values generated either by the ratio- or intensity based ANOVA models (Figure 6C). Regardless of the size of the top-ranked gene lists (n=10-1,000, increments of 10), the intensity model outperforms the ratio model: more genes are reproduced by the intensity model.

The results from the p-value rank-based reproducibility experiments suggest that it is preferable to exclude the array factor in the linear model. To provide further evidence that the intensity model is indeed superior to the ratio model, we applied the Bayesian information criterion (BIC) for model selection on the ratio- and intensity-based ANOVA models (Schwarz 1978). This test does not directly compare the outcomes of the intensity- and ratio-based analysis, but rather determines which of the two analyses is most suitable to analyze the data. A BIC calculation between the ratio and intensity models was performed for each gene. Indeed, for 94.5% of the genes, the intensity model is favorable over the ratio model, as determined by lower BIC values. For 5.5% of the genes, the inclusion of an array effect in the linear model resulted in lower BIC values (Table 1).

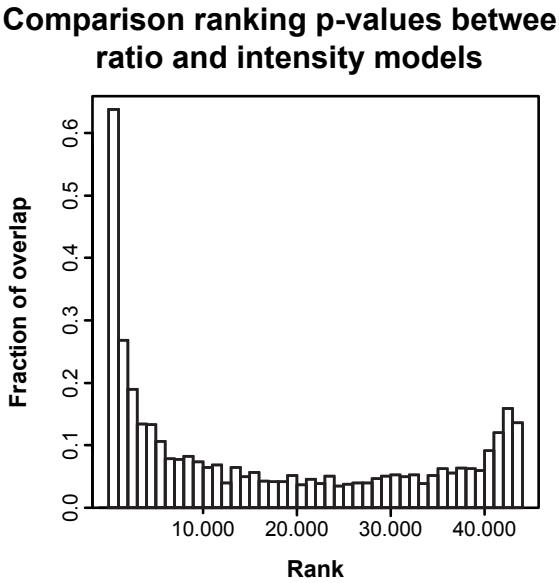

Figure 5 – Ratio- and intensity-based analysis results in similar sets of differentially expressed genes. For the cell line dataset C1, p-values generated by the ratio and intensity ANOVA models were ranked from low to high, and assigned to bins containing 1000 genes. The fraction of overlap represents the proportion of genes occurring in both sets.

Analysis of an independent dataset confirms the gain in reproducibility and sensitivity when using intensity-based models

The cell line experiments demonstrated that intensity-based analysis of dual-color data provide more reproducible results, and is more sensitive in the detection of differentially expressed genes. It is however unknown how these results translate to other types of experiments, consisting of different sample types and experimental setups. We therefore analyzed a separate dataset, consisting of 49 human prefrontal cortex samples, divided over 7 equally sized groups. Samples were obtained from different human subjects, thus the biological variance in this dataset is expected to be large (no biological variation is present in the cell line dataset). Consequently, samples were not pooled, but hybridized individually. As each biological sample was hybridized two times, we expected the distribution of intensities from the two separate hybridizations to be very similar. Indeed, as previously observed in the cell line experiments, an unsupervised hierarchical clustering of all single channels showed that the two intensity measurements of the same biological sample clustered together (Figure 7).

The human brain experiment was not designed with full technical replication in mind. However, as we performed duplicate measurements for each sample, it was possible to divide the dataset into 2 identical biological datasets B1 and B2. To assess

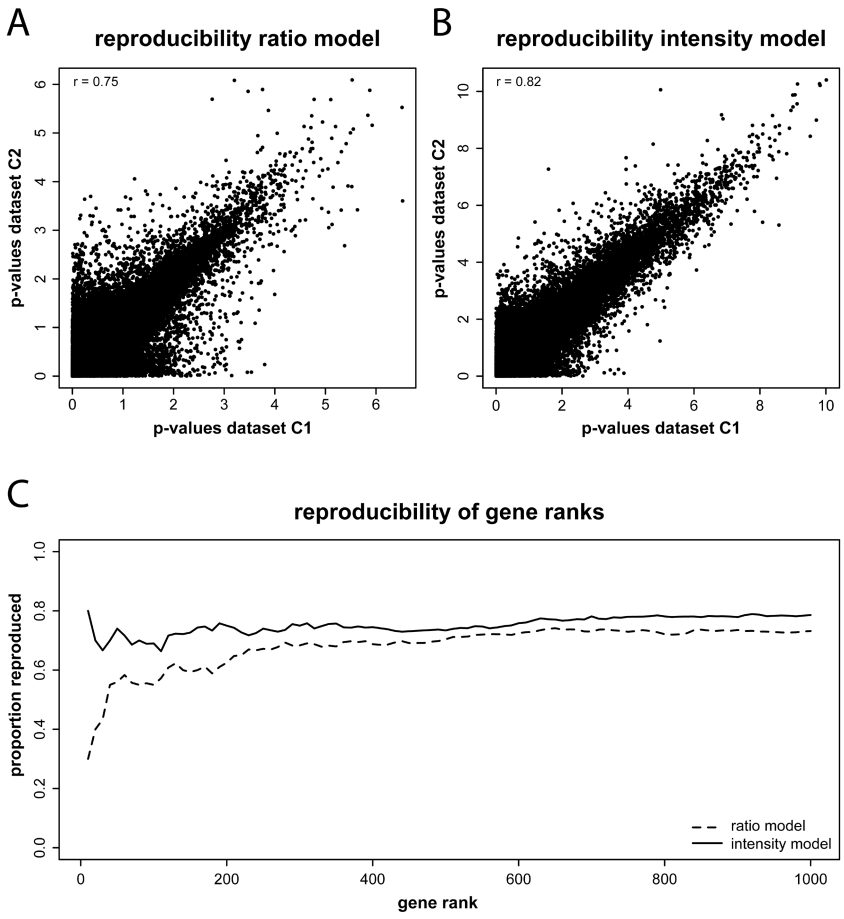

Figure 6 – Intensity models provide more reproducible results than ratio models.
A, B) Comparison between the reproducibility of p-values between technically duplicated experiments, generated by the ratio model (A) and the intensity model (B). Note the higher correlation for the intensity model. p-values are given as –log10(p-value): higher p-values are more significant. C) proportion of genes reproduced by either the ratio on intensity model, for sets of equally ranked genes between the replicate datasets C1 and C2.

the reproducibility between these two replicate datasets, we again compared the p-values generated both by the ratio and the intensity models. We found a surprising lack of correlation (r=0.05) for p-values based on the ratio model between replicates (Figure 8A). The p-values generated by the intensity model however showed a far better correlation (r=0.46, Figure 8B). Indeed, when determining, for increasing numbers of genes (10-1,000 genes, increments of 10), the overlap between the highest ranked genes based on the p-values of the replicate measurements of either

	Ratio	Intensity	Total
Cell line dataset			
Genes	2382	40976	43358
Percentage	5.49%	94.51%	100.00%
Brain dataset			
Genes	4	39413	39417
Percentage	0.01%	99.99%	100.00%

Table 1 – Results of the per-gene BIC model selection for both the cell line and human brain datasets. The column Ratio represents the number or percentage of genes with lower BIC values as opposed to the intensity model. The Intensity column represents the number or percentage of genes with lower BIC values as opposed to the ratio model.

the ratio- or intensity based ANOVA models, we observed a substantial proportion of reproduced genes in the intensity model. Almost no genes were reproduced between the two ratio-based analyses (Figure 8C). Not surprisingly, model selection according to the BIC showed that for 99.99% of the genes, the intensity model outperforms the ratio model. For only 4 genes, the array component was large enough to justify incorporation in the ANOVA model (Table 1). Thus, also in this second experimental dataset, there is clear evidence that the intensity model is to be preferred over the ratio model.

As the brain dataset is based on human subjects, the biological variation is large, which is reflected in overall less significant p-values than the cell line dataset. Consequently, replication on the p-value level is less pronounced than for the cell line dataset. We therefore also analyzed replication in the human brain dataset on the treatment effect level. For the two replicate datasets, the size of the treatment effect between different pairwise sample group comparisons (positioned at different distances in the loop design) was estimated using ANOVA models with and without the array factor (Figure 9). In all comparisons, the intensity-based analysis resulted in better correlations between M-values from the two replicate datasets.

A power perspective on intensity versus ratio-based models

In both the cell line and human brain datasets, the factors treatment and array are partially confounded (since one cannot assign every treatment to each array). In the MAQC dataset, which consists of 10 technical replications of two commercially available RNA samples, these factors are not confounded. A BIC analysis revealed that the model without array effect is preferable for 71% of the genes in the MAQC dataset. Thus, even though dropping the array effect is beneficial for roughly 2 out of every 3 genes, this percentage is lower than in the other two data sets. This is however not unexpected: BIC includes a penalty which is proportional to the sam-

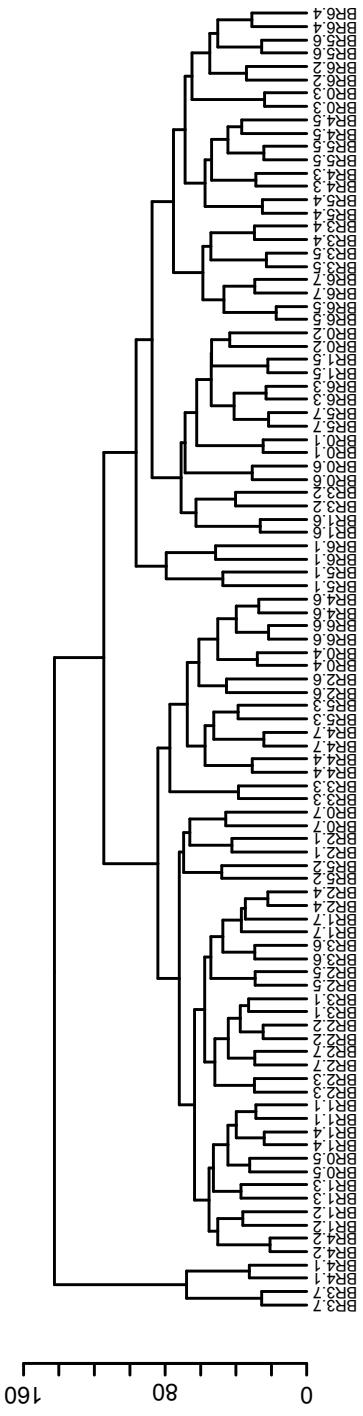

Figure 7 – Hierarchical clustering of log2-transformed single channel intensities of the human brain experiment. Only genes with an average intensity A > 7 were used. Note that, for all 49 individuals, the two replicate measurements cluster together.

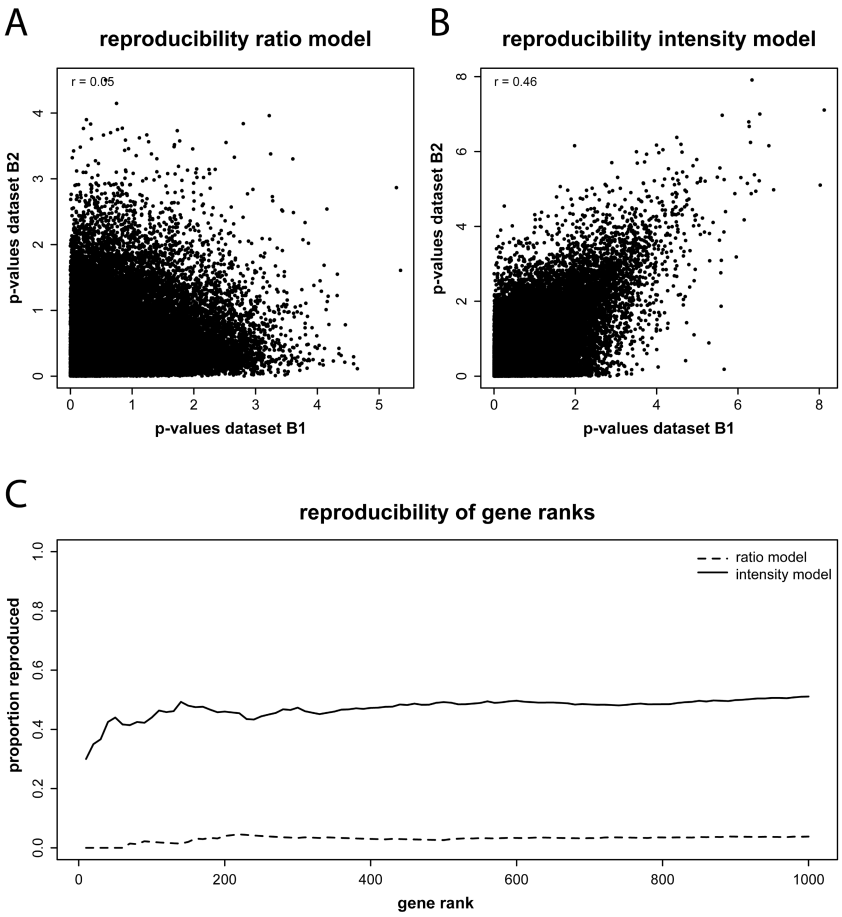

Figure 8 – Comparison between ratio and intensity model-based reproducibility in the brain dataset. A, B) Comparison between the reproducibility of p-values between the split brain datasets B1 and B2, generated by the ratio model (A) and the intensity model (B). Note the absence of correlation between p-values calculated with the ratio model. p-values are given as –log10(p-value): higher p-values are more significant. C) proportion of genes reproduced in sets of equally ranked genes between the replicate datasets.

ple size (number of arrays) for the model with array effect while constant for the other model, and the sample size of the MAQC dataset is smaller than those of the other two data sets. The simple repeated measurements design of the MAQC data set allowed us to study the trade-off between less degrees of freedom and variance reduction caused by inclusion of the array effect from a power perspective. Figure 10A-C shows the power curves for probes A_32_P215304, A_23_P201338 and A_32_P211558, assuming that the estimated treatment effect sizes are real (the

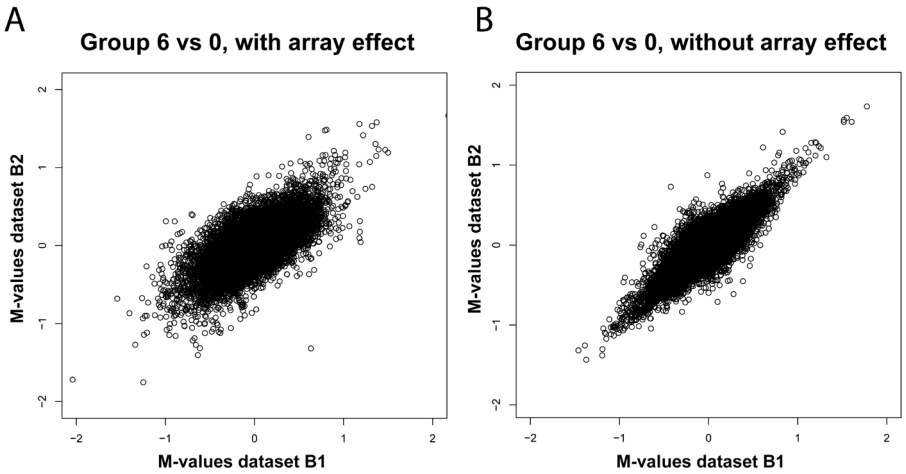

Figure 9 – Reproducibility of ANOVA-derived treatment effects between group 0 and group 6 in replicate brain datasets B1 and B2. Panel A: reproducibility of treatment effects derived from the ratio model. Panel B: reproducibility of treatment effects derived from the intensity model. Note the enhanced reproducibility when using the intensity-based ANOVA model.

treatment effect sizes are the same for both the ratio and intensity models). While one analysis may dominate the other for all sample sizes (Figure 8A and 8B), we observe the aforementioned trade-off from the crossing curves in Figure 8C. In all cases the power curve for the analysis including the array effect is steeper, confirming our expectations that when sample size increases, the loss of degrees of freedom is less harmful. We also considered the average power (the expected number of genes declared significant) over the entire MAQC dataset (Figure 8D). The gene set was restricted to those with an estimated treatment effect size larger than 0.25 to emulate a set that contains differential signal. The average power was higher for the model with array effect for total sample size larger or equal to 12 while smaller otherwise. Differences were small, though: a maximum difference of 1% was found. As expected the power curves converge again when the sample size increases. As opposed to the reproducibility results, these power calculations assumed the array effects to be fixed, as implied by the model. While this may be too optimistic, it is good to notice that the aforementioned trade-off is visible from a power perspective.

Discussion

Our results demonstrate that the analysis of dual-color microarray gene expression experiments using intensity-based linear models outperforms the standard ratio-

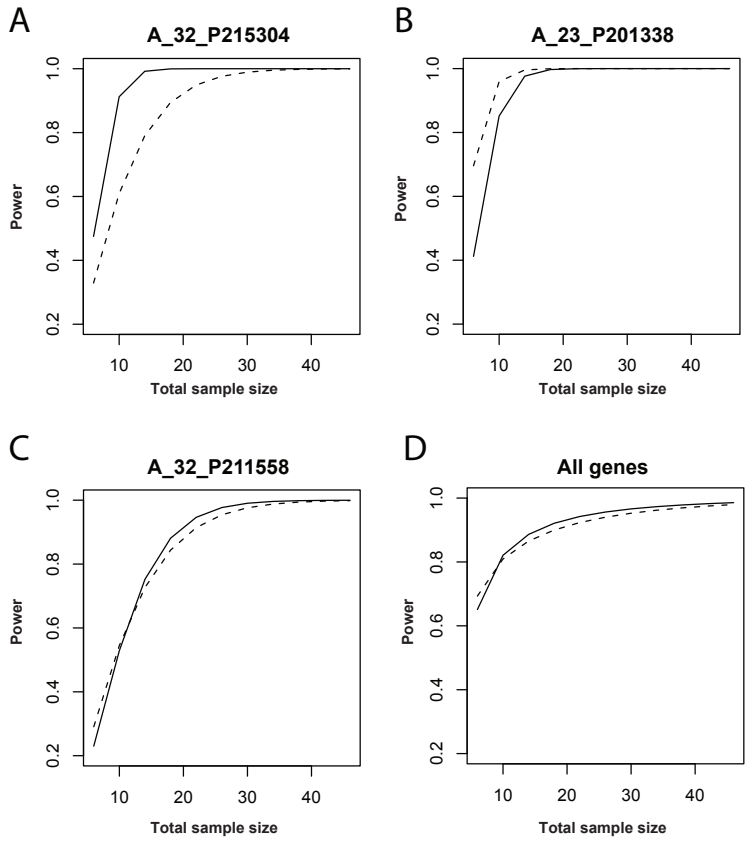

Figure 10 – Power curves for intensity and ratio models for the MAQC dataset. A-C) Power curves for probes A_32_P215304, A_23_P201338 and A_32_P211558 using treatment effect sizes equal to their estimated values, -0.34, -0.35, -0.50. D) Average power for all probes in the MAQC dataset. Only probes with an estimated effect size larger than 0.25 were taken into account. Solid line: model including array effect; dashed line: model without array effect.

based analysis. Both reproducibility and sensitivity were enhanced in detecting differential gene expression in two independent datasets.

By analyzing technically replicated experiments we determined the effect of both models on the reproducibility of gene rankings. Our studies show that for both the cell line and brain datasets the intensity-based analysis provides more reproducible gene rankings than the ratio-based analysis of the same dataset. For the cell line dataset, 78% of the 1,000 most significant genes is reproduced between the two duplicate datasets C1 and C2 when using the intensity analysis, whereas only 73% of the genes is reproduced with the ratio analysis (see Figure 4C). For the brain datasets B1 and B2, the difference between ratio- and intensity-based reproducibility is far

more pronounced: only 4% of the top 1,000 genes are reproduced in the ratio analysis, while there is still a substantial overlap of 51% between intensity-based gene rankings (Figure 6C). The underlying reasons behind the apparent discrepancy between the cell line and brain datasets will be addressed later. An independent line of evidence, based on model selection, also indicated that intensity-based models are preferred over ratio-based models for the analysis of dual-color microarray data. When performing Bayesian Information Criterion model selection calculations, we found that for 95% of the transcripts in the cell line experiment, and virtually all transcripts in the human brain experiment, the intensity model was favored over the ratio model. Furthermore, for both the cell line dataset and a publicly available third dataset, a comparison between ANOVA-based array and treatment effect sizes revealed that the treatment effects are much larger.

Combining the gene ranking, relative effect size and model selection results, we argue that simply by selecting the intensity model instead of the ratio model for the analysis of the same set of gene expression measurements, more reproducible results are obtained.

It should be noted that the relative advantage of dropping the array effect depends on the complexity of the design and the sample size (the number of arrays). For the relatively simple MAQC data set BIC selects the model with array effect for 29% of the genes, much more frequently than for both the brain and cell line data sets. The beneficial effect of dropping the array effect from the model seems more pronounced in experiments that employ direct designs to address complex comparisons, such as time series and multifactorial experiments.

Adding to the enhanced reproducibility, intensity-based analysis is more sensitive in the detection of differential gene expression, as derived from more significant p-values. It is important to note that, by selecting the ratio-based p-value of the 1000th most significant gene as a cutoff, almost all of the 1000 genes (89% for dataset C1, 92% for dataset C2) are also significant in the intensity-based analysis using the same cutoff. Interestingly, this analysis also reveals that 3335 genes, not selected by the ratio model, are reproducibly more significant than the 1000th gene in the ratio results. This provides additional evidence for the enhanced sensitivity of the intensity model over the ratio model. Due to the poor reproducibility of the ratio-based results in the brain dataset, such calculations were not meaningful for that dataset.

Enhanced sensitivity due to ignoring the array effect in the linear model

The observation that ratio-derived p-values can be improved by intensity-based models can be attributed to the inclusion of the array effect in the ratio-based linear model. Pairing of data is a powerful concept for removing subject specific bias. In particular, when the quality of the spot printing procedure is not constant (often the case with in-house spotted arrays), it is essential to account for an array effect in the ANOVA model (Wolfinger *et al.* 2001). But there is a price to pay: degrees of

freedom (Hoen *et al.* 2004). The total number of degrees of freedom equals the number of samples. The array effect consumes almost half of the degrees of freedom. However, due to the high quality of commercially available dual-color oligonucleotide microarrays, we and others observed that the ratios of the same sample pair, measured on different arrays, are strongly correlated (Patterson *et al.* 2006), which means that the array effect is likely to be very small. When using a ratio-based model to analyze the data, many degrees of freedom are used to estimate the array effect, explaining only a small proportion of the variability. This ultimately results in less significant p-values, a lower correlation between p-values from the two replicate experiments, and a smaller proportion of reproduced top-ranked genes. Indeed, the results from the model selection experiments clearly indicate that the model without array effect is the preferred model for both datasets. It should be noted that we do not state that the array effect is absent: our analyses in fact show that an array effect is present in modern dual color microarray experiment. Furthermore, the results from the power calculations for the MAQC dataset show that including the array effect can be slightly beneficial for certain sample sizes. However, we conclude from our experiments that for both the brain and cell line datasets, the array effect is too small in comparison to the main factor of interest (treatment) to justify incorporation into the ANOVA model.

A possible argument for the inclusion of the array effect is the potential competition for spot binding between the co-hybridized samples. However, our and other studies suggest that competition is not an issue (Buffart *et al.* 2008; Hoen *et al.* 2004). This can be derived from the strong correlation between the real and in silico reconstructed ratios (average correlation 0.78, range 0.47-0.88, data not shown), and the hierarchical clustering in Figures 1 and 5. Our study was however not conducted to demonstrate that ratios can be reconstructed in silico by using separate intensities. Indeed, this has been demonstrated before (Hoen *et al.* 2004). Our specific aim was to compare the performance of ratio- and intensity-based methods based on the main outcome of comparative gene expression experiments: a list of ranked genes. As this gene ranking provides the basis for further research, it needs to be robust and reproducible. We show here that intensity-based methods provide more reproducible results and is more sensitive in detecting differential gene expression, and thus outperform the standard ratio-based analysis.

Biological variation negatively affects ratio-based, but not intensity-based, replication

As indicated earlier, in the human brain experiment, we observed a striking lack of reproducibility (r=0.05) between p-values generated by the ratio model on the replicate datasets B1 and B2, whereas the intensity-based p-values reproduced quite well (r=0.46). These findings can be attributed to the following. First of all, the overall p-values (both intensity- and ratio-based) are less significant in the human brain experiment than in the cell line experiment, due to the large biological variation between individuals. Second, due to the relatively low level of biological replication,

few degrees of freedom are left for estimating the biological effect. Third, the brain experiment was not designed with splitting the data into two technical replicates in mind. While the two data sets are biologically identical, the samples are paired differently on the arrays between the two replicate datasets. Since this pairing is more or less arbitrary, the results should be robust against this artifact, but this is not necessarily the case for the ratio-based analysis. When the biological variation is large, different sample pairings may result in differences in measured ratios, a phenomenon we observed in the brain dataset (Figure 7 and Figure S4). The intensity-based analysis of brain datasets B1 and B2 does not suffer from these drawbacks: no ratios are calculated, and more degrees of freedom are left for estimating the biological effect of interest, resulting in a substantial proportion of reproducible findings (51% of the 1,000 most significant genes), and a relatively high correlation between p-values (r=0.46). In a setting with many biological replicates per level (e.g. comparison of two large groups) the differences in correlation between the ratio-based and intensity-based analysis are likely to be smaller.

Our studies indicate that the reliability of gene rankings obtained from dual-color microarray experiments can be improved by using intensity-based models. An added benefit of the intensity-based analysis is that intensity models do not suffer from the drawbacks of ratio models in the analysis of complex direct dual-color experiments. Designs such as the interwoven loop design address the increased complexity of microarray experiments, which have progressed from "simple" two-group comparisons to multifactorial or time-course experiments. The aforementioned direct designs are efficient, but often bias certain comparisons over others and lack the possibility to extend the experiment by adding more groups or samples. There are no such limitations when analyzing dual-color experiments with intensity-based models (Hoen *et al.* 2004). Finally, the LIMMA software package also uses intensity data from dual-color experiments, but mainly as a solution to compare samples which are unconnected in the hybridization design (Smyth 2005). Here, we provide evidence that it is beneficial to perform an intensity-based analysis for connected designs as well.

Conclusions

In conclusion, our results indicate that intensity-based models are very powerful in the analysis of dual-color gene expression data when these are obtained from a high-quality platform. Most importantly, intensity models yield more reproducible results, and are more sensitive in the detection of differential gene expression than standard ratio-based analysis methods on the same microarray dataset. The gain in reproducibility and sensitivity are most pronounced in complex designs such as the interwoven loop design. We argue that the intensity-based models outperform ratio-based models, and thus are the preferred models for the analysis of dual-color gene expression datasets derived from commercial oligo-based array platforms.

Authors' contributions

KB generated the human brain dataset, conceived of the study, performed statistical analyses, and drafted the manuscript. RHB and SJS generated the human keratinocyte cell line dataset. BY and JV participated in the design of the study and helped to draft the manuscript. MAW conceived of the study, performed statistical analyses and helped to draft the manuscript. All authors read and approved the final manuscript.

Acknowledgements

Funding for the human keratinocyte cell line experiment was provided by the EU Research Sixth Framework programme, project DISMAL, project number LSHC-CT-2005-018991. The human brain experiment received funding from the Royal Dutch Academy of Sciences, Innovation Fund and Solvay Pharmaceuticals.

CHAPTER 5

Gene expression changes in the human prefrontal cortex during the progression of Alzheimer's Disease

Koen Bossers, Gideon Meerhoff, Anke Essing,
Jeroen van Dongen, Pieter Houba, Chris G. Kruse,
Joost Verhaagen, Dick F. Swaab

Submitted

Abstract

Despite extensive research efforts, the molecular biological changes underlying Alzheimer's Disease remain poorly understood. We have therefore performed a systematic search for gene expression changes during the progression of AD, using the Braak staging for neurofibrillary changes as an objective measure AD disease staging. We measured transcript levels in the prefrontal cortex (PFC). In this brain area, neurofibrillary changes only start to appear around Braak stage III, allowing for the possible detection of gene expression changes before, during and after the onset of AD neuropathology.

We detected clusters of tightly co-regulated genes, that represent an early increase in neuronal activity, before the onset of neuropathology in the PFC. Subsequently, when the first plaques and tangles start to appear in the PFC, this initial increase in activity turns into a reduction in neuronal activity, coinciding with the clinical diagnosis of mild cognitive impairment. We hypothesize that this early activation represents a coping mechanism against increased soluble Aβ levels, as we observed several genes involved in APP and Aβ processing in these clusters. Furthermore, we detected clusters of genes with a roughly opposite pattern of expression. We also observed evidence for the interaction of the ApoE gene with the expression levels of the genes involved in these clusters, suggesting an accelerating role for ApoE4 in AD disease progression.

Introduction

Alzheimer's disease (AD) is the most common form of dementia, and its prevalence increases exponentially with age. Neuropathologically, AD is characterized by the presence of extracellular deposits β-amyloid protein (Aβ) in diffuse and neuritic plaques, and neurofibrillary changes (NFC) comprised of intracellular deposits of hyperphosphorylated tau protein in neurofibrillary tangles, dystrophic neurites and neuropil threads (Braak *et al.* 1998). AD disease propagation can be monitored by the presence of tangle-bearing neurons in well-defined brain areas, and is classified this way into 6 Braak stages (Braak I-VI) (Braak and Braak 1991; Braak *et al.* 2006). A Braak stage of 0 means that no NFCs are detected in any part of the brain. Braak stages I and II are characterized by the presence of only a few NFCs in the transentorhinal region of the brain. These stages are not associated with any sign of cognitive decline. Braak stages III and IV, clinically manifested as mild cognitive impairment, are defined by increased NFC pathology in the transentorhinal cortical area, the hippocampus and limbic areas. In these stages, the first NFCs in the prefrontal cortex (PFC) can also be observed. Finally, when NFC-associated neuropathology spreads throughout most parts of the neocortex, Braak stages V and VI are accompanied by the clinical diagnosis of dementia.

In the last two decades, mutations in APP, PSEN1 and PSEN2 have been found to cause autosomal dominant, early onset familial AD (reviewed in Bertram and Tanzi 2005). Interestingly, these genes are all involved in altering normal Aβ levels, which is the main component of extracellular plaques in AD. However, the autosomal dominant variants only account for a small subset of AD cases; the vast majority (> 95%) of AD cases is of sporadic origin. The main risk factor for sporadic AD is age (Yankner *et al.* 2008). Variations in the ApoE gene significantly alter the susceptibility for AD, but are not causal to AD. Carriers of 1 or 2 copies of the ApoE4 allele have a 3 to 5-fold higher risk of developing AD than non-ApoE4 carriers (Mayeux 2006). Despite extensive research efforts in the last few decades, the biological processes that cause sporadic AD remain poorly understood.

In order to elucidate the fundamental molecular mechanisms underlying the progression of AD-associated neuropathology, we have generated genome-wide gene expression profiles from the medial frontal gyrus of 49 clinically well characterized subjects, stratified according to Braak score for NFC pathology. For each Braak stage, 7 patients were included. We selected the prefrontal cortex (PFC), because it is affected relatively late in the AD disease process (Braak and Braak 1991). This makes it possible to investigate potential gene expression alterations before, during and after the onset of AD-associated neuropathological changes. Braak stage profiles were reconstructed from the gene expression data for all transcripts, to monitor transcript alterations over the course of the AD process.

Methods

Subjects

Snap-frozen human medial frontal gyrus brain samples were obtained from the Netherlands Brain Bank, Amsterdam (NBB). Written informed consent for a brain autopsy and the use of the material and clinical information for research purposes was obtained by the NBB from the donor or the next of kin. All individuals were neuropathologically systematically investigated as described earlier (van de Nes *et al.* 1998). For each individual, both full neuropathological reports, including Braak staging for NFC and neuritic plaques (Braak and Braak 1991), and clinical reports were available. For each of the 6 Braak stages for NFC, 7 individuals were included. Furthermore, 7 individuals without any NFC pathology were included as Braak stage 0. No neuropathology other than characteristic for AD or associated with normal aging was observed in any of the individuals. Included patients showed no signs of neuropathological or psychiatric disease, and were not treated with corticosteroids except prednison in two Braak 0 cases. Per Braak stage, the median value of plaques levels (no, few, substantial or many plaques) in the prefrontal cortex was determined, and the number of patients with NFC pathology per Braak stage was assessed (Figure 1).

Samples were matched as closely as possible for sex, age, postmortem interval and pH of the cerebrospinal fluid (CSF), and ApoE genotype (Table 1). It is now

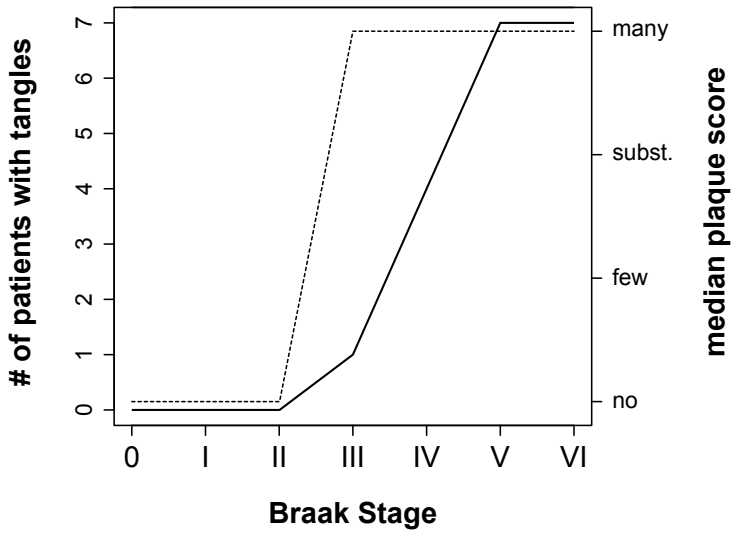

Figure 1 – Neurofibrillary tangle and senile plaque pathology in the prefrontal cortex . Representation of AD-associated neuropathological alterations in the PFC of patients included in this study. The solid line represents the number of patients with tangles (left y-axis). The dotted line represents the median senile plaque pathology (right y-axis).

evident that agonal state is a major confounder in gene expression studies (Tomita *et al.* 2004). CSF pH is a marker for agonal state, therefore only samples with high CSF pH values were included (mean pH 6.6, range 6.2-7.4). Furthermore, as microarray experiments are sensitive to RNA degradation, only samples with a relatively high RNA integrity number (RIN, mean RIN 8.3, range 6.5-9.6) were used (also see section on RNA isolation). Due to the stringent pH and RIN selection criteria, the final set of samples contained small but significant differences between Braak groups for age, post mortem interval and RIN (Kruskal-Wallis test, p-value < 0.05). The minor differences in RNA integrity have, however not influenced our conclusions, as we were able to confirm transcripts levels in our dataset by qPCR analysis, which is insensitive to the amount of RNA degradation observed in our dataset (Fleige and Pfaffl 2006). Furthermore, very few genes correlated with age or post mortem interval, and we observed no overlap between these genes, and the genes selected by the Braak stage ANOVA (data not shown, for description of ANOVA-based gene selection see below).

Tissue dissection and RNA isolation

Tissue dissection was performed using a cryostat. For each sample, between 20 and 30 sections of 50µm were cut. Grey matter areas were identified macroscopically and dissected out using pre-chilled scalpels. Care was taken to keep the tissue frozen at all times. Grey matter was collected in pre-chilled 2ml tubes and immediate-

Braak	Sex	Age	pH	BW	RIN	PMD	ApoE-ε4
0	4M/3F	70.6±9.6	6.7±0.4	1290±170	8.1±1.1	6.8±1.4	3+/4-
1	3M/4F	80.3±5.6	6.6±0.2	1250±140	8.7±1	5.9±0.9	2+/5-
2	3M/4F	76.7±7.8	6.7±0.2	1290±150	9.1±0.1	7.3±1.6	3+/4-
3	3M/4F	85±6.4	6.7±0.4	1230±160	7.7±0.9	6.2±2.6	2+/5-
4	3M/4F	82.3±4.9	6.6±0.2	1150±170	8.2±0.8	5±1.6	3+/4-
5	4M/3F	74.3±6.5	6.5±0.2	1200±120	8.3±0.8	5.4±1.2	4+/3-
6	3M/4F	70.3±7.8	6.8±0.2	1120±150	7.6±0.5	4.8±0.9	4+/3-
	p	*0.674*	*0.767*	*0.016*	*0.084*	*0.007*	

Table 1 – Patient grouping. RIN: RNA Integrity Number. PMD: post mortem delay (hours). P: ANOVA-based p-value between Braak stages. The significant interaction between Braak stage and brain weight is due to brain atrophy associated with AD.

ly put on dry ice. Tissue yields were typically around 50mg. Total RNA was isolated using a combination of Trizol-based and RNeasy Mini Kit RNA isolation methods. Briefly, samples were homogenized in ice-cold Trizol (Life Technologies, Grand Island, New York, 3ml Trizol per 100mg tissue). After phase separation by addition of chloroform, the aqueous phase was transferred to a new RNAse-free 1.5ml tube, and mixed with an equal volume of 70% RNAse-free ethanol. Samples were then applied to an RNeasy Mini column (Qiagen, Valencia, California), and processed according to the RNeasy Mini Protocol for RNA Cleanup (version June 2001, from step 3). RNA yields and purity were determined using a NanoDrop ND-1000 spectrophotometer (NanoDrop Technologies, Wilmington, Delaware). RNA integrity was determined by the RNA Integrity Number (RIN) as measured by the Agilent 2100 bioanalyzer (Agilent Technologies, Palo Alto, California). Overall, the isolated RNA was of high integrity (average RIN of 8.3, range 6.5-9.6, see Table 1).

Sample labeling and microarray hybridization

For microarray analysis, Agilent 44K Whole Human Genome arrays (Agilent Technologies, Part Number G4112A) were used. Sample labeling and microarray hybridization and processing were performed according to manufacturer's instructions. Briefly, for each sample, two aliquots of 500ng of RNA were linearly amplified and fluorescently labeled with either Cy3-CTP or Cy5-CTP (Perkin Elmer) with the Agilent Low RNA Input Fluorescent Linear Amplification Kit (Agilent Technologies, protocol version 2.0, August 2003). Prior to hybridization, equal amounts (1 µg) of Cy3 and Cy5 labeled RNA were hydrolyzed for 30 minutes at 60°C in 1x fragmentation buffer (Agilent Technologies). The fragmented targets were hybridized to a microarray by incubating for 17 hours at 60°C in 1x target solution (Agilent Technologies) in a rotating hybridization chamber. The most efficient hybridization scheme was calculated with the od function of the SMIDA package (version 0.1) in

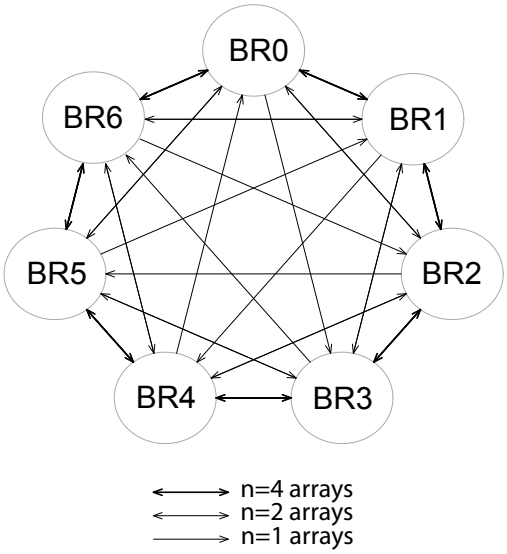

Figure 2 - Hybdridization setup brain experiment. BR = Braak stage.

the R statistical processing environment (http://www.r-project.org). The resulting hybridization scheme can be found in Figure 2. After hybridization, the arrays were washed at RT for 5 minutes in 6xSSPE/0.005% N-Lauroylsarcosine (Sigma-Aldrich, St Louis, Missouri), 1 minute in 0.06xSSPE/0.005% N-Lauroylsarcosine, and 30 seconds in acetonitrile (Sigma-Aldrich) and dried in a nitrogen flow. Microarrays were scanned using an Agilent DNA Microarray Scanner at 5μm resolution and 100% PMT setting. Microarray scans were quantified using Agilent Feature Extraction software (version 8.5.1).

Microarray normalization and single gene analysis

Raw expression data generated by the Feature Extraction software was imported into the R statistical processing environment using the LIMMA package in Bioconductor (http://www.bioconductor.org). All features for which one or more foreground measurements were flagged as saturated or as a non-uniformity outlier by the Feature Extraction software were excluded from further analysis. 39510 features passed these constraints. As overall background levels were very low, no background correction was performed. The intensity distributions within and between arrays were normalized using the quantile algorithm in LIMMA. After normalization, the individual intensities were extracted from the ratio measurements. The log2-transformed intensity measurements per sample were used in all following analyses. In order to check for hybridization artifacts, the individual intensities were clustered using a hierarchical clustering method (data not shown). As each sample was hybridized twice, possible outliers could be identified by an aberrant distance between the duplicate measurements. Four such cases were detected. For these cases, the corresponding hybridization was repeated, and the outlier was re-

moved from further analysis. The mean expression for each feature per sample was calculated by averaging the two measured intensities, to yield the final normalized dataset.

In order to detect genes with a significant interaction with Braak score, a one-way analysis of variance (ANOVA) approach using Braak as grouping factor was applied to the log2-transformed intensity levels for each feature. We chose not to merge data of transcripts encoding for the same gene, as this would preclude the detection of expression differences between transcript variants. The p-value was calculated as the probability of the F statistic accepting the null hypothesis. Raw p-values were corrected for multiple testing using the Benjamini-Hochberg algorithm. Corrected p-values < 0.05 were considered as significant.

Cluster analysis of Braak stage profile data

In order to follow the expression of individual transcripts during the course of AD, the consecutive Braak stages were used as markers of disease progression. For each transcript, the expression value per Braak stage was calculated by averaging the 7 individual intensity measurements. For each transcript, the Braak stage profile was centered on zero by subtracting the mean expression level of all subjects. To enable Gene Ontology overrepresentation analysis (which is a gene-level annotation, see below) on sets of transcripts with similar profiles, all profiles of transcripts belonging to the same gene were averaged. The final Braak stage profile dataset contained profiles associated with the expression of 29813 genes and expressed sequence tags (ESTs) over the Braak stages. A soft clustering approach based on fuzzy c-means using the MFuzz package (version 1.6.0) in Bioconductor was then applied to group transcripts with similar profiles. Soft clustering is robust against noise, and performs better in detecting clusters that are not well separated, and was therefore chosen over more conventional hard clustering approaches (Futschik and Carlisle 2005). The fuzzyness parameter M was determined by randomizing the Braak labels and stepwise increasing the M value until no significant clusters were observed in the randomized data set (as described in the MFuzz manual). The resulting M value of 1.55 was used for subsequent analyses. The Braak stage dataset was clustered into 24 separate clusters, to allow for the detection of the possible occurrence of small but significant differences between clusters. For each transcript, the final cluster assignment was made by selecting the cluster for which the MFuzz-assigned cluster membership was maximal. Finally, for each cluster, the percentage of features with a significant gene-Braak ANOVA p-value was calculated, to estimate the significance of the cluster profile.

Gene ontology overrepresentation analysis

The features on the array were annotated with Gene Ontology (GO) identifiers using the hgug4112a library (version 2.0.1) in Bioconductor. Out of the 29813 features encoding for unique genes and ESTs, 16693 features were annotated with one or more GO classes. A total of 6065 unique GO classes were represented on the array.

Gene	Forward	Reverse
DHX16	TTGACTCGGAGTGGCTACCG	AGCGTGGCTGTTGCTCAAAGA
ERBP	GGCTTCCCCAAGTACTTCCA	AGCCAGCAGTTCTTCCACAA
KLHDC5	AGGATGCGTGGAATTTTGTG	TTCATGTTCCGGTCTCTGGT
TM9SF4	CCAGCTGTGTGCAGAGGATT	TCCACGATGTCCAGCTTGTT
SNW1	CTTCTCCCACCTTTCAGCAT	CTCACTGTGGTTGGGGTAACT
AURKAIP1	GCCTCAAATTCAGTGCAAAA	CTCGAACTTGATCTGCTTGC
ISOC2	TGAGACAGAGTGGTGCCTTC	TTCTGGATCTCCTTGAACTGG
PCSK1	TGCCCACTCCTACACTAAGCGA	CCTGCCTAACAGAAGATGCGG
IMP4	TATTTCCCGTGCCCAAAGAT	GTTGCGGTGGTCTGTCTTCT
IGFBP5	GTGCTGTGTACCTGCCCAAT	GCAGCTTCATCCCGTACTTG
CENTD2	CCTCCCAACAAACTCCAGAA	CCTGTAGAAGCTCAGCCAAGAG
HSPA2	CCACCATCGAAGAAGTGGAC	CGTACTTGGCACAAGGACATT
MRAS	AATGTCGACAAAGCCTTCCA	CGCCATTTGGTTTTCTTCTTC
KEAP1	TGAGGCACTTTTGTTTCTTGG	TCCCGGAAGATGGGTTATTT
ZBTB34	GCTGTGAATTCAACCTTTGGA	TGGTCATTCTCAAACAAACCAG
DSCR1L1	TGAAAGTCAGAATCGCCTCA	CACGTGCACAAATGATTCAG
MT1G	ACCTCCTGCAAGAAGAGCTG	CACTCTATTTGTACTTGGGAGCA
MT1B	CTCCTGCAAGTGCAAAGAGT	TCCCAACATCAGGCACAG
LAMP2	TTATCAATCCCAGCATTTTGA	CAAGTTTGTCTCCAGGACCA
CSRP1	TTAAGGACCCCAAAGTCAGG	CAGGGTTAAGGCCAGAGATAA

Table 2 - primer sequences used for qPCR reactions

For the 24 groups of genes as defined by the cluster analysis, we determined significantly overrepresented GO classes associated with each cluster with the TopGO package (version 1.4.0) (Alexa *et al.* 2006). The TopGO algorithm incorporates the hierarchical structure of the GO tree into the calculation of overrepresented GO classes. This facilitates the biological interpretation of the processes associated with the clusters, as the algorithm eliminates less specific GO terms from the results. GO classes were scored with the weight algorithm. GO classes with a weight-corrected p-value of < 0.05 were considered significant. Only GO classes containing 5 or more genes, for which at least one gene was represented in the cluster under investigation, were included in the final result table.

Reverse transcription and quantitative PCR

Each sample was reversely transcribed using 1µg of total RNA, random hexamer primers and SuperScript II Reverse Transcriptase (Invitrogen, Carlsbad, California). 1/250 of the total cDNA yield was used for each qPCR reaction. Transcript quantifications were carried out on an ABI 7300 sequence detection system (Applied Biosystems, Foster City, California). Each reaction was performed with the appropriate amount of cDNA, 3pmol of forward and reverse primers and 10ul 2x SYBR green ready reaction mix (Applied Biosystems) in a total volume of 20µl. Forward and reverse primer sequences can be found in Table 2. To check for primer dimers, dissociation curves were generated for all wells. No primer dimers were observed.

For between-sample normalization, genes were selected that were not regulated between Braak stages using expression stability measurements and geometric averaging of multiple internal reference genes (Vandesompele *et al.* 2002). Briefly, an initial selection of 10 genes was made based on the gene expression data and reference gene data from literature. The 6 most stable genes between Braak stages were selected (DHX16, ERBP, KLHDC5, TM9SF4, SNW1, AURKAIP1 and ISOC2), and for each sample a normalization factor was determined by geometric averaging of the expression values of the reference genes.

Results

Identification of single gene changes in AD

In order to gain insight in gene expression changes associated with the progression of AD, we performed microarray experiments on the prefrontal cortex of a set of 49 individuals with varying levels of AD-associated NFC (n=7 per Braak stage. An ANOVA analysis on the normalized microarray dataset was performed to detect transcripts with significant changes between Braak stages. In total, 1071 features (2.7% of all features) representing 922 genes were found to have an interaction between expression level and Braak stage (Benjamini-Hochberg corrected p-value < 0.05, Table S1). All features with $p < 0.01$ are given in Table 3. qPCR measurements on a selection of 13 genes were highly correlated with microarray data (average r^2=.57), and for 12 out of 13 genes, confirmed the significant differences between Braak stages for all genes (Table 4). Several transcriptional alterations observed in our dataset are in line with earlier findings in end stage AD and thus confirm our approach. For example, we observed a strong decrease in somatostatin (SST) levels in more advanced Braak stages, which has been found to be reduced in the AD neocortex and CSF already 25 years ago (Davies *et al.* 1980; Wood *et al.* 1982). CRH levels (May *et al.* 1987) and KLK7 levels (Diamandis *et al.* 2004) are also severely decreased in AD CSF, observations which we corroborated in the AD PFC. Two members of the small heat shock protein family, HSPA2 and HSPB2, and the class I metallothioneins MT1B and MT1G are induced in end stage AD in our dataset, and have been reported to be associated with Aβ pathology in AD (Hidalgo *et al.* 2006; Lukiw 2004; Wilhelmus *et al.* 2006).

Detection of concerted gene expression changes over Braak stages

The selection of significant genes by the ANOVA analysis alone does not provide insight in the potential involvement of the selected transcripts in the development of AD neuropathology. It is theoretically possible that all of the changes for example occur between Braak stage V and VI, which then most likely represent changes in response to NFC and plaque pathology, as opposed to gene changes causative to AD neuropathology.

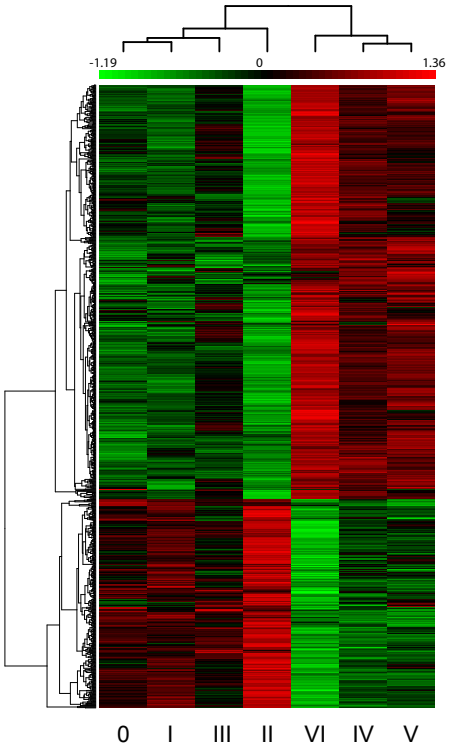

Figure 3 – Clustering of significant transcripts associated with AD. Hierachical clustering of all transcripts significantly changed in the Braak stage ANOVA. Note the clear separation between Braak stages before onset of pathology in the PFC (Braak 0-II) and Braak stages after onset of pathology (Braak IV-VI), suggesting an interaction between the expression levels of these transcripts and neuropathology in AD.

Therefore, for each transcript, the average expression per Braak stage was used to construct a profile, corresponding to the expression pattern of that transcript over the consecutive Braak stages. Next, we performed a hierarchical clustering on the average levels per Braak stage for the significantly regulated transcripts (Figure 3). Interestingly, we observed a clear separation between the early stages of NFC pathology (Braak stages 0-III, before or at the onset of NFC pathology in the PFC) and later stages (Braak IV-VI, after appearance of NFC in the PFC) based on the expression of the genes with a significant interaction between expression level and Braak

Table 3 (following pages) - List of most significantly altered transcripts during the progression of AD. Braak stage data: log2-transformed fold change against average of all measurements. P value: Benjamini-Hochberg-corrected ANOVA p-value. Fold Change: maximum fold change between Braak stages. Cluster: cluster assignment (see Figure 4). Only genes with $p < 0.01$ are given. The full list of significantly altered genes can be found in Table S1.

GeneName	Description
ZBTB34	Homo sapiens mRNA for KIAA1993 protein. [AB082524]
BC004287	Homo sapiens, clone IMAGE:3618365, mRNA. [BC004287]
POGK	Homo sapiens pogo transposable element with KRAB domain (POGK), mRNA [NM_017542]
SCG3	Homo sapiens secretogranin III (SCG3), mRNA [NM_013243]
TLE4	Homo sapiens transducin-like enhancer of split 4 (E(sp1) homolog, Drosophila) (TLE4), mRNA [NM_007005]
PHF15	Homo sapiens PHD finger protein 15 (PHF15), mRNA [NM_015288]
MRGPRF	Homo sapiens MAS-related GPR, member F (MRGPRF), mRNA [NM_145015]
AF131834	Homo sapiens clone 24841 mRNA sequence. [AF131834]
KIAA1737	Homo sapiens KIAA1737 (KIAA1737), mRNA [NM_033426]
PTPLB	Homo sapiens protein tyrosine phosphatase-like (proline instead of catalytic arginine), member b (PTPLB), mRNA [NM_198402]
GTF3C5	Homo sapiens general transcription factor IIIC, polypeptide 5, 63kDa (GTF3C5), mRNA [NM_012087]
AK025758	Homo sapiens cDNA: FLJ22105 fis, clone HEP17660. [AK025758]
SPON2	Homo sapiens spondin 2, extracellular matrix protein (SPON2), mRNA [NM_012445]
CRYBA2	Homo sapiens crystallin, beta A2 (CRYBA2), transcript variant 1, mRNA [NM_005209]
PPP1R1A	Homo sapiens protein phosphatase 1, regulatory (inhibitor) subunit 1A (PPP1R1A), mRNA [NM_006741]
SIRT1	Homo sapiens sirtuin (silent mating type information regulation 2 homolog) 1 (S. cerevisiae) (SIRT1), mRNA [NM_012238]
PHYHIPL	Homo sapiens mRNA for KIAA1796 protein, partial cds. [AB058699]
RFP2	Homo sapiens ret finger protein 2 (RFP2), transcript variant 3, mRNA [NM_213590]
CR600106	full-length cDNA clone CS0DJ008YP03 of T cells (Jurkat cell line) Cot 10-normalized of Homo sapiens (human). [CR600106]
ENST00000278590	Homo sapiens mRNA for KIAA1726 protein, partial cds. [AB051513]
PCSK1	Homo sapiens proprotein convertase subtilisin/kexin type 1 (PCSK1), mRNA [NM_000439]
KEAP1	Homo sapiens kelch-like ECH-associated protein 1 (KEAP1), transcript variant 1, mRNA [NM_203500]
ENST00000330777	Homo sapiens mRNA for FLJ00269 protein. [AK122582]
ZCCHC14	Homo sapiens zinc finger, CCHC domain containing 14 (ZCCHC14), mRNA [NM_015144]
RNF184	Homo sapiens ring finger protein 184 (RNF184), mRNA [NM_018133]
OPHN1	Homo sapiens oligophrenin 1 (OPHN1), mRNA [NM_002547]
THC2336533	Unknown
CENTD2	Homo sapiens centaurin, delta 2 (CENTD2), transcript variant 1, mRNA [NM_139181]
A_32_P38228	Unknown
LOC348840	Homo sapiens hypothetical protein LOC348840 (LOC348840), mRNA [NM_182631]
ZNF235	Homo sapiens zinc finger protein 235 (ZNF235), mRNA [NM_004234]
LTBP3	Homo sapiens latent transforming growth factor beta binding protein 3 (LTBP3), mRNA [NM_021070]
IMP4	Homo sapiens IMP4, U3 small nucleolar ribonucleoprotein, homolog (yeast) (IMP4), mRNA [NM_033416]
ARHGAP6	Homo sapiens Rho GTPase activating protein 6 (ARHGAP6), transcript variant 2, mRNA [NM_001174]
STARD10	Homo sapiens START domain containing 10 (STARD10), mRNA [NM_006645]
CP110	Homo sapiens CP110 protein (CP110), mRNA [NM_014711]
C18orf10	Homo sapiens chromosome 18 open reading frame 10 (C18orf10), mRNA [NM_015476]

BR0	BR1	BR2	BR3	BR4	BR5	BR6	P value	Fold Change	Cluster
-0.21	-0.06	-0.24	-0.07	0.09	0.15	0.35	0.000	1.51	2
-0.29	-0.14	-0.28	-0.26	0.17	0.39	0.41	0.000	1.62	24
-0.28	-0.11	-0.30	-0.14	0.22	0.23	0.38	0.000	1.60	24
0.54	0.21	0.54	0.23	-0.34	-0.49	-0.69	0.001	2.35	23
-0.19	-0.06	-0.32	-0.21	0.25	0.17	0.36	0.001	1.60	24
-0.16	-0.14	-0.21	-0.06	0.09	0.30	0.18	0.001	1.42	2
-0.29	-0.23	-0.40	-0.27	0.29	0.34	0.58	0.001	1.98	24
0.18	0.15	0.40	0.16	-0.17	-0.26	-0.47	0.001	1.82	23
-0.29	-0.12	-0.20	-0.17	0.16	0.34	0.27	0.001	1.54	24
-0.25	-0.05	-0.16	-0.10	0.09	0.20	0.27	0.001	1.44	2
-0.14	-0.18	-0.26	-0.03	0.12	0.22	0.26	0.001	1.43	24
-0.09	-0.15	-0.21	0.05	0.10	-0.00	0.31	0.001	1.43	24
0.39	0.41	0.93	0.46	-0.46	-0.57	-1.14	0.001	4.19	6
0.14	0.06	0.42	-0.02	-0.18	-0.09	-0.33	0.001	1.67	23
-0.22	-0.17	-0.14	-0.23	0.16	0.34	0.26	0.001	1.48	24
-0.17	-0.03	-0.24	-0.04	0.09	0.08	0.31	0.001	1.46	24
-0.24	-0.14	-0.21	-0.07	0.13	0.24	0.29	0.001	1.44	24
-0.21	-0.06	-0.22	-0.16	0.16	0.20	0.29	0.001	1.42	2
-0.17	-0.15	-0.23	-0.04	0.12	0.20	0.27	0.001	1.41	24
-0.25	-0.20	-0.35	0.02	0.16	0.28	0.34	0.002	1.62	24
0.15	0.54	0.65	0.12	-0.31	-0.52	-0.62	0.002	2.42	6
-0.21	-0.17	-0.19	-0.09	0.13	0.27	0.26	0.002	1.39	24
0.33	0.37	0.37	0.06	-0.35	-0.32	-0.47	0.002	1.79	23
-0.17	-0.06	-0.41	-0.03	0.13	0.19	0.35	0.002	1.69	2
-0.18	-0.10	-0.12	-0.07	0.12	0.11	0.23	0.002	1.33	2
-0.01	-0.07	-0.31	0.01	0.13	-0.04	0.27	0.002	1.50	19
-0.37	-0.07	-0.12	-0.22	0.26	0.21	0.32	0.002	1.61	24
-0.11	-0.10	-0.21	-0.11	0.13	0.13	0.27	0.002	1.40	24
-0.07	-0.12	-0.18	-0.09	0.15	0.10	0.21	0.002	1.32	2
0.00	0.14	0.22	-0.01	-0.08	-0.10	-0.16	0.002	1.30	9
-0.16	0.02	-0.14	-0.08	0.09	0.09	0.18	0.002	1.27	4
-0.14	-0.19	-0.40	-0.01	0.17	0.20	0.35	0.002	1.68	19
0.06	0.16	0.26	0.05	-0.10	-0.04	-0.39	0.002	1.58	23
-0.13	-0.16	-0.28	-0.07	0.10	0.19	0.35	0.002	1.55	2
-0.18	-0.17	-0.25	-0.10	0.16	0.22	0.32	0.002	1.48	24
-0.28	-0.11	-0.23	-0.16	0.13	0.25	0.40	0.002	1.60	24
0.19	0.20	0.50	0.02	-0.27	-0.34	-0.30	0.003	1.79	23

Table 3 (continued)

GeneName	Description
STARD7	Homo sapiens START domain containing 7 (STARD7), transcript variant 1, mRNA [NM_020151]
HIPK1	Homo sapiens homeodomain interacting protein kinase 1 (HIPK1), transcript variant 1, mRNA [NM_198268]
WNT10A	Homo sapiens wingless-type MMTV integration site family, member 10A (WNT10A), mRNA [NM_025216]
PCGF4	Human prot-oncogene (BMI-1) mRNA, complete cds. [L13689]
ZNF395	Homo sapiens zinc finger protein 395 (ZNF395), mRNA [NM_018660]
TAF4	Homo sapiens TAF4 RNA polymerase II, TATA box binding protein (TBP)-associated factor, 135kDa (TAF4), mRNA [NM_003185]
SPIRE1	Homo sapiens spire homolog 1 (Drosophila) (SPIRE1), mRNA [NM_020148]
ZNF300	Homo sapiens zinc finger protein 300 (ZNF300), mRNA [NM_052860]
A_32_P232437	Unknown
THC2341745	Unknown
MRAS	Homo sapiens muscle RAS oncogene homolog (MRAS), mRNA [NM_012219]
MTSS1	Homo sapiens metastasis suppressor 1 (MTSS1), mRNA [NM_014751]
LOC342892	Homo sapiens mRNA; cDNA DKFZp686J154 (from clone DKFZp686J154). [CR627133]
KPTN	Homo sapiens kaptin (actin binding protein) (KPTN), mRNA [NM_007059]
AF086044	Homo sapiens full length insert cDNA clone YX74D05. [AF086044]
LRRC1	Homo sapiens leucine rich repeat containing 1 (LRRC1), mRNA [NM_018214]
TMEM4	Homo sapiens transmembrane protein 4, mRNA (cDNA clone IMAGE:3344788), complete cds. [BC001027]
PDZK11	Homo sapiens PDZ domain containing 11 (PDZK11), mRNA [NM_016484]
THC2341688	Q86UA3 (Q86UA3) MYG1 protein, partial (11%) [THC2341688]
THC2306982	Q9VGZ7 (Q9VGZ7) CG18545-PA, partial (10%) [THC2306982]
MGC39606	Homo sapiens hypothetical protein MGC39606 (MGC39606), mRNA [NM_203306]
PCGF4	Homo sapiens polycomb group ring finger 4 (PCGF4), mRNA [NM_005180]
BOLA3	Homo sapiens bolA-like 3 (E. coli) (BOLA3), mRNA [NM_212552]
ENST00000321482	Unknown
COG2	Homo sapiens component of oligomeric golgi complex 2 (COG2), mRNA [NM_007357]
NIN	Homo sapiens ninein (GSK3B interacting protein) (NIN), transcript variant 1, mRNA [NM_182944]
MRPS25	Homo sapiens mitochondrial ribosomal protein S25 (MRPS25), nuclear gene encoding mitochondrial protein, mRNA [NM_022497]
BX490547	BX490547 DKFZp686B2084_s1 686 (synonym: hlcc3) Homo sapiens cDNA clone DKFZp686B2084 3', mRNA sequence [BX490547]
A_24_P349489	Unknown
A_24_P933135	Unknown
SLC22A18	Homo sapiens solute carrier family 22 (organic cation transporter), member 18 (SLC22A18), transcript variant 2, mRNA [NM_183233]
MID1IP1	Homo sapiens MID1 interacting protein 1 (gastrulation specific G12-like (zebrafish)) (MID1IP1), mRNA [NM_021242]
CAPS	Homo sapiens calcyphosine (CAPS), transcript variant 1, mRNA [NM_004058]
CASC3	Homo sapiens cancer susceptibility candidate 3 (CASC3), mRNA [NM_007359]
FLJ14627	Homo sapiens hypothetical protein FLJ14627 (FLJ14627), mRNA [NM_032814]
ZC3H11A	Homo sapiens zinc finger CCCH-type containing 11A (ZC3H11A), mRNA [NM_014827]
NDUFA7	Homo sapiens NADH dehydrogenase (ubiquinone) 1 alpha subcomplex, 7, 14.5kDa (NDUFA7), mRNA [NM_005001]

BR0	BR1	BR2	BR3	BR4	BR5	BR6	P value	Fold Change	Cluster
-0.31	-0.19	-0.11	-0.13	0.21	0.36	0.18	0.003	1.60	24
-0.25	-0.08	-0.24	0.02	0.13	0.10	0.32	0.003	1.48	19
0.14	0.08	0.27	0.04	-0.20	-0.15	-0.18	0.003	1.38	9
-0.24	-0.04	-0.15	-0.21	0.22	0.16	0.26	0.003	1.41	2
-0.14	-0.20	-0.51	0.04	0.22	0.16	0.44	0.003	1.93	20
-0.20	-0.07	-0.30	-0.06	0.13	0.17	0.34	0.003	1.56	24
-0.16	-0.11	-0.16	-0.12	0.15	0.28	0.13	0.003	1.36	4
-0.08	-0.10	-0.16	-0.03	0.07	0.17	0.13	0.004	1.25	2
0.05	0.19	0.32	0.21	-0.25	-0.12	-0.41	0.004	1.66	23
0.06	0.43	0.65	0.04	-0.15	-0.29	-0.74	0.004	2.62	6
-0.36	-0.16	-0.48	0.02	0.21	0.23	0.54	0.004	2.03	12
-0.19	-0.15	-0.13	-0.06	0.11	0.18	0.24	0.004	1.35	24
-0.07	-0.05	-0.07	-0.09	0.03	0.11	0.16	0.004	1.19	4
-0.08	-0.10	-0.14	-0.15	0.18	0.13	0.16	0.005	1.26	2
-0.33	-0.17	-0.57	-0.26	0.21	0.41	0.70	0.005	2.41	12
-0.27	-0.21	-0.53	-0.04	0.28	0.19	0.59	0.005	2.19	24
0.24	0.14	0.41	0.20	-0.39	-0.27	-0.34	0.005	1.75	23
0.13	0.11	0.14	0.05	-0.10	-0.05	-0.28	0.005	1.33	9
0.12	0.09	0.28	0.08	-0.25	-0.02	-0.31	0.005	1.51	23
0.22	0.32	0.72	0.01	-0.42	-0.25	-0.60	0.006	2.50	6
0.16	0.26	0.44	0.04	-0.30	-0.12	-0.48	0.006	1.89	23
-0.23	-0.03	-0.14	-0.25	0.25	0.15	0.26	0.006	1.42	2
0.19	0.14	0.45	0.08	-0.30	-0.32	-0.25	0.006	1.71	23
0.09	0.17	0.30	0.01	-0.14	-0.11	-0.33	0.006	1.55	23
-0.17	-0.12	-0.11	-0.07	0.12	0.26	0.10	0.006	1.35	2
-0.16	-0.03	-0.16	-0.06	0.11	0.07	0.23	0.006	1.32	4
0.12	0.18	0.52	0.10	-0.17	-0.29	-0.46	0.006	1.97	23
-0.10	-0.08	-0.20	0.00	0.03	0.04	0.32	0.006	1.43	24
0.05	0.10	0.39	0.05	-0.07	-0.01	-0.51	0.006	1.87	23
0.28	0.14	0.34	-0.06	-0.27	-0.12	-0.30	0.006	1.56	23
0.14	0.16	0.25	0.03	-0.19	-0.07	-0.32	0.006	1.49	9
-0.28	-0.32	-0.66	-0.09	0.34	0.53	0.49	0.006	2.28	12
-0.24	-0.23	-0.35	-0.01	0.13	0.15	0.55	0.006	1.87	12
-0.26	-0.16	-0.44	0.02	0.20	0.22	0.42	0.006	1.81	24
0.06	0.15	0.33	0.04	-0.20	-0.03	-0.34	0.006	1.60	23
-0.19	-0.12	-0.32	-0.14	0.20	0.21	0.35	0.006	1.59	24
0.16	0.05	0.30	0.21	-0.21	-0.14	-0.36	0.006	1.59	23

Table 3 (continued)

GeneName	Description
MYOZ3	Homo sapiens myozenin 3 (MYOZ3), mRNA [NM_133371]
MGC5576	Homo sapiens hypothetical protein MGC5576 (MGC5576), mRNA [NM_024056]
ZNF318	Homo sapiens zinc finger protein 318 (ZNF318), mRNA [NM_014345]
AXIN2	Homo sapiens axin 2 (conductin, axil) (AXIN2), mRNA [NM_004655]
PCIA1	Homo sapiens cross-immune reaction antigen PCIA1 (PCIA1), mRNA [NM_024050]
THC2404169	Unknown
AK055372	Homo sapiens cDNA FLJ30810 fis, clone FEBRA2001440. [AK055372]
EFHD1	Homo sapiens EF-hand domain family, member D1 (EFHD1), mRNA [NM_025202]
CAB39L	Homo sapiens calcium binding protein 39-like (CAB39L), mRNA [NM_030925]
C21orf62	Homo sapiens chromosome 21 open reading frame 62 (C21orf62), mRNA [NM_019596]
POGK	Homo sapiens pogo transposable element with KRAB domain (POGK), mRNA [NM_017542]
HNRPH3	Homo sapiens heterogeneous nuclear ribonucleoprotein H3 (2H9) (HNRPH3), transcript variant 2H9, mRNA [NM_012207]
USP37	Homo sapiens ubiquitin specific protease 37 (USP37), mRNA [NM_020935]
CDH23	Homo sapiens cadherin-like 23 (CDH23), transcript variant 1, mRNA [NM_022124]
SFRP2	Homo sapiens secreted frizzled-related protein 2 (SFRP2), mRNA [NM_003013]
IGFBP5	Homo sapiens insulin-like growth factor binding protein 5 (IGFBP5), mRNA [NM_000599]
BOLA3	Homo sapiens bolA-like 3 (E. coli) (BOLA3), mRNA [NM_212552]
ENST00000331920	Homo sapiens cDNA FLJ42602 fis, clone BRACE3011271, moderately similar to Patched protein. [AK124593]
ENST00000325151	Homo sapiens, clone IMAGE:5248278, mRNA, partial cds. [BC037171]
KIAA1181	Homo sapiens endoplasmic reticulum-golgi intermediate compartment 32 kDa protein, mRNA (cDNA clone MGC:16233 IMAGE:3677787), complete cds. [BC012766]
LEAP-2	Homo sapiens liver-expressed antimicrobial peptide 2 (LEAP-2), mRNA [NM_052971]
STX10	Homo sapiens syntaxin 10 (STX10), mRNA [NM_003765]
FLJ35696	Homo sapiens FLJ35696 protein (FLJ35696), mRNA [NM_207387]
FZD7	Homo sapiens frizzled homolog 7 (Drosophila) (FZD7), mRNA [NM_003507]
MGC4172	Homo sapiens short-chain dehydrogenase/reductase (MGC4172), mRNA [NM_024308]
DVL2	Homo sapiens dishevelled, dsh homolog 2 (Drosophila) (DVL2), mRNA [NM_004422]
MYLK2	Homo sapiens myosin light chain kinase 2, skeletal muscle (MYLK2), mRNA [NM_033118]
NRP1	Homo sapiens neuropilin 1 (NRP1), transcript variant 1, mRNA [NM_003873]
RASGRF1	Homo sapiens Ras protein-specific guanine nucleotide-releasing factor 1 (RASGRF1), transcript variant 1, mRNA [NM_002891]
RAF1	Homo sapiens v-raf-1 murine leukemia viral oncogene homolog 1 (RAF1), mRNA [NM_002880]
AK125038	Homo sapiens cDNA FLJ43048 fis, clone BRTHA3004502. [AK125038]
PLXDC2	Homo sapiens plexin domain containing 2 (PLXDC2), mRNA [NM_032812]
CSRP1	Homo sapiens cysteine and glycine-rich protein 1 (CSRP1), mRNA [NM_004078]
HSPA2	Homo sapiens heat shock 70kDa protein 2 (HSPA2), mRNA [NM_021979]
SFRP2	Homo sapiens secreted frizzled-related protein 2 (SFRP2), mRNA [NM_003013]
OR7A5	Homo sapiens olfactory receptor, family 7, subfamily A, member 5 (OR7A5), mRNA [NM_017506]
RPRM	Homo sapiens reprimo, TP53 dependant G2 arrest mediator candidate (RPRM), mRNA [NM_019845]

BR0	BR1	BR2	BR3	BR4	BR5	BR6	P value	Fold Change	Cluster
-0.04	0.09	0.40	0.10	-0.15	-0.14	-0.26	0.006	1.58	9
-0.21	-0.10	-0.31	-0.04	0.20	0.15	0.31	0.006	1.54	24
-0.17	-0.10	-0.16	-0.15	0.11	0.20	0.27	0.006	1.35	2
-0.23	-0.12	-0.14	0.03	0.07	0.20	0.20	0.006	1.35	2
0.03	0.05	0.22	0.06	-0.03	-0.04	-0.30	0.006	1.43	23
-0.28	-0.17	-0.38	0.00	0.13	0.19	0.51	0.006	1.85	12
0.13	-0.04	0.24	0.47	-0.22	-0.20	-0.37	0.006	1.79	9
-0.30	-0.22	-0.65	0.02	0.30	0.35	0.50	0.006	2.21	12
-0.27	-0.19	-0.22	-0.01	0.18	0.12	0.38	0.007	1.57	24
-0.19	-0.23	-0.35	-0.10	0.21	0.25	0.41	0.007	1.68	24
-0.18	-0.13	-0.33	-0.25	0.25	0.31	0.34	0.007	1.58	24
-0.12	-0.09	-0.30	-0.13	0.21	0.12	0.30	0.007	1.51	24
-0.12	-0.08	-0.22	-0.04	0.14	0.10	0.22	0.007	1.36	2
-0.11	-0.09	-0.13	0.02	0.05	0.09	0.17	0.007	1.23	2
-0.46	0.04	-0.27	-0.47	0.34	0.37	0.46	0.007	1.91	2
-0.26	-0.26	-0.47	-0.08	0.15	0.45	0.47	0.007	1.91	24
0.07	0.14	0.32	0.05	-0.13	-0.12	-0.33	0.007	1.56	23
-0.31	-0.15	-0.28	0.17	0.05	0.19	0.33	0.007	1.56	24
0.07	0.13	0.23	0.12	-0.10	-0.08	-0.38	0.007	1.52	23
0.02	-0.30	-0.24	-0.06	0.10	0.22	0.27	0.007	1.49	2
-0.15	-0.17	-0.23	0.01	0.09	0.12	0.32	0.007	1.47	24
-0.13	-0.09	-0.16	-0.08	0.16	0.18	0.12	0.007	1.27	2
0.09	0.09	0.40	0.16	-0.17	-0.17	-0.41	0.007	1.75	23
-0.18	-0.08	-0.35	-0.01	0.19	0.04	0.39	0.007	1.67	24
0.11	0.15	0.29	0.03	-0.14	-0.09	-0.35	0.007	1.56	23
-0.14	-0.09	-0.28	-0.05	0.13	0.17	0.26	0.007	1.46	24
0.08	-0.11	0.33	0.15	-0.18	-0.09	-0.18	0.007	1.43	9
0.25	0.00	0.15	0.06	-0.06	-0.18	-0.22	0.007	1.38	18
0.00	0.17	0.48	0.03	-0.18	-0.20	-0.31	0.007	1.73	23
-0.12	-0.09	-0.24	-0.04	0.14	0.13	0.21	0.007	1.36	24
-0.28	-0.22	-0.57	-0.13	0.22	0.47	0.52	0.007	2.13	12
0.00	-0.01	-0.40	-0.06	0.13	-0.13	0.46	0.007	1.81	20
-0.24	-0.45	-0.69	-0.02	0.28	0.58	0.54	0.008	2.40	12
-0.31	-0.33	-0.57	-0.06	0.15	0.52	0.60	0.008	2.25	12
-0.18	-0.01	-0.20	-0.17	0.14	0.18	0.24	0.008	1.36	2
-0.29	-0.21	-0.34	-0.22	0.39	0.41	0.26	0.008	1.68	24
-0.19	-0.15	-0.21	-0.44	0.10	0.45	0.43	0.009	1.86	24

Gene	Description	P value		
		Microarray	qPCR	r^2
PCSK1	Homo sapiens proprotein convertase subtilisin/kexin type 1 (PCSK1), mRNA [NM_000439]	0.0016	3.70E-06	0.85
IMP4	Homo sapiens IMP4, U3 small nucleolar ribonucleoprotein, homolog (yeast) (IMP4), mRNA [NM_033416]	0.0020	0.015	0.34
IGFBP5	Homo sapiens insulin-like growth factor binding protein 5 (IGFBP5), mRNA [NM_000599]	0.0067	9.33E-06	0.81
CENTD2	Homo sapiens centaurin, delta 2 (CENTD2), transcript variant 1, mRNA [NM_139181]	0.0018	0.043	0.56
HSPA2	Homo sapiens heat shock 70kDa protein 2 (HSPA2), mRNA [NM_021979]	0.0076	0.007	0.64
MRAS	Homo sapiens muscle RAS oncogene homolog (MRAS), mRNA [NM_012219]	0.0041	5.66E-08	0.76
KEAP1	Homo sapiens kelch-like ECH-associated protein 1 (KEAP1), transcript variant 1, mRNA [NM_203500]	0.0016	0.004	0.18
ZBTB34	Homo sapiens mRNA for KIAA1993 protein. [AB082524]	0.0001	0.694	0.12
DSCR1L1	Homo sapiens Down syndrome critical region gene 1-like 1 (DSCR1L1), mRNA [NM_005822]	0.0374	0.001	0.63
MT1G	Homo sapiens metallothionein 1G (MT1G), mRNA [NM_005950]	0.0356	0.042	0.54
MT1B	Homo sapiens metallothionein 1B (functional) (MT1B), mRNA [NM_005947]	0.0220	0.003	0.75
LAMP2	Homo sapiens lysosomal-associated membrane protein 2 (LAMP2), transcript variant LAMP2A, mRNA [NM_002294]	0.0212	0.008	0.67
CSRP1	Homo sapiens cysteine and glycine-rich protein 1 (CSRP1), mRNA [NM_004078]	0.0076	0.002	0.61

Table 4 – Validation of differential expression of 13 transcripts using qPCR.
Microarray P value: Benjamini-Hochberg corrected p-value as determined by gene-level ANOVA analysis between Braak stages.
qPCR P value: ANOVA-based p value between Braak stages. r^2 – Pearson's correlation coefficient.

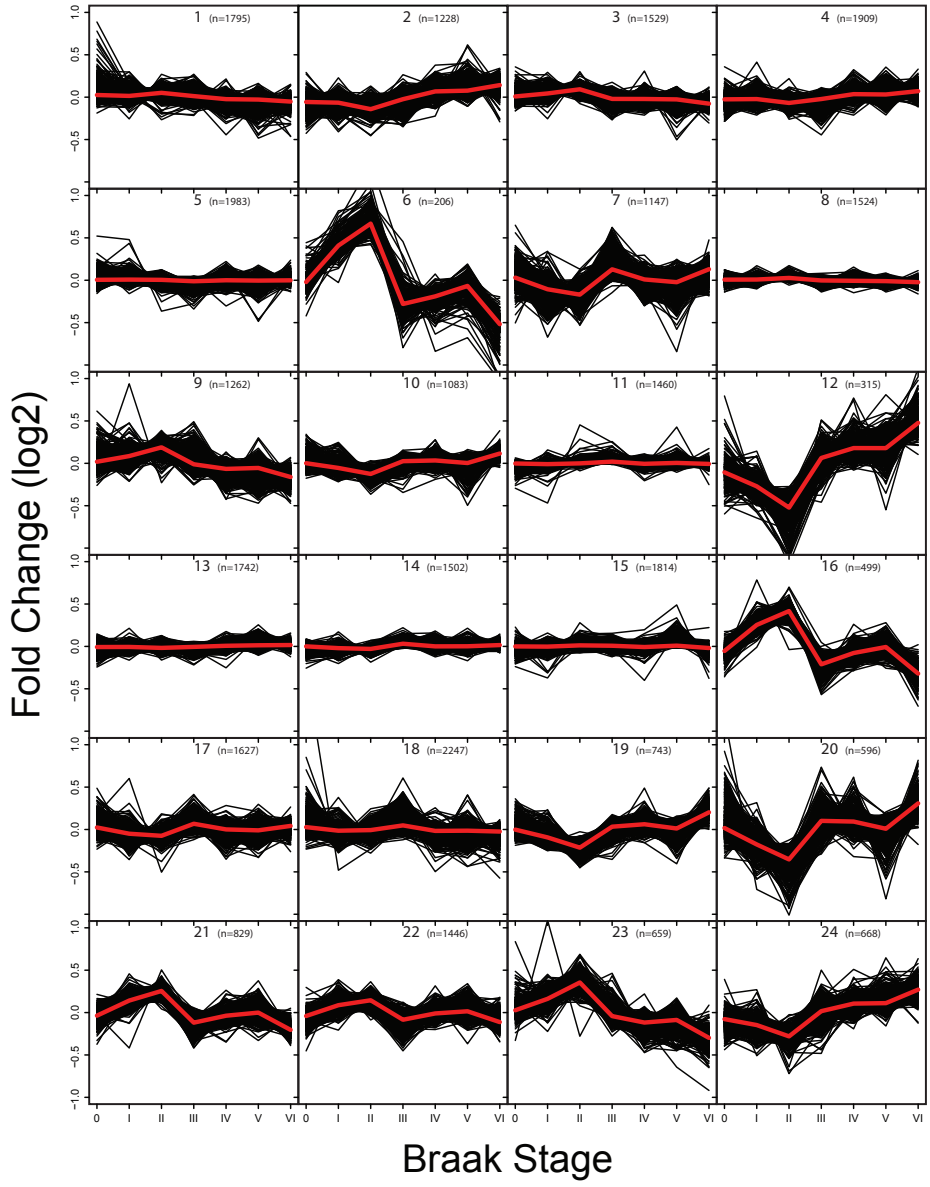

Figure 4 – Division of Braak stage profiles for all transcripts into 24 clusters with correlated expression patterns. The red line represents the average Braak stage profile for that cluster. The cluster number corresponds to the numbers mentioned in the text. 'n' denotes the number of transcripts assigned to a particular cluster.

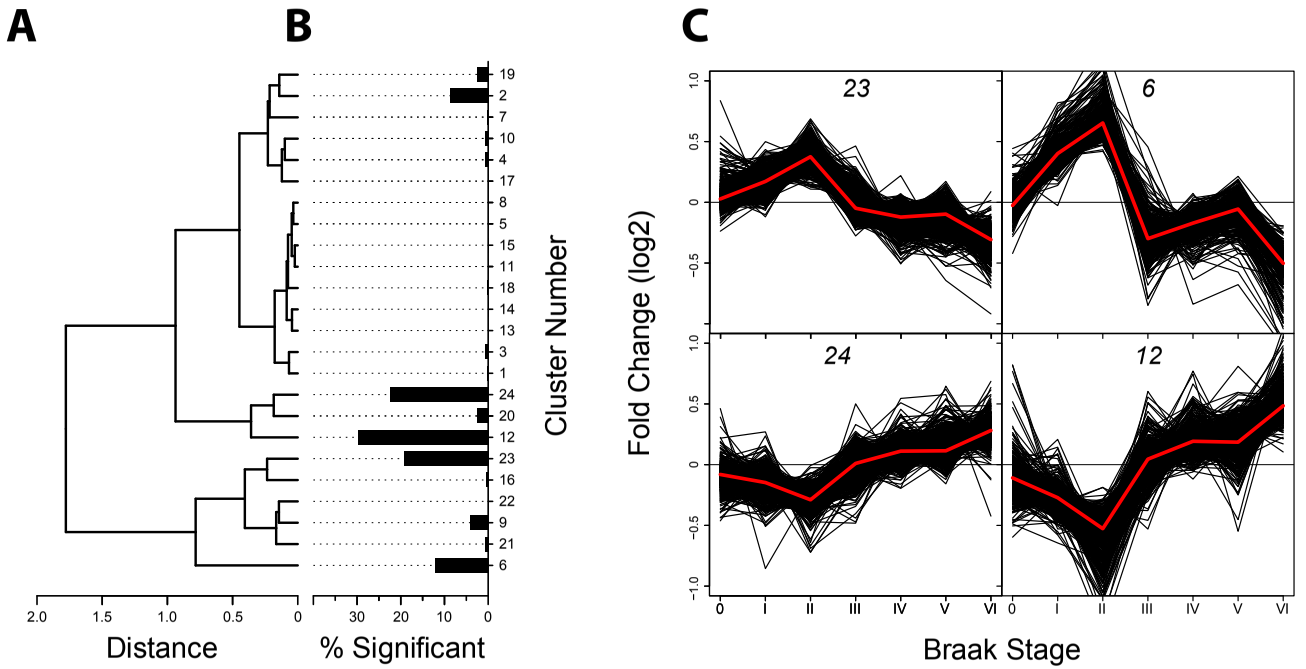

Figure 5 – A) Hierarchical clustering of mean expression patterns for the Braak stage cluster, demonstrating the relationship between Braak stage clusters. B) Percentage of significant genes (as determined by the transcript-level ANOVA between Braak stages) per Braak stage cluster. The numbers to the right correspond to the cluster numbers in Figure 4. C) The four most significant clusters (defined as the largest fraction of significant genes) during the progession of AD. The numbers in each plot correspond to the cluster numbers in Figure 4.

stage. This finding suggests a relationship between the observed transcriptional alterations and AD-associated NFC neuropathology.

Furthermore, using Braak stage profiles, it becomes possible to group transcripts with similar expression patterns over the Braak stages. The presence of such groups of transcripts might indicate co-regulation and/or functional interaction between these transcripts. Also, alterations in gene expression over successive Braak stages possibly provide insight in the sequence of events ultimately leading to AD-associated neuropathology and -degeneration. Clusters of transcripts displaying alterations in early Braak stages are expected to contain more expression changes causative to MCI and AD, whereas alterations in later Braak stages possibly represent secondary effects.

After merging profiles of transcripts encoding for the same gene, a cluster analysis on the resulting 29813 Braak stage profiles divided the dataset in 24 groups of transcripts with strongly coupled expression levels (Figure 4). As expected, a number of clusters consisted of transcripts that were unaltered during the course of the disease. More interestingly, we also detected several clusters with pronounced and distinct alterations over the Braak stages. As the shapes of some profiles shared similarities with other profiles, a second cluster analysis was performed on the average shapes of the clusters to assess the relationship between the Braak stage clusters (Figure 5A). Also, for each cluster, we calculated the fraction of genes differentially expressed according to the ANOVA analysis. This provided us with an indication of the significance of the observed alterations over the Braak stages (Figure 5B).

Several clusters stood out due to the shape of regulation over the consecutive Braak stages, and the high percentage of significantly altered transcripts within these clusters (Figure 5C). Two gross patterns could be observed: 1) an increase in expression in early Braak stages, followed by a decline in expression in later stages (clusters 6 and 23 in Figure 4&5, the UPDOWN clusters) and 2) a decrease in expression in early Braak stages, followed by an increase in expression in later stages (cluster 12 and 24 in Figure 4&5, the DOWNUP clusters). Interestingly, the most profound changes in gene expression were detected between Braak stages II and III, just before or at the onset of NFC pathology in the PFC, suggesting a link between specific Braak profile clusters and AD-associated NFC in the PFC.

Functional annotation of Braak stage profile clusters

To gain insight in the biological processes associated with the different clusters of Braak stage profiles, we first annotated the genes represented on the microarray with identifiers according to the Gene Ontology (GO) database. Next, for each of the four DOWNUP and UPDOWN clusters, an overrepresentation analysis was performed to determine which GO identifiers were significantly enriched within that cluster. The resulting lists of significantly overrepresented GO identifiers are presented in Table S2. A selection of the most significant GO identifiers ($p < 0.01$) associated with the UPDOWN and DOWNUP clusters are given in Table 5 and 6, respectively.

GO ID	Description	Cluster	Annotated	In Cluster	P Value
Biological Process					
GO:0007399	nervous system development	6	682	25	3.80E-06
GO:0006120	mitochondrial electron transport, NADH to ubiquinone	23	34	7	1.10E-05
GO:0015986	ATP synthesis coupled proton transport	23	37	7	1.90E-05
GO:0007018	microtubule-based movement	6	106	7	6.90E-05
GO:0007268	synaptic transmission	6	263	17	7.60E-05
GO:0007186	G-protein coupled receptor protein signaling pathway	6	756	19	2.80E-04
GO:0006813	potassium ion transport	6	153	7	6.70E-04
GO:0006418	tRNA aminoacylation for protein translation	23	47	6	7.20E-04
GO:0006821	chloride transport	6	44	4	8.10E-04
GO:0006118	electron transport	23	332	23	1.22E-03
GO:0051258	protein polymerization	6	56	4	2.00E-03
GO:0043648	dicarboxylic acid metabolic process	23	15	4	2.96E-03
GO:0050679	positive regulation of epithelial cell proliferation	23	13	3	2.99E-03
GO:0042254	ribosome biogenesis and assembly	23	92	7	5.55E-03
GO:0008543	fibroblast growth factor receptor signaling pathway	23	16	3	5.56E-03
GO:0006383	transcription from RNA polymerase III promoter	23	32	4	6.15E-03
GO:0006334	nucleosome assembly	6	86	4	9.30E-03
GO:0051258	protein polymerization	23	56	5	9.51E-03
GO:0007267	cell-cell signaling	6	631	25	9.97E-03
Cellular Component					
GO:0043005	neuron projection	6	72	11	8.90E-11
GO:0044455	mitochondrial membrane part	23	95	16	8.40E-10
GO:0045202	synapse	6	211	12	1.00E-06
GO:0005883	neurofilament	6	6	3	1.80E-05
GO:0045259	proton-transporting ATP synthase complex	23	19	5	6.80E-05
GO:0030054	cell junction	6	379	13	8.30E-05
GO:0008021	synaptic vesicle	6	58	5	2.40E-04
GO:0030426	growth cone	6	15	3	3.80E-04
GO:0005666	DNA-directed RNA polymerase III complex	23	9	3	1.00E-03
GO:0008180	signalosome	23	9	3	1.00E-03
GO:0031970	organelle envelope lumen	23	21	4	1.40E-03
GO:0005874	microtubule	6	226	8	1.65E-03
GO:0005625	soluble fraction	6	238	8	2.27E-03
GO:0005678	chromatin assembly complex	6	8	2	2.53E-03
GO:0005739	mitochondrion	23	871	49	2.60E-03
GO:0005874	microtubule	23	226	13	3.20E-03
GO:0005737	cytoplasm	23	5841	186	5.70E-03
GO:0030130	clathrin coat of trans-Golgi network vesicle	6	14	2	7.91E-03

GO ID	Description	Cluster	Annotated	In Cluster	P Value
Molecular Function					
GO:0015077	monovalent inorganic cation transmembrane transporter activity	23	103	14	1.10E-07
GO:0005184	neuropeptide hormone activity	6	25	5	2.50E-06
GO:0008137	NADH dehydrogenase (ubiquinone) activity	23	38	7	2.30E-05
GO:0051537	2 iron, 2 sulfur cluster binding	23	10	4	5.30E-05
GO:0003924	GTPase activity	23	201	14	2.50E-04
GO:0004812	aminoacyl-tRNA ligase activity	23	47	6	7.20E-04
GO:0030955	potassium ion binding	6	121	6	7.80E-04
GO:0004890	GABA-A receptor activity	6	21	3	8.40E-04
GO:0005267	potassium channel activity	6	126	6	9.60E-04
GO:0005254	chloride channel activity	6	52	4	1.21E-03
GO:0031404	chloride ion binding	6	53	4	1.30E-03
GO:0003924	GTPase activity	6	201	7	2.25E-03
GO:0030276	clathrin binding	6	9	2	2.77E-03
GO:0005509	calcium ion binding	6	901	17	2.92E-03
GO:0004289	subtilase activity	6	11	2	4.18E-03
GO:0005251	delayed rectifier potassium channel activity	23	15	3	4.57E-03
GO:0008603	cAMP-dependent protein kinase regulator activity	23	15	3	4.57E-03
GO:0030976	thiamin pyrophosphate binding	23	5	2	5.12E-03
GO:0004993	serotonin receptor activity	6	14	2	6.79E-03
GO:0030552	cAMP binding	6	15	2	7.79E-03
GO:0016247	channel regulator activity	23	35	4	8.44E-03
GO:0042803	protein homodimerization activity	6	141	5	8.86E-03
GO:0030594	neurotransmitter receptor activity	6	92	4	9.46E-03
GO:0005525	GTP binding	23	358	16	9.58E-03

Table 5 – Table of the most significantly regulated GO identifiers in the UPDOWN clusters, listing all GO identifiers overrepresented in clusters 6 and 23 with a $p < 0.01$. Annotated: number of genes on the array with a specific GO identifier. In cluster: number of genes in that cluster with a specific GO identifier. P value: TopGO p value.

GO ID	Description	Cluster	Annotated	In Cluster	P Value
Biological Process					
GO:0002504	antigen processing and presentation of peptide or polysaccharide antigen via MHC class II	24	24	6	2.70E-05
GO:0007205	protein kinase C activation	12	22	4	2.30E-04
GO:0008354	germ cell migration	24	7	3	5.60E-04
GO:0046330	positive regulation of JNK cascade	12	13	3	7.20E-04
GO:0016049	cell growth	12	172	9	7.70E-04
GO:0007368	determination of left/right symmetry	12	18	3	1.95E-03
GO:0043392	negative regulation of DNA binding	12	6	2	2.89E-03
GO:0001501	skeletal development	12	230	10	3.81E-03
GO:0019048	virus-host interaction	12	7	2	4.00E-03
GO:0019827	stem cell maintenance	12	7	2	4.00E-03
GO:0035088	establishment or maintenance of apical/basal cell polarity	12	7	2	4.00E-03
GO:0006817	phosphate transport	24	102	8	5.08E-03
GO:0008589	regulation of smoothened signaling pathway	12	8	2	5.29E-03
GO:0007169	transmembrane receptor protein tyrosine kinase signaling pathway	12	189	8	5.54E-03
GO:0007160	cell-matrix adhesion	12	89	6	5.72E-03
GO:0015758	glucose transport	12	27	3	6.38E-03
GO:0042471	ear morphogenesis	12	27	3	6.38E-03
GO:0009953	dorsal/ventral pattern formation	12	28	3	7.07E-03
GO:0006355	regulation of transcription, DNA-dependent	24	2193	75	8.28E-03
GO:0045930	negative regulation of mitotic cell cycle	12	10	2	8.34E-03
GO:0042632	cholesterol homeostasis	24	17	3	9.04E-03
Cellular Component					
GO:0042613	MHC class II protein complex	24	21	6	1.20E-05
GO:0031252	leading edge	24	79	7	4.50E-03
GO:0043235	receptor complex	12	86	5	6.80E-03
Molecular Function					
GO:0046870	cadmium ion binding	12	6	6	6.40E-12
GO:0005507	copper ion binding	12	61	8	1.80E-06
GO:0032395	MHC class II receptor activity	24	22	6	1.60E-05
GO:0008307	structural constituent of muscle	12	43	5	3.00E-04
GO:0003779	actin binding	24	302	18	1.10E-03
GO:0015250	water channel activity	24	9	3	1.30E-03
GO:0008307	structural constituent of muscle	24	43	5	5.10E-03
GO:0008060	ARF GTPase activator activity	24	5	2	6.50E-03
GO:0008147	structural constituent of bone	24	5	2	6.50E-03
GO:0004181	metallocarboxypeptidase activity	12	29	3	7.30E-03
GO:0046790	virion binding	12	10	2	7.90E-03
GO:0005547	phosphatidylinositol-3,4,5-trisphosphate binding	24	6	2	9.60E-03

Table 6 (opposite page) – Table of the most significantly regulated GO identifiers in the DOWNUP clusters, listing all GO identifiers overrepresented in clusters 12 and 24 with a $p < 0.01$. Annotated: number of genes on the array with a specific GO identifier. In cluster: number of genes in that cluster with a specific GO identifier. P value: TopGO p value.

Cluster 6, one of the UPDOWN clusters, is strongly associated with gene groups involved in synaptic transmission (e.g. GO classes *Synaptic Transmission* and *Synapse*) and nervous system development and plasticity (e.g. GO classes N*ervous System Development* and *Growth Cone)*. Interestingly, although the overall shape of cluster 23 resembles that of cluster 6, cluster 23 contains genes associated with quite different processes, such as ATP synthesis (e.g. GO classes *ATP Synthesis Coupled Proton Transport*, *Electron Transport* and *Mitochondrion*) and ribosome assembly and rRNA and tRNA transcription and processing (e.g. GO classes *tRNA Metabolic Process*, *Ribosome Biogenesis* and *Assembly and Ribonuclease P Complex*). The DOWNUP cluster 12 contains several gene groups involved in differentiation and proliferation (e.g. GO classes *Protein Kinase C Activation*, *Positive Regulation of JNK Cascade*, *Brain Development* and *Notch Signaling Pathway*) and metal ion binding (GO classes *Response to Metal Ion*, *Cadmium Ion Binding* and *Copper Ion Binding*). Cluster 24 is strongly associated with antigen processing gene groups (e.g. GO classes *Antigen Processing and Presentation of Peptide or Polysaccharide Antigen via MHC Class II*, *MHC Class II Protein Complex* and *MHC Class II Receptor Activity*) and regulation of transcription (e.g. GO classes *DNA-dependent Regulation of Transcription*, *Negative Regulation of Transcription Factor Activity* and *DNA Binding*).

Interaction of ApoE genotype with Braak stage profile clusters

The ApoE genotype is currently the only known genetic factor that modulates the risk of developing sporadic AD. To study the potential interaction between ApoE genotype and the clusters of co-regulated genes, we divided the sample set into two groups: (i) individuals with either one (n=20) or two (n=1) copies of the ApoE4 allele (the carrier group), and (ii) individuals without an ApoE4 allele (n=28, the non-carrier group). As each Braak stage contained 7 individuals, further subdividing these stages into carrier and non-carrier would have resulted in groups too small for proper statistical testing. We therefore grouped the Braak stages into 3 groups: the preclinical "control" group (stages 0-II), the "MCI" group (stages III and IV) and the "AD" group (stages V and VI). For all of the UPDOWN and DOWNUP clusters, within each of the three groupings, we compared the average expression levels of genes contained in that cluster between carriers and non-carriers. We did not observe, for any of the clusters, any significant differences between carriers and non-carriers in the control or AD group. However, for both DOWNUP clusters, we observed a significant increase in expression of the ApoE4 carriers as compared to the non-carriers in the MCI group (Wilcoxon rank sum test < .05, Figure6A&B). In the UPDOWN clusters, we observed a trend in the opposite direction, which did, how-

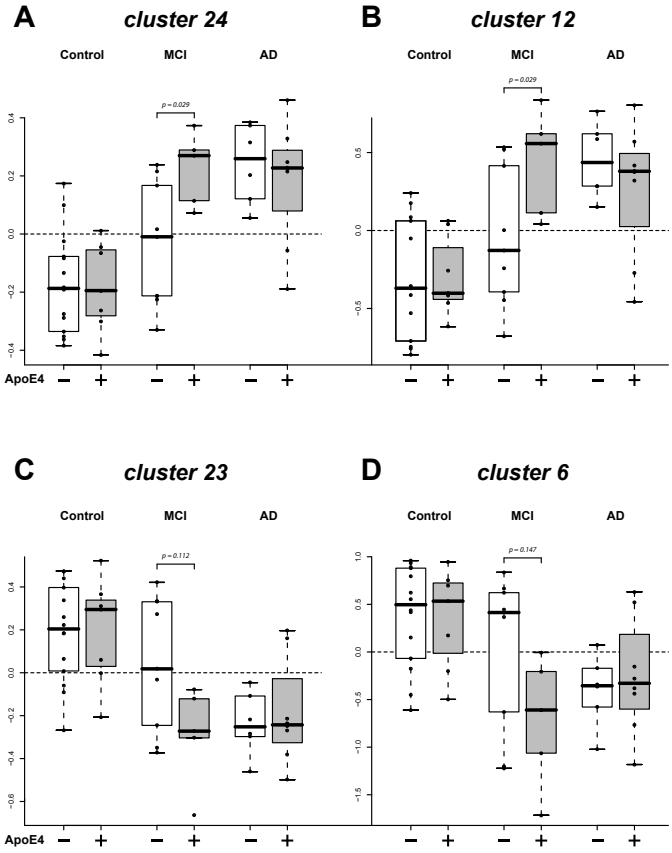

Figure 6 – Interaction between UPDOWN and DOWNUP clusters and ApoE genotype. For the 4 most significant Braak stage clusters, the average expression per cluster was determined by calculating the mean expression of all genes in that cluster the groups "controls" (Braak 0-II), "MCI" (Braak III and IV) and "AD" (Braak V and VI). These groups were further subdivided in ApoE4 carriers and non-carriers. P-values were calculated by the Wilcoxon rank sum test. Note the significant ApoE-dependent differences in the MCI group for the DOWNUP clusters, and the trend in the UPDOWN clusters.

ever, not reach statistical significance (Wilcoxon rank sum test < .15, Figure 6C&D). Interestingly, in the MCI group for both the DOWNUP and UPDOWN clusters, the expression levels of the carriers resembled those of the AD group, whereas the distribution of the non-carriers more resembled a transition phase between the control group and the AD group.

Discussion

In this study, genome-wide gene expression profiles of grey matter isolated from a large set (n=49) of human PFC samples were stratified according to the Braak staging for NFC in order to study transcriptional alterations associated with AD. As this part of the neocortex is affected relatively late in the disease process, we were able to follow gene expression changes associated with AD neuropathology from the earliest stages onwards. We observed a number of gene clusters with remarkable concerted alterations in gene expression over the consecutive Braak stages. The gene clusters with the most significant alterations can roughly be divided into two expression patterns: UPDOWN and DOWNUP. Genes associated with UPDOWN clusters (clusters 6 and 23, Figure 5C) increase in expression between Braak 0 and Braak II, and then steeply decline to Braak III, followed by a more gradual decline in the advanced Braak stages. This pattern was selectively enriched for genes implicated in neuronal activity. The DOWNUP clusters (clusters 12 and 24, Figure 5C), that for instance include genes involved in differentiation and proliferation, follow a roughly mirrored pattern of expression over the Braak stages. Interestingly, when examining the samples included in this study on a neuropathological level, we observed the most prominent alterations in the PFC between Braak II and III: the median amyloid plaque score changed dramatically from no plaques at Braak II, to many plaques at Braak stage III (Figure 1). Also, the first NFC only started to appear after Braak II. Thus, in the transition between Braak 0 and II, profound gene expression changes are already observed before any of the classical AD-associated neuropathological changes are present in the PFC. It is noteworthy that the patients in these Braak stages came into the Netherlands Brain Bank as "controls", and were cognitively unaffected. Furthermore, the transition between Braak II and III appeared to be very important in AD disease progression, both in terms of neuropathological alterations and gene expression changes. As the UPDOWN and DOWNUP gene groups already showed strong alterations before the onset of the neuropathological changes in the PFC, the individual genes and/or biological processes represented by these gene groups might be causally involved in the development of neuropathology during the progression of AD. In this discussion, we will highlight these potential causative mechanisms.

The appearance of AD neuropathology is preceded by changes in gene expression that point to an increased neuronal plasticity and activity in the PFC in Braak stage I-II

The UPDOWN clusters were selectively and significantly enriched for genes involved in synaptic transmission, synaptic plasticity, oxidative phosphorylation and general metabolism (Table 5 and S2). Examples of genes present in UPDOWN clusters that play a role in synaptic plasticity and transmission include CHL1 and DCAMKL1 (both involved in neuron migration and axon outgrowth; Koizumi *et al.* 2006; Deuel *et al.* 2006; Schmid and Maness 2008), PAK1 (implicated in activi-

ty-dependent synaptogenesis; Saneyoshi *et al.* 2008), GLRB (a regulator of synaptic connectivity via postsynaptic inhibition; Xu and Tian 2008), MEF2C (a transcription factor facilitating learning by negative regulation of synapse numbers; Barbosa *et al.* 2008), RTN4 (also known as NOGO, a well-known neurite growth-inhibitory protein that suppresses experience-driven plasticity in the visual cortex; McGee *et al.* 2005) and STMN2 (involved in altering microtubular structures during axon extension; Li *et al.* 2009). Interestingly, the expression of EGR3, also present in the UPDOWN cluster, is regulated by synaptic activity (Li *et al.* 2007). Transcriptional evidence for alterations in energy synthesis can be derived from the presence of members of the mitochondrial electron (NDUFA10, NDUFA6, NDUFA7, NDUFA9, NDUFB5, NDUFS1, NDUFV2) and proton (ATP5C1, ATP5F1, ATP5G1, ATP5H, ATP5O, ATP6AP1, ATP6V0E2L) transport complexes.

The biological molecular functions of the genes described above, combined with the expression pattern of the UPDOWN clusters over the Braak stages, suggest an increase in neuronal activity during the progression from Braak stage 0 to II. This is an intriguing finding; individuals in these Braak stages are cognitively unaffected, and these early changes in neuronal activity are not paralleled by any –visible- neuropathological alteration in the PFC. We therefore hypothesize that the increased neuronal activity might be indicative for deleterious alterations that have a negative effect on synaptic transmission. In this light, the upregulation of synaptic transmission represents a coping mechanism, where the brain has to "work" harder to maintain normal cognitive levels. Furthermore, the deleterious alterations might also be causally involved in the development of AD-associated neuropathology, as they occur just before the onset of pathology in the PFC.

Recent evidence from functional imaging experiments supports our findings of increased activity in cognitively intact controls, prior to the onset of AD pathology. Two fMRI studies comparing aged, but non-demented controls at risk for AD and non-demented controls not at risk (defined as having or not having a parent who suffered from AD), demonstrated that the at-risk group showed enhanced activation of the frontal lobe (Bassett *et al.* 2006; Yassa *et al.* 2008). Furthermore, in a FAD family characterized by a C410Y mutation in the PSEN1 gene, a cognitively normal 21-year old carrier exhibited enhanced brain activity as compared to age-matched controls during memory-related tasks (Mondadori *et al.* 2006). Interestingly, evidence for a compensatory increase in neuronal activity can also be found in subcortical areas. For example, metabolic activity in the nucleus basalis of Meynert is increased in control cases without an ApoE4 allele, and in patients with mild cognitive impairment (Braak stages III-IV) (Dubelaar *et al.* 2004; Dubelaar *et al.* 2006).

We here provide evidence that, in the absence of senile plaque or NFC pathology, an early increase in neuronal activity in the prefrontal cortex (as represented by the specific upregulation of genes involved in processes such as synaptic transmission, synaptic plasticity and oxidative phosphorylation) might represent a coping mechanism against decreased synaptic efficacy. The potential causative mechanisms underlying the decrease in synaptic efficacy are discussed below.

Increased levels of soluble Aβ might underlie the compensatory neuronal activity at Braak I-II

The important question arises which process(es) elicit the compensatory response of increased neuronal activity at Braak I-II. Elevations in intracellular Aβ concentrations have been shown to precede plaque formation in both AD (Gouras *et al.* 2000) and DS (Gyure *et al.* 2001; Mori *et al.* 2002), and in several transgenic mouse models for AD (Oakley *et al.* 2006; Oddo *et al.* 2006). As mentioned earlier, the transition from Braak II-III is accompanied by a drastic and sudden increase in prefrontal plaque load (Figure 1), which suggests that soluble Aβ levels are increased before Braak III. Furthermore, in recent years, compelling evidence has emerged pointing to the inhibitory actions of increased soluble Aβ levels on synaptic transmission and plasticity (reviewed in LaFerla *et al.* 2007). Direct evidence for a transient impairment of cognitive function by intracerebroventricular infusion of physiological concentrations of Aβ oligomers has been demonstrated in nontransgenic rats (Cleary *et al.* 2005), thus excluding potential confounding effects of APP overexpression via other mechanisms than Aβ. In the 3xTg-AD mouse model, the accumulation of intraneuronal Aβ appeared to cause the earliest cognitive defects (Billings *et al.* 2005), coinciding with a decline in LTP (Oddo *et al.* 2003). Removal of the intracellular Aβ by immunotherapy reversed the cognitive defects (Billings *et al.* 2005). Furthermore, both in vitro and in vivo, soluble Aβ-mediated synaptic silencing was observed in neurons overexpressing APP, by specifically targeting postsynaptic AMPA receptors and by reducing presynaptic vesicle recycling (Shemer *et al.* 2006; Ting *et al.* 2007). Taken together, there is substantial evidence that plaque formation is preceded by increased soluble Aβ levels, and that soluble Aβ negatively affects synaptic transmission, even at physiological levels. In this light, we hypothesize that rising soluble Aβ levels are a potential cause of the observed increased neuronal activity in Braak I and II. Namely, more soluble Aβ would reduce synaptic efficacy and elicit a compensatory response to maintain normal levels of synaptic transmission. Furthermore, the sudden appearance of senile plaques in Braak stage III is likely to be preceded by increased Aβ levels. An alternative explanation might be that via polysynaptic pathways the first AD changes in the entorhinal and hippocampal regions affect the function of the neocortex and NBM. For this possibility no evidence is available at present. Also, additional studies are needed to confirm the elevated levels of soluble Aβ in the prefrontal cortex in Braak stages I-II, for example by using antibodies specific for oligomeric forms of Aβ (Wang *et al.* 2009).

Transcriptional alterations in the UPDOWN cluster point to increased soluble Aβ levels

Based upon our hypothesis of increased soluble Aβ levels in early Braak stages (0-II), we systematically studied the list of genes that were 1) significantly changed between Braak stages, and 2) were member of the UPDOWN or DOWNUP cluster, in order to identify genes that might be involved in altering Aβ levels. Indeed, in the UPDOWN clusters, we identified a set of genes (PSEN2, EGR1, RER1, PACAP, SST,

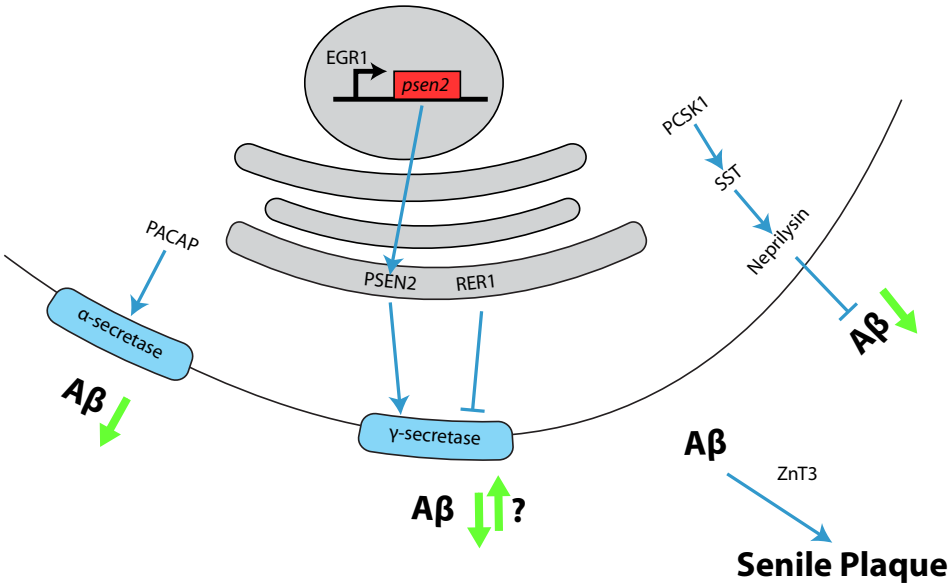

Figure 7 – Gene expression changes related to APP processing and Aβ metabolism. In the UPDOWN clusters, several genes (EGR1, PSEN2, RER1, PACAP, PCSK1, SST and ZnT3) are involved in altering the levels of Aβ. The expression of these genes is increased in Braak stage II, and decreased in Braak stage IV. This picture reflects the situation at Braak stage II. A detailed description of the specific roles of the genes mentioned here on Aβ levels can be found in the text.

PCSK1 and ZnT3) known to be involved in the generation, breakdown or aggregation of Aβ. The regulatory pattern of these transcripts (upregulated in Braak I and II) over the Braak stages provides support for an increased soluble Aβ load in Braak stages I and II.

Three of these genes (PSEN2, EGR1 and RER1) are involved in gamma-secretase mediated APP processing. PSEN2 is a member of the gamma-secretase complex, and directly catalyzes the cleavage of APP into Aβ (Zhang and Xu 2007). As PSEN2 contains an EGR1-responsive element in the promoter region, EGR1 regulates the expression of PSEN2 (Renbaum *et al.* 2003). RER1 mediates the assembly and intracellular location of gamma-secretase (Kaether *et al.* 2007; Spasic *et al.* 2007).

PACAP regulates Aβ levels by promoting the non-amyloidogenic alpha-secretase pathway of APP processing (Kojro *et al.* 2006), and is capable of attenuating Aβ42-mediated cell death in PC12 cells(Onoue *et al.* 2002). SST regulates Aβ levels by increasing the activity of neprilysin, the main proteolytic degrading enzyme of Aβ(Saito *et al.* 2005), and SST levels are increased after administration of Aβ25-35 in cultured cortical neurons (Geci *et al.* 2007). PCSK1, alternatively named PC-1, converts the inactive proprotein pro-SST into SST, and is coexpressed with SST over the Braak stages. Finally, the synaptic zinc transporter ZnT3 releases Zn2+ into the

synaptic cleft upon neuronal activity, which can accelerate plaque formation (Ha *et al.* 2007). Indeed, in hAPP+/ZnT3-/- transgenic mice, a significant reduction in plaque load has been observed as compared with hAPP+/ZnT3+/+ mice (Lee *et al.* 2002). Thus, in Braak stages I and II, the increased levels of PACAP, SST and PCSK1 are possibly a response to increased Aβ levels, whereas PSEN2, EGR1, RER1 and ZnT3 might induce higher levels of Aβ (Figure 7).

The effect of Aβ on synaptic transmission and mitochondria possibly underlies the progression from control to MCI/AD

As discussed earlier, to maintain normal levels of synaptic transmission when confronted with increased levels of Aβ at Braak I/II, a compensatory increase in neuronal activity is required, which is represented in our gene expression dataset as an upregulation of synaptic transmission and mitochondrial gene expression. Intriguingly, recent evidence has emerged demonstrating that the release of intraneuronal Aβ into the extracellular space is directly regulated by neuronal activity. In hippocampal slices of APPSWE mice, neuronal activity modulates the secretion of Aβ, and this secretion results in selective and reversible NMDA-R dependent depression of excitatory synaptic transmission (Kamenetz *et al.* 2003). Furthermore, Cirrito et al very elegantly provided direct in vivo evidence for the relation between synaptic activity and interstitial Aβ levels (Cirrito *et al.* 2005). By simultaneously stimulating the perforant pathway, recording activity in the hippocampus, and sampling interstitial fluid (ISF), the authors showed that after 1 hour of continuous stimulation, ISF Aβ levels increased by 30%. Furthermore, by blocking neuronal activity with tetrodotoxin or tetanus toxin, a respective 40% and 70% decrease in ISF Aβ levels was observed. All of the changes in Aβ levels were reversible, providing compelling evidence that extracellular Aβ levels are directly modulated by synaptic activity. Thus, the combined observation that synaptic activity increases extracellular Aβ levels and that soluble Aβ inhibits synaptic transmission, suggest that under normal physiological conditions, Aβ is part of a negative feedback loop preventing neuronal hyperexcitability (Kamenetz *et al.* 2003).

Taken together, our dataset suggests that an imbalance in this feedback loop might underlie the sudden appearance of senile plaques in Braak III after prolonged periods of increased neuronal activity. In Braak I and II, synaptic activity gradually increases as a compensatory response to decreased synaptic efficacy (as a result of increased Aβ levels, or age-related alterations in synaptic function, or a combination of both). As Aβ secretion is regulated by synaptic activity, more Aβ is released into the extracellular space, further decreasing synaptic efficacy. In order to maintain normal cognitive function, neuronal activity/plasticity must be increased even further. This could lead to a self-amplifying cascade which ultimately, after reaching a threshold where neurons are at their maximal metabolic capacity and soluble Aβ starts to aggregate, leads to the formation of extracellular plaques.

In addition to its negative effects on synaptic transmission, APP and Aβ are also associated with mitochondrial dysfunction. Accumulation of APP and derivatives

of APP are found to block mitochondrial import channels in AD (Devi *et al.* 2006). In Tg2576 AD mice, Aβ monomers and oligomers are located on mitochondrial membranes in a transmembrane arrested form (Anandatheerthavarada *et al.* 2003). Thus, the combined effect of Aβ on the expression of genes involved in energy synthesis and synaptic transmission/plasticity are a possible explanation for the transition from Braak II to Braak III, where decreased neuronal activity is accompanied by a sudden increase in senile plaque load.

The ApoE4 allele potentially accelerates AD progression by amplifying gene group changes in the UPDOWN and DOWNUP clusters

In Braak stages III and IV, we observed a striking effect of the ApoE genotype on the magnitude of gene expression changes in the UPDOWN and DOWNUP clusters (Figure 4). Regardless of the direction of regulation, carriers of the ApoE4 allele exhibited more pronounced alterations in gene expression than non-carriers, suggesting a faster disease progression. Indeed, individuals with one or two ApoE4 alleles are known to progress faster from MCI to AD (Belbin *et al.* 2007; Craft *et al.* 1998). The differential effect of ApoE4 versus ApoE3 has been studied extensively (reviewed in Mahley *et al.* 2006). Amongst others, ApoE4 negatively affects neurite outgrowth and remodeling (Nathan *et al.* 2002; Ji *et al.* 2003), enhances Aβ deposition (Holtzman *et al.* 2000), is associated with altered CNS glucose metabolism (Wishart *et al.* 2006; Reiman *et al.* 2004; Dubelaar *et al.* 2004) and causes mitochondrial dysfunction (Chang *et al.* 2005; Devi *et al.* 2006). There is a striking overlap between processes differentially modulated by the ApoE alleles, and the gene groups in the UPDOWN clusters. Thus, the observed changes in gene expression provides strong evidence that during the progression of AD, ApoE4 specifically amplifies processes underlying neurodegeneration, such as reduced synaptic transmission and mitochondrial dysfunction.

Neuronal apoptosis and the role of sirtuins in early and late Braak stages

Whereas the gene groups associated with the UPDOWN clusters are in general associated with neuronal activity, the biological interpretation of the DOWNUP results in the context of AD is more difficult. For example, 7 out of 9 genes in the GO class "Cell Growth" are found in cancers or function as tumor suppressor genes. Inflammation and cellular differentiation and/or development appear to be the most important categories. As cellular differentiation or development is usually associated with alterations in transcription factor activities, we more closely examined the genes in the GO class "regulation of transcription, DNA-dependent" for their involvement in AD-associated neurodegeneration. We observed a concerted upregulation of TGFB1 and SMAD7 in end-stage AD. Interestingly, the expression of these genes is increased in the TgCRND8 mouse model for AD as a response to Aβ, and causes neuronal apoptosis (Salins *et al.* 2008). The increased levels of RELA and NFKB1 are also indicative for neuronal apoptosis in the latest Braak stages (Pizzi *et*

al. 2009). Furthermore, the upregulation of ID1 and ID3 is implicated in Rett Syndrome, a neurodevelopmental disorder. Together, these transcriptional alterations are indicative for neurodegenerative events leading to neuronal dysfunction or neuronal loss in the latest Braak stages. Interestingly, the histone deacetylase SIRT1 is coregulated with these genes. SIRT1 has recently gained attention as a neuroprotective enzyme in AD and its expression is regulated by resveratrol, a red wine polyphenol associated with a reduced risk for AD (Anekonda and Reddy 2006). Indeed, SIRT1 protects against microglia-dependent Aβ toxicity by increasing the acetylation of RELA, thereby inhibiting NF-kappaB signaling (Chen *et al.* 2005).

Being a member of the DOWNUP cluster, the expression of SIRT1 is decreased in Braak I-II. This downregulation thus occurs at a point in time when the levels of soluble Aβ and the metabolic demand (and associated levels of oxidative stress) are increased. One could thus hypothesize that decreased levels of SIRT1 (or rather: SIRT1-mediated neuroprotection against Aβ and apoptosis) concomitant with changes in biological processes in the UPDOWN clusters described above (APP processing & Aβ clearance, synaptic plasticity and oxidative phosphorylation) are potential causative molecular changes in the progression from control to MCI/AD. This would also provide a potential mechanistic explanation for the reduced risk for AD associated with resveratrol intake. However, this also implies that resveratrol treatments should be started before the first clinical signs of the disease, when SIRT1 levels are lowest. These data warrant further investigation of the role of sirtuins in the earliest Braak stages.

Conclusion

In conclusion, by measuring gene expression profiles in a large set of well characterized PFC samples, we report several clusters of genes with concerted alterations over the consecutive Braak stages and their possible involvement in AD pathogenesis. Intriguingly, the most profound changes occur just before the onset of senile plaque pathology, and involve a compensatory increase of neuronal activity and metabolism, possibly as a response to increased soluble Aβ levels. As synaptic activity both regulates the secretion of Aβ and is negatively affected by Aβ, we hypothesize that disturbances in this balance might cause a positive feedback loop where increasing levels of neuronal activity are paralleled by a buildup of Aβ. This might ultimately lead to senile plaque formation and a reduction of neuronal activity. These events take place before the first appearance of NFC pathology, and involve alterations in genes concerned in Aβ formation or clearance. Thus, our data provide support for the amyloid cascade hypothesis where Aβ is the initiating event in AD-associated neuropathology, and in this respect draw a parallel between genetic and sporadic forms of AD. Furthermore, our findings illustrate the importance of early intervention and suggest that treatment strategies that reduce Aβ levels in the earliest stages of AD might prevent the development of this devastating disease.

Supplementary data

Space constraints prevent the printing of the supplementary data for this chapter. The data is available from the author upon request.

Table S1 - List of all significantly altered transcripts during the progression of AD, as determined by transcript-level ANOVA. Braak stage data: log2-transformed fold change against average of all measurements. P value: Benjamini-Hochberg-corrected ANOVA p-value. Fold Change: maximum fold change between Braak stages. Cluster: cluster assignment (see Figure 4).

Table S2 – List of all significantly overrepresented GO identifiers in the UPDOWN and DOWNUP clusters. The UPDOWN table contains all GO identifiers overrepresented in clusters 6 and 23 with a $p < 0.01$. The DOWNUP table contains all GO identifiers overrepresented in clusters 12 and 24 with a $p < 0.01$ (see Figures 4 and 5). Annotated: number of genes on the array with a specific GO identifier. In cluster: number of genes in that cluster with a specific GO identifier. P value: TopGO p value.

CHAPTER 6

A meta-analysis of microarray-based gene expression studies in Alzheimer's disease

Koen Bossers, Sasja Heetveld, Dick F. Swaab,
Joost Verhaagen

manuscript in preparation

Abstract

Alzheimer's disease (AD) is the leading cause of dementia, and its prevalence increases exponentially with age. Despite extensive research efforts, the origin of this devastating disease remains poorly understood. Genome-wide gene expression studies can provide novel insights into changes in the transcriptome in AD and form the basis for studies on molecular pathways that are affected in AD. Due to the substantial variation inherently associated with gene expression studies in the postmortem human brain, independent validation of microarray results is very important. We therefore performed a meta-analysis on the combined data of five recent large-scale gene expression studies in postmortem AD brains. Most studies concerned end stage AD. The main outcome of this analysis was a set of 69 genes that was reproducibly detected as differentially expressed in three or more studies. The meta-analysis revealed a robust dysregulation of genes involved in the regulation of intracellular Ca2+ levels, suggesting an important role of Ca2+ regulation in AD-associated neurodegeneration. Furthermore, a number of genes involved in mitochondrial function, DNA damage, cell cycle regulation, synaptic transmission, inflammation and cholesterol metabolism were reproducibly detected in 3 or more studies. The dysregulation of these genes points to molecular pathways underlying AD neuropathology and can provide the basis for the design of novel drugs.

Introduction

Alzheimer's disease (AD) is a slowly progressive degenerative disorder of the human central nervous system. At age 70, around 1% of the population suffers from AD, and the prevalence doubles every 5 years (Rocca *et al.* 1991). In total, approximately 15% of elderly people over the age of 65 years is diagnosed with AD. Despite extensive research efforts, the origin of AD pathogenesis remains poorly understood. AD is mostly considered to be a multifactorial disease with age as the main risk factor. In recent years, microarray technology has revolutionized the way researchers can approach such complex disorders, by the measurement of gene expression levels of essentially all genes at the same time. As such, gene expression profiling studies are unbiased, which maximizes the possibility for detecting previously undiscovered pathways that contribute to the pathogenesis in AD.

Since the advent of microarray technology, a relatively small number of microarray studies have been conducted comparing affected and unaffected brain structures between AD patients and age-matched controls. These studies identified alterations in biological processes such as activation of apoptotic and neuroinflammatory signaling, and reduced expression of genes involved in synaptic vesicle trafficking and cytoskeleton integrity (reviewed in Reddy and McWeeney 2006). Almost all studies focused on gene expression differences between end-stage AD patients and age-matched controls. Notable exceptions are a study by Blalock et al, which distinguished between incipient and late AD (Blalock *et al.* 2004) and a study by Katsel

et al, which correlated gene expression levels to CERAD rating scores for clinical dementia (Katsel *et al.* 2007). Altogether, these studies suggest that multiple cellular pathways are involved in AD pathogenesis. Interestingly, each gene array study of postmortem AD brains has identified previously unreported genes that may be involved in AD pathogenesis. This may be due to the wide variety of brain regions profiled, number and clinico-pathological characteristics of AD and control subjects, statistical approaches and array platforms used. Since genome-wide expression studies are associated with high levels of false positives and false negatives, it is very important to know which of the findings are replicated in independent studies.

Therefore, in this article, we present a meta-analysis of five recent, high quality genome-wide microarray studies on AD postmortem brain samples. The common genes and pathways identified in the independent datasets will be discussed in the context of their potential involvement in AD-associated neurodegeneration, and may help to elucidate the most important biological processes underlying the pathological changes observed in AD.

Methods

The starting point of this meta-analysis was a query of the PubMed database including the Mesh terms "Gene array", "Alzheimer" and limits set to studies published in the last three years. We decided to limit the studies to the most recent three years, as we aimed to incorporate only studies utilizing genome-wide microarrays. This prevents confounding effects from the inclusion of "biased" microarrays covering only a specific subset of the human genome, such as the specialized ORF microarray used in the study of Bensemain et al (Bensemain *et al.* 2009). The PubMed search yielded 69 results. From this list of 69 papers we extracted all microarray studies performed on human brain samples. Subsequently, we selected those studies that used a genome-wide microarray platform. Furthermore, it was important that the full lists of differentially expressed genes were available for our analysis. Only 3 studies fulfilled these criteria: the studies by Parachikova et al (Parachikova *et al.* 2007), by Emilsson et al (Emilsson *et al.* 2006) and by Xu et al (Xu *et al.* 2006). We therefore decided to include a study by Blalock et al (Blalock *et al.* 2004) which was slightly older, but of very high quality and fulfilling all other selection criteria described above. As a fifth and final study, we included the microarray study we have generated (see Chapter 5 of this thesis). Details of the final selection of studies are given in Table 1. For all these studies, we obtained the original published lists of differentially expressed genes, focusing only on the comparison control versus end-stage AD. We then defined all genes, present in three or more lists, as reliably detected.

Dataset	Brain area	Subjects	Array platform	Number of significant genes
Bossers *et al.* 2009	Frontal medial gyrus	49 subjects, 7 patients per Braak stage for tangles (Braak I-VI), and 7 subjects without neurofibrillary tangle or plaque pathology	Aligent 44k Whole human genome (44000 probes)	992
Blalock *et al.* 2004	Hippocampus	9 controls (average Braak score for tangles: II), 22 AD patients (average Braak score for tangles: V, varying MMSE score)	Affymetrix Human Genome U133A GeneChip (> 22000 genes)	1495
Emilsson *et al.* 2006	Frontal cortex, Brodmann areas 8 and 9	61 AD samples (31 females/30 males) and 53 samples from individuals without psychiatric disorder (27 females/26 males), pooled design	cDNA microarrays: "UU arrays" (7762 cDNA clones) and "RIT arrays" (20000 cDNA clones)	2907
Parachikova *et al.* 2007	Hippocampus and prefrontal cortex	10 AD patients (amyloid load 2.7-13.5%, MMSE 17-22, BRAAK IV-V) and 14 non-demented controls (amyloid load 0-13.5%, MMSE 25-30, BRAAK I-V)	Affymetrix U95Av2 GeneChip, (> 12000 genes)	113
Xu *et al.* 2006	Hippocampus	4 APOE4/4 AD, 5 APOE3/4 AD, 3 APOE3/3 AD and 3 control samples	Affymetrix Human Genome U133A GeneChip (>22000 genes)	133

Table 1. Overview of the five gene expression studies used for the meta-analysis.

Results and discussion

The comparison of genes that were significantly regulated in end stage AD described in five genome-wide gene expression studies yielded 6 genes differentially regulated in four studies, and 63 genes in three studies (see Table 2 for the upregulated genes and Table 3 for the downregulated genes).

In the list of robustly detected genes, we observed sets of transcripts that could be categorized into functionally related groups. Here, we will discuss the most interesting gene groups and their members and their possible implications for AD. Furthermore, we will discuss the practical limitations of the meta-analysis approach presented here.

Alterations in Ca2+ homeostasis in AD

One of the most interesting findings was the dysregulation of a group of genes (ITPKB, Bcl-2, TFII-I) involved in regulating intracellular Ca2+ levels. The upregulation of Type B inositol 1,4,5-triphosphate 3-kinase (ITPKB) was observed in four out of five studies. ITPKB affects calcium signaling downstream of phospholipase C, via phosphorylation of inositol 1,4,5-triphosphate (IP3) to inositol 1,3,4,5-tetraphosphate (IP4) (Irvine *et al.* 1986). IP3 is an essential second messenger that triggers the release of Ca2+ from intracellular stores. IP3 can be rapidly converted into IP4 by the action of ITPKB to maintain Ca2+ homeostasis. Thus, the observed upregulation of ITPKB in AD patients is expected to lead to increased phosphorylation of IP3 to IP4, reducing calcium release from intracellular stores.

Release of Ca2+ from intracellular stores occurs through two channels in the ER membrane: the IP3 receptor and the ryanodine receptor. Bcl-2, which we found to be upregulated in three studies, interacts with the IP3 receptor to inhibit IP3-mediated Ca2+ release from the ER (Chen *et al.* 2004). Further support for the Ca2+ dysregulation hypothesis can be deduced from the upregulation of the transcription factor TFII-I. TFII-I, upregulated in four studies, acts outside the nucleus as a negative regulator of agonist-induced calcium entry (Caraveo *et al.* 2006). Thus, we hypothesize that the combinated upregulation of ITPKB, Bcl-2 and TFII-I together act to decrease calcium levels in the cytosol, and might therefore represent a protective mechanism against neuronal dysfunction and apoptosis (Figure 1).

The data described above suggests that neurons in end-stage AD brain are under considerable calcium homeostasis-related stress, potentially leading to changes in synaptic transmission, plasticity and neuronal survival (Mattson 2007). Although alterations in calcium homeostasis have already been linked to AD for a long time, it is important to note that these findings are almost exclusively based on in vitro experiments or familial forms of AD. For example, mutations in presenilin-1 and 2, causing familial AD, lead to overfilling of ER calcium stores (Akbari *et al.* 2004; Leissring *et al.* 2000; Mattson *et al.* 2001). The present meta-analysis suggests that calcium homeostasis is disturbed in sporadic AD as well.

Symbol	Gene name	Blalock	Bossers	Emilsson	Parachikova	Xu
AEBP1	AE binding protein 1	■	■	■		
ARID1A	AT rich interactive domain 1A (SWI-like)	■	■	■		
ATBF1	AT-binding transcription factor 1	■	■	■		
AXL	AXL receptor tyrosine kinase	■		■	■	
BAZ2B	Bromodomain adjacent to zinc finger domain, 2B	■	■	■		
BCL-2	B-cell CLL/lymphoma 2	■	■	■		
BIN1	Bridging integrator 1	■		■		■
BMPR1A	Bone morphogenetic protein receptor, type IA	■	■	■		
BTG1	B-cell translocation gene 1, anti-proliferative		■	■	■	
CASC3	Cancer susceptibility candidate 3	■	■		■	
CD59	CD59 molecule, complement regulatory protein	■	■	■	■	
CDK2AP1	CDK2-associated protein 1	■	■	■	■	
CHES1	Checkpoint suppressor 1	■	■		■	
CLIC1	Chloride intracellular channel 1	■		■	■	
CTDSP2	CTD (carboxy-terminal domain, RNA polymerase II, polypeptide A) small phosphatase 2	■	■	■		
DHCR7	7-dehydrocholesterol reductase	■	■	■		
ECE1	Endothelin converting enzyme 1	■	■	■		
ECM2	Extracellular matrix protein 2, female organ and adipocyte specific	■	■	■		
GPC4	Glypican 4	■	■	■		
GPRC5B	G protein-coupled receptor, family C, group 5, member B	■		■	■	
GTF2I	General transcription factor II, i	■	■	■		■
HIST2H2BE	Histone cluster 2, H2be	■		■	■	
HRBL	HIV-1 Rev binding protein-like	■	■	■		
ITPKB	Inositol 1,4,5-trisphosphate 3-kinase B	■	■	■	■	
LRDD	Leucine-rich repeats and death domain containing	■	■	■		
M6PRBP1	Mannose-6-phosphate receptor binding protein 1	■	■	■		
MAN2A2	Mannosidase, alpha, class 2A, member 2	■	■	■		
MXI1	MAX interactor 1	■		■	■	■
MYST3	MYST histone acetyltransferase (monocytic leukemia) 3	■	■	■		
PABPC1	Poly(A) binding protein, cytoplasmic 1	■		■	■	
PLEC1	Plectin 1, intermediate filament binding protein 500kDa	■	■	■		
PPP1R1A	Protein phosphatase 1, regulatory (inhibitor) subunit 1A	■	■	■		
PSMF1	Proteasome (prosome, macropain) inhibitor subunit 1 (PI31)	■		■	■	
SDCCAG3	Serologically defined colon cancer antigen 3	■	■	■		
SLC6A12	Solute carrier family 6 (neurotransmitter transporter, betaine/GABA), member 12		■	■	■	
VAT1	Vesicle amine transport protein 1 homolog (T. californica)	■	■	■		

Table 2 - Genes found to be significantly upregulated in end-stage AD in three or more studies.

Symbol	Gene name	Blalock	Bossers	Emilsson	Parachikova	Xu
ACOT7	Acyl-CoA thioesterase 7	■		■	■	
ARPP-19	Cyclic AMP phosphoprotein, 19 kD	■		■		■
ATP1B1	ATPase, Na+/K+ transporting, beta 1 polypeptide	■		■		■
ATP5J2	ATP synthase, H+ transporting, mitochondrial F0 complex, subunit F2		■	■		■
ATP6V1H	ATPase, H+ transporting, lysosomal 50/57kDa, V1 subunit H	■		■	■	
BSCL2	Bernardinelli-Seip congenital lipodystrophy 2 (seipin)	■		■		■
CAP2	CAP, adenylate cyclase-associated protein, 2 (yeast)	■		■	■	
CHCHD2	Coiled-coil-helix-coiled-coil-helix domain containing 2	■	■	■		■
CLIP3	CAP-GLY domain containing linker protein 3	■		■		■
COPS7A	COP9 constitutive photomorphogenic homolog subunit 7A (Arabidopsis)	■	■	■		
COX8A	Cytochrome c oxidase subunit 8A (ubiquitous)	■		■		■
CRH	Corticotrophin releasing factor	■	■	■		
CRYM	Crystallin, mu	■		■	■	
CYCS	Cytochrome c, somatic	■	■	■		
DNAJA1	DnaJ (Hsp40) homolog, subfamily A, member 1	■		■		■
DUSP6	Dual specificity phosphatase 6	■	■	■		
ENO2	Enolase 2 (gamma, neuronal)	■		■		■
F8	Coagulation factor VIII, procoagulant component (hemophilia A)	■	■	■		
GABRA2	Gamma-aminobutyric acid (GABA) A receptor, alpha 2	■	■	■		
IDS	Iduronate-2 sulfatase (Hunter syndrome)	■	■	■		
ME3	Malic enzyme 3, NADP(+)-dependent, mitochondrial	■	■	■		
MECR	Mitochondrial trans-2-enoyl-CoA reductase	■	■	■		
MTHFD1	Methylenetetrahydrofolate dehydrogenase (NADP+ dependent) 1, methenyltetrahydrofolate cyclohydrolase, formyltetrahydrofolate synthetase	■	■	■		
PDE4DIP	Phosphodiesterase 4D interacting protein (myomegalin)	■	■	■		
PNMA2	Paraneoplastic antigen MA2	■		■		■
RTN1	Reticulon 1	■		■		■
SLC25A3	Solute carrier family 25 (mitochondrial carrier; phosphate carrier), member 3		■	■		■
TAC1	Tachykinin, precursor 1	■		■	■	
TUBB	Tubulin, beta		■	■		■
TUBB4	Tubulin, beta 4	■	■			■
VAMP1	Vesicle-associated membrane protein 1 (synaptobrevin 1)	■		■	■	
VAMP2	Vesicle-associated membrane protein 2 (synaptobrevin 2)	■		■		■
WIF1	WNT inhibitory factor 1	■	■		■	

Table 3 - Genes found to be significantly downregulated in end-stage AD in three or more studies.

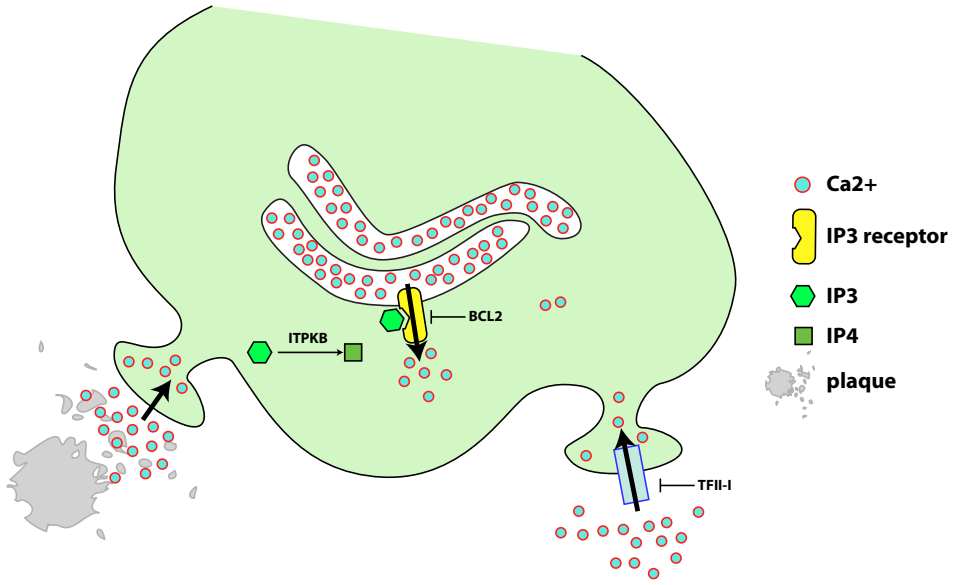

Figure 1 – Compensatory gene expression changes to dysregulation of calcium homeostasis in AD. Cytosolic calcium levels are increased in end-stage AD (in part through Aβ-mediated changes in spine function, see below). In response, IKTPB converts IP3 to IP4, thereby preventing Ca2+ release from the ER via the IP3 receptor. Bcl-2 blocks ER calcium flow through the IP3 receptor. TFII-I blocks the entrance of agonist-dependent extracellular calcium entry. Together, these gene expression alterations counteract Ca2+-induced changes in spine morphology and synaptic plasticity.

Interestingly, two very recent studies also provide compelling evidence for the involvement of calcium in sporadic forms of AD. A study by Dreses-Werringloer et al revealed that a polymorphism in the CALHM1 (calcium homeostasis modulator 1) gene influences calcium homeostasis, Aβ production and AD disease risk (Dreses-Werringloer *et al.* 2008). Furthermore, a very elegant study by Kuchibhotla et al demonstrated that, in transgenic mice, Aβ plaques can locally induce calcium overload in dendritic spines close to the plaque (Kuchibhotla *et al.* 2008). The raised calcium levels in the affected spines are associated with an abnormal morphology, and as synaptic plasticity is dependent on large rises in postsynaptic calcium levels, these data for the first time link the proximity to plaques to functional alterations in synaptic plasticity. The authors did not comment on the potential source of the calcium increase. Our data suggests that calcium release from the ER might be a good candidate, and the presence of the ER in close proximity to dendritic spines strengthens such a hypothesis (Kennedy and Ehlers 2006). In this respect, the observed changes of genes involved in calcium release from the ER might represent a compensatory mechanism against an even further increase in cytosolic calcium load. An alternative calcium source is the local synapse itself, where calcium can

enter the spine cytosol via for example NMDA receptor activation-mediated release from intracellular stores (Emptage *et al.* 1999), or via the influx of extracellular calcium through Aβ-induced membrane pores (Demuro *et al.* 2005). Interestingly, intracellular Ca2+ exacerbates Aβ aggregation (Mattson *et al.* 1993b; Mattson *et al.* 1993a), suggesting a positive feedback loop between Aβ-mediated calcium influx and Aβ formation.

As the gene expression datasets in this meta-analysis are based on end-stage AD, we cannot conclude from these data whether calcium dysfunction precedes Aβ formation or that alterations in Aβ precede calcium changes. Indeed, there is considerable debate in the scientific community on this topic and evidence for both hypotheses can be found in literature (Buxbaum *et al.* 1994; Querfurth and Selkoe 1994; Leissring *et al.* 2002; Mark *et al.* 1995). Anyhow, changes in calcium levels appear to play an essential role in end-stage AD neurodegeneration. It would therefore be of interest to study local changes in spine calcium levels in brain sections from all Braak stages, and to specifically search for gene expression changes related to calcium homeostasis in early Braak stages. Furthermore, we hypothesize that alterations in genes involved in synaptic transmission (discussed below) might be related to pre- and post-synaptic changes in calcium homeostasis, strengthening the role of Ca2+ as a central player in AD-associated dysfunction of synaptic transmission, ultimately leading to neurodegeneration.

Mitochondria and apoptosis

Previous studies have highlighted that mitochondrial abnormalities and oxidative stress play an important role in the early pathology of AD (Zhu *et al.* 2006; Hauptmann *et al.* 2006). The meta-analysis revealed the downregulation of a substantial number of genes associated with mitochondrial function. The expression of COX8A, one of the nuclear-encoded subunits of cytochrome c oxidase, is decreased in three studies. Interestingly, cytochrome c oxidase activity is known to be reduced in AD platelets and post mortem brain samples (Cardoso *et al.* 2004; Kish *et al.* 1992). In addition, we found both cytochrome c (CYCS) and the mitochondrial phosphate carrier SLC25A3, involved in CYCS release (Alcala *et al.* 2008), to be downregulated in three studies. Several other genes implicated in mitochondrial function are also downregulated, such as ATP5J2, MECR, ME3 and CHCHD2 (Inui *et al.* 1986; Pongratz *et al.* 2007; Xie *et al.* 2007; Yagi and Hatefi 1987). Mitochondrial dysfunction might be one of the prime causes for AD-associated neuronal atrophy. Furthermore, mitochondria have an important role in apoptosis, which is one of the possible mechanisms of neuronal cell loss in AD (Nagy and Esiri 1997; de la Monte *et al.* 1997). For example, CYCS triggers apoptosis when it is released from mitochondria and BCL-2, which is localized to the outer mitochondrial membrane, is the anti-apoptotic member of a large family of proteins involved in the modulation of cell death (Chao and Korsmeyer 1998). It has been demonstrated that increased expression of BCL-2 (upregulated in three studies) in APP transgenic mice is associated with neuroprotection (Karlnoski *et al.* 2007). In addition, we found

LRDD to be upregulated in three studies. This protein is isoform 2 of a p53-induced protein with a death domain (PIDD), and known to counteract the pro-apoptotic function of isoform 1 (Cuenin *et al.* 2008). Taken together, the upregulation of Bcl-2 and PIDD, and the downregulation of CYCS in end-stage AD appear to represent a protective response to apoptotic signals.

In addition to regulating apoptosis, mitochondria are intimately connected (Rizzuto *et al.* 1998; Babcock *et al.* 1997; Rizzuto *et al.* 1993) with calcium homeostasis. Mitochondria shape Ca2+ signals (Jouaville *et al.* 1995) by buffering the release of Ca2+ from the ER (Hajnoczky *et al.* 1999) and the influx of Ca2+ across the plasma membrane (Bernardi and Rasola 2007), or by providing a local source of Ca2+ for ER refilling (Arnaudeau *et al.* 2001). For example, as discussed earlier, BCL-2 inhibits ER calcium release through the IP3 receptor. Therefore, alterations in mitochondrial bioenergetics are likely to influence intracellular Ca2+ balance, and potentially contribute to Ca2+ dysregulation as described earlier in this chapter.

DNA damage, cell cycle regulators and tau phosphorylation

Alterations in the levels of proteins that control cell cycle progression have recently gained attention in relation to neurodegeneration as observed in AD (Webber *et al.* 2005). This meta-analysis revealed the regulation of several genes involved in cell cycle regulation to be altered in end-stage AD. For example, the transcription factor TFII-I, required for c-fos activated cell cycle entry (Roy 2007), is upregulated in four studies. Two enzyme families involved in transcriptional and cell cycle regulation are histone acetyl transferases (HATs, which make DNA more accessible to transcriptional regulators by acetylizing histones) and histone deacetylases (HDACs, which condense DNA by deacetylizing histones). We observed an upregulation of the histone acetyltransferase MYST3 in three out of five studies. Alterations in the acetylation state of histones are implicated in neuronal dysfunction and the balance between degeneration and survival. For example, the overexpression of certain HAT family members is neuroprotective (Rouaux *et al.* 2003). In this respect, the observed upregulation of MYST3 might be to protect neurons from AD-associated neuropathological mechanisms. This finding is particularly interesting in relation to the recently discovered neuroprotective function of sirtuins, a family of NAD+-dependent HDACs, in aging and AD (Anekonda and Reddy 2006).

On the other hand however, altered histone-DNA interactions may make DNA more susceptible to oxidative damage: the acetylated histone can dissociate from DNA, increasing the likelihood of oxidative modifications (Butterfield *et al.* 2001; Drake *et al.* 2004). In addition, a member of the Histone 2B family (HIST2H2BE) , and two genes involved in chromatin remodeling (ARID1A and BAZ2B), were found to be upregulated in three studies, potentially adding to the vulnerability of DNA to oxidative damage (Nie *et al.* 2000; Jones *et al.* 2000). Indeed, enhanced DNA and RNA oxidation has been observed in AD (reviewed in Moreira *et al.* 2008). Interestingly, the transcription factor CHES1 (upregulated in three studies), can

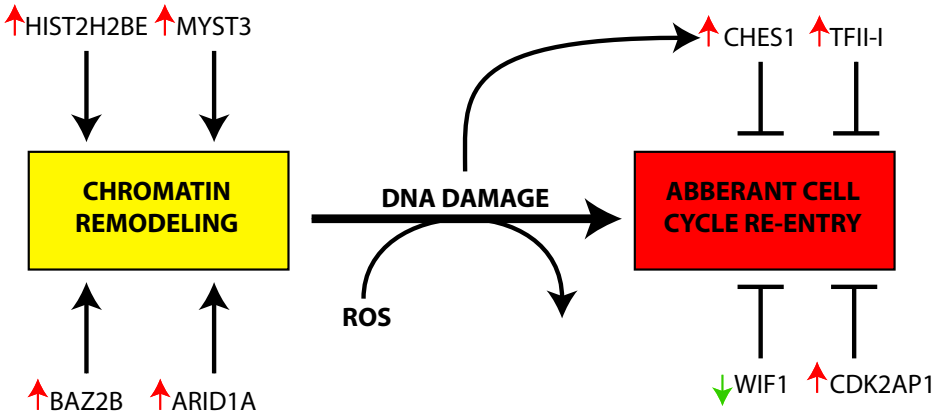

Figure 2 – Interaction between chromatin remodeling, DNA damage and aberrant cell cycle re-entry in AD. The genes involved in chromatin remodeling and histone acetylation are all upregulated, leading to exposed DNA. Subsequently, reactive oxygen species (ROS) lead to DNA damage, triggering aberrant cell cycle re-entry. In response, several genes act to restore cell cycle arrest, whereas the downregulation of WIF1 promotes cell cycle re-entry. Together, these alterations suggest increased DNA damage and disturbances in cell cycle control in AD. For details, see text.

restore cell cycle arrest in response to DNA damaged-induced cell cycle re-entry (Busygina *et al.* 2006) (Figure 2).

In relation to chromatin remodeling, histone (de)-acetylation and DNA damage-induced cell cycle re-entry, several other cell cycle proteins are abnormally upregulated in brains of AD patients (Busser *et al.* 1998; McShea *et al.* 1997). For example, there is growing evidence for the involvement of cyclin-dependent protein kinases (CDKs) in neurodegenerative disorders (Husseman *et al.* 2000; Park *et al.* 2000). In our analysis, three studies reported an upregulation of CDK2 associated protein 1 (CDK2AP1), a protein that negatively regulates CDK2 activity (Shintani *et al.* 2000). Interestingly, pharmacological inhibitors of CDKs protect cultured cortical neurons from death evoked by Aβ (Giovanni *et al.* 1999). CDKs are phylogenetically closely related to glycogen synthase kinase-3β (GSK-3β). GSK-3β participates directly in the pathological hyperphosphorylation of tau seen in AD (Wang *et al.* 2007; Sengupta *et al.* 2006; Bennecib *et al.* 2000; Flaherty *et al.* 2000) and is a well-established component target of the Wnt signaling pathway. Activation of the pathway leads to inhibition of GSK-3β and consequently a reduced phosphorylation of tau protein (Takashima *et al.* 1998). Wnt inhibitory factor-1 (WIF-1), downregulated in three studies, is a secreted antagonist of Wnt signaling (Reguart *et al.* 2004) which, via the mechanisms described above, might lead to the activation of GSK-3β and subsequently tau phosphorylation. Furthermore, WIF1 is involved in G1 arrest (Tang *et al.* 2009). Mitogen-activated protein (MAP) kinases are also directly involved in tau hyperphosphorylation, and increased MAP kinase activity is observed in the AD

brain (Swatton *et al.* 2004). MKP3, a negative regulator of MAP kinases, is downregulated in three studies. We hypothesize that decreased MKP3 levels lead to increased tau phosphorylation.

Synaptic alterations in AD

Loss of synapse function and/or synapse loss is thought to play an important role in AD (Masliah *et al.* 1991; Masliah *et al.* 1989; Hamos *et al.* 1989) and strongly correlates with cognitive decline (Terry *et al.* 1991; DeKosky and Scheff 1990). Our meta-analysis revealed a number of genes (VAMP1/2, CRH, GABRA2, GAT2, BIN1) involved in synaptic transmission to be regulated in AD. Three studies report downregulation of both isoforms of the synaptic protein synaptobrevin (VAMP1 and VAMP2). Synaptobrevin is one of the SNARE proteins involved in synaptic vesicle docking and fusion with target membranes (Jagadish *et al.* 1996; Osen-Sand *et al.* 1996). Synaptobrevin levels are known to be significantly decreased in AD brains (Shimohama *et al.* 1997), a finding which we corroborate here. Furthermore, we observed a downregulation of corticotrophin-releasing hormone (CRH), a regulator of synaptic transmission within specific neuronal circuits in the CNS (Gallagher *et al.* 2008; Orozco-Cabal *et al.* 2006), in three studies. We also observed a downregulation of GABRA2, the alpha2 subunit of GABA receptor complex, in combination with an upregulation of GAT2/BGT-1, a GABA transporter (Takanaga *et al.* 2001). GABA is considered to be the primary inhibitory neurotransmitter in the mammalian brain. Although there is only a modest loss of GABA neurons in AD (Lowe *et al.* 1988; Reinikainen *et al.* 1988; Mountjoy *et al.* 1984; Rossor *et al.* 1982), alterations in levels of subunit components of the GABA receptor complex have been demonstrated in AD patients (Armstrong *et al.* 2003; Mizukami *et al.* 1998b; Mizukami *et al.* 1998a). Furthermore, amphiphysin II (BIN1) is upregulated in three studies and plays a key role in clathrin-mediated endocytosis of synaptic vesicles (Zhang and Zelhof 2002). Abnormalities of the endosomal-lysosomal system are prominent in AD (Cataldo *et al.* 1996; Cataldo *et al.* 2004; Nixon *et al.* 2001) and upregulation of this system is especially observed in cell populations that are more vulnerable to the disease process (Cataldo *et al.* 1995).

Taken together, the transcriptional alterations of neurotransmission-related genes described here may be important players in the decline of synaptic function as observed in AD. Interestingly, the local effects of calcium on spine morphology and function as discussed earlier in this chapter may be intimately connected to the gene expression changes of the neurotransmission-related gene group.

Inflammation

Inflammatory events mediated by microglial activation accompany several neurodegenerative processes, including AD (Kalaria 1999; McGeer and McGeer 1998; McGeer *et al.* 1994). Activation of microglial cells leads to the production of various cytokines and toxic substances, which may ultimately cause neuronal injury and death (Benveniste *et al.* 2001; Combs *et al.* 2001; Styren *et al.* 1998). The chloride

intracellular channel-1 (CLIC1), is a chloride ion channel known to be associated with macrophage activation, and is upregulated in three studies. CLIC1 mediates Aβ-induced generation of reactive oxygen species (Milton *et al.* 2008). Interestingly, in vitro data suggests that blockade of the CLIC1 channel both inhibits the generation of microglial-derived reactive oxygen species and increases Aβ phagocytosis (Paradisi *et al.* 2008).

Reactive microglial cells are involved in activation of the complement cascade (Bellander *et al.* 2004; Singhrao *et al.* 1999). CD59, a complement regulatory protein that inhibits the formation of the membrane attack complex, is one of the genes found to be upregulated in four studies and increased expression of this gene has been demonstrated in AD brains (McGeer *et al.* 1991). In vitro, CD59 can protect neurons against complement-mediated damage (Pedersen *et al.* 2007), and the absence of CD59 results in exacerbated neuropathology after traumatic brain injury in vivo (Stahel *et al.* 2009). As the aggregation of Aβ strongly activates the complement system (Rogers *et al.* 1992), the observed upregulation of CD59 may be an attempt by neurons to defend themselves against complement-mediated cell lysis.

Cholesterol metabolism in AD

There is a growing body of evidence for the involvement of cholesterol in AD pathogenesis. The most important genetic risk factor for sporadic AD is a polymorphism in the ApoE gene, the major carrier of cholesterol in the CNS. Individuals carrying one or two copies of the ApoE-ε4 allele have a higher risk of developing the disease (Corder *et al.* 1993; Ferrer and Marti 1998), compared to those carrying the ApoE-ε2 or ApoE-ε3 types. Furthermore, there are cardio-vascular riskfactors for AD, and previous studies found an association between atherosclerosis and dementia, which was particularly strong in individuals carrying the ApoE-ε4 genotype (Corder *et al.* 1993; Hofman *et al.* 1997). In addition, it has been observed that patients with cardiovascular disease undergoing cholesterol lowering therapy with cholesterol synthesis inhibitors (statins) have a lower risk of developing AD (Jick *et al.* 2000; Wolozin *et al.* 2000). In APP/PS transgenic mice, a treatment with a cholesterol-lowering drug that inhibits DHCR7, reduced cholesterol levels and Aβ accumulation (Refolo *et al.* 2001). Interestingly, 7-dehydrocholesterol reductase (DHCR7), which catalyzes the conversion of 7-dehydrocholesterol to cholesterol (Wilton *et al.* 1968), was upregulated in three studies. The upregulation of DHCR7 might therefore lead to Aβ accumulation.

Methodological considerations

Although we were successful in identifying a set of genes robustly detected across 3 or 4 studies, we were unable to detect genes that were significantly dysregulated in all 5 studies under investigation. There are several potentials explanations for this somewhat unexpected finding. First of all, different classification criteria (such as Mini Mental State Examination, Aβ immunoreactivity and Braak scores for plaques

and tangles) have been used for AD disease severity. Also, due to different sample sizes, array platforms and statistical methods employed, the size of the lists of differentially expressed genes differ to a great extent between the included studies. For example, in the study by Emilsson et al, roughly 14% (2907 out of 20000) of all genes was differentially expressed, whereas in the study of Xu et al, this number was less than 1% (133 out of 22000). The lack of overlap between the relatively short lists of the studies of Xu et al (133) and Parachikova et al (113) is therefore not surprising, even more so when taking into account that the former was performed in the hippocampus, whereas the majority of the data from the latter study has been obtained from the prefrontal cortex. The hippocampus and frontal cortex are obviously very different structures with respect to the moment in the disease process and the degree to which the brain is affected, the cell type composition and functional characteristics. On the other hand, one could also hypothesize that AD-associated neuropathology induces (at least in part) similar gene expression changes in neurons throughout the brain. The combined effect of limited numbers of significantly regulated genes, and the confounding effect of gene expression differences between brain areas, may have prevented the detection of such genes.

A second limitation imposed on this meta-analysis is that the full datasets (the expression levels for all probes on the array) were not available. Having access to the full datasets allows for a more unbiased comparison. A possible approach would be to compare the overlap between gene lists of equal size (for example by sorting gene expression measurements on p-value, and selecting the top 1000 genes from each dataset) or gene lists based on a certain percentage (for example the top 5% of every dataset, sorted on p-value). Furthermore, when the full datasets of all individual arrays are available, it becomes possible to perform the same statistical analyses on all sets, further eliminating potential bias. Fortunately, more and more journals are now making the deposition of full microarray datasets into publically available databases mandatory upon acceptance. Such datasets will be of tremendous value for future meta-analyses.

One of the most important findings in Chapter 5 of this thesis, which describes the transcriptional alterations associated with the progression of AD, is the presence of very early changes in gene expression, which are potentially causative to the disease. It is important to note that current literature defines "early" changes as changes occurring in MCI (roughly Braak stage III/IV), whereas we found the most important changes to occur in Braak stage II. Therefore, we believe that future meta-analyses should focus on gene expression changes very early in the disease process, in cognitively unaffected individuals, to maximize the potential for detecting transcript changes related to the onset and progression of AD.

As briefly mentioned in the Methods section, an initial meta-analysis of high-throughput gene expression studies in human AD brain tissue has been published a few years ago (Reddy and McWeeney 2006). In contrast to our meta-analysis, the Reddy et al study was limited to the comparison of the major (biological process-based) conclusions between studies, whereas we directly compared expression changes of single genes in search of commonalities. Interestingly, the main biologi-

cal processes described in the Reddy et al study largely overlap with the biological processes, in which the genes reported by us to be robustly detected across 3 or more studies, are involved. This provides further support for the relevance of the findings described in this manuscript.

Conclusions

The meta-analysis of gene expression changes in human AD brain as described in this chapter identified a set of 69 genes identified in three or more studies, and provides insight into a number of molecular pathways that may be important in AD pathophysiology. The observation of transcriptional alterations involved in calcium homeostasis is of particular interest. Changes in calcium homeostasis appear to play a central role in neuronal dysfunction as observed in AD, by inducing synaptic alterations, apoptosis and the formation of reactive oxygen species. Indeed, gene expression changes related to all these processes are present in the set of 69 genes. Furthermore, the strong interaction between Aβ and calcium (Aβ membrane pores induce calcium entry, and calcium triggers Aβ aggregation) further stresses the importance of calcium-related gene expression changes in AD. Another very interesting observation is the interaction between chromatin remodeling, DNA damage and aberrant cell cycle re-entry. The mechanism of action of resveratrol, a polyphenol found in red wine and associated with reduced risk for developing AD, is thought to be via effects on histone acetylation (reviewed in Vingtdeux *et al.* 2008). It would be of interest to study the effects of resveratrol on the expression of the genes involved in chromatin remodeling and cell cycle control.

Finally, a meta-analysis of five genome-wide gene expression datasets in end-stage AD allowed us to focus on transcriptional alterations robustly detected across three or more studies. These findings warrant further investigations towards the potential therapeutic relevance of these gens. We hope that, in the near future, medium-throughput functional studies, such as siRNA-mediated knockdown, will result in new target genes for drug development programs.

CHAPTER 7

Neurosteroid biosynthetic pathways changes in the Alzheimer's disease prefrontal cortex

Sabina Luchetti, Koen Bossers, Saskia Van de Bilt, Vincent Agrapart, Rafael Ramirez Morales, Giovanni Vanni Frajese, Dick F. Swaab

Submitted

Abstract

Expression of the genes for enzymes involved in neurosteroid biosynthesis was studied in human prefrontal cortex (PFC) in the course of Alzheimer's disease (AD) (n=49). Quantitative RT-PCR (qPCR) revealed that mRNA levels of diazepam binding inhibitor (DBI), which is involved in the first step of steroidogenesis and in GABAergic transmission, were increased, as were mRNA levels for several neurosteroid biosynthetic enzymes. Aromatase, 17β-hydroxysteroid dehydrogenase type 1 (HSD17B1) and aldo-keto reductase 1C2 (AKR1C2), were all increased in the late stages of AD. Several GABA-A subunits were significantly reduced in AD. Increased expression of aromatase in the PFC was confirmed by immunohistochemistry and was found to be localized predominantly in astrocytes. These data suggest a role for estrogens and allopregnanolone produced by astrocytes in the PFC in AD, possibly as part of a rescue program. The reduced gene expression of some synaptic and extra-synaptic GABA-A subunits may indicate a deficit of modulation of GABA-A receptors by neuroactive steroids, which may contribute to the neuropsychiatric characteristics of this disease.

Introduction

The sex steroids, i.e. estrogens, androgens and progesterone, when synthesized and metabolized in the central nervous system (CNS), are known as neurosteroids (Baulieu 1998). In neural tissue, the enzymes involved in steroidogenesis are present both in glial cells and neurons (Stoffel-Wagner 2001; Do Rego *et al.* 2009; Mellon and Vaudry 2001). A scheme of the sex steroid biosynthesis pathway in the brain and the abbreviations used in the text are shown in Figure 1. There is substantial evidence suggesting that sex steroids can mediate neuroprotection and influence neuronal survival, neuronal and glial differentiation and myelination in the CNS by regulating gene expression of neurotrophic factors and anti-inflammatory molecules (Melcangi *et al.* 2008; Djebaili *et al.* 2005; Behl 2002; Schumacher *et al.* 2007; Bialek *et al.* 2004).

Progesterone, testosterone and estradiol have been shown to prevent neuronal loss in the CNS in animal models of neurodegenerative diseases such as Alzheimer's disease (AD), where they show neuroprotective and regenerative effects (Vongher and Frye 1999; Schumacher *et al.* 2003; Gouras *et al.* 2000). On the other hand, some metabolites of pregnenolone, progesterone, testosterone and deoxycorticosterone (DOC) are also regarded as "neuroactive" because of their ability to modulate neurotransmitter activity. Among these, 3α5α-tetrahydro progesterone (3α5α-THP or allopregnanolone), androstanediol and 3α5α-tetrahydro DOC (3α5α-THDOC) are positive allosteric modulators of ionotropic γ-amino-butyric acid (GABA-A) receptors. In particular, allopregnanolone is considered the most potent allosteric modulator of GABA-A receptors, acting in a benzodiazepine (BDZ)-like manner (Belelli and Lambert 2005).

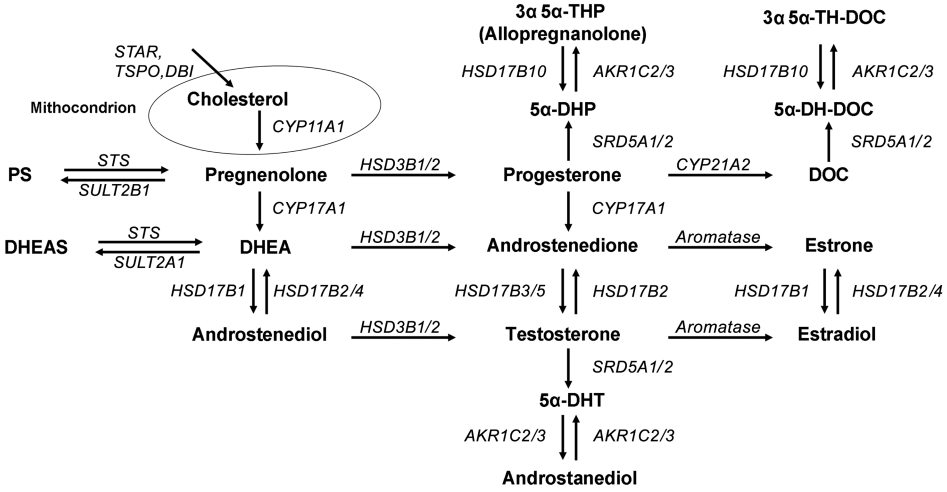

Figure 1 - Sex steroid biosynthetic pathway. All the main steps of sex steroids synthesis are shown, including the initial transport of cholesterol into the mitochondria, mediated by the complex: STAR, TSPO and DBI. Numbers after the enzyme name indicate the isoform type. Abbreviations: AKR1C, aldo-keto reductase 1C; CYP11A1, cytochrome P450scc; CYP17A1, cytochrome P450c17A1; CYP21A2, cytochrome P450c21B; DBI, diazepam binding inhibitor; DOC, deoxycorticosterone; 5α-DH-DOC, 5α-dehydro- doxycorticosterone; DHEA, dehydroepiandrosterone; 5α-DHP, 5α-dehydro-progesterone; HSD3B, 3β-hydroxysteroid dehydrogenase; HSD17B, 17β-hydroxysteroid dehydrogenase; STAR, steroid acute regulator; SRD5A, 5α-reductase; SULT, sulfotransferase; STS, steroid-sulfatase; 3α5α-THDOC, 3α 5α- tetrahydro-deoxycorticosterone; 3α5α-THP, 3α5α-tetrahydroprogesterone; TSPO, 18kDa translocator protein.

The modulatory activity of neuroactive steroids involves post-synaptic GABA-A receptors, most commonly containing the α1 (GABRA1), β2 (GABRB2) and γ2 (GABRG2) subunits, and extrasynaptic GABA-A receptors commonly containing α4 (GABRA4), δ (GABRD) or ε (GABRE) subunits (Farrant and Nusser 2005). Neuroactive steroids can also regulate the expression of GABA-A receptor subunit genes in vitro and in vivo (Biggio *et al.* 2001). As a consequence of these properties, allopregnanolone and the other neuroactive compounds modulate memory processes, anxiety, sleep processes, responses to stressful stimuli and seizure susceptibility and may influence cognitive and neuropsychiatric symptoms such as those seen in AD (Dubrovsky 2005) .

While a role for sex steroids in neuroprotection has been demonstrated in animal studies including AD models (Carroll *et al.* 2007; Ciriza *et al.* 2004; He *et al.* 2004), information is lacking about the neurosteroid biosynthetic pathway in the human

CNS during neurodegenerative processes in AD, partly because of the difficulty in obtaining suitable human brain tissue. Decreased blood levels of sex steroids with aging have been associated with an increased risk of AD (Cholerton *et al.* 2002; Pike *et al.* 2006). Combined with evidence of reduced levels of steroids such as testosterone in human AD brain (Rosario *et al.* 2004), this raises the possibility that alterations in gene expression of the enzymes which synthesize neurosteroids may be involved in the pathology of AD, which may in turn result in reduced neuroprotective actions.

The goal of the present study is to elucidate the gene expression of the enzymes involved in the synthesis of neurosteroids in the human prefrontal cortex (PFC) during the neuropathological progression of AD. Using quantitative RT-PCR (qPCR) we analyzed a list of 37 genes including the key biosynthetic enzymes, the steroid hormone receptors, and the GABA-A receptor subunits on which the neurosteroids exert their modulatory actions in the brain. Immunohistochemistry (IHC) experiments were also performed to confirm the main qPCR findings at the protein level.

Materials and methods

Subjects

Postmortem human brain tissue was obtained from The Netherlands Brain Bank, Netherlands Institute for Neuroscience, Amsterdam (NBB). Donors or their next of kin gave written informed consent to the NBB to allow the brain autopsy and to use the material and clinical information for research purposes.

Donors were grouped by Braak stage according to neuropathological diagnosis (Braak and Braak 1991). Based on the distribution of neurofibrillary tangles, 7 patients were chosen for each Braak stage (BR1 to 6) and 7 subjects with no tangles (BR0) and no neurological or psychiatric disease were included as controls. Subsequently patients were grouped based on the cognitive characteristics associated with each Braak stage as follows: BR0-2 = no cognitive impairment; BR 3-4 = mild cognitive impairment; BR5-6 = fully developed AD (Bancher *et al.* 1996).

In addition, the same subjects were also divided into three groups based on the amount of amyloid plaques (Braak and Braak 1991): A (absent or low amount), B (moderate amount), C (high amount). Subjects that were administered with indomentacin, hormone therapies and corticosteroids up to 1 month or less before death were excluded from the study. Alzheimer's patients were treated with benzodiazepine and opioids, which are routinely administered in the last days of hospitalization, but controls were matched for such treatment to minimize variability of the results. Subjects of each group were matched by age, gender, brain pH and postmortem delay. Neuropathological information is summarized in table 1.

Braak	Sex	Age	pH	BW	RIN	PMD	ApoE-ε4
0	4M/3F	70.6±9.6	6.7±0.4	1290±170	8.1±1.1	6.8±1.4	3+/4-
1	3M/4F	80.3±5.6	6.6±0.2	1250±140	8.7±1	5.9±0.9	2+/5-
2	3M/4F	76.7±7.8	6.7±0.2	1290±150	9.1±0.1	7.3±1.6	3+/4-
3	3M/4F	85±6.4	6.7±0.4	1230±160	7.7±0.9	6.2±2.6	2+/5-
4	3M/4F	82.3±4.9	6.6±0.2	1150±170	8.2±0.8	5±1.6	3+/4-
5	4M/3F	74.3±6.5	6.5±0.2	1200±120	8.3±0.8	5.4±1.2	4+/3-
6	3M/4F	70.3±7.8	6.8±0.2	1120±150	7.6±0.5	4.8±0.9	4+/3-
	p	*0.674*	*0.767*	*0.016*	*0.084*	*0.007*	

Table 1 – Patient grouping. RIN: RNA Integrity Number. PMD: post mortem delay (hours). P: ANOVA-based p-value between Braak stages. The significant interaction between Braak stage and brain weight is due to brain atrophy associated with AD.

RNA isolation and cDNA synthesis

Snap-frozen postmortem frontal medial gyrus samples were used. From each sample, approximately 30 sections of 50µm were cut using a cryostat, and grey matter was dissected out using scalpels. RNA isolation and cDNA synthesis were performed as described previously (Bossers *et al.* 2009) using 1µg of Dnase-treated RNA input for cDNA synthesis. RNA purity was determined using a NanoDrop ND-1000 spectrophotometer (Nanodrop Technologies, Wilmington, Delaware). RNA Integrity Number (RIN) was measured on the Agilent 2100 bioanalyzer (Agilent Technologies, Palo Alto, California). All RNA samples used in this study had RIN values of at least 6.5. A dilution of 1:10 of the total cDNA yield was used for the qPCR experiments.

Quantitative PCR

Sequences of the primer pairs and product sizes are shown in Supplementary Table 1. For the AKR1C gene isoforms 1, 2 and 3, which are highly similar, specific primer pairs were generated. Where possible, primer pairs were designed to span the 3'-most intron to avoid amplification of DNA templates that may be present in trace amounts in the RNA samples. The qPCR reaction contained 10 µl of 2X SYBR Green Mastermix (Applied Biosystems, Foster City, CA, USA), 3 µl of each primer pair (1 µM) and 7 µl of template cDNA (equivalent to 7 ng of total RNA in a 20 µl reaction volume. The PCR was performed in a GeneAmp 7300 thermocycler PCR program: 10 min at 95 ºC, followed by 40 cycles of 15 s at 95 ºC and 1 min at 60 ºC. For the AKR1C1 gene, the long product (280bp) was amplified by increasing the annealing/extension phase to 2 min.

The specificity of the amplification was checked by a melting curve analysis and electrophoresis of the products on an 8% polyacrylamide gel. Sterile water, RNA samples without addition of reverse transcriptase in the cDNA synthesis and DNA

samples were used as controls. Linearity of each qPCR assay was tested by preparing a series of dilutions of the same stock cDNA in multiple plates. The normalization factor was based on the geometric mean of the following 7 reference genes selected by a geNorm analysis (Vandesompele *et al.* 2002) : AURKAIP1; DHX16; ERBP KL-HDC5; ISOC2; SNW1; TM9SF4. The relative absolute amount of target genes was calculated by the formula 1010x E-ct (E=10- (1/slope)) (Pfaffl 2001). The absolute amount of transcript thus determined was then divided by the normalization factor to obtain the relative mRNA expression of the target gene.

Immunohistochemistry

Immunohistochemistry was performed on formalin fixed paraffin sections (6µm thick) of human prefrontal cortex (PFC) from 3 patients per Braak stage (Braak 0 to 6). Sections were mounted on SuperfrostPlus slides (Menzel, Germany) and dried overnight at 58 ºC followed by 24-36 hours at 37 ºC. The sections were deparaffinized and rehydrated in an ethanol series and then rinsed in distilled water. After antigen retrieval treatment (0.01M Citrate Buffer pH6 microwave for 10 min at 90ºC), sections were allowed to cool for 30 min. Primary antibodies and dilutions used were: 1) rabbit polyclonal anti-aromatase (AROM) (Yague *et al.* 2006), 1:2000, kindly provided by Prof. L.M. Garcia Segura, Instituto Cajal, Madrid, Spain; 2) rabbit anti-AKR1C (AKR1C1 to 4) (Lin *et al.* 2004),1:500, kindly provided by Prof. T.M. Penning, University of Pennsylvania School of Medicine, USA; 3) rabbit polyclonal anti-steroid 5α-reductase (SDR5A) (Thigpen *et al.* 1993), 1:500, kindly provided by Prof. D.W. Russell, University of Texas Southwestern Medical Center, Dallas, USA. For AKR1C a blocking step with TBS/5% milk was performed, while for SDR5A sections were blocked with TBS/0.1% milk. A goat-anti rabbit secondary antibody (1:400, Vector Laboratories) was applied, followed by avidin biotin complex (ABC, 1:800, Vector Laboratories) and colour developed with 0.5 mg/ml 3,3-Diaminobenzidine-tetrahydrochloride (Sigma, Zwijndrecht) and ammonium nickel sulphate (2.2 mg/ml).

For glial fibrillary acidic protein (GFAP) immunofluorescent double staining, mouse anti-GFAP (Sigma Aldrich, 1:400) with AROM (1:1000) or AKR1C (1:500) were used. Donkey anti-rabbit (Alexa488-conjugate; 1:400) and donkey anti-mouse (Alexa 594-conjugate; 1:400) were used as secondary antibodies.

Statistical analysis

Statistical analysis was conducted with SPSS (version 16.0, SPSS Incorporation). The differences between the groups were statistically evaluated by one-way ANOVA followed by a Bonferroni post-hoc test. Sex differences were evaluated by a two-way ANOVA. Values of $p<0.05$ were considered significant.

Results

Gene expression changes in neurosteroid biosynthetic pathways

One way ANOVA followed by a Bonferroni post-hoc test between the individual Braak stages (0 to 6) showed no significant differences in gene expression between Braak stages 0, 1 and 2, between Braak 3 and 4 or between Braak 5 and 6. Subsequent analysis on the patients classified by clinical stages as BR0-2 (no cognitive impairment n=21), BR3-4 (mild cognitive impairment, n=14) and BR5-6 (fully developed AD, n=14), found statistically significant changes in transcript levels for several genes.

DBI was found to be increased 1.3 fold in BR3-4 and 1.5 fold in BR5-6 compared to BR0-2 (Figure 2A). AKR1C2 was increased 1.3 fold in BR3-4 and 1.3 fold in BR5-6 (Figure 3A) and HSD17B1 was 2.1 fold increased in BR5-6 compared to BR0-2 (Figure 2B). The enzyme aromatase showed increased mRNA levels in the BR3-4 group (1.8 fold), and reached 2.4 fold higher in BR5-6 (Figure 4A). Transcript levels of the rate-limiting enzyme SRD5A1 were 1.2 fold increased in BR5-6 compared to BR3-4 although this failed to reach significance (p=0.051; data not shown).

In order to understand the influence of the amyloid plaques on the neurosteroid biosynthetic pathway the data were re-analyzed by classifying the subjects on the basis of the amount of amyloid plaques present. Patients were divided into three groups according to plaque load (A=absent or low, n=16; B=medium n=11 and C=high plaque load n=22). The same genes were found to differ significantly between groups as when subjects were classified by Braak stage. DBI and AKR1C2 mRNA levels were significantly increased respectively by 1.5 and 1.3 fold in group C compared to group A (supplementary Figure 1A,B). Furthermore, aromatase was 1.9 fold increased in group C compared to both groups A and B while HSD17B1 was 2.2 and 1.8 fold increased in group C compared to groups A and B respectively (supplementary Figure 1C,D).

Changes in gene expression of GABA-A receptor subunits.

Expression of some of the GABA-A receptor subunits was significantly changed in AD PFC as follows: GABRA1 subunit was 1.5 fold reduced in BR3-4 and BR5-6 compared to BR0-2 (Figure 5A). GABRA2 was significantly decreased (1.3 fold) in BR5-6 compared to BR0-2 (Figure 5B). GABRA4 was also 1.3 fold reduced both in BR3-4 and BR5-6 (Figure 5C), while GABRD was 1.7 fold reduced in BR5-6 compared to BR0-2 (Figure 5D).

As before, data were also analyzed by amyloid plaque load classification. Similarly to the Braak group analysis, expression of GABRA1 and GABRA4 subunits were significantly reduced (respectively by 1.6 and 1.5 fold) in group C compared to group A (supplementary Figure 2A,B). GABRD subunit was 1.4 fold reduced in group C compared to A and to B (supplementary Figure 2D). In addition, in the amyloid plaque classification analysis, expression of GAD1 and GABRB2 showed

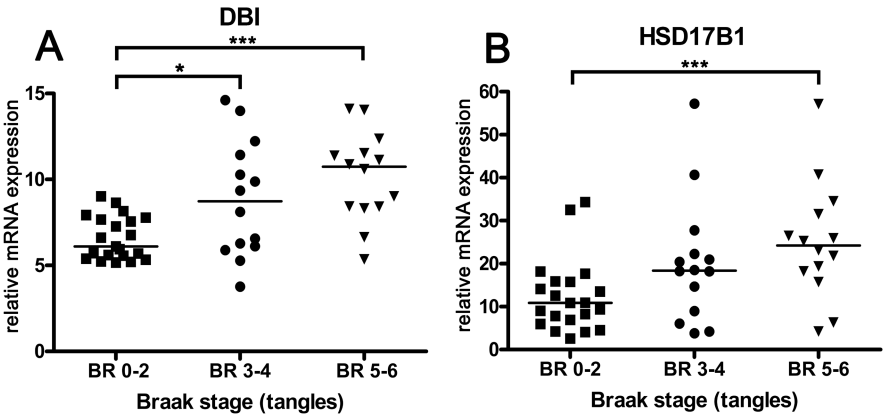

*Figure 2. DBI and HSD17B1 gene expression changes in AD PFC. Results of qPCR are shown as relative mRNA expression for each gene normalized to the housekeeping genes values as described in Subjects and Methods. (A) DBI gene expression was significantly increased in BR3-4 (*p<0.05) and in BR5-6 (***p<0.001) compared to BR0-2. (B) HSD17B1 mRNA expression was increased in BR5-6 (***p<0.001) compared to BR0-2.*

1.5 fold reduced expression in group C compared to group A. (supplementary Figure 2C,E). However, in this analysis, GABRA2 was not significantly changed.

For genes studied other than those described above no significant changes were found. No significant gender differences were found for any genes examined.

Aromatase, AKR1C and SRD5A immunohistochemistry in PFC

We performed IHC on paraffin sections of PFC in order to determine if the main findings of the qPCR were also evident at the protein level, and to determine the cellular localizations of the affected enzymes and their changes in the course of AD. The results were evaluated with a semi-quantitative analysis in which the intensity of the staining was scored in 5 categories ranging from absence (–) to very intense (++++). The staining intensities of Aromatase and AKR1C in neurons and astrocytes are shown in Supplementary Table 2 and 3.

Aromatase staining was greatly increased in layer 1 astrocytes in BR5-6 compared to the other stages (Figure 4B, C, D). Moderate staining of aromatase was found in neurons at all the Braak stages (Figure 4E, F, G). As shown in Figure 3B, C and D, AKR1C staining was present predominantly in astrocytes and was increased in BR3-4 compared to BR0-2 and BR5-6 in agreement with the qPCR data.

Expression of aromatase and AKR1C in astrocytes was confirmed by double stainings with glial fibrillary acidic protein (GFAP). GFAP-aromatase (Figure 6A, C, E) and GFAP-AKR1C (Figure 6B, D, F) colocalization was found both in the reactive astrocytes rich in GFAP and other astrocytes expressing moderate amounts of

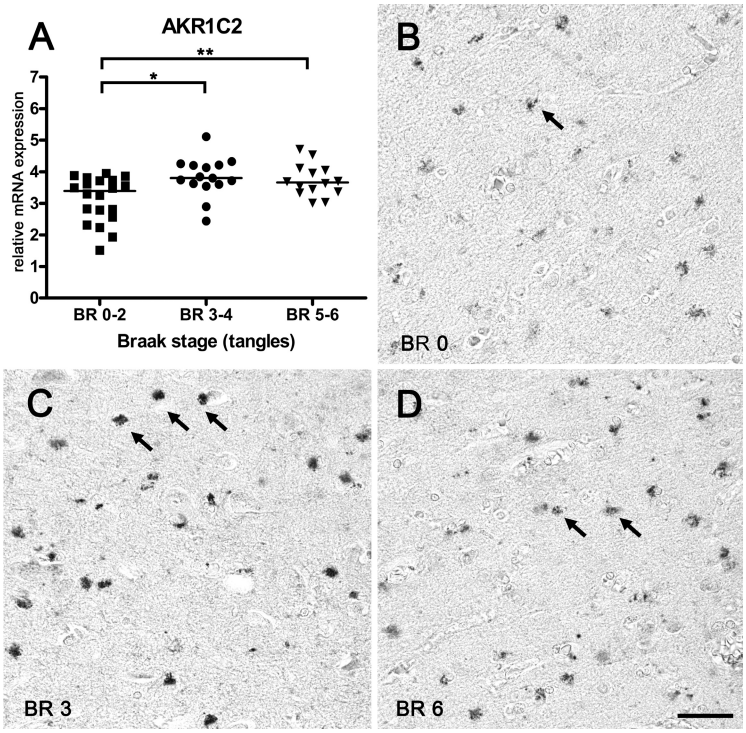

*Figure 3 - AKR1C2 gene expression and immunocytochemical changes in AD PFC. (A) Expression of AKR1C2 is significantly increased in BR3-4 (**p<0.01) and BR5-6 (*p<0.05). (B-D) Photomicrographs of AKR1C immunostaining in PFC sections (layer 1-2) show increased staining in BR3 (C) compared to BR0 (B) and BR6 (D). Arrows indicate astrocytes where expression is predominantly found. Scale bar = 25 μm*

GFAP. SDR5A moderately stained neurons but no clear increase was found in the BR5-6 compared to other Braak stages (data not shown).

Discussion

Neurosteroid biosynthetic pathway changes in AD

To our knowledge, we are the first to report changes in the pathway of neurosteroid synthesis in the human brain, during the course of AD. The qPCR data analysis of 37 genes showed that the neurosteroid biosynthesis pathway is altered in the PFC of AD patients during the course of the disease. Changes occur already in the early stages (BR3-4) and become more pronounced in the late stages of AD (Braak 5-6).

While some caution is necessary in interpreting the results, changes in regulation of mRNAs for neurosteroid synthetic enzymes are indicative of changes in the production of the enzyme themselves, which would have consequences for the balance

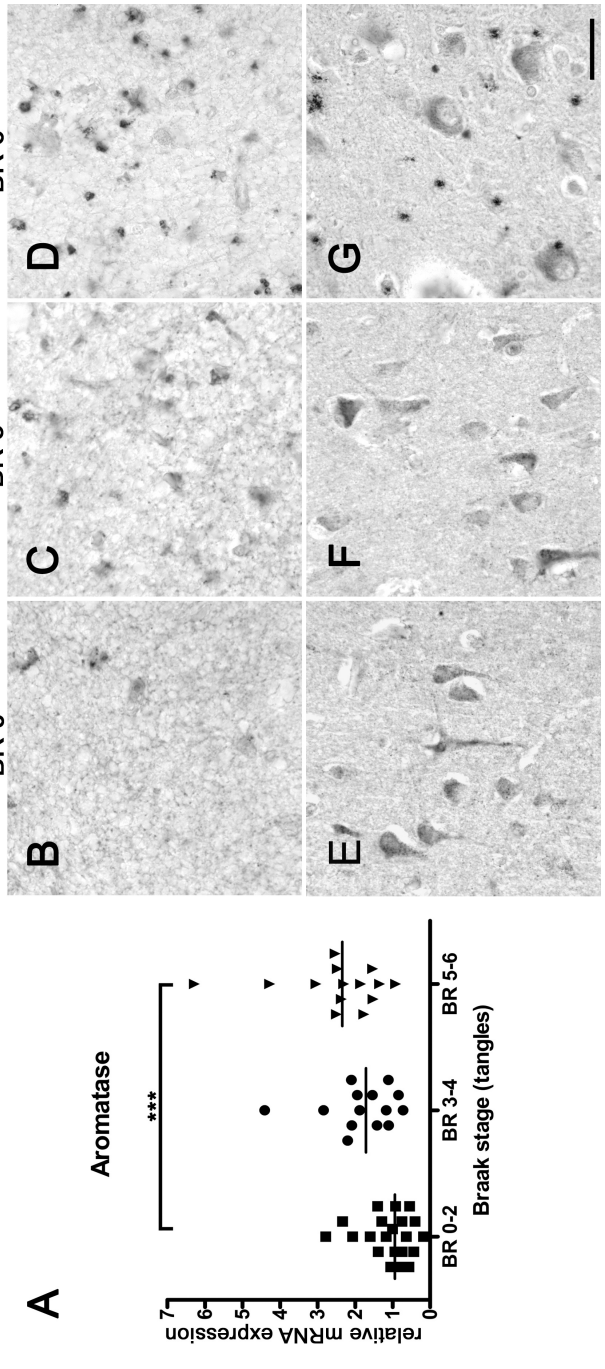

Figure 4. Aromatase gene expression and immunocytochemical changes in AD PFC.
*(A) Graph shows increased mRNA expression of the enzyme aromatase in BR5-6 compared to BR0-2 (***$p<0.001$).*
(B-G) Photomicrographs of aromatase immunostaining of the PFC in BR 0 (B,E), BR 3 (C,F) and BR 6 (D,G). In layer 1 (B,C,D) staining is increased in astrocytes. In layers 2-3 (E, F, G) aromatase expression in PFC increases with the progression of the disease and the cellular localization changes: it is found mainly in neurons in BR3 (F) but more in astrocytes in BR6 (G). Scale bar = 25µm.

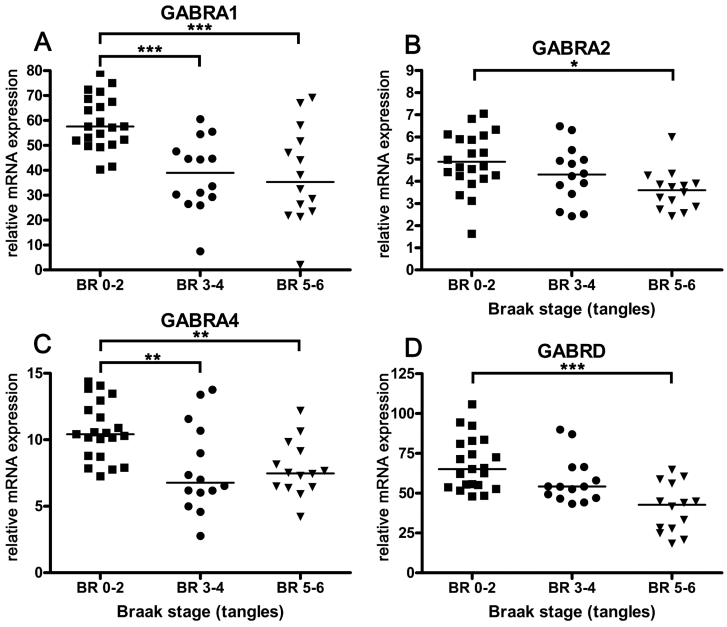

*Figure 5. GABA-A receptor subunit gene expression changes in AD PFC. (A) Reduced GABRA1 subunit expression in BR3-4 and BR5-6 (***p<0.001). (B) Reduced GABRA2 expression in BR5-6 (*p<0.05). (C) Reduced GABRA4 expression in BR3-4 and BR5-6 (**p<0.01). (D) Reduced GABRD expression in BR5-6 (***p<0.001).*

of synthesis or metabolism of the various neurosteroids. Likewise, the reduction in mRNA for neuromodulation-sensitive GABA receptor subunits suggests changes in production of these subunits, which would be expected to influence neurotransmission in the affected brain areas. However, further experiments are necessary to determine relative quantities of the steroids themselves in the brain and this would help with the full interpretation of the changes we observed.

First, the increased mRNA expression of DBI that we found in BR3-4 and BR5-6 suggests a specific involvement of cholesterol transport in the development of the disease, starting already in the stage of mild cognitive impairment (BR3-4). DBI promotes the loading of cholesterol into the mitochondrial inner membrane, both directly and via interaction with peripheral benzodiazepine receptor (PBR), recently renamed 18kDa translocator protein (TSPO) (Papadopoulos *et al.* 2006). This is a rate-limiting step for the whole neurosteroid biosynthetic pathway (Papadopoulos *et al.* 1997; Costa *et al.* 1994). Our findings suggest that in early AD, there is an attempt to increase the biosynthesis of neurosteroids and neuroactive steroids through increased mitochondrial import of cholesterol. Previously, measurements of enzyme levels in cerebrospinal fluid (CSF) showed that DBI protein levels were increased in AD patients with severe cognitive impairment (Ferrarese *et al.* 1990) although other studies failed to find any increase (Barbaccia *et al.* 1986; Ferrero *et*

al. 1988), a discrepancy which maybe related to differences in AD cognitive impairment and age range of the subjects.

Second, we found increased expression of AKR1C2 mRNA in PFC of AD patients starting from BR3. In the brain this enzyme directs the reduction of 5α-DHP into allopregnanolone and 5α DH-DOC to 5α TH-DOC (Penning *et al.* 2003) while it has been suggested that the reverse reaction is preferentially mediated by HSD17B10 (He *et al.* 2005). As we were unable to find differences in HSD17B10 gene expression, we presume that the increased amount of AKR1C2 directs the reaction towards the synthesis of allopregnanolone and 5α TH-DOC.

Allopregnanolone levels in the PFC have been evaluated in several studies but the results were not concordant. Weill Engerer *et al.* (Weill-Engerer *et al.* 2002) found no differences between BR4-6 AD and BR1-3 control brains while Marx *et al.* (Marx *et al.* 2006) recently found reduced levels of allopregnanolone in PFC of BR4-5 AD compared to BR1-3 male patients. Differences in internal standards used for gas chromatography mass spectrometry (GC/MS) measurement, small patient samples and lack of gender matching between groups of the first study may be involved in the discrepancy. In a previous study (Bossers *et al.* submitted), a large increase in tangles was found in the patients at BR3 compared to Braak 0, 1and 2 which suggests BR3 may be a critical stage in the development of the disease. Increased AKR1C2 expression beginning at BR3, as we observed, would promote an increase in allopregnanolone synthesis. One possibility is that this is a compensatory mechanism of the PFC to raise the levels of allopregnanolone. Alternatively, the elevated amount of AKR1C2 may lead to the synthesis of other neuroactive steroids such as 3α5α-THDOC and 5α-DHT (see Figure 1). Future studies analyzing the amount of these compounds would be helpful to clarify this point.

Third, we found increased expression of aromatase and HSD17B1 in AD patients during the course of the disease. By qPCR, aromatase was upregulated in BR5-6 and also in amyloid stages B and C. By IHC we observed that aromatase expression appears to be upregulated in astrocytes in the later stages of AD. Aromatase converts androgens into estrogens and HSD17B1 converts estrone into estradiol. Therefore, in late stages of AD, the balance of the neurosteroid biosynthetic pathways in PFC appears to be shifted towards the synthesis of estradiol specifically in astroglia.

Various studies in the literature are consistent with our results and suggest a neuroprotective action for estradiol in AD. Increased aromatase expression in reactive astroglia was found in response to brain injury provoked by neurotoxic and mechanical lesions (Garcia-Ovejero *et al.* 2005). Additionally, after brain injury, a neuroprotective effect for aromatase has been shown using aromatase deficient mice or mice treated with aromatase inhibitors (Garcia-Segura 2008). Attenuation of tau hyperphosphorylation induced by estradiol in HEK293 cells, suggests a preventive role for estradiol on AD-like tau pathology (Liu *et al.* 2008). In human primary culture of microglia derived from cortex, estradiol administration enhanced uptake of amyloid beta (Li *et al.* 2000). Aromatase-expressing astroglia were observed after brain injury induced by kainic acid administration or by introducing a cannula in the parenchyma in several rodent brain areas suggesting a potential for astrocytes

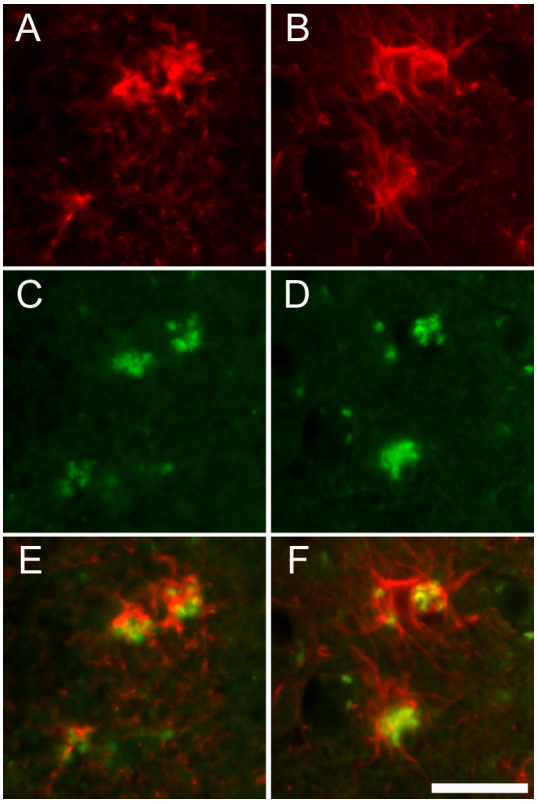

Figure 6. - Expression of aromatase and AKR1C in astrocytes in AD PFC. Photomicrographs of immunofluorescent staining for GFAP (red) and aromatase or AKR1C (green). (A, B) GFAP staining (C) AKR1C staining, (D) aromatase staining, (E) GFAP- AKR1C co-localization (F) GFAP-aromatase colocalization. Scale bar=25µm

to produce estradiol in response to injury. Estrogens are released by astrocytes as trophic factors for damaged neurons and also may be involved in compensatory restructuring of injured brain tissue (Garcia-Ovejero *et al.* 2005). Therefore, increased aromatase expression may be an attempt to induce estrogen synthesis in PFC, potentially as a part of a rescue program that takes place in brain tissue affected by a neurodegenerative process such as AD.

GABA-A receptor subunit gene expression changes

Pregnane steroids (e.g allopregnanolone and THDOC) are considered potent positive allosteric GABA-A modulators, enhancing GABA-induced Cl- currents. Studies from Biggio and colleagues (Biggio *et al.* 2006) indicated that their fluctuation may also modulate gene expression of some GABA-A receptor subunits (Concas *et al.* 1999; Follesa *et al.* 2005). This would suggest that changes in their levels in the brain may both directly and indirectly affect GABA-A receptor plasticity and consequently GABAergic transmission.

To better understand if changes in steroidogenesis in AD affect the GABAergic system, we studied the gene expression of the GABA-A receptor subunits known to be modulated by neuroactive steroids. Studies indicate that all alpha subunits are

modulated by pregnane steroids (Belelli *et al.* 2002). Beta subunits are not modulated while gamma 2 but not gamma 1 subunits are sensitive (Belelli *et al.* 2002; Herd *et al.* 2007).

Post-synaptic GABA-A receptors mediate phasic inhibition in the CNS (Farrant and Nusser 2005) and receptors containing α1 or α2 subunits are the most abundant (Mohler 2006). In this context, the reduced amount of α1 and α2 GABA-A subunit expression we found in BR3-4 and BR5-6 suggests a loss of GABAergic phasic inhibition in PFC, starting from the preclinical phases of the disease.

When patients were grouped based on amyloid plaques amount, decreased mRNA levels of GABRB2 and GAD but not of GABRA2 were found in amyloid stage C compare to A. However, reduced mRNA levels for the GABRB2 subunit and GAD, which is responsible for synthesis of GABA, would also suggest a deficit of GABAergic transmission in PFC occurring at the last stages of the disease.

Interestingly, the δ subunit, found in the extrasynaptic receptors, increases the sensitivity of the GABA-A receptor to neuroactive steroids (Belelli *et al.* 2002; Stell *et al.* 2003). In combination with α4 and β2, it is implicated in the generation of tonic inhibition in rat and mouse thalamo-cortical neurons (Farrant and Nusser 2005). In addition, its deletion in transgenic mice, if associated with α4 loss, reduces the tonic receptor activation in granule cells of the dentate gyrus by 3α5α-THDOC, leading to increased neuronal excitability (Stell *et al.* 2003).

From this perspective the down-regulation of GABA-A receptor subunits α4 and δ found during the last stages of AD would suggest that a reduced tonic activity may occur in PFC. Consistent with this, in a transgenic mouse model of Alzheimer's (Busche *et al.* 2008), a proportion of neurons near to plaques were hyperactive, as revealed by imaging of calcium transients. This hyperactivity was reduced by diazepam suggesting impairment of GABA-ergic inhibition around the plaques.

In support of the hypothesis that abnormalities of GABAergic transmission occur in the course of AD is the increased mRNA expression of DBI that we found in BR3-4 and BR5-6. DBI may inhibit GABAergic transmission by acting at the extracellular allosteric modulatory BZD binding site on GABA-A receptor alpha subunits (Papadopoulos *et al.* 1997; Costa *et al.* 1994). It is possible that DBI may participate in GABAergic modulation in PFC starting from mild cognitive impairment stages of AD.

Changes in GABAergic activity may induce imbalances in inhibitory neurotransmission in the PFC and may play an important role in the cognition and behavioral alterations such as agitation, dysphoria, anxiety, euphoria, apathy, depression, disinhibition, irritability, and aberrant motor behavior occurring in AD (Birzniece *et al.* 2006; Lanctot *et al.* 2007).

In this context, activation of synthesis of neuroactive steroids such as allopregnanolone and 3α5α-THDOC by the enzyme AKR1C2 may be part of a compensatory reaction to increase GABAergic activity at both the postsynaptic and extrasynaptic level in the course of AD.

Clinical relevance

Reduced blood or brain levels of estrogens in women after the menopause have been associated with the decline of cognitive performances in AD (Manly *et al.* 2000; Rosario *et al.* 2009). Clinical studies of hormone replacement or estrogen replacement therapy have had mixed results with the largest study being inconclusive (Mulnard 2005). In our experiments, aromatase and HSD17B1 start to be upregulated in the PFC from BR3-4 suggesting that estrogens are already synthesized in the brain in the stage of mild cognitive impairment. This supports the idea that administration of estrogens may be beneficial before these stages, probably during the peri-menopause when the treatment would have highest efficacy (Garcia-Ovejero *et al.* 2005; Lethaby *et al.* 2008; Genazzani *et al.* 2007).

Few studies have also shown reduced levels of testosterone in the aging brain as well as in AD male patients (Rosario *et al.* 2009; Weill-Engerer *et al.* 2002). Our data also suggest a possible role for testosterone metabolites such as 5α-DHT or androstanediol in AD, as indicated by the increase in AKR1C2 gene expression. Testosterone represents a potential treatment for AD in men due not only to its own neuroprotective properties but potentially also through its aromatization into estrogens. Testosterone replacement therapy improved cognitive scores in healthy men (Leichtnam *et al.* 2006; Cherrier *et al.* 2005), but had minimal effects on cognition in the development of the disease (Lu *et al.* 2006; Hogervorst 2008). Therefore, as with HRT in women, testosterone replacement therapy in aging men may be more beneficial if provided before the pathological process is too advanced.

Increasing attention has been given to progesterone and allopregnanolone as anti-apoptotic, neuroprotective and neuroregenerative agents (Wang *et al.* 2007). Indeed, our finding of increased expression of AKR1C2 and unchanged HSD17B10 suggests a role of allopregnanolone synthesis in AD as a neuroprotective or neurotransmitter modulating factor. However, administration of allopregnanolone or its precursors progesterone or medroxyprogestone had deleterious effects (Kask *et al.* 2008; Shumaker *et al.* 2003; van Wingen G. *et al.* 2007). Further clinical studies in AD are necessary to elucidate the potential of progesterone and allopregnanolone as a therapeutic agent in neurodegenerative diseases.

In summary these data provide insight into the regulation of neurosteroid and neuroactive steroid synthesis and their modulatory activity on GABA-A function in the course of AD. Our findings of increased gene expression of some key enzymes suggest a biosynthetic pathway favoring the synthesis of estradiol and allopregnanolone. These compounds exert either a neuroprotective action or have modulatory effects on GABA-A receptors, suggesting a compensatory mechanism which may partly protect the PFC from development of the disease. In addition, the reduced gene expression of some synaptic and extra-synaptic GABA-A subunits suggests a deficit of modulation of GABA-A receptors by neuroactive steroids, which may play a role in the cognitive impairment and neuropsychiatric characteristics of this disease.

Acknowledgments

Authors would like to thank, R. Balesar, B. Fisser, A. Sluiter, U. Unmehopa, J.J. Van Heerikhuize for technical assistance, Dr M. Hofman for statistical advises, Dr. M.R.J. Mason and Dr. W. Kamphuis for critical comments of the paper. SL was supported by funds from the Istituto Dermopatico Immacolata (IDI-IRCCS to Prof. G. Frajese) and the Santa Lucia Foundation (Santa Lucia-IRCCS to Prof G. Bernardi), Rome, Italy. Experimental materials were funded by the Netherlands Institute for Neuroscience to DFS. We thank the Netherlands Brain Bank for providing the human material.

Supplementary data

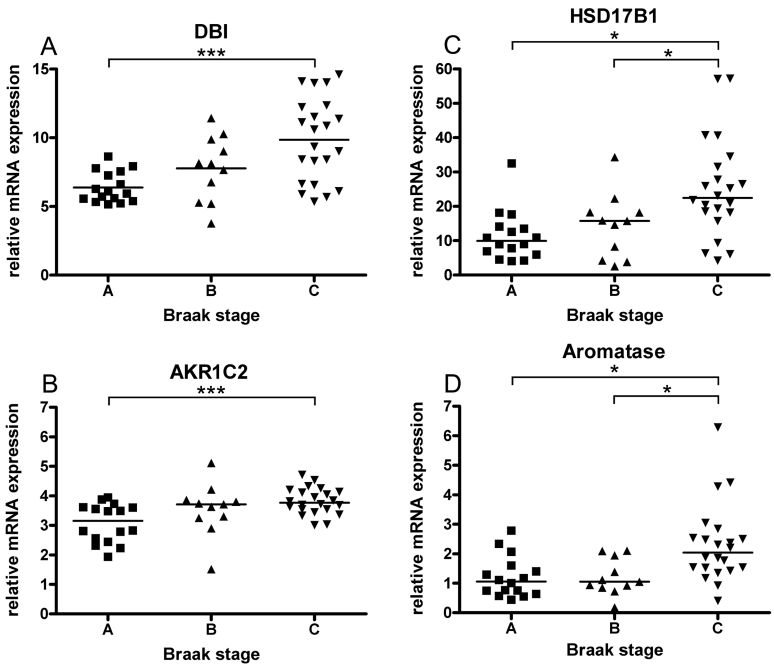

*Supplementary Figure 1. Gene expression changes of neurosteroid biosynthetic enzymes and regulator proteins in PFC of patients classified by amyloid plaque load. (A, B) DBI and AKR1C2 mRNA levels were significantly increased in group C compared to group A (***p<0.001). (C) Furthermore, HSD17B1 was increased in group C respect to groups A and B (*p<0.05). (D) Aromatase mRNA was increased in group C compared to groups A and B (*p<0.05).*

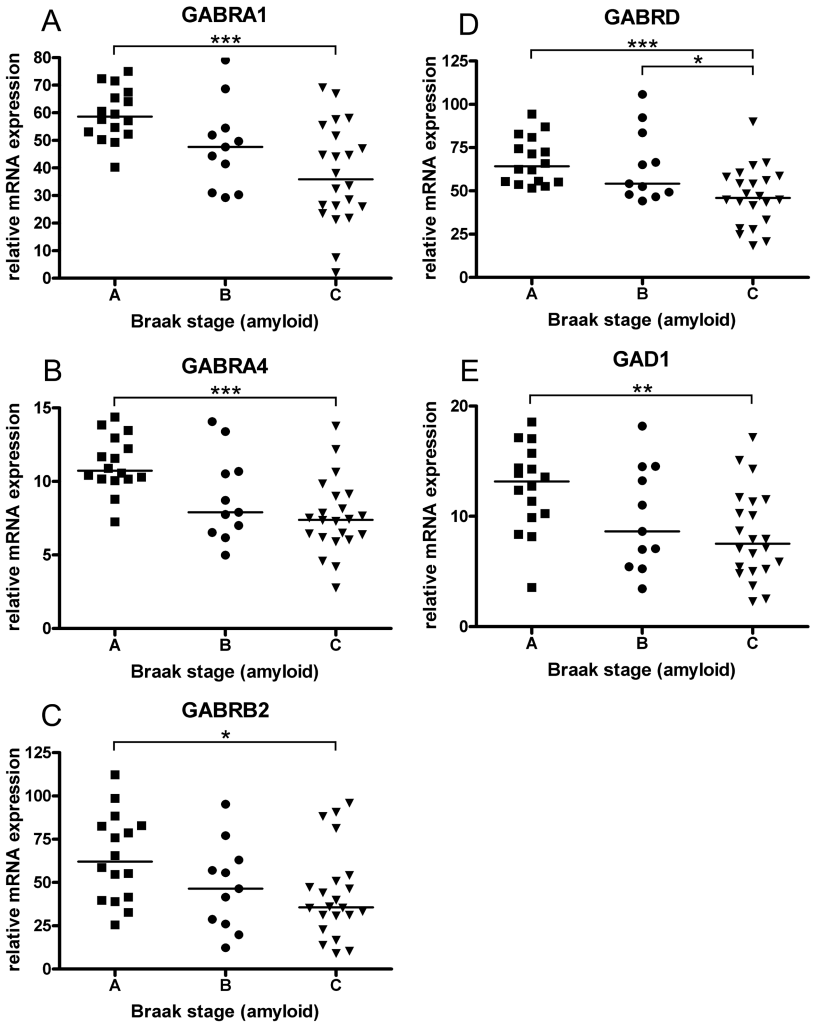

*Supplementary Figure 2. Graphs show the gene expression changes of GABA-A subunit receptor enzymes and in PFC of patients classified by amyloid plaque load. (A, B) Expression of GABRA1 (A) and GABRA4 (B) subunits mRNA were significantly reduced in group C compared to group A (***p<0.001). (C) GABRB2 subunit (*p<0.05) showed reduced gene expression in group C compared to group A. (D) GABRD subunit was reduced in group C compared to A (***p<0.001) and to B (*p<0.05). (E) In addition, mRNA expression of GAD1 was decreased in group C compared to A (**p<0.01).*

(opposite page) Supplementary Table 1 - qPCR primer sequences

Gene	Forward primer	Reverse primer	Accession numbers
Enzymes			
AKR1C1	CACAGCTTGTGTAAGACTG	GCTTCAATTGCCAATTTGGT	NM_001353
AKR1C2	GTTGTTTGAAAGTGTGTAGCA	GTCTTCACTTGGCTGGCA	NM_001354
AKR1C3	GGAGGGCTTTGCCTGATGT	GCTAAACAGGACGGATTTAAGT	NM_003739
CYP11A1	CAGTCGTCTGTCCCAAGT	CTGAGAACCCATTCAACC	NM_000781
CYP17A1	GTCATCTCCTTGATCTGCT	CTCAGGTTGTCTATGATGC	NM_000102
CYP19A1	TGCAGGAAAGTACATCGCCAT	TCCTTGCAATGTCTTCACGTG	NM_000103
CYP21A2	GGAGACAAGATCAAGGAC	CAATTTGGATGGACCAGT	NM_000500
GAD1	CTAAGAACGGTGAGGAGCAAAC	TGGTGTGGGTGATGAAAGTCC	NM_000817, NM_013445
HSD3B1-2	CGTATAAGCCACTCTACAGC	CCACAAGGGAACCAACC	NM_000862
HSD17B1	GGGGTCCACTTGAGCCTGAT	TGCCCAACACCTTCTCCATG	NM_000413
HSD17B2	CTGGGCTTCACGGTATTT	AGCAGGTTCTTCGCAATT	NM_002153
HSD17B3	CTTCTGGGATAGCCCTGTT	CTGGATGATGACTTCTTTTGC	NM_000197
HSD17B4	GCCTATGCCCTGGCTTTT	TCCTTTGAAGTCCCCTCC	NM_000414
HSD17B6	CTGAGGCGTGAGATTCAAC	GTTTGTCATTCCCGTTCTG	NM_003725
HSD17B7	GCAGGCATTCTTACACCAA	GCTCAAGGTCACCTGGATC	NM_016371
HSD17B10	CCAGCGAGTTCTTGATGTG	GCAGTGTTGATGATGACCC	NM_004493, NM_001037811
SRD5A1	TCCTCGTCCACTACGGGCAT	ACGCTTTCCTCCTCGCATC	NM_001047
SRD5A2	GCCTCTTCTGCCTACATTACT	GCAGTGCCTCTGAGAATGAG	NM_000348
STS	GGGGATGCTGTTGAGGAA	GTCCGATGTGAAGTAGATGAGG	NM_000351
SULT2A1	TGAGGAGCTGAAACAGGA	AAGTTCAGTTCTTCGGGTTC	NM_003167
SULT2B1	CGTTGTGGTCTCCCTCTATCA	AACTGCACTTCGCCTTTGAG	NM_004605, NM_177973
Receptors and regulator proteins			
AR	CAACTCCAGGATGCTCTACTTC	AGGTGCCTCATTCGGACA	NM_000044
DBI	GGCGACATAAATACAGAACG	TTCCAGGCATCCCACTT	NM_020548, NM_001079863-2
ESR1	TCTTGGACAGGAACCAGGGAA	CGGAACCGAGATGATGTAGCC	NM_000125
ESR2a	TGCTTTGGTTTGGGTGATTG	TTCCATGCCCTTGTTACTCG	NM_001437
GABRA1	ATGCCCAACAAACTCCTGC	ATAGGGAAGTCCTCCAAATGC	NM_000806
GABRA2	CTTGGGATGGGAAGAGTGTAGT	GTTCTGTATCATAACGGAAGCCT	NM_000807, NM_001114175
GABRA4	TGGGCAAACCGTATCAAGTG	GAGGTGGAAGTAAACCGTCATAA	NM_000809
GABRB1	AGCCAGAGTCGCACTAGGAAT	CCAGCAGAGCCAGGAACAC	NM_000812
GABRB2	CGGTGGATAGACTCCTGAA	TGGCAATGTCAATGTTCATC	NM_000813
GABRD	ATCGTGAACGCCAAGTCG	TGGAGGTGATTCGGATGCT	NM_000815
GABRE	CATCCTCGTATCAATAGCCGTG	GCTCCTCTCCATCACTTCCCT	NM_004961
GABRG2	CGTCCTATCCTGGGTGTCTTTC	CAATGGTGCTGAGGGTGGTC	NM_000816, NM_198903-4
GABRQ	CCTGGGAAGGACGATTACT	CCCTCTGAACCTGGAACTT	NM_018558
PGR	TCAGGCTGTCATTATGGTGTCC	GCAGTCATTTCTTCCAGCACAT	NM_000926
STAR	GGGCTCAGGAAGGACGAA	GCAAATGTGGCAGTGGTG	NM_000349
TSPO	TCTGGAAAGAGCTGGGAGG	TTGTCGGGCACCAAAGAAG	NM_000714
Housekeeping genes			
AURKAIP1	GCCTCAAATTCAGTGCAAAA	CTCGAACTTGATCTGCTTGC	NM_017900
DHX16	TTGACTCGGAGTGGCTACCG	AGCGTGGCTGTTGCTCAAAGA	NM_003587
ERBP	GGCTTCCCCAAGTACTTCCA	AGCCAGCAGTTCTTCCACAA	NM_014597
KLHDC5	AGGATGCGTGGAATTTTGTG	TTCATGTTCCGGTCTCTGGT	NM_020782
ISOC2	TGAGACAGAGTGGTGCCTTC	TTCTGGATCTCCTTGAACTGG	NM_024710
SNW1	CTTCTCCCACCTTTCAGCAT	CTCACTGTGGTTGGGGTAACT	NM_012245
TM9SF4	CCAGCTGTGTGCAGAGGATT	TCCACGATGTCCAGCTTGTT	NM_014742

Braak	Sex	Age	Neurons	Astrocytes
0	F	64	+	++
0	M	78	++	+++
0	F	74	-	+
1	M	83	-	+++
1	M	79	++	-
1	F	82	-	++
2	M	79	++	+
2	F	78	++	+
2	F	89	++	-
3	M	87	+	++
3	M	81	++	++
3	M	93	++	+
4	F	86	+	++
4	M	79	-	-
4	F	84	++	++
5	F	69	++	++++
5	F	71	+	++++
5	F	79	++	+++
6	M	80	++	+++
6	F	80	+	++++
6	M	67	-	++++

Supplementary Table 2 - Aromatase immunohistochemical staining intensity in the prefrontal cortex. Staining intensity is evaluated as: - absent; + weak; ++ moderate; +++ strong; ++++ very strong.

Braak	Sex	Age	Neurons	Astrocytes
0	F	64	-	+++
0	M	78	-	++
0	F	74	-	++
1	M	83	-	++
1	M	79	-	+
1	F	82	-	+++
2	M	79	+	++
2	F	78	++	+++
2	F	89	++	+++
3	M	87	-	+++
3	M	81	-	++++
3	M	93	-	+++
4	F	86	-	++++
4	M	79	-	+++
4	F	84	++	++
5	F	69	-	++
5	F	71	-	+++
5	F	79	-	+++
6	M	80	-	++++
6	F	80	-	+++
6	M	67	-	++

Supplementary Table 3 - AKR1C immunohistochemical staining intensity in the prefrontal cortex. Staining intensity is evaluated as: - absent; + weak; ++ moderate; +++ strong; ++++ very strong.

CHAPTER 8

General discussion

Koen Bossers, Dick F. Swaab, Joost Verhaagen

Scope of general discussion

In the studies presented in this thesis, we have identified a large number of transcriptional alterations associated with PD or AD. Molecular mechanisms in which these alterations might have a role have been postulated, and we have outlined how these mechanisms may contribute to the process of neurodegeneration.

In this general discussion we will first elaborate on three topics directly related to the findings described in this thesis, including 1) the potential influence of ApoE polymorphisms in the earliest stages of AD, 2) the role of aging in AD and 3) the observed alterations in the DAergic phenotype and axon guidance cues in PD.

The second part of the general discussion will focus on a number of methodological limitations that potentially arise when working with human postmortem brain tissue and we will illustrate the problems that might occur by briefly describing our own experience with a set of brain tissue samples of schizophrenia patients. Furthermore, additional bioinformatics methodology will be discussed that can overcome some of the drawbacks of gene ontology-based analysis of microarray datasets.

Finally, we will highlight experimental approaches that will be employed in the future by us to further unravel the complex changes in transcriptional networks involved in AD and PD pathogenesis, by means of state-of-the-art bioinformatics tools and by characterizing the potential role of the observed transcriptional alterations in relevant in vitro and in vivo models for PD and AD.

Alzheimer's Disease

The role of ApoE in the development and progression of AD

A polymorphism in the apolipoprotein E (ApoE) gen (ApoE-ε4) is the most prevalent genetic risk factor for AD. In Chapter 5, we have described the differential effect of ApoE-ε4 and ApoE-ε3 isoforms on the expression levels of the two main clusters of regulated genes during the progression of AD. Specifically, in MCI patients (defined as having Braak III-IV), the amplitude of differential gene expression is more pronounced in ApoE-ε4 carriers and is close to the levels as observed in end-stage AD, suggesting greater vulnerability and/or faster disease progression for AD-associated neuropathological alterations. Due to the number of individuals per Braak stage (n=7), our experimental design was underpowered for the detection of significant differential effects of ApoE genotype per Braak stage. Taking this limitation into account, discrimination of gene expression levels per Braak stage by further subdivision into ApoEε4 carriers and non-carriers can provide useful insights into potential trends of the effect of ApoE genotype on the gene expression changes that occur in the earliest Braak stages. In Figure 1, for each Braak stage, the mean expression level of the two UPDOWN clusters (Figure 1A&C) and two DOWNUP clusters (Figure 1B&D) are given for the ApoE4 carriers and non-carriers.

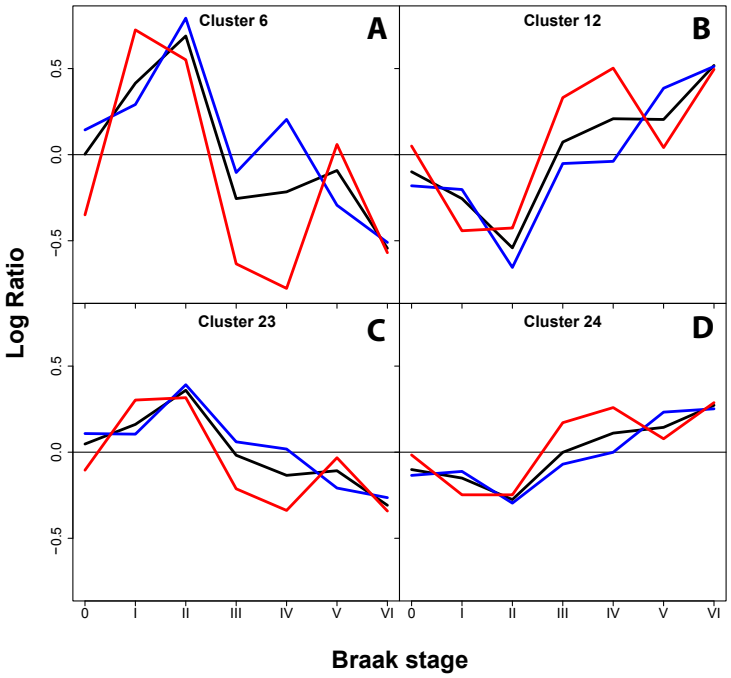

Figure 1 – Differential effect of ApoE genotype on Braak stage clusters. The mean expression levels of transcripts assigned to the four most significant Braak stage clusters (see also Chapter 5) were separated by ApoE genotype. The black lines represent the original clustering with all 7 patients per timepoint. The red line represents the time profile of ApoE-ε4 carriers, the blue line represent the time profile of ApoE-ε4 non-carriers. Note the differential expression levels at Braak stages 0-I between ApoE-ε4 carriers and non-carriers, in addition to the differences at Braak III-IV already described in Chapter 5.

In addition to the previously described differences in Braak III and IV, the ApoE genotype appears to differentially affect gene expression levels in Braak stages 0 and I. In the Braak 0 group, ApoE-ε4 carriers exhibits lower transcript levels than non-carriers for the genes in the UPDOWN clusters. As mentioned earlier, these clusters are associated with synaptic transmission and mitochondrial energy synthesis. Interestingly, in both young (29-39 years old) and aged (65-75 years old) human subjects, the ApoE-ε4 allele is associated with lower glucose utilization levels in the hippocampus and cortex (Reiman *et al.* 2004), and healthy ApoE-ε4 homozygotes in their 60s have higher cognitive domain decline and brain atrophy rates compared to heterozygotes and non-carriers (Chen *et al.* 2007; Caselli *et al.* 2007). Thus, the combined evidence of our gene expression dataset and the studies described above suggest that neuronal activity levels in the brains of ApoE-ε4 carriers are by default lower than in non-carriers. We hypothesized in Chapter 5 that one of the specific insults underlying AD is an increase in soluble Aβ levels be-

tween Braak 0 and Braak II resulting in reduced efficacy in synaptic transmission, and that the brain responds by a compensatory increase in neuronal activity. Interestingly, already in Braak I, this compensation is observed for ApoE-ε4 carriers, whereas non-carriers remain unaffected (Figure 1A&C). This suggests that ApoE-ε4 carriers might be more sensitive to increased levels of Aβ. Also, the compensatory response (increased neuronal activity in Braak I-II) in ApoE-ε4 carriers appears to be somewhat less robust (as determined by the amplitude of the UP movement in the UPDOWN clusters) than in non-carriers. These findings provide evidence that the enhanced vulnerability of ApoE-ε4 carriers to Aβ levels might originate from a reduced compensatory capacity in neuronal activity.

The differential properties of ApoE genotypes have been studies extensively (reviewed in Mahley *et al.* 2006). The three possible genotypes are based on amino acid variations at positions 112 and 158. In ApoE-ε2, both positions are cysteines, and in ApoE-ε4 both are arginines. ApoE-ε3 consists of Cys-112 and Arg-158. These amino acid variations result in an altered folding behavior for ApoE-ε4 specifically (Mahley *et al.* 2006). Interestingly, the biological effects of different ApoE isoforms are profound. For example, Aβ deposition is enhanced 10-fold in ApoE-ε4/APP transgenic mice as opposed to ApoE-ε3/APP transgenic mice (Holtzman *et al.* 2000). Furthermore, aged ApoE-ε4 transgenic mice show memory deficits in the Morris water maze test, while ApoE-ε3 transgenic mice perform as controls (Raber *et al.* 2000). An overview of the detrimental effects of ApoE-ε4 in relation to neurodegeneration can be found in Table 1 of the review of Mahley et al (Mahley *et al.* 2006). Summarizing, the differential characteristics of ApoE isoforms, mainly due to their interactions with cognitive performance and Aβ deposition, combined with the observed differences in gene expression during the progression of AD, suggest that ApoE-ε4 carriers are indeed more vulnerable to Aβ-induced neurotoxicity (possibly due to reduced metabolic activity associated with the ApoE-ε4 isoform as suggested by our data and earlier findings of our group; see Dubelaar *et al.* 2004). Importantly, we have not observed indications for differences in neurodegenerative pathways between the two isoforms: ApoE isoforms do not alter the fundamental characteristics (i.e. transcriptional activity profiles) of AD, but are most likely involved in disease vulnerability and rate of disease progression.

It must be noted that the individual variation in the AD dataset is quite large, thus care should be taken in the interpretation of the cluster data separated by ApoE genotype. For example, there is a distinct spike at Braak V for ApoE-ε4 carriers, which is difficult to interpret. However, in the light of the overwhelming data on the effect of ApoE isoforms on AD, the differential clusters presented here are very interesting, and warrant further investigation.

The relationship between aging and AD

Aging is the single largest risk factor for AD. In the brain, Aβ deposition in the form of diffuse plaques is part of the normal aging process, and can be observed in cognitively normal individuals (reviewed in Keller 2006). The question therefore arises whether there are any commonalities between molecular mechanisms underlying normal aging and AD, and which aspects of AD may be accounted for by age-related transcriptional alterations. In other words, is AD a form of premature, accelerated aging, or are the transcriptional alterations found in AD distinctly different than those found in aging?

To gain insight into this question, a comparison is needed between the effects of aging on brain function and the molecular pathways that are dysregulated during the progression of AD. In general, a decline of cognitive function is observed with age in healthy individuals. The most notable changes in memory function are reductions in short-term recall, delayed recall of verbal information and reduced speed of processing information (Albert *et al.* 1987). Long-term memory and implicit memory remain relatively well preserved during the process of aging. Interestingly, the selective loss of short term recall is also one of the main features in AD stages. The cognitive decline during the normal aging process correlates with reduced activity of the prefrontal cortex (Logan *et al.* 2002; Persson *et al.* 2004) and a loss of functional synapses (Brun *et al.* 1995). Elderly people activate larger parts of the prefrontal cortex during executive tasks, which might represent a compensatory mechanism to cope with the reduced activation (reviewed in Minati *et al.* 2007).

Genome-wide expression studies in the aging human brain

To this date, a limited number of studies have been performed that aim to monitor transcriptional alterations during the process of brain aging, mainly in rodents (Yankner *et al.* 2008). Of particular importance to this thesis are, of course, brain aging studies in human postmortem brain tissue. In 2004, Lu et al measured genome-wide transcript levels in the frontal pole of 30 individuals ranging from 26 to 106 years old (Lu *et al.* 2004). They observed that gene expression patterns were relatively homogeneous in two sample groups composed of relatively young individuals (≤42 years) or aged individuals (≥73 years). Analysis of gene expression between these two groups showed that ~450 genes were differentially expressed. More importantly, the expression levels of these genes were negatively correlated between the two groups: highly expressed genes in the "young" group were lower expressed in the "old" group, and vice versa. Gene ontology analysis revealed that transcript levels of genes involved in synaptic transmission, Ca2+ homeostasis and signaling, and mitochondrial genes were selectively reduced in the aged frontal cortex. The upregulated genes were highly enriched for genes associated with stress response, DNA repair and inflammation. Building upon these observations, the authors hypothesized that oxidative DNA damage might have selectively occurred in downregulated genes, leading to reduced transcript levels and evoking a DNA repair re-

sponse. Indeed, a comparison of the levels of DNA damage in the promoter region of stably expressed, upregulated and downregulated genes, showed that significantly more DNA damage accumulated in the downregulated genes. Furthermore, in vitro experiments on SH-SY5Y neuroblastoma cells confirmed the selective effect of oxidative stress-induced DNA damage on the transcript levels of several age-downregulated genes, whereas the levels of age-stable genes remained unaffected. Thus, these results are suggestive for the role of DNA damage in the age-related decline of synaptic transmission and oxidative phosphorylation. The mechanisms of why the DNA damage occurs in these specific genes is unknown, but one may hypothesize this is related to gene activity: genes involved in synaptic transmission and oxidative phosphorylation are abundantly transcribed in neurons, which suggests that their promoter regions might be more exposed than other genes (for example, via chromatin remodeling), resulting in greater accumulation of DNA damage.

The main findings in a second large gene expression study by Erraji-Benchekroun et al on aging in the human prefrontal cortex (39 subjects, age range 13-79) (Erraji-Benchekroun *et al.* 2005) are in general agreement with the findings presented by Lu *et al.* Correlation analysis between transcript levels and age detected sets of genes that either increased or decreased in expression with age. Indeed, the authors were able to construct a model based on "molecular" age that predicts chronological age quite well. Furthermore, genes upregulated during aging were highly enriched for glial-specific genes. Conversely, genes downregulated during aging mainly contained neuron-enriched genes. Gene ontology-based functional class scoring showed that synaptic and signal transduction gene groups were strongly suppressed in aged individuals, whereas gene groups involved in cellular defenses such as immune system and complement activation were increased. Although the vast majority of neuron-enriched genes that change during aging were downregulated, a subgroup showed increased expression with age. Interestingly, the functions of these genes are linked to oxidative stress and protection against damage to macromolecules. This provides further evidence for the involvement of DNA damage in age-related transcriptional alterations.

As a follow-up to their initial study (Lu et al 2004), Loerch and coworkers recently published a report on a multi-species comparison on the aging brain transcriptome (Loerch *et al.* 2008). Gene expression profiles were generated from cortical samples of young (n=13, ≤40 years old) and old (n=15, ≥70 years old) humans, young (n=5, 5 months old) and old (n=5, 30 months old) mice, and young (n=5, 5-6 years old) and old (n=6, 28-31 years old) rhesus monkeys. Only a limited set of genes was consistently regulated in all three species. Further analysis of species-specific aging effects showed that rhesus monkeys and humans differed from mice by a dramatic increase in numbers of depressed neuronal genes, mainly involved in synaptic function. Most notably, the GABA-ergic inhibitory system was strongly decreased in aged humans, but not in mice. Furthermore, the data demonstrated that the upregulated genes were enriched for glial genes, while the downregulated genes were enriched in neuron-specific transcripts, which is in agreement with the earlier findings of Erraji-Benchekroun *et al.* The authors hypothesized that the pronounced

reduction of the inhibitory GABA-ergic system might result in broader activation patterns in the prefrontal cortex (Minati *et al.* 2007), as a compensatory mechanism against decreased synaptic transmission. These results indicate that the process of aging is distinctly different in humans as compared to mice, which underscores the necessity for studying the biological mechanism(s) of aging and age-related neurodegenerative disorders in human brain tissue.

Expression patterns of genes modulated by age in AD

When comparing the main age-related transcriptional changes of the studies discussed above, and the patterns of gene expression during the progression of AD as presented in Chapter 5, several interesting commonalities appear. In end-stage AD, we observed a strong reduction in transcripts involved in synaptic transmission and the mitochondrial electron transport chain. Notable upregulated gene groups include antigen processing, defense response against virus and cytoskeletal reorganization. The specific downregulation of transcripts involved in synaptic transmission and mitochondrial energy synthesis, and the upregulation of inflammation-related transcript found in aging suggest that similar pathways are affected in AD and aging. This is perhaps not surprising, as the incidence of AD increases dramatically with age. However, AD is, by definition, characterized by neuropathological alterations not observed in normal aging. Most notably, normal aging is not accompanied by extensive senile plaque formation and tau hyperphosporylation and massive neuron loss in the entorhinal cortex and hippocampus. Thus, the accelerated decrease in neuronal activity combined with neuronal loss and plaque and tangle formation, together suggest that in addition to changes observed in normal aging, distinct insult(s) and/or gene expression changes exist in AD that interact with groups of genes that normally change during aging. The experimental approaches described in the Future Perspectives section below are therefore specifically aimed at pinpointing and characterizing these AD-specific transcriptional alterations.

As described in Chapter 5, we hypothesize that a buildup in the levels of soluble Aβ is the main trigger for AD-associated transcriptional alterations. This results in an initial upregulation of genes mainly involved in synaptic transmission and oxidative phosphorylation in early Braak stages (0-II), followed by a decrease in later Braak stages (III-VI). These gene expression patterns should be interpreted in the context of normal age-related transcriptional alterations and the accelerated cognitive decline in AD. Accelerated cognitive decline is not observed in the earliest Braak stages (0-II): it is not until Braak stage III-IV that the progression of AD-associated neuropathology is associated with cognitive defects compared to age-matched controls. We therefore hypothesized that the Aβ-induced decrease in synaptic function (illustrated by decreased LTP, increased LTD and reduced dendritic spine density; Origlia *et al.* 2009; Shankar *et al.* 2008) is paralleled by increased neuronal activity, in order to maintain normal cognitive performance levels. Thus, corrected for age, synaptic efficacy decreases during the progression of AD, which is initially counterbalanced by increased neuronal activity. In later stages, compensatory neuronal activation is no longer sufficient (see Figure 2). Interestingly, the

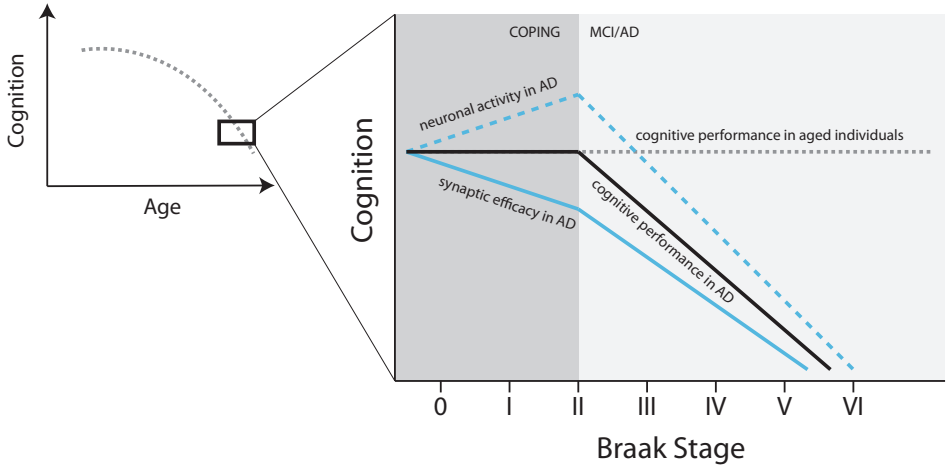

Figure 2 – (left panel) Cognitive performance in aging and AD. Cognitive performance declines with aging. (right panel) In the earliest Braak stages (0-II), a decline in synaptic efficacy is compensated by increased neuronal activity, thus cognitive performance remains unaffected by the first neuropathological alterations. In AD/MCI, synaptic activity declines even further, and the compensatory increase of neuronal activity is lost. Consequently, cognitive decline is accelerated in AD as compared to normal aging.

strong interaction between DNA damage and transcript levels of genes involved in neuronal activity suggest that when a compensatory activation is required, buildup of DNA damage might be accelerated. This suggests a "double-hit" mechanism in AD: the first hit is an increase in soluble Aβ which requires the compensatory activation of specific genes involved in synaptic transmission, plasticity and neuronal activity. As it still remains uncertain whether Aβ indeed is the first hit (although our data supports this hypothesis since we observed altered transcript levels of several genes involved in APP and Aβ processing), alternative "first hits" can be the result of genetic background (for example the ApoE-ε4 isoform) or changes in the vasculature in the aging brain (Viswanathan *et al.* 2009). The second hit may represent an increased buildup of DNA damage in these genes due to higher transcriptional activation (DNA more exposed) and increased ROS levels (as a consequence of higher metabolic activity). This second hit might trigger a self-amplifying feedback loop ultimately resulting in AD-associated neurodegeneration.

Finally, recent clinical trials based on immunization against Aβ-42 have shown remarkable results when it comes to reducing the plaque load in end-stage AD (Holmes *et al.* 2008). However, Aβ immunotherapy, when administered late in the disease process, did not result in improved cognition or enhanced survival rates, and therefore did not prevent progressive neurodegeneration. Based upon the results presented in this thesis, we predict that Aβ immunotherapy administered very early in

the disease process stands a better chance at slowing down AD-associated cognitive decline and neurodegeneration.

Parkinson's Disease

Alterations in the DAergic phenotype in relation to PD

Even after correcting for the reduction in neuronal density, we observed a highly significant decrease of several genes determining the DAergic phenotype of SN DAergic neurons (including VMAT2, NURR1 and ALDH1A1, see Chapter 3), indicating that phenotypical alterations and/or reduced activity are events that occur early in PD. Interestingly, transcription factors that control the DAergic phenotype are not only important during the development of the DAergic system, but remain essential throughout life for the long-term maintenance and survival of DAergic neurons. NURR1 for example is a key regulator of DA synthesis in mesencephalic DAergic neurons: without NURR1 expression, there is no expression of TH, VMAT2 and DAT (Castillo *et al.* 1998; Smits *et al.* 2003). Importantly, NURR1 is directly linked to PD, as point mutations in this gene have been identified that are associated with familial PD (Le *et al.* 2003). These mutations are believed to lower the expression of NURR1, and mice heterozygous for the NURR1 mutation are more sensitive for MPTP (Le *et al.* 1999), and show an age-dependent degeneration of the DAergic system (Jiang *et al.* 2005). Thus, the reduction of NURR1 expression as observed in our dataset possibly indicates that DAergic neurons in PD are more vulnerable to neurodegeneration due to reduced levels of support and maintenance of the DAergic phenotype.

The loss of, or reduction in the DAergic phenotype might also underlie the unexpected finding of an increased density in the number of neuromelanin-negative neurons in the PD SN as compared to control (Chapter 3). Neuromelanin (NM) is a complex polymeric molecule that resembles the structure of melanin found in hair, nails and skin. NM contains high levels of quinones (mainly dopa-quinone), quinone derivatives and metals (predominantly iron) (Zecca *et al.* 2003), and is thought to be formed by sequestering excess catecholamines that are not packaged into synaptic vesicles. In humans, NM starts to appear at 3 years of age, and accumulates throughout life. It is at present unknown whether the formation of NM is reversible: it is however not unlikely that a shutdown of DA synthesis eventually results in a slow clearance of NM. The increased density of non-pigmented neurons in "spared" parts of PD SN might be explained by such a phenomenon. Interestingly, a loss of NM can contribute to PD-associated neurodegeneration, due to its iron-sequestering properties. In the aged SN, iron deposits can be found in NM-negative neurons, whereas these deposits are absent in NM-positive neurons (Zucca *et al.* 2006). The absence of NM is thus possibly associated with higher iron loads, which are known to be toxic for neurons (Gaasch *et al.* 2007). These toxic insults are of particular relevance to DAergic neurons, as these already suffer from high levels

of oxidative stress due to oxidative byproducts of DA itself. The NM-negative neurons might therefore represent a population of neurons that have lost their DAergic phenotype and are prone to degenerate. An alternative possibility for the increased density of NM-negative neurons in the PD SN is that certain subpopulations of neurons, with a different ratio of NM-positive and –negative cells, are preferentially preserved during the course of PD. This might result in a bias in the density measurements. Nevertheless, the observation of an increased density of NM-negative neurons in PD (Chapter 3) warrants further investigations, for example by studying the phenotypic characteristics of the NM-negative neurons in PD and control subjects by immunohistochemical and in situ hybridization-based detection of NURR1 in the different stages of PD.

Axon guidance cues in Parkinson's Disease

The discovery of several molecules possibly involved in axon guidance (ROBO2, RGMA, SLITRK5, NETO2, SDC2 and Sema5A, see Chapter 3) raises interesting questions about the potential involvement of axon guidance cues as an early event in PD-associated neurodegeneration. Axon guidance cues are well known for their roles during the development of the nervous system and after nerve injury. Examples of axon guidance cues after injury include the upregulation of RGMA after ischemic brain injury (Schwab *et al.* 2005) and the increased expression of semaphorin 3A (Sema3A) in scar tissue after injury to the spinal cord, where it contributes to the non-permissive character of the neuronal scar (De Winter *et al.* 2002). In this sense, the observed upregulation of RGMA in the SN of PD patients might be involved in the formation of an inhibitory scar. ROBO2 on the other hand is downregulated in the PD SN. Interestingly, increased expression of ROBO2 is observed in the lumbar dorsal root ganglia after sciatic nerve injury, but not after injury to the central DRG axons by means of dorsal rhizotomy (Yi *et al.* 2006). Furthermore, axon guidance cues can have both chemoattractant and chemorepellent properties, for example depending on their interaction with specific components of extracellular matrix (see also discussion on sema5A below). The upregulation of SDC2 is an indication for an altered extracellular matrix in the PD SN. Taken together, the observation of alterations in axon guidance in the PD SN might be attributable to the formation of scar tissue after the DAergic neurodegeneration. In this light, these changes would be secondary effects that are not directly involved in the early stages of the demise of DAergic neurons but may contribute to neuronal degeneration during the later stages of the disease process.

However, functional axon guidance cues are not restricted to the injured or developing nervous system. Studies in the rodent CNS have revealed that axon guidance signaling occurs in the fully developed, intact adult nervous system. For example, the chemorepulsive Sema3A protein can be found in perineuronal nets in the visual cortex and the hippocampus (Tam Vo and Joost Verhaagen, personal communications), and is expressed on neuromuscular junction of type IIb muscle fibers (De Winter *et al.* 2006). Addition of Sema3A or Sema3F to acute cultures of adult

hippocampal slices modulates synaptic transmission (Bouzioukh *et al.* 2006; Sahay *et al.* 2005). Similarly, in the adult hippocampus, glial-derived ephrin-A3 (a receptor protein-tyrosine kinase) can alter dendritic spine density (Bourgin *et al.* 2007; Murai *et al.* 2003), and ephrin receptor signaling is involved in synapse formation and plasticity (reviewed in Aoto and Chen 2007). It is therefore hypothesized that axon guidance molecules might be involved in regulating synaptic plasticity and neurotransmission in the adult nervous system. Thus, an alternative hypothesis hypothesis of the axon guidance molecular changes would be that the dysregulation of axon guidance cues causes local changes in connectivity to the SN. For example, if the alterations in guidance cues result in loss of synaptic contacts between the dendritic component of SN DAergic neurons and axons innervating the SN, the SN might become dysfunctional. In such a case axon guidance molecules may be interesting novel therapeutic targets in PD. There is also evidence supporting alterations in the striatum that ultimately affect SN DAergic function. It has been reported that PD starts within the striatum, and that SN DAergic neurons degenerate in a dying-back phenomenon (Herkenham *et al.* 1991; Wu *et al.* 2003). The fact that the loss of innervation of the putamen is more severe than the caudate nucleus, argues in favor of differences at the level of the striatum, although alterations in innervation patterns at the level of the SN could also be a reason for such differences. However, we have not observed alterations in the expression of axon guidance genes in the putamen and caudate nucleus datasets, which suggests that the transcriptional changes originate from the SN itself. It is possible that expression changes in DAergic neurons in the SN result, via anterograde protein transport, in altered axon guidance cues in the striatum. Another possibility is that alterations in the SN itself contribute to DAergic neurodegeneration in PD. A possible way of determining whether altered axon guidance cues occur at the level of the striatum or the SN, is by the detection of RGMA, SDC2 and Sema5A using immunohistochemical and in situ hybridization techniques. We are currently engaged in these experiments, which are described in more detail later in this discussion.

Genetic alterations in axon guidance cues in relation to PD

Although not significantly different in our comparison of 7 PD and 8 controls, our dataset seems to suggest a robust upregulation of Sema5A in a subgroup of PD patients (Figure 3). This finding is particularly interesting as two genetic association studies identified a SNP in the Sema5A gene to be linked with increased risk of developing PD (Ding *et al.* 2008; Maraganore *et al.* 2005), although this finding was not reproduced in other studies (Bialecka *et al.* 2006; Clarimon *et al.* 2006). We therefore hypothesize that within a subset of PD patients, alterations on DNA sequence level and/or expression of the Sema5A gene result in increased vulnerability to develop PD. This increased vulnerability might already originate from Sema5A-dependent effects on the development of the DAergic system, resulting in system that is slightly differently wired and is more sensitive to certain insults. Such a mechanism has already been observed for other diseases. In several families, partial haploinsufficiency of ROBO1 contributes to dyslexia, most likely due to

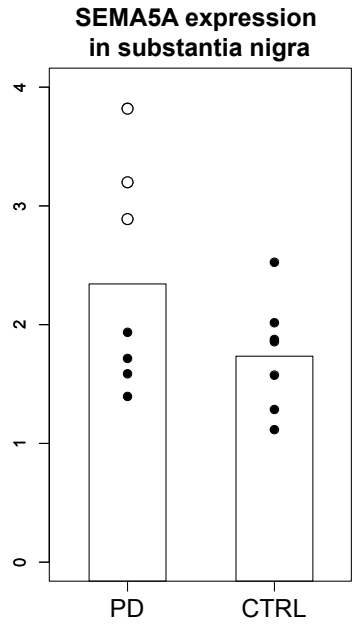

Figure 3 – SEMA5A expression in the substantia nigra of PD patients and controls, as determined by quantitative PCR. Note the high expression levels in a subset of PD patients, indicated by the open circles. Y-axis: arbitrary expression level.

small alterations in midline crossing or dendrite organization (Hannula-Jouppi *et al.* 2005). The question why Sema5A expression is increased in only a subset of patients is unclear. There are no obvious communalities between the subjects with high Sema5A expression in terms of age, sex, RNA integrity and cause of death. Possibly, the SNP in the SEMA5A gene might be involved. Further investigations are needed to investigate this intriguing topic.

A separate line of evidence linking gene-level alterations in axon guidance mechanisms to PD has recently emerged from genome-wide SNP analyses. A study by Lesnick et al combined data from genome-wide association studies with a pathway analysis focused on axon guidance genes (Lesnick *et al.* 2007). Their approach was based on the hypothesis that genetic contributions to a complex disorder such as PD might occur as SNPs in sets of genes that are involved in similar biological processes. Specifically, the authors used SNP data in more than 100 genes involved in axon guidance (being member of the KEGG pathway hsa04360 "Axon Guidance") to construct models predicting PD susceptibility, survival free of PD and age of onset. Indeed, in two independent datasets, these models were able to segregate PD and control patients with high confidence, and the associated p-values were highly significant. Interestingly, as the two datasets differed to a large extent in measured SNP markers, the replication of the interaction between axon guidance pathways

and PD becomes even stronger. Furthermore, several of the SNPs significantly interacting with PD occurred in genes (CDC42, PAK3, PAK4, ROBO2, SLIT2, CXCR4 and SEMA4D) found to be dysregulated in the SN, caudate nucleus or putamen according to a recent microarray study of PD (Papapetropoulos *et al.* 2006). Thus, this study provides compelling data for the involvement of axon guidance cues in PD. Unfortunately, as already mentioned in the introduction of this thesis, the interpretation of these SNP-based data sets remains cumbersome, with one study confirming the observations of Lesnick et al (Srinivasan *et al.* 2008), and one study negating the findings (Li *et al.* 2008).

Summarizing, the data of our and other gene expression studies in PD, combined with the data of single- and genome-wide association studies, suggest that axon guidance cues have a role in PD-associated neurodegeneration. Further research into the exact role of these genes is warranted, and we will therefore include axon guidance genes in the follow-up studies described later in this chapter.

Human postmortem brain material: practical limitations

Although many human diseases have been modeled in experimental animals, most of these animal models do only recapitulate a particular aspect of the disease process. This is particularly true for age-related neurodegenerative diseases like AD and PD. Therefore, the availability of human postmortem brain tissue is of great importance for biological studies on human neurodegenerative and psychiatric diseases. There are, however, also inherent limitations of the use of postmortem human tissue that could confound measuring the biological effect of interest. We will discuss potential issues that have to be taken into account when using human brain samples in general, and with a special focus on human gene expression profiling studies.

Sample matching

The process of selecting human samples in such a way that biological variance is minimized is extremely difficult. Sample selection is of course limited by the samples available in postmortem tissue repositories. For example, The Netherlands Brain Bank (NBB) has a large collection consisting of brain samples of ~2000 donors. However, this collection is not necessarily a reflection of the general population. Aside from the obvious age-bias towards elderly individuals, the demographics of donors that enroll into a brain bank program might be biased towards sex, certain ethnicities or levels of education (Tsuang *et al.* 2005a). The effect of such a bias might not be an issue when studying most diseases, but it is for example known that the risk of developing dementia is lower in men (Azad *et al.* 2007) and in individuals with a better education (Gatz *et al.* 2006), but the disease progresses more

rapidly in the latter group (Hall *et al.* 2007). The researcher should be aware of such potential confounders when extrapolating results to the general population.

Basic sample matching is usually performed by matching on age, sex and diagnosis. Especially in the case of genomics and proteomics experiments, the agonal state and prolonged periods of post mortem delay should be taken into account as well due to their detrimental effect on RNA and protein integrity, and the different half-lives of certain protein and RNA species (Catts *et al.* 2005). The effect of RNA integrity on measuring transcript levels will be discussed in detail later in this section.

In addition to basic sample matching, more advanced sample selection procedures aid in reducing variation. It is important to take into account drugs that influence gene expression in the brain. Notable examples are drugs of abuse, which are, amongst others, known to influence the expression of genes regulating the circadian clock (Perreau-Lenz and Spanagel 2008) and immediate-early genes in the prefrontal cortex (Harlan and Garcia 1998). But in principle all psycho-active drugs might have large confounding effects on transcript levels in the brain. On numerous occasions, we have encountered the use of morphine for pain relief purposes in the last few days before death. It is very important to try to match for such parameters as well. Furthermore, we have excluded patients treated with corticosteroid, as these compounds were found to influence gene expression as well (Erkut *et al.* 2002; Alkemade *et al.* 2005; Liu *et al.* 2006). There are of course situations where it is impossible to match for drug intake. For example in PD, almost all patients receive some sort of DA replacement therapy, mostly in the form of L-dopa.

Agonal factors

In the last several years, it has become apparent that agonal factors have a significant influence on gene expression profiles measured in human brain. A study by Tomita et al showed that the main source of variation in a study examining gene expression changes in bipolar disorder and major depression was agonal state, and not the clinical diagnosis (Tomita *et al.* 2004). While one could argue that transcriptional alterations in these two disorders might be very small, agonal factors also had a larger effect on measured transcript levels than gender, age and postmortem factors. This can be attributed to the detrimental effect of specific agonal conditions such as coma, hypoxia and pyrexia on brain acidosis and RNA integrity. Agonal factors are not readily quantifiable, but correlate very well with brain tissue pH (Stan *et al.* 2006; Tomita *et al.* 2004). Indeed, in the initial selection phase of caudate nucleus samples in the PD study, we observed a trend between RNA integrity and pH of cerebrospinal fluid (Mann-Whitney U-test, $p=0.12$, data not shown). Thus, a practical means of excluding samples with large agonal effects is to discard samples with low brain pH. Furthermore, when examining the cause of death of the same sample group, it was found that a slow course of death was associated with low RNA quality (Fisher Exact test, $p=0.04$, data not shown). RNA quality determination was based on the ratio between 18S and 28S ribosomal RNA peaks. After sample amplification and labeling, we were unable to observe differences in distribution of transcript

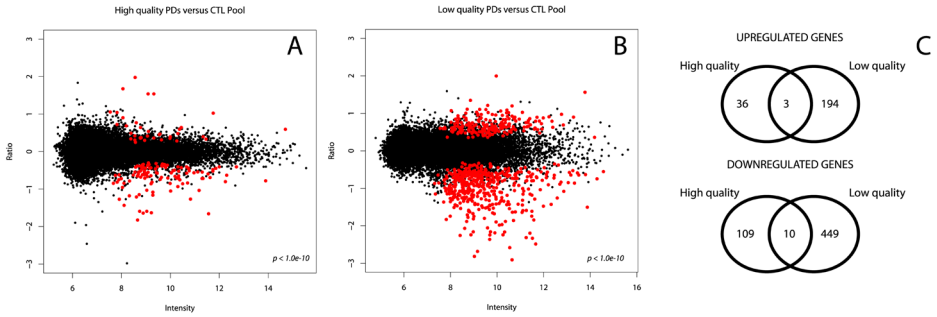

Figure 4 – Comparison of gene expression profiles of samples with high and low RNA quality. A) 3 high quality PD caudate nucleus samples versus a pool of control samples (n=8), B) 3 low quality PD caudate nucleus samples versus the same control pool. Red dots represent significantly regulated genes. C) Overlap between significant genes from the high and low quality datasets.

lengths between high and low quality samples. We therefore decided to examine the effect of RNA integrity on gene expression profiles. To this end, we hybridized 3 PD caudate nucleus samples of lower RNA quality, and 3 PD caudate nucleus samples of high RNA quality against a pool of control samples (n=8). All samples were hybridized twice, and data were analyzed in Rosetta Resolver. We observed a large difference between sets of differentially expressed genes in the high and low RNA quality datasets. Visual inspection of regulated genes (uncorrected p-value < 1e-10) revealed that the low RNA quality dataset contained a large number of mainly downregulated genes that were absent in the high quality dataset. Indeed, the overlap between the two analyses was very poor (Figure 4). Only 3 genes were found to be upregulated in both datasets, out of 39 in the high quality dataset and 197 in the low quality dataset. The findings for downregulated genes were similar: out of 119 genes in the high quality set and 459 genes in the low quality set, only 10 genes overlapped. Although we would now have approached the data analysis in a more robust manner (for example by determining the correlation between the at that time unavailable RNA Integrity Number and gene expression levels), the discrepancy between results from the high and low RNA quality datasets is evident.

RNA integrity and gene expression

The introduction of the RNA Integrity Number (RIN) as a quantitative measure of RNA integrity allows for a more systematic approach in quality control and inclusion/exclusion procedures for gene expression studies. A study by Fleige et al systematically examined the effect of RIN values on qPCR gene expression measure-

ments (Fleige and Pfaffl 2006). The authors studied interaction between RIN values and the Cycle threshold (Ct) value of four different mRNA species (28S, 18S, β-actin and interleukin 1-β). An inverse correlation between RIN value and Ct value was observed, indicating that absolute transcript levels decline with lower RIN values. However, most qPCR and microarray applications use relative expression values. This implies that as long as the relative ratios between the genes of interest and internal control genes are not affected by RNA degradation, the sample can still be used. The authors concluded that the internal ratio between genes remains unaffected when RIN values are > 5, and recommend that samples below this RIN value should be excluded from qPCR experiments. However, microarray experiments are more sensitive to RNA degradation artifacts than qPCR experiments. This is mainly due to the cDNA synthesis strategy, as cDNA synthesis is based on priming with oligo-dT primers. Thus, cDNA products are biased towards the 3'-end of the mRNA molecule. To minimize the potential bias on gene expression measurements, probes on Agilent arrays are designed against transcript regions within 1200 nucleotides of the 3'-end. Reliable detection of transcript levels would however still require the generation of relatively long amplicons. This is certainly not the case for RNA with lower RIN values (Fleige *et al.* 2006). Wherever possible, we employ a RIN cutoff > 7 to minimize artifacts originating from differences in RNA integrity.

A good example of the application of RIN values in the process of quality control can be found in the RNA isolation phase of our AD study. RNA isolation was carried out in 11 batches of 4-6 samples. After measuring RIN values of all samples, we found evidence for a small but significant batch effect resulting in lower RIN num-

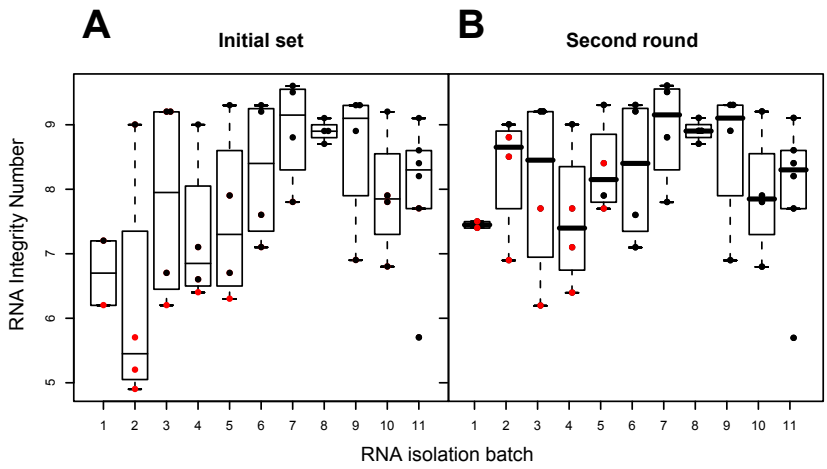

Figure 5 – The use of RNA Integrity Number (RIN) for RNA quality control purposes. A) RIN calculations revealed that in the first batches of RNA isolation, several samples yielded RNA of lower quality than usual (samples marked in red). B) After a second round of RNA isolation of all samples with low RNA quality in batches 1-5, the batch effect disappeared (repeated samples marked in red).

bers in the first few batches (r2=0.125, p=0.01, Figure 5A). After re-isolating RNA from affected samples, the batch effect disappeared (r2=0.02, p=0.50, Figure 5B).

Interestingly, after controlling for a batch effect and selecting for high quality RNA, we observed a trend towards an interaction between Braak stage and RIN number (one-way ANOVA, p=0.08, data not shown). RIN values tend to be higher in Braak stages I and II than in other Braak stages, which can potentially confound gene expression measurements, even though the numbers are very high in all Braak stages (> 7). However, there are indications that in this particular dataset, RIN calculations might be confounded by the disease process. This idea is based on the fact that RIN differences in the range 7-10 are almost exclusively based on alterations in the levels of the 18S and 28S peaks: typical RNA degradation peaks in the low-molecular weight region only occur with lower RIN values. It is known that during the progression of AD, the amount of RNA in ribosomes decreases, and the levels of RNA oxidation of ribosomal RNA increases (Ding *et al.* 2006). Furthermore, one of our main results from the AD microarray study indicates an increased neuronal activity in Braak I and II. Synaptic activity and plasticity are known to be associated with alterations in translation and protein synthesis (Costa-Mattioli *et al.* 2009; Wang and Tiedge 2004), indicating that the RIN value variations might be due to the differences in activity-dependent ribosomal content. Importantly, qPCR validation experiments were also in agreement with microarray-derived gene regulation data. Taken together, the apparent bias towards higher RIN values in Braak stages I and II suggests that the formula used to calculate the RIN values can lead to slightly higher RIN-values that are not necessarily reflecting an actual higher overall RNA quality, but are the result of a genuine biological process

Summarizing, there are a number of important parameters that need to be taken into account when selecting samples for gene expression studies, including age, sex, postmortem delay, agonal state, brain pH, medication and drug use. In our experience, high RNA quality is the single most important determinant influencing gene expression measurements. Therefore, we recommend to only use samples with a RIN value of > 7. As brain pH is correlated with RNA quality, we only select samples with a pH bigger than 6.3.

The critical role of sample matching and sample quality in gene expression experiments: a case study

An example where the cumulative negative effects of several sample parameters on or just below the acceptable threshold can be observed, is a study where we aimed to identify gene expression changes in the frontal cortex of schizophrenia patients. As the number of schizophrenia samples is quite low in the Netherlands Brain Bank (NBB), we obtained 8 additional schizophrenia samples from the Harvard Brain Bank (n=11 in total). All control samples (n=10) originated from the NBB. Sample characteristics can be found in Table 1.

The variation in several critical parameters, such as age (range 36-85) and post mortem delay (range 6:00-19:00 hours), was very large: we therefore decided to use

Diagnosis	Age	Sex	RIN	PMD	Sample origin
Schizophrenia	68	m	7.5	12:35	NBB
Non-demented control	71	m	6.9	06:00	NBB
Schizophrenia	68	m	7.1	7:05	NBB
Non-demented control	73	m	7.1	6:00	NBB
Schizophrenia	80	m	8.1	11:00	NBB
Non-demented control	82	m	6.6	13:35	NBB
Schizophrenia	85	f	6.9	16:04	BOSTON
Non-demented control	82	f	7.5	11:30	NBB
Schizophrenia	52	f	6.8	16:00	BOSTON
Non-demented control	54	f	7.1	08:00	NBB
Schizophrenia	68	f	6.5	10:20	BOSTON
Non-demented control	72	f	6.7	9:10	NBB
Schizophrenia	83	f	6.5	7:55	BOSTON
Non-demented control	83	f	7.4	07:45	NBB
Schizophrenia	36	m	6.9	23:16	BOSTON
Non-demented control	45	m	7.6	08:50	NBB
Schizophrenia	62	m	7.1	7:55	BOSTON
Non-demented control	68	m	7.1	10:10	NBB
Non-demented control	56	m	7.3	09:15	BOSTON
Schizophrenia	49	m	8	19:00	NBB
Schizophrenia	46	m	7.5	16:04	BOSTON
Non-demented control	45	m	7.6	08:50	NBB

Table 1 – Sample description of schizophrenia study. RIN: RNA Integrity Number. PMD: post mortem delay (hours). NBB: Netherlands Brain Bank.

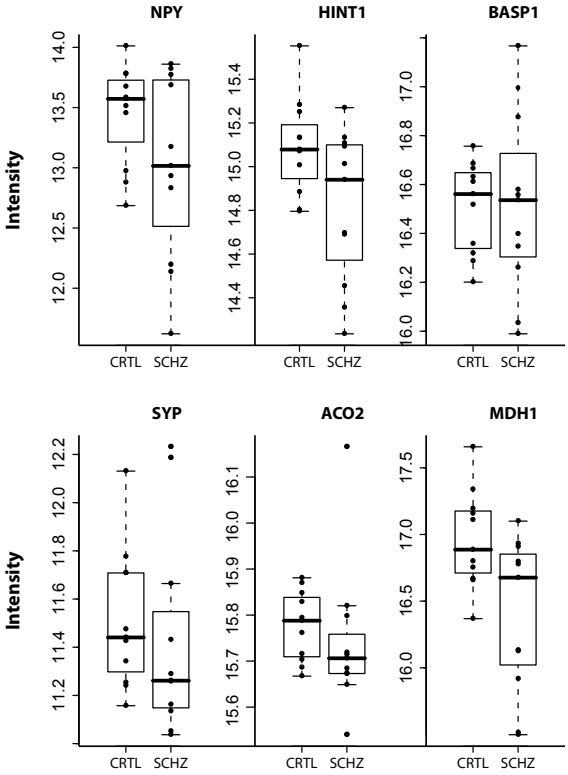

Figure 6 – Microarray gene expression levels of genes previously reported to be dysregulated in schizophrenia. Expression levels of control (n=10) and schizophrenia (n=11) of NPY, HINT1, BASP1, SYP, ACO2 and MDH1. We were unable to confirm differential expression of any of these genes (Mann-Whitney U test, p > 0.05). X-axis: log2 of intensity levels as measured on the array.

a matched pair design: each schizophrenia sample was matched as closely as possibly with a control sample from the NBB. Two schizophrenia patients were quite young (36 and 46, respectively). We were unable to select two different controls for these samples, and therefore chose to use a single matched control for both schizophrenia samples. The brain area used in this study was the superior frontal gyrus. Tissue dissection and RNA isolation was performed according to the protocol used in the AD study (Chapter 5). Overall, RNA integrity was quite low: the average RIN number was 7.2 (range 6.5-8.2). Matched pairs were hybridized twice (using a dye swap). Importantly, the technical replicates yielded highly similar results: in a single channel clustering of normalized data, replicated samples invariably clustered together (data not shown, clustering performed as described in Chapter 4). Furthermore, we observed a strong correlation between the ratios of the same sample pair, but measured on different arrays (average correlation r=.93, range .81-0.99). However, we were unable to robustly detect differential gene expression between schizophrenia

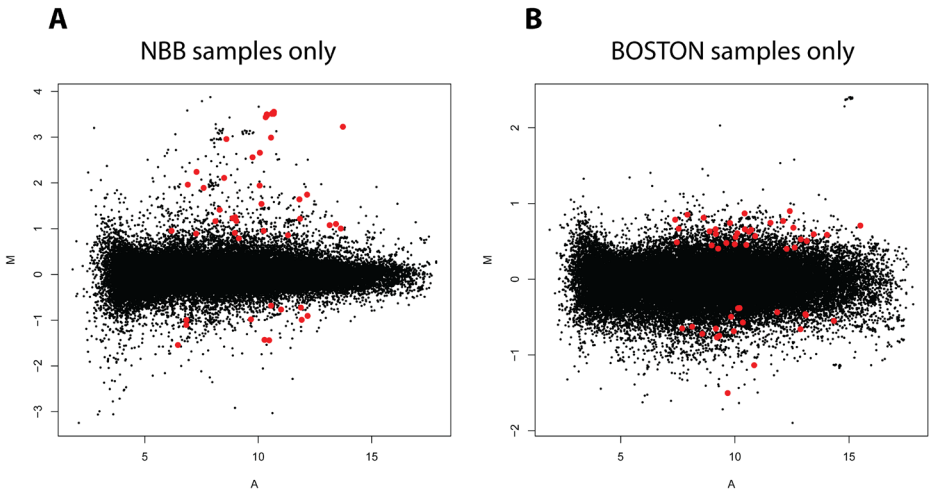

Figure 7 – M versus A plots of the schizophrenia dataset, separated by sample origin. Red dots represent the 50 most significantly regulated genes.

and controls. Two separate analysis approaches were employed, one based on linear models (using the LIMMA package in Bioconductor), the other using paired t-tests (both methods were ratio-based). After multiple testing correction using the Benjamini-Hochberg method, both analyses identified a single gene as differentially expressed, namely UBB (Ubiquitin B). This gene is upregulated 1.73-fold compared to controls. The finding of only a single regulated gene was unexpected: the biological replication seems sufficient (n=11), samples were carefully matched, quality control demonstrated that the technical execution of the experiment was sound, and the Benjamini-Hochberg method for multiple testing correction is not very stringent.

To see whether our gene expression dataset was in general agreement with the gene expression differences known to exist between schizophrenia and controls, we compared the expression levels of several genes in our dataset with the regulatory patterns as described in literature (Figure 6). The NPY gene is previously shown to be downregulated in the frontal cortex of schizophrenia patients, although the variance was very high: control and schizophrenia groups overlapped significantly (Kuromitsu *et al.* 2001). We observed a similar trend which lacked statistical significance. The metabolic enzymes HINT1 and MDH1 are also downregulated in the frontal cortex in schizophrenia (Vawter *et al.* 2004), trends we observed as well. We were unable to confirm a recent report on the increased expression of BASP1 in schizophrenia (Behan *et al.* 2008). Synaptophysin is decreased in the dentate gyrus in schizophrenia, but not in the frontal cortex (Chambers *et al.* 2005; Halim *et al.* 2003), and shows a downward trend in our dataset. Aconitase 2 (ACO2) is not changed in schizophrenia, in accordance to our findings (note the fold change on the Y-axis) (Bubber *et al.* 2004).

Thus, in general, our dataset is not in disagreement with current literature, but fails to reach statistical significance. This might be due to the fact that the average RNA quality is just above the threshold of 7. Also, the large differences in post-mortem delay likely introduce substantial variation. Furthermore, we measured gene expression in grey matter only, whereas others used homogenates of both grey and white matter. An alternative possibility underlying of the lack of differentially expressed genes might result from the different sample origins (n=8 schizophrenia samples from Harvard Brain Bank, n=3 schizophrenia samples from the NBB). One could think of differences in disease diagnosis, brain dissection, measurement of post mortem delay and brain pH, method of freezing, storage conditions etcetera. We therefore performed a separate analysis on the NBB samples alone, and on the Boston samples alone (all control samples are obtained from the NBB).

The analysis of the NBB samples did not yield significant differences, which is not surprising given the low level of biological replication (n=3). The MA plot (Figure 7A) however reveals that several genes show a trend towards differential gene expression. To gain some insight into the data, a literature search was performed for the 50 most significant genes to see whether they have been mentioned with schizophrenia before. SERPINA3 is known to be upregulated in schizophrenia (Arion *et al.* 2007; Saetre *et al.* 2007), which we corroborate here. S100A9 has been used as a biomarker to discriminate schizophrenia from bipolar disorder (Tsuang *et al.* 2005b), although a recent study failed to replicate this (Yao *et al.* 2008). MMP9 is found to be upregulated by antipsychotic treatment in rat adipocytes (Minet-Ringuet *et al.* 2007): we observed an upregulation as well. A SNP in IL18RAP (upregulated in our dataset) is associated in schizophrenia; the authors further suggest an interaction between herpes simplex infection, schizophrenia and polymorphisms in IL18RAP (Shirts *et al.* 2008). Several publications report on the downregulation of GFAP in schizophrenia (Webster *et al.* 2005; Toro *et al.* 2006; Le Niculescu *et al.* 2007), whereas we observed an upregulation.

The separate analysis of the 8 Harvard Brain Bank samples did yield significant results: 75 genes were found to be differentially expressed. However, the distribution of the M values in the MA plot (Figure 7B) does not look very reliable: the spread of M-values around 0 is not intensity-dependent (this is expected, as the signal-to-noise ratios are better at high A values), a feature that is present in the NBB-only analysis. Such a "wide" MA plot was also observed in the low quality PD caudate nucleus microarray dataset discussed earlier in this section. Also, it is important to note that all control samples originated from the NBB; the different sample origins might contribute to the aberrant MA plot. A literature search revealed that 3 genes out of the 50 most significantly regulated genes are co-mentioned with schizophrenia. RIMS2 is upregulated at the protein level (not mRNA level) in the amygdala of schizophrenia patients (Weidenhofer *et al.* 2008), and is mildly upregulated in this analysis (fold change of 1.4). GRM5 appears to be part of a schizophrenia breakpoint locus (Semple *et al.* 2001), and the TGM2 gene is associated with schizophrenia in a British cohort (Bradford *et al.* 2008). Most notably, there is no overlap between

the 50 most significant genes in the NBB-only analysis, and the 50 most significant genes in the Harvard-only analysis.

Summarizing, several factors, including low RNA quality, different sample origins, and a broad range in parameters such as age and postmortem delay, added additional variation into the dataset. Even though we matched parameters as carefully as possible, the accumulation of these confounding factors eventually resulted in the failure to identify significantly differentially expressed genes.

Bioinformatics approaches to identify key genes and pathways

With the advent of high-throughput genomic technology, bioinformatics algorithms that aid in the analysis of the enormous amounts of data produced by microarray experiments have become a essential tool to the experimenter. In the early days of microarray technology, the main focus of the bioinformatics community has been on the reliable identification of differential gene expression. Methods for proper spot identification and quantification, background correction and normalization were developed and optimized, followed by statistical methods for the determination of regulated genes. Although high quality standardized methods are now in place, new algorithms addressing these aspects of microarray experiments are continuously being developed. In fact, we describe an improved method for the detection of differential gene expression in dual-color gene expression experiments in Chapter 4 of this thesis.

The second wave of bioinformatics algorithm development has focused on pattern detection in gene expression datasets. For example, in time course experiments, co-regulated genes are expected to exhibit a similar temporal response. The development of clustering methods and correlation analysis of microarray data allows for the identification of groups of co-expressed genes, and yield new insights into the functional connection of members of these gene groups (Wu and Dewey 2006; Green *et al.* 2006). Furthermore, large functional annotation databases such as the Gene Ontology (GO) (Ashburner *et al.* 2000) database and the Kyoto Encyclopedia for Genes and Genomes (Ogata *et al.* 1999) (KEGG) have opened up new possibilities for the interpretation of microarray datasets. Algorithmic tools called overrepresentation analyses exploit the information stored in these databases for the identification of biological themes or molecular pathways associated with lists of differentially expressed genes, and are now routinely used in microarray experiments. In this thesis, we have applied two improved approaches for the functional annotation of the PD and AD datasets. The functional class scoring approach (see Chapter 3) does not rely on the division of a dataset into regulated and non-regulated genes (which is a relatively arbitrary division), but uses weights based for example on p-values or fold changes (Pavlidis *et al.* 2002). Therefore, the results are not dependent on a user-defined cutoff; different cutoffs can lead to profoundly different results. The TopGO method (used in Chapter 5) makes use of the hierarchical

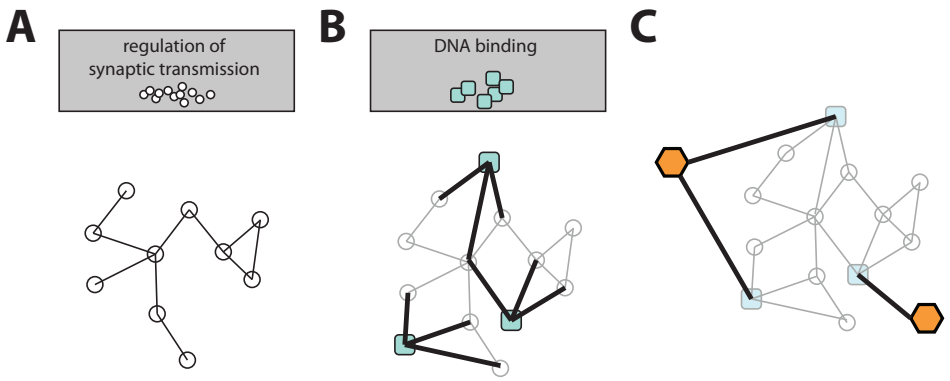

Figure 8 – Example of an Ingenuity Pathway Analysis workflow. A) Build a network of genes out of the GO-based gene group "regulation of synaptic transmission". B) Add transcription factors regulating the expression of pathway genes from the GO-based gene group "DNA binding". C) Find significantly regulated genes that modulate the activity or expression of the transcription factors. These "hub" genes play a central role in the pathway, and are therefore potential candidates for therapeutic approaches.

organization of the Gene Ontology database, which results in more targeted lists of GO classes (Alexa *et al.* 2006).

The GO database is the most widely used source for gene annotations. This can be attributed to the excellent coverage of the genome. In humans, 81.7% of the genes encoding for proteins are annotated with at least 1 GO classifier. In mouse, this number is 67.4%, and in the rat 95.8% of the protein-encoding genes is annotated (Rhee *et al.* 2008). However, one has to keep in mind that the majority of annotations is not derived from "wet" experimental evidence, but is based on computational data or indirectly derived from experimental data. In humans, only 28.1% of the genes is annotated with one or more GO classifiers that are backed by experimental evidence. For the rat genome, this number is only 20.7%. The annotation of the mouse genome is relatively solid, with experimental evidence for ~57% of GO-annotated genes (Rhee *et al.* 2008). Thus, caution should be observed when interpreting the results from GO-based overrepresentation analysis. Furthermore, although GO annotations allow the researcher to group genes into functionally related categories, they do not provide clear indications as to which genes or proteins specifically interact. For example, a specific overrepresentation of the GO classes "regulation of synaptic plasticity" (GO:0048167) and "DNA binding" (GO:0003677) yields no insight in the potential relationship, if any, between these two processes. To find such a relationship, the researcher has to manually evaluate the lists of genes associated with these GO classes, including exhaustive literature searches. As a result, one might find that specific transcription factors in the "DNA binding" group drive the expression of several modulators of synaptic morphology in the "regulation of synaptic transmission" group.

The two main limitations in GO-based analysis of microarray datasets (underrepresentation of evidence-based annotation, and lack of insight at the level of direct gene-gene, gene-protein or protein-protein interaction) are addressed in new state-of-the-art pathway analysis tools such as Ingenuity Pathway Analysis (IPA, www.ingenuity.com). The IPA system is based on a knowledgebase that contains experimentally verified interaction data between genes and/or proteins, which are derived by manual inspection of PubMed abstracts. IPA provides tools for the analysis of gene expression datasets using this knowledgebase. For example, IPA can automatically build networks of gene-gene interactions from the set of 287 differentially expressed genes in the PD SN (Chapter 3).

One of the biggest advantages of the IPA system is that the resulting networks are interactive. This allows the researcher to ask very specific questions. In our example of the interaction between the GO classes "DNA binding" and "regulation of synaptic transmission", a possible analysis approach would be the following. First, a network is build from the genes in the "regulation of synaptic transmission" group to gain insight in the specific involvement of genes with synaptic activity (Figure 8A). Secondly, a specific search can be done for genes in the "DNA binding" group that affect the expression of only those genes involved in synaptic transmission (Figure 8B). Once these transcription factors have been identified and added to the network, one could even go further: find in the list of differentially expressed genes that modulate the activity of these transcription factors (Figure 8C). Such genes that alter the behavior of a large set of downstream targets are called hub genes, and are excellent targets for in vitro and in vivo validation studies, and hopefully provide new entry points for the development of new therapeutics. Importantly, it is very well possible that a hub gene, although differentially expressed, does not belong to a GO class that is overrepresented, and would have been overlooked when focusing on GO-based results alone.

We anticipate that pathway analysis tools such as IPA will become very important in bridging the gap between "broad" data analysis methods such as GO-based overrepresentation, and single gene-based in vitro functional validation experiments. We are currently engaged in performing network and pathway analyses on both the AD and PD datasets using the IPA system, in close collaboration with Solvay Pharmaceuticals. In the near future, we expect a tight in silico integration between data from different –omics approaches (such as gene expression datasets, proteomics, genome-wide SNP datasets) and data from newly emerging medium-to-high throughput in vitro and in vivo functional characterization tools. Examples of these new tools include genome-wide siRNA and overexpression libraries to knock down or overexpress any gene of interest in relevant in vitro models (for examples see Future Perspectives). Hits from these secondary screens can now be easily followed up in vivo as (conditional and unconditional) knockout mice and rats for any gene of interest are now commercially available. Crossbreeding these animals with established models for AD and PD will yield direct insight into the potential disease-modifying role of the gene of interest. Integrative bio-informatics tools will be able to combine data from all these data sources, and will hopefully enable the

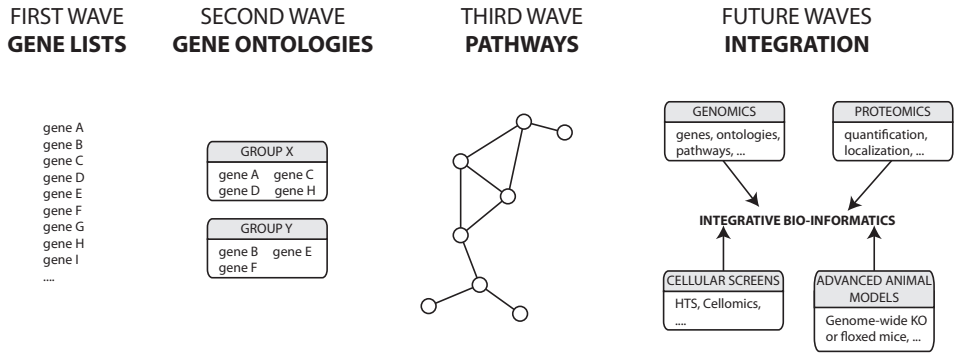

Figure 9 – Schematic overview of advances in bio-informatics for the analysis of high-throughput gene expression datasets.

research community to identify key pathways and processes that can be targeted with therapeutics (Figure 9).

Future perspectives

In this thesis, we have described extensive sets of altered genes and molecular pathways previously unidentified in AD and PD. Some of these genes might represent new entry points for the development of treatment strategies for these disorders. However, as the data are solely on the transcriptional level, additional experiments are needed to strengthen the evidence for the interaction between these genes or gene networks, their protein product(s) and the pathogenic events as they occur during the development and progression of AD and PD. Here, we will discuss experimental approaches (several of them currently ongoing or starting in the near future) to further elucidate the exact role of candidate genes with respect to neurodegenerative events in AD and PD.

Gene expression profiling during the progression of PD

A major strength of the AD microarray study lies in the fact that we were able to follow gene expression changes over the full disease course by selecting samples from each of the Braak stages for tangles. This allowed us to group genes with similar expression patterns over the Braak stages. The co-expression of these transcripts is a strong indication for a functional interaction or relation between the group members. Furthermore, we were able to discriminate between early and late transcriptional events in AD pathogenesis. Recently, a staging system for the progression of PD was proposed by Braak et al (Braak *et al.* 2003) based on the occurrence of Lewy body pathology in different brain areas. This staging system can be used as the basis for a gene expression study during the progression of PD. Interestingly, the earliest neuropathological alterations in PD appear in the brainstem or the olfactory bulb, whereas the substantia nigra is only involved at later stages. A microarray study of

the substantia nigra in all Braak stages for PD might therefore reveal transcriptional alterations that are causative to DAergic neurodegeneration, and can provide more insight in the gene expression profiles of spared parts of the PD SN as presented in this thesis. Unfortunately, as the Braak staging system for PD is relatively new, a selection of high quality, well characterized postmortem samples is difficult to obtain at this moment. Furthermore, the lack of correlation between Braak stage for PD and clinical symptoms, and the finding of substantial numbers of PD cases which do not fit in the staging system, suggests that the staging system needs to be refined (Jellinger 2008; Burke *et al.* 2008; Braak *et al.* 2003). Nevertheless, we anticipate that future microarray studies following the progression of PD will provide very interesting data on causative molecular mechanisms in PD.

Protein and mRNA localization and quantification studies on human postmortem brain tissue

In order to validate the transcriptional alterations in the human brain, extensive mRNA and protein localization and quantification studies are currently ongoing on a large set of brain samples, using in situ hybridization and immunohistochemical techniques. First of all, these experiments will provide insight in the (sub-)cellular location of the transcripts and proteins under investigation. Secondly, we will be able to determine whether the transcriptional alterations are also observed at the protein level. These data will aid in the testing of hypotheses put forward in this thesis, and help to formulate potential new hypotheses. For example, when the upregulation of RER1 is observed in astrocytes but not in neurons, we have to adjust our hypothesis on the involvement of RER1 in intraneuronal Abeta levels (see Chapter 5). Preliminary results from an immunohistochemical study of a set of ~40 proteins differentially expressed in the PD SN indicate that the majority of the proteins is indeed expressed in DAergic neurons, supporting their potential role in PD-associated neurodegeneration. Unfortunately, quantification of protein levels by immunohistochemical methods has proven to be very difficult due to the quenching of the fluorescence signal by neuromelanin (personal communications, Asia Korecka, Dick Swaab and Joost Verhaagen).

In vitro and in vivo assays to study the functional role of target genes

In the following section, we will discuss experimental strategies to examine the role of target genes in cellular assays. As we will employ different assays for PD and AD, the two approaches are discussed separately.

In vitro assays - PD

In order to study the functional role of dysregulated genes detected in our PD study (see chapter 3), a robust cellular assay is needed that recapitulates cardinal features of the disease. Several toxin-induced cellular models (such as the MPP+ and 6-OH-DA models, see also Chapter 1) are well suited to study certain aspects of PD, most

notably processes directly or indirectly linked to mitochondrial defects. It is important to note that mitochondrial dysfunction is also one of our main findings in the PD SN, and has been reported by other groups as well (Chapter 3). Taking into account that PD-associated neurodegeneration happens over the course of years to decades, we are particularly interested in models where a chronic low-dose application of a toxin results in a cell that is compromised, but not dying. To this end, we are now in the process of characterizing a model in which SH-SY5Y neuroblastoma cells, differentiated with retinoic acid into a neuronal phenotype, are treated with low, sublethal concentrations of MPP+ over prolonged periods (20 days). The exact transcriptional makeup of the neuron-like phenotype of the differentiated neuroblastoma cells, and the effect of MPP+ on cellular health and survival will be assessed by means of microarray gene expression profiling. This would allow for a direct comparison between the effects of mitochondrial complex I inhibition by MPP+ in these cells, and the gene expression changes observed in our human PD brain dataset. Also, it will be very interesting to compare both the MPP+-induced transcriptional alterations and the PD brain dataset to a very recent study where laser capture techniques and microarrays were employed to indentify transcriptional alterations in DAergic neurons in the PD SN (Simunovic et al. 2008). These comparisons will aid in discriminating between mitochondrial dysfunction-related transcriptional networks and gene expression changes that are part of other neurodegenerative origin.

Furthermore, the SH-SY5Y-based MPP+ model will be used to study the effect of modulating the expression of target genes on MPP+-induced neurotoxicity. We will select genes of interest from a genome-wide siRNA library (Dharmacon), and subsequently knock down the expression of these genes individually, and measure the functional outcome with an automated fluorescence microscopic imaging system designed for high content screening and high content analysis (Cellomics). In this manner, we will be able to monitor the interaction of gene knockdown with parameters such as mitochondrial membrane potential, cytoskeletal integrity, cellular viability and neuronal outgrowth in the context of MPP+ toxicity. Furthermore, although mitochondrial dysfunction is a key event in PD-associated neurodegeneration, it is important to examine the function of the selected genes of interest in other cellular models of PD. Therefore, we will repeat these knockdown screening experiments with several other SH-SY5Y models where genes involved in genetic forms of PD (such as DJ-1 and PINK-1, see Chapter 1 of this thesis) are knocked down first, followed by a knockdown of target genes. These medium-throughput screening experiments can be complemented by overexpression studies of selected genes. This might be especially relevant for genes that are found to be upregulated in PD (most of the differentially expressed genes in the PD SN are downregulated, Chapter 3). Also, in the light of the multifactorial origin of PD, combinatorial approaches that are based on pools of siRNAs targeting different gene products at once can be very potent in generating a more "PD-like" phenotypic response. However, these experiments are very complex both in terms of planning (which combination of genes to knock down) and interpretation. The above discussed plans are executed

in collaboration with the research groups of Prof. Guus Smit, dr. Ronald van Kesteren and Prof. Peter Heutink at the Vrije Universiteit Amsterdam.

In vitro assays - AD

To assess the involvement of genes of interest in AD, we will take a similar in vitro approach as discussed for the PD follow-up studies. As described in Chapter 5, profound differences in gene expression can already be observed in Braak stage II, before the appearance of clinical symptoms and extensive plaque pathology. As these changes precede plaque formation, they are highly interesting in the light of early therapies. Our data and those of other research groups suggest that the early alterations are due to an increase of soluble forms of Aβ. We therefore intend to develop an AD model based upon differentiated SH-SY5Y cells which are stressed by the addition of Aβ into the culture medium. An important question that remains to be answered is which Aβ assembly state (oligomeric or fibrillar) is associated with the observed transcriptional alterations in our microarray experiments. Both aggregation states are toxic to cells, but act via distinct molecular pathways. For example, oligomeric species are involved in endoplasmic reticulum stress (Chafekar *et al.* 2007) and impair long term potentiation (Shankar *et al.* 2008; Walsh *et al.* 2002), whereas fibrillar forms trigger inflammatory responses (Eikelenboom *et al.* 2002). The specific effect of oligomeric Aβ on synaptic function (Walsh *et al.* 2002) is most interesting with respect to our findings. Also, when added to the culture medium, oligomeric species of Aβ are readily taken up by differentiated neuroblastoma cells, whereas fibrillar forms of Aβ bind to the cell membrane, but remain extracellular (Chafekar *et al.* 2008). Thus, the addition of sublethal concentrations of oligomeric Aβ may be a potent model to elucidate the functional involvement of genes of interest with the observed alterations in neuronal activity. Again, the use of a genome-wide siRNA library would allow for the modulation of the genes of interest, this time in the context of Aβ -induced toxicity. These experiments can be expanded by overexpressing different isoforms of ApoE, to study the interaction between ApoE3 or ApoE4, Aβ -induced toxicity and the genes found to be regulated in AD.

An alternative to the addition of synthetic Aβ would be using cell lines that stably express (mutant or wildtype) APP. Such a model does however represent a more artificial situation, as the overexpression of APP will affect the differentiation process of these cells. On the other hand, such a cell-line can be valuable for specific studies focusing on the effect of target genes on the formation and degradation of different forms of Aβ. To this end, we have initiated collaborations with dr. Elly Hol, dr. Willem Kamphuis (Netherlands Institute for Neuroscience), Dr. Wiep Scheper (Neurogenetics, AMC, Amsterdam) and Prof. Guus Smit and dr. Ronald van Kesteren (Vrije Universiteit, Amsterdam).

In vivo experiments - PD

We aim to develop two approaches for the in vivo characterization of genes of interest as derived from the human brain experiments and in vitro experiments. Both approaches are based on viral-vector based gene silencing or overexpression. The first

set of experiments will determine whether the knockdown or overexpression of a target gene by itself is sufficient to induce neurodegenerative events in the mouse SN. In parallel, we will use a toxin-based PD mouse model to study the effect of gene modulation in a PD "background". Several well-characterized toxin-induced rodent models that mimic PD are already available, and the ones using MPTP as a neurotoxin causing DAergic neurodegeneration are arguably amongst the best PD models (discussed in the Introduction of this thesis). We are currently in the process of testing which adeno-associated viral vector serotypes are most suitable to target the mouse SN.

In vivo experiments - AD

As already discussed in Chapter 1, the order of neuropathological events in several transgenic mouse models of AD (3xTG-AD, PS1APP) closely mimics that as observed during the progression of AD in the human prefrontal cortex. The main finding from our AD microarray study in Chapter 5 is the compensatory increase in neuronal activity in Braak stage II, just before the onset of plaque formation. It is at present unknown whether the cognitive decline in AD mouse models is preceded by such a compensatory event as well. Furthermore, as our hypotheses are centered round the role of soluble forms of Aβ, we are very much interested in the transcriptional alterations associated with increased concentrations of soluble Aβ. To our best knowledge, there are no published gene expression data that studied these alterations. Therefore, we intend to perform genome-wide microarray studies on prefrontal cortex tissue samples of the 3xTg-AD mouse and the PS1APP mouse. The resulting datasets will allow us to compare transcriptional profiles of Aβ -induced stress in mice with and without tau mutations, and the human dataset. In this manner, we will be better equipped to discriminate between neurodegenerative events associated with Aβ, or from other origin in the human AD brain. Furthermore, we are collaborating with DNage, a company that developed transgenic mice that have defects in the DNA repair machinery (nucleotide excision repair). These mice are characterized by accelerated aging and neurodegeneration. As discussed earlier in this General Discussion, aging and DNA damage are intimately linked, and gene groups affected by aging are also affected in AD. We will therefore study the similarities and differences between the transcriptional profiles of the DNage mice, the AD mouse models and the human AD dataset.

To further characterize the function of genes that are found to have an effect in the in vitro experiments, we will study the role of specific target genes by viral vector-mediated gene overexpression or knockdown. These experiments can be performed in wildtype mice, and in AD mouse models. The AD mouse models are characterized by neuropathological events in multiple brain areas. It will be very challenging to target all these brain areas at once with adeno-associated viral vectors. Alternatively, we can opt for transduction of the hippocampus only, and study the performance of these mice on hippocampal-dependent memory tasks. Another possibility is to transduce only a limited portion of the cortex, and examine the effect of gene knockdown or overexpression on neurodegenerative hallmarks in the

transduced brain area, or to transduce larger brain areas with plasmid expression vectors during early post-natal stages of development using an in vivo electroporation approach (Matsuda and Cepko 2007).

Final remarks: towards novel therapeutics for PD and AD

In the future, the gene expression data generated by the experiments described in this thesis will be further employed to pinpoint the most promising targets for the development of new drugs. As a first approach, the pharmaceutical industry can scan our datasets and focus on "drugable targets", such as G-protein coupled receptors, kinases, and enzymes. Small molecules against these drugable targets can be identified with tried and tested classical high throughput screens (HTS). The most promising small compounds identified in HTS are the starting point for drug design.

Complementary to the approach of HTS screening of regulated drugable targets, alternative medium-throughput high-content screening (MTHCS) strategies are now starting to be applied, mainly by academic research groups and small-to-medium sized enterprises. We have highlighted such an approach in the Future Perspectives section above. One of the main advantages from MTHCS approaches is that the lists of regulated genes can be approached in an unbiased manner, whereas large pharma companies tend to focus on drugable targets alone. The outcome of MTHCS (a list of genes that, when modulated, give rise to a relevant phenotype) serves as a basis for the development of new state-of-the-art therapeutic strategies (such as stem cell therapy, gene therapy etc), but can also be exploited to generate new entry points for classical small molecule approaches. For example, when targeting alterations in axon guidance cues for the development of treatment strategies in PD, one could directly interfere with the binding of RGMA to its receptor (neogenin) by locally expressing neogenin receptor bodies lacking the transmembrane signaling part, thereby acting as scavengers to reduce the extracellular concentration of RMGA. Alternatively, a detailed analysis of the molecular pathway downstream of RGMA-mediated signaling might reveal that the modulation of the activity of a specific kinase results in a beneficial effect. A HTS screen using this specific kinase can potentially identify compounds that are therapeutically equally powerful. Therefore, the aim in the near future is to identify new and innovative targets that can serve as a basis for preventive or restorative therapeutics for AD and PD.

List of references

Aarsland D, Zaccai J, Brayne C (2005) A systematic review of prevalence studies of dementia in Parkinson's disease. *Mov Disord.* **20,** 1255-1263.
Agulhon C *et al* (2008) What is the role of astrocyte calcium in neurophysiology? *Neuron* **59,** 932-946.
Akbari Y *et al* (2004) Presenilin regulates capacitative calcium entry dependently and independently of gamma-secretase activity. *Biochem.Biophys.Res.Commun.* **322,** 1145-1152.
Albert M, Duffy FH, Naeser M (1987) Nonlinear changes in cognition with age and their neuropsychologic correlates. *Can.J.Psychol.* **41,** 141-157.
Albrecht DE, Froehner SC (2004) DAMAGE, a novel alpha-dystrobrevin-associated MAGE protein in dystrophin complexes. *J Biol Chem* **279,** 7014-7023.
Alcala S, Klee M, Fernandez J, Fleischer A, Pimentel-Muinos FX (2008) A high-throughput screening for mammalian cell death effectors identifies the mitochondrial phosphate carrier as a regulator of cytochrome c release. *Oncogene* **27,** 44-54.
Alexa A, Rahnenfuhrer J, Lengauer T (2006) Improved scoring of functional groups from gene expression data by decorrelating GO graph structure. *Bioinformatics.* **22,** 1600-1607.
Alkemade A, Unmehopa UA, Wiersinga WM, Swaab DF, Fliers E (2005) Glucocorticoids decrease thyrotropin-releasing hormone messenger ribonucleic acid expression in the paraventricular nucleus of the human hypothalamus. *J.Clin.Endocrinol.Metab* **90,** 323-327.
Alvarez-Fischer D *et al* (2008) Modelling Parkinson-like neurodegeneration via osmotic minipump delivery of MPTP and probenecid. *J.Neurochem.* **107,** 701-711.
Alzheimer A, Stelzmann RA, Schnitzlein HN, Murtagh FR (1995) An English translation of Alzheimer's 1907 paper, "Uber eine eigenartige Erkankung der Hirnrinde". *Clin.Anat.* **8,** 429-431.
Anandatheerthavarada HK, Biswas G, Robin MA, Avadhani NG (2003) Mitochondrial targeting and a novel transmembrane arrest of Alzheimer's amyloid precursor protein impairs mitochondrial function in neuronal cells. *J.Cell Biol.* **161,** 41-54.
Anekonda TS, Reddy PH (2006) Neuronal protection by sirtuins in Alzheimer's disease. *J.Neurochem.* **96,** 305-313.
Aoto J, Chen L (2007) Bidirectional ephrin/Eph signaling in synaptic functions. *Brain Res.* **1184,** 72-80.
Arion D, Unger T, Lewis DA, Levitt P, Mirnics K (2007) Molecular evidence for increased expression of genes related to immune and chaperone function in the prefrontal cortex in schizophrenia. *Biol.Psychiatry* **62,** 711-721.
Armstrong DM, Sheffield R, Mishizen-Eberz AJ, Carter TL, Rissman RA, Mizukami K, Ikonomovic MD (2003) Plasticity of glutamate and GABAA receptors in the hippocampus of patients with Alzheimer's disease. *Cell Mol.Neurobiol.* **23,** 491-505.
Arnaudeau S, Kelley WL, Walsh JV, Jr., Demaurex N (2001) Mitochondria recycle Ca(2+) to the endoplasmic reticulum and prevent the depletion of neighboring endoplasmic reticulum regions. *J.Biol.Chem.* **276,** 29430-29439.
Ashburner M *et al* (2000) Gene ontology: tool for the unification of biology. The Gene Ontology Consortium. *Nat Genet* **25,** 25-29.
Auer S, Reisberg B (1997) The GDS/FAST staging system. *Int.Psychogeriatr.* **9 Suppl 1,** 167-171.
Azad NA, Al Bugami M, Loy-English I (2007) Gender differences in dementia risk factors. *Gend.Med.* **4,** 120-129.
Babcock DF, Herrington J, Goodwin PC, Park YB, Hille B (1997) Mitochondrial participation in the intracellular Ca2+ network. *J.Cell Biol.* **136,** 833-844.
Bancher C, Jellinger K, Lassmann H, Fischer P, Leblhuber F (1996) Correlations between mental state and quantitative neuropathology in the Vienna Longitudinal Study on Dementia. *Eur.Arch.Psychiatry Clin.Neurosci.* **246,** 137-146.
Bao AM, Hestiantoro A, Van Someren EJ, Swaab DF, Zhou JN (2005) Colocalization of corticotropin-releasing hormone and oestrogen receptor-alpha in the paraventricular nucleus of the hypothalamus in mood disorders. *Brain* **128,** 1301-1313.
Barbaccia ML *et al* (1986) Diazepam-binding inhibitor. A brain neuropeptide present in human spinal fluid: studies in depression, schizophrenia, and Alzheimer's disease. *Arch.Gen.Psychiatry.* **43,** 1143-1147.
Barbosa AC *et al* (2008) MEF2C, a transcription factor that facilitates learning and memory by negative regulation of synapse numbers and function. *Proc.Natl.Acad.Sci.U.S.A* **105,** 9391-9396.
Bassett SS, Yousem DM, Cristinzio C, Kusevic I, Yassa MA, Caffo BS, Zeger SL (2006) Familial risk for Alzheimer's disease alters fMRI activation patterns. *Brain* **129,** 1229-1239.
Bauer, M., Meixner, A., and Ueffing, M. Investigation of Developmental and Disease-Related Genes in Primary Neuronal Systems using Lenti-Viral Vector-Based Technology. 2005. NGFN, Bonn, Germany.
Baulieu EE (1998) Neurosteroids: a novel function of the brain. *Psychoneuroendocrinology.* **23,** 963-987.
Behan A, Byrne C, Dunn MJ, Cagney G, Cotter DR (2008) Proteomic analysis of membrane microdomain-associated proteins in the dorsolateral prefrontal cortex in schizophrenia and bipolar disorder reveals alterations in LAMP, STXBP1 and BASP1 protein expression. *Mol.Psychiatry.*
Behl C (2002) Oestrogen as a neuroprotective hormone. *Nat.Rev.Neurosci.* **3,** 433-442.

Belbin O *et al* (2007) Regulatory region single nucleotide polymorphisms of the apolipoprotein E gene and the rate of cognitive decline in Alzheimer's disease. *Hum.Mol.Genet.* **16,** 2199-2208.
Belelli D, Casula A, Ling A, Lambert JJ (2002) The influence of subunit composition on the interaction of neurosteroids with GABA(A) receptors. *Neuropharmacology* **43,** 651-661.
Belelli D, Lambert JJ (2005) Neurosteroids: endogenous regulators of the GABA(A) receptor. *Nat.Rev. Neurosci.* **6,** 565-575.
Bellander BM, Bendel O, Von EG, Ohlsson M, Svensson M (2004) Activation of microglial cells and complement following traumatic injury in rat entorhinal-hippocampal slice cultures. *J.Neurotrauma* **21,** 605-615.
Bennecib M, Gong CX, Grundke-Iqbal I, Iqbal K (2000) Role of protein phosphatase-2A and -1 in the regulation of GSK-3, cdk5 and cdc2 and the phosphorylation of tau in rat forebrain. *FEBS Lett.* **485,** 87-93.
Bensemain F *et al* (2009) Evidence for induction of the ornithine transcarbamylase expression in Alzheimer's disease. *Mol.Psychiatry* **14,** 106-116.
Benveniste EN, Nguyen VT, O'Keefe GM (2001) Immunological aspects of microglia: relevance to Alzheimer's disease. *Neurochem.Int.* **39,** 381-391.
Bergman O *et al* (2008) PITX3 polymorphism is associated with early onset Parkinson's disease. *Neurobiol.Aging.*
Bernardi P, Rasola A (2007) Calcium and cell death: the mitochondrial connection. *Subcell.Biochem.* **45,** 481-506.
Bernheimer H, Birkmayer W, Hornykiewicz O, Jellinger K, Seitelberger F (1973) Brain dopamine and the syndromes of Parkinson and Huntington. Clinical, morphological and neurochemical correlations. *J.Neurol.Sci.* **20,** 415-455.
Bertram L, McQueen MB, Mullin K, Blacker D, Tanzi RE (2007) Systematic meta-analyses of Alzheimer disease genetic association studies: the AlzGene database. *Nat.Genet.* **39,** 17-23.
Bertram L, Tanzi RE (2005) The genetic epidemiology of neurodegenerative disease. *J.Clin.Invest* **115,** 1449-1457.
Betarbet R *et al* (2006) Intersecting pathways to neurodegeneration in Parkinson's disease: effects of the pesticide rotenone on DJ-1, alpha-synuclein, and the ubiquitin-proteasome system. *Neurobiol.Dis.* **22,** 404-420.
Betarbet R, Sherer TB, MacKenzie G, Garcia-Osuna M, Panov AV, Greenamyre JT (2000) Chronic systemic pesticide exposure reproduces features of Parkinson's disease. *Nat Neurosci* **3,** 1301-1306.
Bhattacharyya A, Watson FL, Pomeroy SL, Zhang YZ, Stiles CD, Segal RA (2002) High-resolution imaging demonstrates dynein-based vesicular transport of activated Trk receptors. *J Neurobiol* **51,** 302-312.
Bialecka M, Kurzawski M, Klodowska-Duda G, Opala G, Tan EK, Drozdzik M (2006) Polymorphism in semaphorin 5A (Sema5A) gene is not a marker of Parkinson's disease risk. *Neurosci.Lett.* **399,** 121-123.
Bialek M, Zaremba P, Borowicz KK, Czuczwar SJ (2004) Neuroprotective role of testosterone in the nervous system. *Pol.J.Pharmacol.* **56,** 509-518.
Biggio F, Gorini G, Caria S, Murru L, Mostallino MC, Sanna E, Follesa P (2006) Plastic neuronal changes in GABA(A) receptor gene expression induced by progesterone metabolites: in vitro molecular and functional studies. *Pharmacol.Biochem.Behav.* **84,** 545-554.
Biggio G, Follesa P, Sanna E, Purdy RH, Concas A (2001) GABAA-receptor plasticity during long-term exposure to and withdrawal from progesterone. *Int.Rev.Neurobiol.* **46,** 207-241.
Billings LM, Oddo S, Green KN, McGaugh JL, LaFerla FM (2005) Intraneuronal Abeta causes the onset of early Alzheimer's disease-related cognitive deficits in transgenic mice. *Neuron* **45,** 675-688.
Binder LI, Frankfurter A, Rebhun LI (1985) The distribution of tau in the mammalian central nervous system. *J.Cell Biol.* **101,** 1371-1378.
Birzniece V *et al* (2006) Neuroactive steroid effects on cognitive functions with a focus on the serotonin and GABA systems. *Brain Res.Rev.* **51,** 212-239.
Blalock EM *et al* (2005) Harnessing the power of gene microarrays for the study of brain aging and Alzheimer's disease: statistical reliability and functional correlation. *Ageing Res Rev* **4,** 481-512.
Blalock EM, Geddes JW, Chen KC, Porter NM, Markesbery WR, Landfield PW (2004) Incipient Alzheimer's disease: microarray correlation analyses reveal major transcriptional and tumor suppressor responses. *Proc Natl Acad Sci U S A* **101,** 2173-2178.
Bohlen und HO, Minichiello L, Unsicker K (2005) Haploinsufficiency for trkB and trkC receptors induces cell loss and accumulation of alpha-synuclein in the substantia nigra. *FASEB J* **19,** 1740-1742.
Bolstad BM, Irizarry RA, Astrand M, Speed TP (2003) A comparison of normalization methods for high density oligonucleotide array data based on variance and bias. *Bioinformatics* **19,** 185-193.
Bonifati V *et al* (2003) Mutations in the DJ-1 gene associated with autosomal recessive early-onset parkinsonism. *Science* **299,** 256-259.
Bonifati V *et al* (2005) Early-onset parkinsonism associated with PINK1 mutations: frequency, genotypes, and phenotypes. *Neurology* **65,** 87-95.

Borchelt DR *et al* (1996) Familial Alzheimer's disease-linked presenilin 1 variants elevate Abeta1-42/1-40 ratio in vitro and in vivo. *Neuron* **17,** 1005-1013.
Bosboom JL, Stoffers D, Wolters EC (2004) Cognitive dysfunction and dementia in Parkinson's disease. *J.Neural Transm.* **111,** 1303-1315.
Bossers K, Meerhoff G, Balesar R, van Dongen JW, Kruse CG, Swaab DF, Verhaagen J (2009) Analysis of gene expression in Parkinson's disease: possible involvement of neurotrophic support and axon guidance in dopaminergic cell death. *Brain Pathol.* **19,** 91-107.
Bossers, K., Meerhoff, G., Essing, A. et al. Gene expression changes in the human prefrontal cortex during the progression of Alzheimer's Disease. 2009.
Bourgin C, Murai KK, Richter M, Pasquale EB (2007) The EphA4 receptor regulates dendritic spine remodeling by affecting beta1-integrin signaling pathways. *J.Cell Biol.* **178,** 1295-1307.
Bouzioukh F, Daoudal G, Falk J, Debanne D, Rougon G, Castellani V (2006) Semaphorin3A regulates synaptic function of differentiated hippocampal neurons. *Eur.J.Neurosci.* **23,** 2247-2254.
Bove J, Prou D, Perier C, Przedborski S (2005) Toxin-induced models of Parkinson's disease. *NeuroRx.* **2,** 484-494.
Braak H, Alafuzoff I, Arzberger T, Kretzschmar H, Del Tredici K (2006) Staging of Alzheimer disease-associated neurofibrillary pathology using paraffin sections and immunocytochemistry. *Acta Neuropathol.(Berl)* **112,** 389-404.
Braak H, Braak E (1991) Neuropathological stageing of Alzheimer-related changes. *Acta Neuropathol. (Berl)* **82,** 239-259.
Braak H, de Vos RA, Jansen EN, Bratzke H, Braak E (1998) Neuropathological hallmarks of Alzheimer's and Parkinson's diseases. *Prog.Brain Res.* **117,** 267-285.
Braak H, Del Tredici K, Rub U, de Vos RA, Jansen Steur EN, Braak E (2003) Staging of brain pathology related to sporadic Parkinson's disease. *Neurobiol Aging* **24,** 197-211.
Bradford M, Law MH, Stewart AD, Shaw DJ, Megson IL, Wei J (2008) The TGM2 gene is associated with schizophrenia in a British population. *Am.J.Med.Genet.B Neuropsychiatr.Genet.*
Brun A, Liu X, Erikson C (1995) Synapse loss and gliosis in the molecular layer of the cerebral cortex in Alzheimer's disease and in frontal lobe degeneration. *Neurodegeneration.* **4,** 171-177.
Bubber P, Tang J, Haroutunian V, Xu H, Davis KL, Blass JP, Gibson GE (2004) Mitochondrial enzymes in schizophrenia. *J.Mol.Neurosci.* **24,** 315-321.
Buffart TE, Israeli D, Tijssen M., Vosse S.J., Mrsic A, Meijer G.A., Ylstra B (2008) Across array comparative genomic hybridization; a strategy to reduce reference channel hybridizations. *Genes, Chromosomes & Cancer.*
Burke RE, Dauer WT, Vonsattel JP (2008) A critical evaluation of the Braak staging scheme for Parkinson's disease. *Ann.Neurol.* **64,** 485-491.
Busche MA *et al* (2008) Clusters of hyperactive neurons near amyloid plaques in a mouse model of Alzheimer's disease. *Science* **321,** 1686-1689.
Busser J, Geldmacher DS, Herrup K (1998) Ectopic cell cycle proteins predict the sites of neuronal cell death in Alzheimer's disease brain. *J.Neurosci.* **18,** 2801-2807.
Busygina V, Kottemann MC, Scott KL, Plon SE, Bale AE (2006) Multiple endocrine neoplasia type 1 interacts with forkhead transcription factor CHES1 in DNA damage response. *Cancer Res.* **66,** 8397-8403.
Butterfield DA, Drake J, Pocernich C, Castegna A (2001) Evidence of oxidative damage in Alzheimer's disease brain: central role for amyloid beta-peptide. *Trends Mol.Med.* **7,** 548-554.
Buxbaum JD, Ruefli AA, Parker CA, Cypess AM, Greengard P (1994) Calcium regulates processing of the Alzheimer amyloid protein precursor in a protein kinase C-independent manner. *Proc.Natl.Acad. Sci.U.S.A* **91,** 4489-4493.
Cai XD, Golde TE, Younkin SG (1993) Release of excess amyloid beta protein from a mutant amyloid beta protein precursor. *Science* **259,** 514-516.
Cammermeyer J (1967) Artifactual displacement of neuronal nucleoli in paraffin sections. *J.Hirnforsch.* **9,** 209-224.
Caraveo G, van Rossum DB, Patterson RL, Snyder SH, Desiderio S (2006) Action of TFII-I outside the nucleus as an inhibitor of agonist-induced calcium entry. *Science* **314,** 122-125.
Cardoso SM, Proenca MT, Santos S, Santana I, Oliveira CR (2004) Cytochrome c oxidase is decreased in Alzheimer's disease platelets. *Neurobiol.Aging* **25,** 105-110.
Carmine BA, Westerlund M, Bergman O, Nissbrandt H, Lind C, Sydow O, Galter D (2007) S18Y in ubiquitin carboxy-terminal hydrolase L1 (UCH-L1) associated with decreased risk of Parkinson's disease in Sweden. *Parkinsonism.Relat Disord.* **13,** 295-298.
Carroll JC, Rosario ER, Chang L, Stanczyk FZ, Oddo S, LaFerla FM, Pike CJ (2007) Progesterone and estrogen regulate Alzheimer-like neuropathology in female 3xTg-AD mice. *J.Neurosci.* **27,** 13357-13365.
Caselli RJ *et al* (2007) Cognitive domain decline in healthy apolipoprotein E epsilon4 homozygotes before the diagnosis of mild cognitive impairment. *Arch.Neurol.* **64,** 1306-1311.

Castillo SO *et al* (1998) Dopamine biosynthesis is selectively abolished in substantia nigra/ventral tegmental area but not in hypothalamic neurons in mice with targeted disruption of the Nurr1 gene. *Mol. Cell Neurosci.* **11,** 36-46.
Cataldo AM *et al* (1995) Gene expression and cellular content of cathepsin D in Alzheimer's disease brain: evidence for early up-regulation of the endosomal-lysosomal system. *Neuron* **14,** 671-680.
Cataldo AM *et al* (2004) Presenilin mutations in familial Alzheimer disease and transgenic mouse models accelerate neuronal lysosomal pathology. *J.Neuropathol.Exp.Neurol.* **63,** 821-830.
Cataldo AM, Hamilton DJ, Barnett JL, Paskevich PA, Nixon RA (1996) Properties of the endosomal-lysosomal system in the human central nervous system: disturbances mark most neurons in populations at risk to degenerate in Alzheimer's disease. *J.Neurosci.* **16,** 186-199.
Catts VS, Catts SV, Fernandez HR, Taylor JM, Coulson EJ, Lutze-Mann LH (2005) A microarray study of post-mortem mRNA degradation in mouse brain tissue. *Brain Res.Mol.Brain Res.* **138,** 164-177.
Chafekar SM, Baas F, Scheper W (2008) Oligomer-specific Abeta toxicity in cell models is mediated by selective uptake. *Biochim.Biophys.Acta* **1782,** 523-531.
Chafekar SM, Hoozemans JJ, Zwart R, Baas F, Scheper W (2007) Abeta 1-42 induces mild endoplasmic reticulum stress in an aggregation state-dependent manner. *Antioxid.Redox.Signal.* **9,** 2245-2254.
Chambers JS, Thomas D, Saland L, Neve RL, Perrone-Bizzozero NI (2005) Growth-associated protein 43 (GAP-43) and synaptophysin alterations in the dentate gyrus of patients with schizophrenia. *Prog. Neuropsychopharmacol.Biol.Psychiatry* **29,** 283-290.
Chandra S, Gallardo G, Fernandez-Chacon R, Schluter OM, Sudhof TC (2005) Alpha-synuclein cooperates with CSPalpha in preventing neurodegeneration. *Cell* **123,** 383-396.
Chang S, ran MT, Miranda RD, Balestra ME, Mahley RW, Huang Y (2005) Lipid- and receptor-binding regions of apolipoprotein E4 fragments act in concert to cause mitochondrial dysfunction and neurotoxicity. *Proc.Natl.Acad.Sci.U.S.A* **102,** 18694-18699.
Chao DT, Korsmeyer SJ (1998) BCL-2 family: regulators of cell death. *Annu.Rev.Immunol.* **16,** 395-419.
Chen J *et al* (2005) SIRT1 protects against microglia-dependent amyloid-beta toxicity through inhibiting NF-kappaB signaling. *J.Biol.Chem.* **280,** 40364-40374.
Chen K *et al* (2007) Correlations between apolipoprotein E epsilon4 gene dose and whole brain atrophy rates. *Am.J.Psychiatry* **164,** 916-921.
Chen R *et al* (2004) Bcl-2 functionally interacts with inositol 1,4,5-trisphosphate receptors to regulate calcium release from the ER in response to inositol 1,4,5-trisphosphate. *J.Cell Biol.* **166,** 193-203.
Cheng FC, Ni DR, Wu MC, Kuo JS, Chia LG (1998) Glial cell line-derived neurotrophic factor protects against 1-methyl-4-phenyl-1,2,3,6-tetrahydropyridine (MPTP)-induced neurotoxicity in C57BL/6 mice. *Neurosci.Lett.* **252,** 87-90.
Cherrier MM *et al* (2005) Testosterone improves spatial memory in men with Alzheimer disease and mild cognitive impairment. *Neurology.* **64,** 2063-2068.
Chishti MA *et al* (2001) Early-onset amyloid deposition and cognitive deficits in transgenic mice expressing a double mutant form of amyloid precursor protein 695. *J.Biol.Chem.* **276,** 21562-21570.
Cholerton B, Gleason CE, Baker LD, Asthana S (2002) Estrogen and Alzheimer's disease: the story so far. *Drugs Aging* **19,** 405-427.
Christophersen NS *et al* (2007) Midbrain expression of Delta-like 1 homologue is regulated by GDNF and is associated with dopaminergic differentiation. *Exp.Neurol.* **204,** 791-801.
Ciriza I, Azcoitia I, Garcia-Segura LM (2004) Reduced progesterone metabolites protect rat hippocampal neurones from kainic acid excitotoxicity in vivo. *J.Neuroendocrinol.* **16,** 58-63.
Cirrito JR *et al* (2005) Synaptic activity regulates interstitial fluid amyloid-beta levels in vivo. *Neuron* **48,** 913-922.
Clarimon J *et al* (2006) Conflicting results regarding the semaphorin gene (SEMA5A) and the risk for Parkinson disease. *Am.J.Hum.Genet.* **78,** 1082-1084.
Clark IE *et al* (2006) Drosophila pink1 is required for mitochondrial function and interacts genetically with parkin. *Nature* **441,** 1162-1166.
Cleary JP, Walsh DM, Hofmeister JJ, Shankar GM, Kuskowski MA, Selkoe DJ, Ashe KH (2005) Natural oligomers of the amyloid-beta protein specifically disrupt cognitive function. *Nat.Neurosci.* **8,** 79-84.
Combs CK, Karlo JC, Kao SC, Landreth GE (2001) beta-Amyloid stimulation of microglia and monocytes results in TNFalpha-dependent expression of inducible nitric oxide synthase and neuronal apoptosis. *J.Neurosci.* **21,** 1179-1188.
Concas A, Follesa P, Barbaccia ML, Purdy RH, Biggio G (1999) Physiological modulation of GABA(A) receptor plasticity by progesterone metabolites. *Eur.J.Pharmacol.* **375,** 225-235.
Conrad C, Vianna C, Freeman M, Davies P (2002) A polymorphic gene nested within an intron of the tau gene: implications for Alzheimer's disease. *Proc.Natl.Acad.Sci.U.S.A* **99,** 7751-7756.
Corder EH *et al* (1993) Gene dose of apolipoprotein E type 4 allele and the risk of Alzheimer's disease in late onset families. *Science* **261,** 921-923.
Costa E *et al* (1994) Pharmacology of neurosteroid biosynthesis. Role of the mitochondrial DBI receptor (MDR) complex. *Ann.N.Y.Acad.Sci.* **746:223-42.,** 223-242.

Costa-Mattioli M, Sossin WS, Klann E, Sonenberg N (2009) Translational control of long-lasting synaptic plasticity and memory. *Neuron* **61,** 10-26.
Craft S *et al* (1998) Accelerated decline in apolipoprotein E-epsilon4 homozygotes with Alzheimer's disease. *Neurology* **51,** 149-153.
Crowder RJ, Enomoto H, Yang M, Johnson EM, Jr., Milbrandt J (2004) Dok-6, a Novel p62 Dok family member, promotes Ret-mediated neurite outgrowth. *J Biol Chem* **279,** 42072-42081.
Cuenin S, Tinel A, Janssens S, Tschopp J (2008) p53-induced protein with a death domain (PIDD) isoforms differentially activate nuclear factor-kappaB and caspase-2 in response to genotoxic stress. *Oncogene* **27,** 387-396.
Damier P, Hirsch EC, Agid Y, Graybiel AM (1999) The substantia nigra of the human brain. II. Patterns of loss of dopamine-containing neurons in Parkinson's disease. *Brain* **122 (Pt 8),** 1437-1448.
Dauer W, Przedborski S (2003) Parkinson's disease: mechanisms and models. *Neuron* **39,** 889-909.
Davies P, Katzman R, Terry RD (1980) Reduced somatostatin-like immunoreactivity in cerebral cortex from cases of Alzheimer disease and Alzheimer senile dementa. *Nature* **288,** 279-280.
Davis GC, Williams AC, Markey SP, Ebert MH, Caine ED, Reichert CM, Kopin IJ (1979) Chronic Parkinsonism secondary to intravenous injection of meperidine analogues. *Psychiatry Res.* **1,** 249-254.
Dawbarn D, Allen SJ (2003) Neurotrophins and neurodegeneration. *Neuropathol.Appl.Neurobiol.* **29,** 211-230.
de la Monte SM, Sohn YK, Wands JR (1997) Correlates of p53- and Fas (CD95)-mediated apoptosis in Alzheimer's disease. *J.Neurol.Sci.* **152,** 73-83.
De Winter F *et al* (2002) Injury-induced class 3 semaphorin expression in the rat spinal cord. *Exp.Neurol.* **175,** 61-75.
De Winter F *et al* (2006) The expression of the chemorepellent Semaphorin 3A is selectively induced in terminal Schwann cells of a subset of neuromuscular synapses that display limited anatomical plasticity and enhanced vulnerability in motor neuron disease. *Mol.Cell Neurosci.* **32,** 102-117.
de Wit J, Eggers R, Evers R, Castren E, Verhaagen J (2006) Long-term adeno-associated viral vector-mediated expression of truncated TrkB in the adult rat facial nucleus results in motor neuron degeneration. *J.Neurosci.* **26,** 1516-1530.
de Wit J, Verhaagen J (2003) Role of semaphorins in the adult nervous system. *Prog.Neurobiol.* **71,** 249-267.
DeKosky ST, Scheff SW (1990) Synapse loss in frontal cortex biopsies in Alzheimer's disease: correlation with cognitive severity. *Ann.Neurol.* **27,** 457-464.
Demuro A, Mina E, Kayed R, Milton SC, Parker I, Glabe CG (2005) Calcium dysregulation and membrane disruption as a ubiquitous neurotoxic mechanism of soluble amyloid oligomers. *J.Biol.Chem.* **280,** 17294-17300.
Deuel TA, Liu JS, Corbo JC, Yoo SY, Rorke-Adams LB, Walsh CA (2006) Genetic interactions between doublecortin and doublecortin-like kinase in neuronal migration and axon outgrowth. *Neuron* **49,** 41-53.
Devi L, Prabhu BM, Galati DF, Avadhani NG, Anandatheerthavarada HK (2006) Accumulation of amyloid precursor protein in the mitochondrial import channels of human Alzheimer's disease brain is associated with mitochondrial dysfunction. *J.Neurosci.* **26,** 9057-9068.
Di Monte DA, Royland JE, Irwin I, Langston JW (1996) Astrocytes as the site for bioactivation of neurotoxins. *Neurotoxicology* **17,** 697-703.
Diamandis EP *et al* (2004) Altered kallikrein 7 and 10 concentrations in cerebrospinal fluid of patients with Alzheimer's disease and frontotemporal dementia. *Clin.Biochem.* **37,** 230-237.
Ding H *et al* (2008) Association study of semaphorin 5A with risk of Parkinson's disease in a Chinese Han population. *Brain Res.*
Ding Q, Markesbery WR, Cecarini V, Keller JN (2006) Decreased RNA, and increased RNA oxidation, in ribosomes from early Alzheimer's disease. *Neurochem.Res.* **31,** 705-710.
Djebaili M, Guo Q, Pettus EH, Hoffman SW, Stein DG (2005) The neurosteroids progesterone and allopregnanolone reduce cell death, gliosis, and functional deficits after traumatic brain injury in rats. *J.Neurotrauma.* **22,** 106-118.
Do Rego JL *et al* (2009) Neurosteroid biosynthesis: enzymatic pathways and neuroendocrine regulation by neurotransmitters and neuropeptides. *Front Neuroendocrinol.*
Dorsey SG *et al* (2006) In vivo restoration of physiological levels of truncated TrkB.T1 receptor rescues neuronal cell death in a trisomic mouse model. *Neuron* **51,** 21-28.
Drake J *et al* (2004) 4-Hydroxynonenal oxidatively modifies histones: implications for Alzheimer's disease. *Neurosci.Lett.* **356,** 155-158.
Dreses-Werringloer U *et al* (2008) A polymorphism in CALHM1 influences Ca2+ homeostasis, Abeta levels, and Alzheimer's disease risk. *Cell* **133,** 1149-1161.
Dubelaar EJ, Mufson EJ, ter Meulen WG, Van Heerikhuize JJ, Verwer RW, Swaab DF (2006) Increased metabolic activity in nucleus basalis of Meynert neurons in elderly individuals with mild cognitive impairment as indicated by the size of the Golgi apparatus. *J.Neuropathol.Exp.Neurol.* **65,** 257-266.

Dubelaar EJ, Verwer RW, Hofman MA, Van Heerikhuize JJ, Ravid R, Swaab DE (2004) ApoE epsilon4 genotype is accompanied by lower metabolic activity in nucleus basalis of Meynert neurons in Alzheimer patients and controls as indicated by the size of the Golgi apparatus. *J.Neuropathol.Exp.Neurol.* **63,** 159-169.
Dubrovsky BO (2005) Steroids, neuroactive steroids and neurosteroids in psychopathology. *Prog.Neuropsychopharmacol.Biol.Psychiatry.* **29,** 169-192.
Duff K *et al* (1996) Increased amyloid-beta42(43) in brains of mice expressing mutant presenilin 1. *Nature* **383,** 710-713.
Duke DC, Moran LB, Kalaitzakis ME, Deprez M, Dexter DT, Pearce RK, Graeber MB (2006) Transcriptome analysis reveals link between proteasomal and mitochondrial pathways in Parkinson's disease. *Neurogenetics.* **7,** 139-148.
Eastwood SL, Law AJ, Everall IP, Harrison PJ (2003) The axonal chemorepellant semaphorin 3A is increased in the cerebellum in schizophrenia and may contribute to its synaptic pathology. *Mol.Psychiatry* **8,** 148-155.
Eikelenboom P, Bate C, Van Gool WA, Hoozemans JJ, Rozemuller JM, Veerhuis R, Williams A (2002) Neuroinflammation in Alzheimer's disease and prion disease. *Glia* **40,** 232-239.
Elbaz A *et al* (2006) Lack of replication of thirteen single-nucleotide polymorphisms implicated in Parkinson's disease: a large-scale international study. *Lancet Neurol.* **5,** 917-923.
Emilsson L, Saetre P, Jazin E (2006) Alzheimer's disease: mRNA expression profiles of multiple patients show alterations of genes involved with calcium signaling. *Neurobiol.Dis.* **21,** 618-625.
Emptage N, Bliss TV, Fine A (1999) Single synaptic events evoke NMDA receptor-mediated release of calcium from internal stores in hippocampal dendritic spines. *Neuron* **22,** 115-124.
Emre M (2003) What causes mental dysfunction in Parkinson's disease? *Mov Disord.* **18 Suppl 6,** S63-S71.
Erkut ZA, Gabreels BA, Eikelenboom J, van Leeuwen FW, Swaab DF (2002) Glucocorticoid treatment is associated with decreased expression of processed AVP but not of proAVP, neurophysin or oxytocin in the human hypothalamus: are PC1 and PC2 involved? *Neuro.Endocrinol.Lett.* **23,** 33-44.
Erraji-Benchekroun L *et al* (2005) Molecular aging in human prefrontal cortex is selective and continuous throughout adult life. *Biol Psychiatry* **57,** 549-558.
Farrant M, Nusser Z (2005) Variations on an inhibitory theme: phasic and tonic activation of GABA(A) receptors. *Nat.Rev.Neurosci.* **6,** 215-229.
Ferrarese C, Appollonio I, Frigo M, Meregalli S, Piolti R, Tamma F, Frattola L (1990) Cerebrospinal fluid levels of diazepam-binding inhibitor in neurodegenerative disorders with dementia. *Neurology.* **40,** 632-635.
Ferrer I, Marti E (1998) Distribution of fibroblast growth factor receptor-1 (FGFR-1) and FGFR-3 in the hippocampus of patients with Alzheimer's disease. *Neurosci.Lett.* **240,** 139-142.
Ferrero P, Benna P, Costa P, Tarenzi L, Baggio G, Bergamasco B, Bergamini L (1988) Diazepam binding inhibitor-like immunoreactivity (DBI-LI) in human CSF. Correlations with neurological disorders. *J.Neurol.Sci.* **87,** 327-349.
Flaherty DB, Soria JP, Tomasiewicz HG, Wood JG (2000) Phosphorylation of human tau protein by microtubule-associated kinases: GSK3beta and cdk5 are key participants. *J.Neurosci.Res.* **62,** 463-472.
Fleige S, Pfaffl MW (2006) RNA integrity and the effect on the real-time qRT-PCR performance. *Mol. Aspects Med.* **27,** 126-139.
Fleige S, Walf V, Huch S, Prgomet C, Sehm J, Pfaffl MW (2006) Comparison of relative mRNA quantification models and the impact of RNA integrity in quantitative real-time RT-PCR. *Biotechnol.Lett.* **28,** 1601-1613.
Follesa P *et al* (2005) Distinct patterns of expression and regulation of GABA receptors containing the delta subunit in cerebellar granule and hippocampal neurons. *J.Neurochem.* **94,** 659-671.
Folstein MF, Folstein SE, McHugh PR (1975) "Mini-mental state". A practical method for grading the cognitive state of patients for the clinician. *J.Psychiatr.Res.* **12,** 189-198.
Foltynie T, Brayne CE, Robbins TW, Barker RA (2004) The cognitive ability of an incident cohort of Parkinson's patients in the UK. The CamPaIGN study. *Brain* **127,** 550-560.
Fornai F *et al* (2005) Parkinson-like syndrome induced by continuous MPTP infusion: convergent roles of the ubiquitin-proteasome system and alpha-synuclein. *Proc.Natl.Acad.Sci.U.S.A* **102,** 3413-3418.
Forno LS (1996) Neuropathology of Parkinson's disease. *J.Neuropathol.Exp.Neurol.* **55,** 259-272.
Forstl H, Kurz A (1999) Clinical features of Alzheimer's disease. *Eur.Arch.Psychiatry Clin.Neurosci.* **249,** 288-290.
Fuchs J *et al* (2007) The transcription factor PITX3 is associated with sporadic Parkinson's disease. *Neurobiol.Aging.*
Funayama M, Hasegawa K, Kowa H, Saito M, Tsuji S, Obata F (2002) A new locus for Parkinson's disease (PARK8) maps to chromosome 12p11.2-q13.1. *Ann.Neurol.* **51,** 296-301.
Futschik ME, Carlisle B (2005) Noise-robust soft clustering of gene expression time-course data. *J.Bioinform.Comput.Biol.* **3,** 965-988.

Gaasch JA, Lockman PR, Geldenhuys WJ, Allen DD, Van der Schyf CJ (2007) Brain iron toxicity: differential responses of astrocytes, neurons, and endothelial cells. *Neurochem.Res.* **32,** 1196-1208.
Gallagher JP, Orozco-Cabal LF, Liu J, Shinnick-Gallagher P (2008) Synaptic physiology of central CRH system. *Eur.J.Pharmacol.* **583,** 215-225.
Games D *et al* (1995) Alzheimer-type neuropathology in transgenic mice overexpressing V717F beta-amyloid precursor protein. *Nature* **373,** 523-527.
Gandhi S *et al* (2006) PINK1 protein in normal human brain and Parkinson's disease. *Brain* **129,** 1720-1731.
Gao T, Furnari F, Newton AC (2005) PHLPP: a phosphatase that directly dephosphorylates Akt, promotes apoptosis, and suppresses tumor growth. *Mol Cell* **18,** 13-24.
Garcia-Ovejero D, Azcoitia I, DonCarlos LL, Melcangi RC, Garcia-Segura LM (2005) Glia-neuron crosstalk in the neuroprotective mechanisms of sex steroid hormones. *Brain Res.Brain Res.Rev.* **48,** 273-286.
Garcia-Segura LM (2008) Aromatase in the brain: not just for reproduction anymore. *J.Neuroendocrinol.* **20,** 705-712.
Gasmi M *et al* (2007) AAV2-mediated delivery of human neurturin to the rat nigrostriatal system: long-term efficacy and tolerability of CERE-120 for Parkinson's disease. *Neurobiol.Dis.* **27,** 67-76.
Gatz M, Prescott CA, Pedersen NL (2006) Lifestyle risk and delaying factors. *Alzheimer Dis.Assoc. Disord.* **20,** S84-S88.
Geci C, How J, Alturaihi H, Kumar U (2007) Beta-amyloid increases somatostatin expression in cultured cortical neurons. *J.Neurochem.* **101,** 664-673.
Genazzani AR, Pluchino N, Luisi S, Luisi M (2007) Estrogen, cognition and female ageing. *Hum. Reprod.Update.* **13,** 175-187.
Gilks WP *et al* (2005) A common LRRK2 mutation in idiopathic Parkinson's disease. *Lancet* **365,** 415-416.
Giovanni A, Wirtz-Brugger F, Keramaris E, Slack R, Park DS (1999) Involvement of cell cycle elements, cyclin-dependent kinases, pRb, and E2F x DP, in B-amyloid-induced neuronal death. *J.Biol.Chem.* **274,** 19011-19016.
Goate A *et al* (1991) Segregation of a missense mutation in the amyloid precursor protein gene with familial Alzheimer's disease. *Nature* **349,** 704-706.
Goedert M (1993) Tau protein and the neurofibrillary pathology of Alzheimer's disease. *Trends Neurosci.* **16,** 460-465.
Goedert M (2005) Tau gene mutations and their effects. *Mov Disord.* **20 Suppl 12,** S45-S52.
Goedert M, Spillantini MG, Jakes R, Rutherford D, Crowther RA (1989) Multiple isoforms of human microtubule-associated protein tau: sequences and localization in neurofibrillary tangles of Alzheimer's disease. *Neuron* **3,** 519-526.
Gouras GK *et al* (2000) Intraneuronal Abeta42 accumulation in human brain. *Am.J.Pathol.* **156,** 15-20.
Gouras GK, Xu H, Gross RS, Greenfield JP, Hai B, Wang R, Greengard P (2000) Testosterone reduces neuronal secretion of Alzheimer's beta-amyloid peptides. *Proc.Natl.Acad.Sci.U.S.A* **97,** 1202-1205.
Green JA, Kim JG, Whitworth KM, Agca C, Prather RS (2006) The use of microarrays to define functionally-related genes that are differentially expressed in the cycling pig uterus. *Soc.Reprod.Fertil. Suppl* **62,** 163-176.
Greene JG, Dingledine R, Greenamyre JT (2005) Gene expression profiling of rat midbrain dopamine neurons: implications for selective vulnerability in parkinsonism. *Neurobiol Dis* **18,** 19-31.
Grunblatt E *et al* (2004) Gene expression profiling of parkinsonian substantia nigra pars compacta; alterations in ubiquitin-proteasome, heat shock protein, iron and oxidative stress regulated proteins, cell adhesion/cellular matrix and vesicle trafficking genes. *J Neural Transm.* **111,** 1543-1573.
Grundke-Iqbal I, Iqbal K, Quinlan M, Tung YC, Zaidi MS, Wisniewski HM (1986) Microtubule-associated protein tau. A component of Alzheimer paired helical filaments. *J.Biol.Chem.* **261,** 6084-6089.
Gyure KA, Durham R, Stewart WF, Smialek JE, Troncoso JC (2001) Intraneuronal abeta-amyloid precedes development of amyloid plaques in Down syndrome. *Arch.Pathol.Lab Med.* **125,** 489-492.
Ha C, Ryu J, Park CB (2007) Metal ions differentially influence the aggregation and deposition of Alzheimer's beta-amyloid on a solid template. *Biochemistry* **46,** 6118-6125.
Habermann B (2004) The BAR-domain family of proteins: a case of bending and binding? *EMBO Rep.* **5,** 250-255.
Hajnoczky G, Hager R, Thomas AP (1999) Mitochondria suppress local feedback activation of inositol 1,4, 5-trisphosphate receptors by Ca2+. *J.Biol.Chem.* **274,** 14157-14162.
Halim ND, Weickert CS, McClintock BW, Hyde TM, Weinberger DR, Kleinman JE, Lipska BK (2003) Presynaptic proteins in the prefrontal cortex of patients with schizophrenia and rats with abnormal prefrontal development. *Mol.Psychiatry* **8,** 797-810.
Hall CB, Derby C, LeValley A, Katz MJ, Verghese J, Lipton RB (2007) Education delays accelerated decline on a memory test in persons who develop dementia. *Neurology* **69,** 1657-1664.

Hamani C, Saint-Cyr JA, Fraser J, Kaplitt M, Lozano AM (2004) The subthalamic nucleus in the context of movement disorders. *Brain* **127,** 4-20.
Hamos JE, DeGennaro LJ, Drachman DA (1989) Synaptic loss in Alzheimer's disease and other dementias. *Neurology* **39,** 355-361.
Hannula-Jouppi K, Kaminen-Ahola N, Taipale M, Eklund R, Nopola-Hemmi J, Kaariainen H, Kere J (2005) The axon guidance receptor gene ROBO1 is a candidate gene for developmental dyslexia. *PLoS. Genet.* **1,** e50.
Hardy J (1992) Framing beta-amyloid. *Nat.Genet.* **1,** 233-234.
Hardy J, Cai H, Cookson MR, Gwinn-Hardy K, Singleton A (2006) Genetics of Parkinson's disease and parkinsonism. *Ann.Neurol.* **60,** 389-398.
Hardy JA, Higgins GA (1992) Alzheimer's disease: the amyloid cascade hypothesis. *Science* **256,** 184-185.
Harlan RE, Garcia MM (1998) Drugs of abuse and immediate-early genes in the forebrain. *Mol.Neurobiol.* **16,** 221-267.
Hastie T, Tibshirani R, Friedman J (2001) 'The Elements of Statistical Learning.' (Springer-Verlag New York, LLC:
Hauptmann S, Keil U, Scherping I, Bonert A, Eckert A, Muller WE (2006) Mitochondrial dysfunction in sporadic and genetic Alzheimer's disease. *Exp.Gerontol.* **41,** 668-673.
He J, Hoffman SW, Stein DG (2004) Allopregnanolone, a progesterone metabolite, enhances behavioral recovery and decreases neuronal loss after traumatic brain injury. *Restor.Neurol.Neurosci.* **22,** 19-31.
He XY, Wegiel J, Yang YZ, Pullarkat R, Schulz H, Yang SY (2005) Type 10 17beta-hydroxysteroid dehydrogenase catalyzing the oxidation of steroid modulators of gamma-aminobutyric acid type A receptors. *Mol.Cell Endocrinol.* **229,** 111-117.
Henn IH *et al* (2007) Parkin mediates neuroprotection through activation of IkappaB kinase/nuclear factor-kappaB signaling. *J.Neurosci.* **27,** 1868-1878.
Herd MB, Belelli D, Lambert JJ (2007) Neurosteroid modulation of synaptic and extrasynaptic GABA(A) receptors. *Pharmacol.Ther.* **116,** 20-34.
Herkenham M, Little MD, Bankiewicz K, Yang SC, Markey SP, Johannessen JN (1991) Selective retention of MPP+ within the monoaminergic systems of the primate brain following MPTP administration: an in vivo autoradiographic study. *Neuroscience* **40,** 133-158.
Hidalgo J *et al* (2006) Expression of metallothionein-I, -II, and -III in Alzheimer disease and animal models of neuroinflammation. *Exp.Biol.Med.(Maywood.)* **231,** 1450-1458.
Hoen PA, Turk R, Boer JM, Sterrenburg E, De Menezes RX, Van Ommen GJ, Den Dunnen JT (2004) Intensity-based analysis of two-colour microarrays enables efficient and flexible hybridization designs. *Nucleic Acids Res* **32,** E41.
Hofman A *et al* (1997) Atherosclerosis, apolipoprotein E, and prevalence of dementia and Alzheimer's disease in the Rotterdam Study. *Lancet* **349,** 151-154.
Hogervorst E (2008) Testosterone supplementation did not prevent cognitive decline or increase bone mineral density in older men. *Evid.Based.Med.* **13,** 71.
Hol EM, van Leeuwen FW, Fischer DF (2005) The proteasome in Alzheimer's disease and Parkinson's disease: lessons from ubiquitin B+1. *Trends Mol.Med.* **11,** 488-495.
Holcomb L *et al* (1998) Accelerated Alzheimer-type phenotype in transgenic mice carrying both mutant amyloid precursor protein and presenilin 1 transgenes. *Nat.Med.* **4,** 97-100.
Holmes C *et al* (2008) Long-term effects of Abeta42 immunisation in Alzheimer's disease: follow-up of a randomised, placebo-controlled phase I trial. *Lancet* **372,** 216-223.
Holtzman DM *et al* (2000) Apolipoprotein E isoform-dependent amyloid deposition and neuritic degeneration in a mouse model of Alzheimer's disease. *Proc.Natl.Acad.Sci.U.S.A* **97,** 2892-2897.
Hsiao K *et al* (1996) Correlative memory deficits, Abeta elevation, and amyloid plaques in transgenic mice. *Science* **274,** 99-102.
Huitinga I, van der CM, Salm L, Erkut Z, van Dam A, Tilders F, Swaab D (2000) IL-1beta immunoreactive neurons in the human hypothalamus: reduced numbers in multiple sclerosis. *J.Neuroimmunol.* **107,** 8-20.
Husseman JW, Nochlin D, Vincent I (2000) Mitotic activation: a convergent mechanism for a cohort of neurodegenerative diseases. *Neurobiol.Aging* **21,** 815-828.
Hutter CM *et al* (2008) Lack of evidence for an association between UCHL1 S18Y and Parkinson's disease. *Eur.J.Neurol.* **15,** 134-139.
Hyun TS *et al* (2004) HIP1 and HIP1r stabilize receptor tyrosine kinases and bind 3-phosphoinositides via epsin N-terminal homology domains. *J.Biol.Chem.* **279,** 14294-14306.
Inui H, Miyatake K, Nakano Y, Kitaoka S (1986) Purification and some properties of short chain-length specific trans-2-enoyl-CoA reductase in mitochondria of Euglena gracilis. *J.Biochem.* **100,** 995-1000.
Irizarry MC, McNamara M, Fedorchak K, Hsiao K, Hyman BT (1997a) APPSw transgenic mice develop age-related A beta deposits and neuropil abnormalities, but no neuronal loss in CA1. *J.Neuropathol.Exp. Neurol.* **56,** 965-973.

Irizarry MC, Soriano F, McNamara M, Page KJ, Schenk D, Games D, Hyman BT (1997b) Abeta deposition is associated with neuropil changes, but not with overt neuronal loss in the human amyloid precursor protein V717F (PDAPP) transgenic mouse. *J.Neurosci.* **17,** 7053-7059.
Irvine RF, Letcher AJ, Heslop JP, Berridge MJ (1986) The inositol tris/tetrakisphosphate pathway--demonstration of Ins(1,4,5)P3 3-kinase activity in animal tissues. *Nature* **320,** 631-634.
Jagadish MN *et al* (1996) Insulin-responsive tissues contain the core complex protein SNAP-25 (synaptosomal-associated protein 25) A and B isoforms in addition to syntaxin 4 and synaptobrevins 1 and 2. *Biochem.J.* **317 (Pt 3),** 945-954.
Jellinger KA (2008) A critical reappraisal of current staging of Lewy-related pathology in human brain. *Acta Neuropathol.* **116,** 1-16.
Ji Y, Gong Y, Gan W, Beach T, Holtzman DM, Wisniewski T (2003) Apolipoprotein E isoform-specific regulation of dendritic spine morphology in apolipoprotein E transgenic mice and Alzheimer's disease patients. *Neuroscience* **122,** 305-315.
Jiang C, Wan X, He Y, Pan T, Jankovic J, Le W (2005) Age-dependent dopaminergic dysfunction in Nurr1 knockout mice. *Exp.Neurol.* **191,** 154-162.
Jick H, Zornberg GL, Jick SS, Seshadri S, Drachman DA (2000) Statins and the risk of dementia. *Lancet* **356,** 1627-1631.
Jokic N *et al* (2006) The neurite outgrowth inhibitor Nogo-A promotes denervation in an amyotrophic lateral sclerosis model. *EMBO Rep.* **7,** 1162-1167.
Jones MH, Hamana N, Nezu J, Shimane M (2000) A novel family of bromodomain genes. *Genomics* **63,** 40-45.
Jouaville LS, Ichas F, Holmuhamedov EL, Camacho P, Lechleiter JD (1995) Synchronization of calcium waves by mitochondrial substrates in Xenopus laevis oocytes. *Nature* **377,** 438-441.
Kaether C *et al* (2007) Endoplasmic reticulum retention of the gamma-secretase complex component Pen2 by Rer1. *EMBO Rep.* **8,** 743-748.
Kalaria RN (1999) Microglia and Alzheimer's disease. *Curr.Opin.Hematol.* **6,** 15-24.
Kamenetz F *et al* (2003) APP processing and synaptic function. *Neuron* **37,** 925-937.
Kantor DB *et al* (2004) Semaphorin 5A is a bifunctional axon guidance cue regulated by heparan and chondroitin sulfate proteoglycans. *Neuron* **44,** 961-975.
Karlnoski R *et al* (2007) Up-regulation of Bcl-2 in APP transgenic mice is associated with neuroprotection. *Neurobiol.Dis.* **25,** 179-188.
Kask K, Backstrom T, Nilsson LG, Sundstrom-Poromaa I (2008) Allopregnanolone impairs episodic memory in healthy women. *Psychopharmacology (Berl).* **199,** 161-168.
Katsel P, Li C, Haroutunian V (2007) Gene expression alterations in the sphingolipid metabolism pathways during progression of dementia and Alzheimer's disease: a shift toward ceramide accumulation at the earliest recognizable stages of Alzheimer's disease? *Neurochem.Res.* **32,** 845-856.
Keeney PM, Xie J, Capaldi RA, Bennett JP, Jr. (2006) Parkinson's disease brain mitochondrial complex I has oxidatively damaged subunits and is functionally impaired and misassembled. *J Neurosci* **26,** 5256-5264.
Keller JN (2006) Age-related neuropathology, cognitive decline, and Alzheimer's disease. *Ageing Res. Rev.* **5,** 1-13.
Kennedy MJ, Ehlers MD (2006) Organelles and trafficking machinery for postsynaptic plasticity. *Annu. Rev.Neurosci.* **29,** 325-362.
Kerr MK, Churchill GA (2001) Experimental design for gene expression microarrays. *Biostatistics* **2,** 183-201.
Kingsbury AE, Daniel SE, Sangha H, Eisen S, Lees AJ, Foster OJ (2004) Alteration in alpha-synuclein mRNA expression in Parkinson's disease. *Mov Disord.* **19,** 162-170.
Kirik D, Georgievska B, Bjorklund A (2004) Localized striatal delivery of GDNF as a treatment for Parkinson disease. *Nat.Neurosci.* **7,** 105-110.
Kirkitadze MD, Bitan G, Teplow DB (2002) Paradigm shifts in Alzheimer's disease and other neurodegenerative disorders: the emerging role of oligomeric assemblies. *J.Neurosci.Res.* **69,** 567-577.
Kish SJ *et al* (1992) Brain cytochrome oxidase in Alzheimer's disease. *J.Neurochem.* **59,** 776-779.
Kitada T *et al* (1998) Mutations in the parkin gene cause autosomal recessive juvenile parkinsonism. *Nature* **392,** 605-608.
Klein C, Grunewald A, Hedrich K (2006) Early-onset parkinsonism associated with PINK1 mutations: frequency, genotypes, and phenotypes. *Neurology* **66,** 1129-1130.
Kobayashi H, Ujike H, Hasegawa J, Yamamoto M, Kanzaki A, Sora I (2006) Identification of a risk haplotype of the alpha-synuclein gene in Japanese with sporadic Parkinson's disease. *Mov Disord.* **21,** 2157-2164.
Koizumi H, Tanaka T, Gleeson JG (2006) Doublecortin-like kinase functions with doublecortin to mediate fiber tract decussation and neuronal migration. *Neuron* **49,** 55-66.

Kojro E, Postina R, Buro C, Meiringer C, Gehrig-Burger K, Fahrenholz F (2006) The neuropeptide PACAP promotes the alpha-secretase pathway for processing the Alzheimer amyloid precursor protein. *FASEB J.* **20,** 512-514.
Korecka JA, Verhaagen J, Hol EM (2007) Cell-replacement and gene-therapy strategies for Parkinson's and Alzheimer's disease. *Regen.Med.* **2,** 425-446.
Kramer ER *et al* (2007) Absence of Ret Signaling in Mice Causes Progressive and Late Degeneration of the Nigrostriatal System. *PLoS.Biol.* **5,** e39.
Kramer ML, Schulz-Schaeffer WJ (2007) Presynaptic alpha-synuclein aggregates, not Lewy bodies, cause neurodegeneration in dementia with Lewy bodies. *J.Neurosci.* **27,** 1405-1410.
Kuchibhotla KV, Goldman ST, Lattarulo CR, Wu HY, Hyman BT, Bacskai BJ (2008) Abeta plaques lead to aberrant regulation of calcium homeostasis in vivo resulting in structural and functional disruption of neuronal networks. *Neuron* **59,** 214-225.
Kurita M, Kuwajima T, Nishimura I, Yoshikawa K (2006) Necdin downregulates CDC2 expression to attenuate neuronal apoptosis. *J.Neurosci.* **26,** 12003-12013.
Kuromitsu J, Yokoi A, Kawai T, Nagasu T, Aizawa T, Haga S, Ikeda K (2001) Reduced neuropeptide Y mRNA levels in the frontal cortex of people with schizophrenia and bipolar disorder. *Brain Res.Gene Expr.Patterns.* **1,** 17-21.
Kuwako K *et al* (2005) Disruption of the paternal necdin gene diminishes TrkA signaling for sensory neuron survival. *J Neurosci* **25,** 7090-7099.
LaFerla FM, Green KN, Oddo S (2007) Intracellular amyloid-beta in Alzheimer's disease. *Nat.Rev. Neurosci.* **8,** 499-509.
Lanctot KL, Herrmann N, Rothenburg L, Eryavec G (2007) Behavioral correlates of GABAergic disruption in Alzheimer's disease. *Int.Psychogeriatr.* **19,** 151-158.
Lange KW, Paul GM, Naumann M, Gsell W (1995) Dopaminergic effects on cognitive performance in patients with Parkinson's disease. *J.Neural Transm.Suppl* **46,** 423-432.
Langston JW, Ballard P, Tetrud JW, Irwin I (1983) Chronic Parkinsonism in humans due to a product of meperidine-analog synthesis. *Science* **219,** 979-980.
Larsen KE *et al* (2006) Alpha-synuclein overexpression in PC12 and chromaffin cells impairs catecholamine release by interfering with a late step in exocytosis. *J.Neurosci.* **26,** 11915-11922.
Le Niculescu H *et al* (2007) Towards understanding the schizophrenia code: an expanded convergent functional genomics approach. *Am.J.Med.Genet.B Neuropsychiatr.Genet.* **144B,** 129-158.
Le W, Conneely OM, He Y, Jankovic J, Appel SH (1999) Reduced Nurr1 expression increases the vulnerability of mesencephalic dopamine neurons to MPTP-induced injury. *J.Neurochem.* **73,** 2218-2221.
Le WD, Xu P, Jankovic J, Jiang H, Appel SH, Smith RG, Vassilatis DK (2003) Mutations in NR4A2 associated with familial Parkinson disease. *Nat.Genet.* **33,** 85-89.
Lee JY, Cole TB, Palmiter RD, Suh SW, Koh JY (2002) Contribution by synaptic zinc to the gender-disparate plaque formation in human Swedish mutant APP transgenic mice. *Proc.Natl.Acad.Sci.U.S.A* **99,** 7705-7710.
Leichtnam ML, Rolland H, Wuthrich P, Guy RH (2006) Testosterone hormone replacement therapy: state-of-the-art and emerging technologies. *Pharm.Res.* **23,** 1117-1132.
Leissring MA *et al* (2002) A physiologic signaling role for the gamma -secretase-derived intracellular fragment of APP. *Proc.Natl.Acad.Sci.U.S.A* **99,** 4697-4702.
Leissring MA, Akbari Y, Fanger CM, Cahalan MD, Mattson MP, LaFerla FM (2000) Capacitative calcium entry deficits and elevated luminal calcium content in mutant presenilin-1 knockin mice. *J.Cell Biol.* **149,** 793-798.
Lesnick TG *et al* (2007) A genomic pathway approach to a complex disease: axon guidance and Parkinson disease. *PLoS.Genet.* **3,** e98.
Lethaby A, Hogervorst E, Richards M, Yesufu A, Yaffe K (2008) Hormone replacement therapy for cognitive function in postmenopausal women. *Cochrane.Database.Syst.Rev.* CD003122.
Lewis SJ, Slabosz A, Robbins TW, Barker RA, Owen AM (2005) Dopaminergic basis for deficits in working memory but not attentional set-shifting in Parkinson's disease. *Neuropsychologia* **43,** 823-832.
Li L, Yun SH, Keblesh J, Trommer BL, Xiong H, Radulovic J, Tourtellotte WG (2007) Egr3, a synaptic activity regulated transcription factor that is essential for learning and memory. *Mol.Cell Neurosci.* **35,** 76-88.
Li R, Shen Y, Yang LB, Lue LF, Finch C, Rogers J (2000) Estrogen enhances uptake of amyloid beta-protein by microglia derived from the human cortex. *J.Neurochem.* **75,** 1447-1454.
Li Y *et al* (2008) Neither replication nor simulation supports a role for the axon guidance pathway in the genetics of Parkinson's disease. *PLoS.ONE.* **3,** e2707.
Li YH, Ghavampur S, Bondallaz P, Will L, Grenningloh G, Puschel AW (2009) Rnd1 regulates axon extension by enhancing the microtubule destabilizing activity of SCG10. *J.Biol.Chem.* **284,** 363-371.

Lin HK, Steckelbroeck S, Fung KM, Jones AN, Penning TM (2004) Characterization of a monoclonal antibody for human aldo-keto reductase AKR1C3 (type 2 3alpha-hydroxysteroid dehydrogenase/type 5 17beta-hydroxysteroid dehydrogenase); immunohistochemical detection in breast and prostate. *Steroids* **69,** 795-801.
Lin L, Rao Y, Isacson O (2005) Netrin-1 and slit-2 regulate and direct neurite growth of ventral midbrain dopaminergic neurons. *Mol Cell Neurosci* **28,** 547-555.
Lincoln S *et al* (1999) Low frequency of pathogenic mutations in the ubiquitin carboxy-terminal hydrolase gene in familial Parkinson's disease. *Neuroreport* **10,** 427-429.
Liu RY, Unmehopa UA, Zhou JN, Swaab DF (2006) Glucocorticoids suppress vasopressin gene expression in human suprachiasmatic nucleus. *J.Steroid Biochem.Mol.Biol.* **98,** 248-253.
Liu XA, Zhu LQ, Zhang Q, Shi HR, Wang SH, Wang Q, Wang JZ (2008) Estradiol attenuates tau hyperphosphorylation induced by upregulation of protein kinase-A. *Neurochem.Res.* **33,** 1811-1820.
Loerch PM *et al* (2008) Evolution of the aging brain transcriptome and synaptic regulation. *PLoS.ONE.* **3,** e3329.
Logan JM, Sanders AL, Snyder AZ, Morris JC, Buckner RL (2002) Under-recruitment and nonselective recruitment: dissociable neural mechanisms associated with aging. *Neuron* **33,** 827-840.
Lowe SL, Francis PT, Procter AW, Palmer AM, Davison AN, Bowen DM (1988) Gamma-aminobutyric acid concentration in brain tissue at two stages of Alzheimer's disease. *Brain* **111 (Pt 4),** 785-799.
Lu J, Helton TD, Blanpied TA, Racz B, Newpher TM, Weinberg RJ, Ehlers MD (2007) Postsynaptic positioning of endocytic zones and AMPA receptor cycling by physical coupling of dynamin-3 to Homer. *Neuron* **55,** 874-889.
Lu PH *et al* (2006) Effects of testosterone on cognition and mood in male patients with mild Alzheimer disease and healthy elderly men. *Arch.Neurol.* **63,** 177-185.
Lu T, Pan Y, Kao SY, Li C, Kohane I, Chan J, Yankner BA (2004) Gene regulation and DNA damage in the ageing human brain. *Nature* **429,** 883-91.
Lukiw WJ (2004) Gene expression profiling in fetal, aged, and Alzheimer hippocampus: a continuum of stress-related signaling. *Neurochem.Res.* **29,** 1287-1297.
Mahley RW, Weisgraber KH, Huang Y (2006) Apolipoprotein E4: a causative factor and therapeutic target in neuropathology, including Alzheimer's disease. *Proc.Natl.Acad.Sci.U.S.A* **103,** 5644-5651.
Manly JJ, Merchant CA, Jacobs DM, Small SA, Bell K, Ferin M, Mayeux R (2000) Endogenous estrogen levels and Alzheimer's disease among postmenopausal women. *Neurology.* **54,** 833-837.
Mann F, Chauvet S, Rougon G (2007) Semaphorins in development and adult brain: Implication for neurological diseases. *Prog.Neurobiol.* **82,** 57-79.
Maraganore DM *et al* (2005) High-resolution whole-genome association study of Parkinson disease. *Am.J.Hum.Genet.* **77,** 685-693.
Mark RJ, Hensley K, Butterfield DA, Mattson MP (1995) Amyloid beta-peptide impairs ion-motive ATPase activities: evidence for a role in loss of neuronal Ca2+ homeostasis and cell death. *J.Neurosci.* **15,** 6239-6249.
Martin ER *et al* (2001) Association of single-nucleotide polymorphisms of the tau gene with late-onset Parkinson disease. *JAMA* **286,** 2245-2250.
Marx CE *et al* (2006) The neurosteroid allopregnanolone is reduced in prefrontal cortex in Alzheimer's disease. *Biol.Psychiatry.* **60,** 1287-1294.
Masliah E, Terry RD, Alford M, DeTeresa R, Hansen LA (1991) Cortical and subcortical patterns of synaptophysinlike immunoreactivity in Alzheimer's disease. *Am.J.Pathol.* **138,** 235-246.
Masliah E, Terry RD, DeTeresa RM, Hansen LA (1989) Immunohistochemical quantification of the synapse-related protein synaptophysin in Alzheimer disease. *Neurosci.Lett.* **103,** 234-239.
Matsuda T, Cepko CL (2007) Controlled expression of transgenes introduced by in vivo electroporation. *Proc.Natl.Acad.Sci.U.S.A* **104,** 1027-1032.
Mattson MP (2007) Calcium and neurodegeneration. *Aging Cell* **6,** 337-350.
Mattson MP, Chan SL, Camandola S (2001) Presenilin mutations and calcium signaling defects in the nervous and immune systems. *Bioessays* **23,** 733-744.
Mattson MP, Lovell MA, Ehmann WD, Markesbery WR (1993a) Comparison of the effects of elevated intracellular aluminum and calcium levels on neuronal survival and tau immunoreactivity. *Brain Res.* **602,** 21-31.
Mattson MP, Tomaselli KJ, Rydel RE (1993b) Calcium-destabilizing and neurodegenerative effects of aggregated beta-amyloid peptide are attenuated by basic FGF. *Brain Res.* **621,** 35-49.
May C, Rapoport SI, Tomai TP, Chrousos GP, Gold PW (1987) Cerebrospinal fluid concentrations of corticotropin-releasing hormone (CRH) and corticotropin (ACTH) are reduced in patients with Alzheimer's disease. *Neurology* **37,** 535-538.
Mayeux R (2006) Genetic epidemiology of Alzheimer disease. *Alzheimer Dis.Assoc.Disord.* **20,** S58-S62.
McGee AW, Yang Y, Fischer QS, Daw NW, Strittmatter SM (2005) Experience-driven plasticity of visual cortex limited by myelin and Nogo receptor. *Science* **309,** 2222-2226.

McGeer EG, McGeer PL (1998) The importance of inflammatory mechanisms in Alzheimer disease. *Exp.Gerontol.* **33,** 371-378.
McGeer PL *et al* (1991) Detection of the membrane inhibitor of reactive lysis (CD59) in diseased neurons of Alzheimer brain. *Brain Res.* **544,** 315-319.
McGeer PL, Walker DG, Akiyama H, Yasuhara O, McGeer EG (1994) Involvement of microglia in Alzheimer's disease. *Neuropathol.Appl.Neurobiol.* **20,** 191-192.
McGowan E *et al* (2005) Abeta42 is essential for parenchymal and vascular amyloid deposition in mice. *Neuron* **47,** 191-199.
McGowan E, Eriksen J, Hutton M (2006) A decade of modeling Alzheimer's disease in transgenic mice. *Trends Genet.* **22,** 281-289.
McNaught KS, Belizaire R, Isacson O, Jenner P, Olanow CW (2003) Altered proteasomal function in sporadic Parkinson's disease. *Exp.Neurol.* **179,** 38-46.
McShea A, Harris PL, Webster KR, Wahl AF, Smith MA (1997) Abnormal expression of the cell cycle regulators P16 and CDK4 in Alzheimer's disease. *Am.J.Pathol.* **150,** 1933-1939.
Melcangi RC, Garcia-Segura LM, Mensah-Nyagan AG (2008) Neuroactive steroids: state of the art and new perspectives. *Cell Mol.Life Sci.* **65,** 777-797.
Mellon SH, Vaudry H (2001) Biosynthesis of neurosteroids and regulation of their synthesis. *Int.Rev. Neurobiol.* **46,** 33-78.
Miller RM, Kiser GL, Kaysser-Kranich TM, Lockner RJ, Palaniappan C, Federoff HJ (2006) Robust dysregulation of gene expression in substantia nigra and striatum in Parkinson's disease. *Neurobiol Dis* **21,** 305-313.
Milton RH *et al* (2008) CLIC1 function is required for beta-amyloid-induced generation of reactive oxygen species by microglia. *J.Neurosci.* **28,** 11488-11499.
Minati L, Grisoli M, Bruzzone MG (2007) MR spectroscopy, functional MRI, and diffusion-tensor imaging in the aging brain: a conceptual review. *J.Geriatr.Psychiatry Neurol.* **20,** 3-21.
Minet-Ringuet J *et al* (2007) Alterations of lipid metabolism and gene expression in rat adipocytes during chronic olanzapine treatment. *Mol.Psychiatry* **12,** 562-571.
Mizukami K, Grayson DR, Ikonomovic MD, Sheffield R, Armstrong DM (1998a) GABAA receptor beta 2 and beta 3 subunits mRNA in the hippocampal formation of aged human brain with Alzheimer-related neuropathology. *Brain Res.Mol.Brain Res.* **56,** 268-272.
Mizukami K, Ikonomovic MD, Grayson DR, Sheffield R, Armstrong DM (1998b) Immunohistochemical study of GABAA receptor alpha1 subunit in the hippocampal formation of aged brains with Alzheimer-related neuropathologic changes. *Brain Res.* **799,** 148-155.
Mizuta I *et al* (2006) Multiple candidate gene analysis identifies alpha-synuclein as a susceptibility gene for sporadic Parkinson's disease. *Hum.Mol.Genet.* **15,** 1151-1158.
Mohler H (2006) GABA(A) receptor diversity and pharmacology. *Cell Tissue Res.* **326,** 505-516.
Mondadori CR *et al* (2006) Enhanced brain activity may precede the diagnosis of Alzheimer's disease by 30 years. *Brain* **129,** 2908-2922.
Moore DJ, West AB, Dawson VL, Dawson TM (2005) Molecular pathophysiology of Parkinson's disease. *Annu.Rev Neurosci* **28,** 57-87.
Moran LB, Duke DC, Deprez M, Dexter DT, Pearce RK, Graeber MB (2006) Whole genome expression profiling of the medial and lateral substantia nigra in Parkinson's disease. *Neurogenetics.* **7,** 1-11.
Moreira PI *et al* (2008) Nucleic acid oxidation in Alzheimer disease. *Free Radic.Biol.Med.* **44,** 1493-1505.
Mori C *et al* (2002) Intraneuronal Abeta42 accumulation in Down syndrome brain. *Amyloid.* **9,** 88-102.
Morris JC, Mohs RC, Rogers H, Fillenbaum G, Heyman A (1988) Consortium to establish a registry for Alzheimer's disease (CERAD) clinical and neuropsychological assessment of Alzheimer's disease. *Psychopharmacol.Bull.* **24,** 641-652.
Mountjoy CQ, Rossor MN, Iversen LL, Roth M (1984) Correlation of cortical cholinergic and GABA deficits with quantitative neuropathological findings in senile dementia. *Brain* **107 (Pt 2),** 507-518.
Mukherjee O, Kauwe JS, Mayo K, Morris JC, Goate AM (2007) Haplotype-based association analysis of the MAPT locus in late onset Alzheimer's disease. *BMC.Genet.* **8,** 3.
Mulnard RA (2005) Methodological issues in estrogen treatment trials for Alzheimer's disease. *Ann.N.Y.Acad.Sci.* **1052:173-81.,** 173-181.
Murai KK, Nguyen LN, Irie F, Yamaguchi Y, Pasquale EB (2003) Control of hippocampal dendritic spine morphology through ephrin-A3/EphA4 signaling. *Nat.Neurosci.* **6,** 153-160.
Myers AJ *et al* (2005) The H1c haplotype at the MAPT locus is associated with Alzheimer's disease. *Hum.Mol.Genet.* **14,** 2399-2404.
Nagy ZS, Esiri MM (1997) Apoptosis-related protein expression in the hippocampus in Alzheimer's disease. *Neurobiol.Aging* **18,** 565-571.
Nakagawa T, Schwartz JP (2004) Gene expression profiles of reactive astrocytes in dopamine-depleted striatum. *Brain Pathol.* **14,** 275-280.

Nakagawa T, Yabe T, Schwartz JP (2005) Gene expression profiles of reactive astrocytes cultured from dopamine-depleted striatum. *Neurobiol.Dis.* **20,** 275-282.
Nathan BP, Jiang Y, Wong GK, Shen F, Brewer GJ, Struble RG (2002) Apolipoprotein E4 inhibits, and apolipoprotein E3 promotes neurite outgrowth in cultured adult mouse cortical neurons through the low-density lipoprotein receptor-related protein. *Brain Res.* **928,** 96-105.
Nie Z, Xue Y, Yang D, Zhou S, Deroo BJ, Archer TK, Wang W (2000) A specificity and targeting subunit of a human SWI/SNF family-related chromatin-remodeling complex. *Mol.Cell Biol.* **20,** 8879-8888.
Niederkofler V, Salie R, Sigrist M, Arber S (2004) Repulsive guidance molecule (RGM) gene function is required for neural tube closure but not retinal topography in the mouse visual system. *J.Neurosci.* **24,** 808-818.
Nixon RA, Mathews PM, Cataldo AM (2001) The neuronal endosomal-lysosomal system in Alzheimer's disease. *J.Alzheimers.Dis.* **3,** 97-107.
Oakley AE *et al* (2007) Individual dopaminergic neurons show raised iron levels in Parkinson disease. *Neurology* **68,** 1820-1825.
Oakley H *et al* (2006) Intraneuronal beta-amyloid aggregates, neurodegeneration, and neuron loss in transgenic mice with five familial Alzheimer's disease mutations: potential factors in amyloid plaque formation. *J.Neurosci.* **26,** 10129-10140.
Oddo S *et al* (2003) Triple-transgenic model of Alzheimer's disease with plaques and tangles: intracellular Abeta and synaptic dysfunction. *Neuron* **39,** 409-421.
Oddo S, Caccamo A, Smith IF, Green KN, LaFerla FM (2006) A dynamic relationship between intracellular and extracellular pools of Abeta. *Am.J.Pathol.* **168,** 184-194.
Ogata H, Goto S, Sato K, Fujibuchi W, Bono H, Kanehisa M (1999) KEGG: Kyoto Encyclopedia of Genes and Genomes. *Nucleic Acids Res* **27,** 29-34.
Olanow CW, McNaught KS (2006) Ubiquitin-proteasome system and Parkinson's disease. *Mov Disord.* **21,** 1806-1823.
Onoue S, Endo K, Ohshima K, Yajima T, Kashimoto K (2002) The neuropeptide PACAP attenuates beta-amyloid (1-42)-induced toxicity in PC12 cells. *Peptides* **23,** 1471-1478.
Origlia N, Capsoni S, Cattaneo A, Fang F, Arancio O, Yan SD, Domenici L (2009) Abeta-Dependent Inhibition of LTP in Different Intra-Cortical Circuits of the Visual Cortex: The Role of RAGE. *J.Alzheimers.Dis.*
Orozco-Cabal L, Pollandt S, Liu J, Shinnick-Gallagher P, Gallagher JP (2006) Regulation of synaptic transmission by CRF receptors. *Rev.Neurosci.* **17,** 279-307.
Osen-Sand A *et al* (1996) Common and distinct fusion proteins in axonal growth and transmitter release. *J.Comp Neurol.* **367,** 222-234.
Papadopoulos V *et al* (1997) Peripheral benzodiazepine receptor in cholesterol transport and steroidogenesis. *Steroids* **62,** 21-28.
Papadopoulos V *et al* (2006) Translocator protein (18kDa): new nomenclature for the peripheral-type benzodiazepine receptor based on its structure and molecular function. *Trends Pharmacol.Sci.* **27,** 402-409.
Papapetropoulos S, Ffrench-Mullen J, McCorquodale D, Qin Y, Pablo J, Mash DC (2006) Multiregional gene expression profiling identifies MRPS6 as a possible candidate gene for Parkinson's disease. *Gene Expr.* **13,** 205-215.
Papapetropoulos S, McCorquodale D (2007) Gene-expression profiling in Parkinson's disease: discovery of valid biomarkers, molecular targets and biochemical pathways. *Future Neurology* **2,** 29-38.
Parachikova A *et al* (2007) Inflammatory changes parallel the early stages of Alzheimer disease. *Neurobiol.Aging* **28,** 1821-1833.
Paradisi S *et al* (2008) Blockade of chloride intracellular ion channel 1 stimulates Abeta phagocytosis. *J.Neurosci.Res.* **86,** 2488-2498.
Park DS, Obeidat A, Giovanni A, Greene LA (2000) Cell cycle regulators in neuronal death evoked by excitotoxic stress: implications for neurodegeneration and its treatment. *Neurobiol.Aging* **21,** 771-781.
Park J *et al* (2006) Mitochondrial dysfunction in Drosophila PINK1 mutants is complemented by parkin. *Nature* **441,** 1157-1161.
Patterson TA *et al* (2006) Performance comparison of one-color and two-color platforms within the MicroArray Quality Control (MAQC) project. *Nat.Biotechnol.* **24,** 1140-1150.
Pavlidis P, Lewis DP, Noble WS (2002) Exploring gene expression data with class scores. *Pac.Symp. Biocomput.* 474-485.
Pedersen ED, Aass HC, Rootwelt T, Fung M, Lambris JD, Mollnes TE (2007) CD59 efficiently protects human NT2-N neurons against complement-mediated damage. *Scand.J.Immunol.* **66,** 345-351.
Penning TM, Jin Y, Heredia VV, Lewis M (2003) Structure-function relationships in 3alpha-hydroxysteroid dehydrogenases: a comparison of the rat and human isoforms. *J.Steroid Biochem.Mol.Biol.* **85,** 247-255.
Perreau-Lenz S, Spanagel R (2008) The effects of drugs of abuse on clock genes. *Drug News Perspect.* **21,** 211-217.

Persson J, Sylvester CY, Nelson JK, Welsh KM, Jonides J, Reuter-Lorenz PA (2004) Selection requirements during verb generation: differential recruitment in older and younger adults. *Neuroimage.* **23,** 1382-1390.
Petit A *et al* (2005) Wild-type PINK1 prevents basal and induced neuronal apoptosis, a protective effect abrogated by Parkinson disease-related mutations. *J.Biol.Chem.* **280,** 34025-34032.
Pfaffl MW (2001) A new mathematical model for relative quantification in real-time RT-PCR. *Nucleic Acids Res.* **29,** e45.
Pike CJ, Rosario ER, Nguyen TV (2006) Androgens, aging, and Alzheimer's disease. *Endocrine.* **29,** 233-241.
Pizzi M, Sarnico I, Lanzillotta A, Battistin L, Spano P (2009) Post-ischemic brain damage: NF-kappaB dimer heterogeneity as a molecular determinant of neuron vulnerability. *FEBS J.* **276,** 27-35.
Plun-Favreau H *et al* (2007) The mitochondrial protease HtrA2 is regulated by Parkinson's disease-associated kinase PINK1. *Nat.Cell Biol.* **9,** 1243-1252.
Polymeropoulos MH *et al* (1997) Mutation in the alpha-synuclein gene identified in families with Parkinson's disease. *Science* **276,** 2045-2047.
Pongratz RL, Kibbey RG, Shulman GI, Cline GW (2007) Cytosolic and mitochondrial malic enzyme isoforms differentially control insulin secretion. *J.Biol.Chem.* **282,** 200-207.
Popken GJ, Farel PB (1997) Sensory neuron number in neonatal and adult rats estimated by means of stereologic and profile-based methods. *J.Comp Neurol.* **386,** 8-15.
Przedborski S, Jackson-Lewis V, Naini AB, Jakowec M, Petzinger G, Miller R, Akram M (2001) The parkinsonian toxin 1-methyl-4-phenyl-1,2,3,6-tetrahydropyridine (MPTP): a technical review of its utility and safety. *J.Neurochem.* **76,** 1265-1274.
Qian L, Flood PM (2008) Microglial cells and Parkinson's disease. *Immunol.Res.*
Querfurth HW, Selkoe DJ (1994) Calcium ionophore increases amyloid beta peptide production by cultured cells. *Biochemistry* **33,** 4550-4561.
Raber J, Wong D, Yu GQ, Buttini M, Mahley RW, Pitas RE, Mucke L (2000) Apolipoprotein E and cognitive performance. *Nature* **404,** 352-354.
Raguz J, Wagner S, Dikic I, Hoeller D (2007) Suppressor of T-cell receptor signalling 1 and 2 differentially regulate endocytosis and signalling of receptor tyrosine kinases. *FEBS Lett.* **581,** 4767-4772.
Reddy PH, McWeeney S (2006) Mapping cellular transcriptosomes in autopsied Alzheimer's disease subjects and relevant animal models. *Neurobiol.Aging* **27,** 1060-1077.
Refolo LM *et al* (2001) A cholesterol-lowering drug reduces beta-amyloid pathology in a transgenic mouse model of Alzheimer's disease. *Neurobiol.Dis.* **8,** 890-899.
Reguart N *et al* (2004) Cloning and characterization of the promoter of human Wnt inhibitory factor-1. *Biochem.Biophys.Res.Commun.* **323,** 229-234.
Reijnders JS, Ehrt U, Weber WE, Aarsland D, Leentjens AF (2008) A systematic review of prevalence studies of depression in Parkinson's disease. *Mov Disord.* **23,** 183-189.
Reiman EM *et al* (2004) Functional brain abnormalities in young adults at genetic risk for late-onset Alzheimer's dementia. *Proc.Natl.Acad.Sci.U.S.A* **101,** 284-289.
Reinikainen KJ, Paljarvi L, Huuskonen M, Soininen H, Laakso M, Riekkinen PJ (1988) A post-mortem study of noradrenergic, serotonergic and GABAergic neurons in Alzheimer's disease. *J.Neurol.Sci.* **84,** 101-116.
Renbaum P, Beeri R, Gabai E, Amiel M, Gal M, Ehrengruber MU, Levy-Lahad E (2003) Egr-1 upregulates the Alzheimer's disease presenilin-2 gene in neuronal cells. *Gene* **318,** 113-124.
Rhee SY, Wood V, Dolinski K, Draghici S (2008) Use and misuse of the gene ontology annotations. *Nat. Rev.Genet.* **9,** 509-515.
Ricotta D, Conner SD, Schmid SL, von Figura K, Honing S (2002) Phosphorylation of the AP2 mu subunit by AAK1 mediates high affinity binding to membrane protein sorting signals. *J.Cell Biol.* **156,** 791-795.
Ritter B *et al* (2007) The NECAP PHear domain increases clathrin accessory protein binding potential. *EMBO J.* **26,** 4066-4077.
Rizzuto R *et al* (1998) Close contacts with the endoplasmic reticulum as determinants of mitochondrial Ca2+ responses. *Science* **280,** 1763-1766.
Rizzuto R, Brini M, Murgia M, Pozzan T (1993) Microdomains with high Ca2+ close to IP3-sensitive channels that are sensed by neighboring mitochondria. *Science* **262,** 744-747.
Rocca WA *et al* (1991) Frequency and distribution of Alzheimer's disease in Europe: a collaborative study of 1980-1990 prevalence findings. The EURODEM-Prevalence Research Group. *Ann.Neurol.* **30,** 381-390.
Roche FM, Hokamp K, Acab M, Babiuk LA, Hancock RE, Brinkman FS (2004) ProbeLynx: a tool for updating the association of microarray probes to genes. *Nucleic Acids Res.* **32,** W471-W474.
Roe CM, Xiong C, Miller JP, Cairns NJ, Morris JC (2008) Interaction of neuritic plaques and education predicts dementia. *Alzheimer Dis.Assoc.Disord.* **22,** 188-193.

Rogaev EI *et al* (1995) Familial Alzheimer's disease in kindreds with missense mutations in a gene on chromosome 1 related to the Alzheimer's disease type 3 gene. *Nature* **376,** 775-778.
Rogers J *et al* (1992) Complement activation by beta-amyloid in Alzheimer disease. *Proc.Natl.Acad. Sci.U.S.A* **89,** 10016-10020.
Roher AE, Lowenson JD, Clarke S, Woods AS, Cotter RJ, Gowing E, Ball MJ (1993) beta-Amyloid-(1-42) is a major component of cerebrovascular amyloid deposits: implications for the pathology of Alzheimer disease. *Proc.Natl.Acad.Sci.U.S.A* **90,** 10836-10840.
Rosario ER, Chang L, Head EH, Stanczyk FZ, Pike CJ (2009) Brain levels of sex steroid hormones in men and women during normal aging and in Alzheimer's disease. *Neurobiol.Aging.*
Rosario ER, Chang L, Stanczyk FZ, Pike CJ (2004) Age-related testosterone depletion and the development of Alzheimer disease. *JAMA.* **292,** 1431-1432.
Rosen WG, Mohs RC, Davis KL (1984) A new rating scale for Alzheimer's disease. *Am.J.Psychiatry* **141,** 1356-1364.
Rossor MN, Garrett NJ, Johnson AL, Mountjoy CQ, Roth M, Iversen LL (1982) A post-mortem study of the cholinergic and GABA systems in senile dementia. *Brain* **105,** 313-330.
Rouaux C, Jokic N, Mbebi C, Boutillier S, Loeffler JP, Boutillier AL (2003) Critical loss of CBP/p300 histone acetylase activity by caspase-6 during neurodegeneration. *EMBO J.* **22,** 6537-6549.
Roy AL (2007) Signal-induced functions of the transcription factor TFII-I. *Biochim.Biophys.Acta* **1769,** 613-621.
Saetre P, Emilsson L, Axelsson E, Kreuger J, Lindholm E, Jazin E (2007) Inflammation-related genes up-regulated in schizophrenia brains. *BMC.Psychiatry* **7,** 46.
Sahay A, Kim CH, Sepkuty JP, Cho E, Huganir RL, Ginty DD, Kolodkin AL (2005) Secreted semaphorins modulate synaptic transmission in the adult hippocampus. *J.Neurosci.* **25,** 3613-3620.
Saito T *et al* (2005) Somatostatin regulates brain amyloid beta peptide Abeta42 through modulation of proteolytic degradation. *Nat.Med.* **11,** 434-439.
Salins P, He Y, Olson K, Glazner G, Kashour T, Amara F (2008) TGF-beta1 is increased in a transgenic mouse model of familial Alzheimer's disease and causes neuronal apoptosis. *Neurosci.Lett.* **430,** 81-86.
Saneyoshi T *et al* (2008) Activity-dependent synaptogenesis: regulation by a CaM-kinase kinase/CaM-kinase I/betaPIX signaling complex. *Neuron* **57,** 94-107.
Santacruz K *et al* (2005) Tau suppression in a neurodegenerative mouse model improves memory function. *Science* **309,** 476-481.
Schapira AH (2008) Mitochondria in the aetiology and pathogenesis of Parkinson's disease. *Lancet Neurol.* **7,** 97-109.
Schapira AH, Cooper JM, Dexter D, Jenner P, Clark JB, Marsden CD (1989) Mitochondrial complex I deficiency in Parkinson's disease. *Lancet* **1,** 1269.
Scheff SW, Price DA (2006) Alzheimer's disease-related alterations in synaptic density: neocortex and hippocampus. *J.Alzheimers.Dis.* **9,** 101-115.
Scheuner D *et al* (1996) Secreted amyloid beta-protein similar to that in the senile plaques of Alzheimer's disease is increased in vivo by the presenilin 1 and 2 and APP mutations linked to familial Alzheimer's disease. *Nat.Med.* **2,** 864-870.
Schmid RS, Maness PF (2008) L1 and NCAM adhesion molecules as signaling coreceptors in neuronal migration and process outgrowth. *Curr.Opin.Neurobiol.* **18,** 245-250.
Schumacher M *et al* (2003) Steroid hormones and neurosteroids in normal and pathological aging of the nervous system. *Prog.Neurobiol.* **71,** 3-29.
Schumacher M, Guennoun R, Stein DG, De Nicola AF (2007) Progesterone: therapeutic opportunities for neuroprotection and myelin repair. *Pharmacol.Ther.* **116,** 77-106.
Schwab JM *et al* (2005) Central nervous system injury-induced repulsive guidance molecule expression in the adult human brain. *Arch.Neurol* **62,** 1561-1568.
Schwarz G (1978) Estimating the dimension of a model. *Annals of Statistics* **6,** 461-464.
Selkoe DJ (1991) The molecular pathology of Alzheimer's disease. *Neuron* **6,** 487-498.
Selkoe DJ (2000) The genetics and molecular pathology of Alzheimer's disease: roles of amyloid and the presenilins. *Neurol.Clin.* **18,** 903-922.
Semple CA, Devon RS, Le Hellard S, Porteous DJ (2001) Identification of genes from a schizophrenia-linked translocation breakpoint region. *Genomics* **73,** 123-126.
Sengupta A, Grundke-Iqbal I, Iqbal K (2006) Regulation of phosphorylation of tau by protein kinases in rat brain. *Neurochem.Res.* **31,** 1473-1480.
Setsuie R *et al* (2007) Dopaminergic neuronal loss in transgenic mice expressing the Parkinson's disease-associated UCH-L1 I93M mutant. *Neurochem.Int.* **50,** 119-129.
Shankar GM *et al* (2008) Amyloid-beta protein dimers isolated directly from Alzheimer's brains impair synaptic plasticity and memory. *Nat.Med.* **14,** 837-842.
Shemer I *et al* (2006) Non-fibrillar beta-amyloid abates spike-timing-dependent synaptic potentiation at excitatory synapses in layer 2/3 of the neocortex by targeting postsynaptic AMPA receptors. *Eur.J.Neurosci.* **23,** 2035-2047.

Sherrington R *et al* (1995) Cloning of a gene bearing missense mutations in early-onset familial Alzheimer's disease. *Nature* **375,** 754-760.
Shi GX, Han J, Andres DA (2005) Rin GTPase couples nerve growth factor signaling to p38 and b-Raf/ERK pathways to promote neuronal differentiation. *J Biol Chem* **280,** 37599-37609.
Shimohama S, Kamiya S, Taniguchi T, Akagawa K, Kimura J (1997) Differential involvement of synaptic vesicle and presynaptic plasma membrane proteins in Alzheimer's disease. *Biochem.Biophys.Res. Commun.* **236,** 239-242.
Shintani S *et al* (2000) p12(DOC-1) is a novel cyclin-dependent kinase 2-associated protein. *Mol.Cell Biol.* **20,** 6300-6307.
Shirts BH, Wood J, Yolken RH, Nimgaonkar VL (2008) Comprehensive evaluation of positional candidates in the IL-18 pathway reveals suggestive associations with schizophrenia and herpes virus seropositivity. *Am.J.Med.Genet.B Neuropsychiatr.Genet.* **147,** 343-350.
Shumaker SA *et al* (2003) Estrogen plus progestin and the incidence of dementia and mild cognitive impairment in postmenopausal women: the Women's Health Initiative Memory Study: a randomized controlled trial. *JAMA.* **289,** 2651-2662.
Simunovic F *et al* (2008) Gene expression profiling of substantia nigra dopamine neurons: further insights into Parkinson's disease pathology. *Brain*.
Singhrao SK, Neal JW, Morgan BP, Gasque P (1999) Increased complement biosynthesis by microglia and complement activation on neurons in Huntington's disease. *Exp.Neurol.* **159,** 362-376.
Singleton AB *et al* (2003) alpha-Synuclein locus triplication causes Parkinson's disease. *Science* **302,** 841.
Sleegers K, van Duijn CM (2001) Alzheimer's Disease: Genes, Pathogenesis and Risk Prediction. *Community Genet.* **4,** 197-203.
Smidt MP, Burbach JP (2007) How to make a mesodiencephalic dopaminergic neuron. *Nat.Rev.Neurosci.* **8,** 21-32.
Smits SM, Burbach JP, Smidt MP (2006) Developmental origin and fate of meso-diencephalic dopamine neurons. *Prog.Neurobiol.* **78,** 1-16.
Smits SM, Ponnio T, Conneely OM, Burbach JP, Smidt MP (2003) Involvement of Nurr1 in specifying the neurotransmitter identity of ventral midbrain dopaminergic neurons. *Eur.J.Neurosci.* **18,** 1731-1738.
Smits SM, Smidt MP (2006) The role of Pitx3 in survival of midbrain dopaminergic neurons. *J.Neural Transm.Suppl* 57-60.
Smyth GK (2005) Limma: linear models for microarray data. In 'Bioinformatics and Computational Biology Solutions using R and Bioconductor'. (Eds R Gentleman, V Carey, S Dudoit, RA Irizarry, and W Huber) pp. 397-420.
Smyth GK, Speed T (2003) Normalization of cDNA microarray data. *Methods* **31,** 265-273.
Spasic D *et al* (2007) Rer1p competes with APH-1 for binding to nicastrin and regulates gamma-secretase complex assembly in the early secretory pathway. *J.Cell Biol.* **176,** 629-640.
Srinivasan BS *et al* (2008) Whole genome survey of coding SNPs reveals a reproducible pathway determinant of Parkinson disease. *Hum.Mutat.*
Stahel PF *et al* (2009) Absence of the complement regulatory molecule CD59a leads to exacerbated neuropathology after traumatic brain injury in mice. *J.Neuroinflammation.* **6,** 2.
Stan AD, Ghose S, Gao XM, Roberts RC, Lewis-Amezcua K, Hatanpaa KJ, Tamminga CA (2006) Human postmortem tissue: what quality markers matter? *Brain Res.* **1123,** 1-11.
Stell BM, Brickley SG, Tang CY, Farrant M, Mody I (2003) Neuroactive steroids reduce neuronal excitability by selectively enhancing tonic inhibition mediated by delta subunit-containing GABAA receptors. *Proc.Natl.Acad.Sci.U.S.A* **100,** 14439-14444.
Stoffel-Wagner B (2001) Neurosteroid metabolism in the human brain. *Eur.J.Endocrinol.* **145,** 669-679.
Storch A, Ludolph AC, Schwarz J (2004) Dopamine transporter: involvement in selective dopaminergic neurotoxicity and degeneration. *J.Neural Transm.* **111,** 1267-1286.
Styren SD, Kamboh MI, DeKosky ST (1998) Expression of differential immune factors in temporal cortex and cerebellum: the role of alpha-1-antichymotrypsin, apolipoprotein E, and reactive glia in the progression of Alzheimer's disease. *J.Comp Neurol.* **396,** 511-520.
Sulzer D (2007) Multiple hit hypotheses for dopamine neuron loss in Parkinson's disease. *Trends Neurosci.* **30,** 244-250.
Sunderland T, Hill JL, Mellow AM, Lawlor BA, Gundersheimer J, Newhouse PA, Grafman JH (1989) Clock drawing in Alzheimer's disease. A novel measure of dementia severity. *J.Am.Geriatr.Soc.* **37,** 725-729.
Swatton JE, Sellers LA, Faull RL, Holland A, Iritani S, Bahn S (2004) Increased MAP kinase activity in Alzheimer's and Down syndrome but not in schizophrenia human brain. *Eur.J.Neurosci.* **19,** 2711-2719.
Sydow O (2008) Parkinson's disease: recent development in therapies for advanced disease with a focus on deep brain stimulation (DBS) and duodenal levodopa infusion. *FEBS J.* **275,** 1370-1376.
Taira T, Saito Y, Niki T, Iguchi-Ariga SM, Takahashi K, Ariga H (2004) DJ-1 has a role in antioxidative stress to prevent cell death. *EMBO Rep* **5,** 213-218.

Takanaga H, Ohtsuki S, Hosoya K, Terasaki T (2001) GAT2/BGT-1 as a system responsible for the transport of gamma-aminobutyric acid at the mouse blood-brain barrier. *J.Cereb.Blood Flow Metab* **21,** 1232-1239.
Takano K *et al* (2007) A dibenzoylmethane derivative protects dopaminergic neurons against both oxidative stress and endoplasmic reticulum stress. *Am.J.Physiol Cell Physiol* **293,** C1884-C1894.
Takashima A *et al* (1998) Activation of tau protein kinase I/glycogen synthase kinase-3beta by amyloid beta peptide (25-35) enhances phosphorylation of tau in hippocampal neurons. *Neurosci.Res.* **31,** 317-323.
Tan EK *et al* (2006) Case-control study of UCHL1 S18Y variant in Parkinson's disease. *Mov Disord.* **21,** 1765-1768.
Tanemura K *et al* (2001) Formation of filamentous tau aggregations in transgenic mice expressing V337M human tau. *Neurobiol.Dis.* **8,** 1036-1045.
Tang Y *et al* (2009) WIF1, a Wnt pathway inhibitor, regulates SKP2 and c-myc expression leading to G1 arrest and growth inhibition of human invasive urinary bladder cancer cells. *Mol.Cancer Ther.* **8,** 458-468.
Teismann P, Schulz JB (2004) Cellular pathology of Parkinson's disease: astrocytes, microglia and inflammation. *Cell Tissue Res.* **318,** 149-161.
Terry RD *et al* (1991) Physical basis of cognitive alterations in Alzheimer's disease: synapse loss is the major correlate of cognitive impairment. *Ann.Neurol.* **30,** 572-580.
Thigpen AE, Silver RI, Guileyardo JM, Casey ML, McConnell JD, Russell DW (1993) Tissue distribution and ontogeny of steroid 5 alpha-reductase isozyme expression. *J.Clin.Invest* **92,** 903-910.
Thomas B, Beal MF (2007) Parkinson's disease. *Hum.Mol.Genet.* **16 Spec No. 2,** R183-R194.
Ting JT, Kelley BG, Lambert TJ, Cook DG, Sullivan JM (2007) Amyloid precursor protein overexpression depresses excitatory transmission through both presynaptic and postsynaptic mechanisms. *Proc. Natl.Acad.Sci.U.S.A* **104,** 353-358.
Tobin JE *et al* (2008) Haplotypes and gene expression implicate the MAPT region for Parkinson disease: the GenePD Study. *Neurology* **71,** 28-34.
Tomita H *et al* (2004) Effect of agonal and postmortem factors on gene expression profile: quality control in microarray analyses of postmortem human brain. *Biol Psychiatry* **55,** 346-52.
Toro CT, Hallak JE, Dunham JS, Deakin JF (2006) Glial fibrillary acidic protein and glutamine synthetase in subregions of prefrontal cortex in schizophrenia and mood disorder. *Neurosci.Lett.* **404,** 276-281.
Tsuang D *et al* (2005a) Evaluation of selection bias in an incident-based dementia autopsy case series. *Alzheimer Dis.Assoc.Disord.* **19,** 67-73.
Tsuang MT *et al* (2005b) Assessing the validity of blood-based gene expression profiles for the classification of schizophrenia and bipolar disorder: a preliminary report. *Am.J.Med.Genet.B Neuropsychiatr. Genet.* **133B,** 1-5.
Um JW, Stichel-Gunkel C, Lubbert H, Lee G, Chung KC (2009) Molecular interaction between parkin and PINK1 in mammalian neuronal cells. *Mol.Cell Neurosci.*
van de Nes JA, Kamphorst W, Ravid R, Swaab DF (1998) Comparison of beta-protein/A4 deposits and Alz-50-stained cytoskeletal changes in the hypothalamus and adjoining areas of Alzheimer's disease patients: amorphic plaques and cytoskeletal changes occur independently. *Acta Neuropathol.(Berl)* **96,** 129-138.
Van Gassen G, Annaert W (2003) Amyloid, presenilins, and Alzheimer's disease. *Neuroscientist.* **9,** 117-126.
van Wingen G., van Broekhoven F., Verkes RJ, Petersson KM, Backstrom T, Buitelaar J, Fernandez G (2007) How progesterone impairs memory for biologically salient stimuli in healthy young women. *J.Neurosci.* **27,** 11416-11423.
Vandesompele J, De Preter K, Pattyn F, Poppe B, Van Roy N, De Paepe A, Speleman F (2002) Accurate normalization of real-time quantitative RT-PCR data by geometric averaging of multiple internal control genes. *Genome Biol.* **3,** RESEARCH0034.
Vawter MP *et al* (2004) Gene expression of metabolic enzymes and a protease inhibitor in the prefrontal cortex are decreased in schizophrenia. *Neurochem.Res.* **29,** 1245-1255.
Vingtdeux V, Dreses-Werringloer U, Zhao H, Davies P, Marambaud P (2008) Therapeutic potential of resveratrol in Alzheimer's disease. *BMC.Neurosci.* **9 Suppl 2,** S6.
Viswanathan A, Rocca WA, Tzourio C (2009) Vascular risk factors and dementia: how to move forward? *Neurology* **72,** 368-374.
Vongher JM, Frye CA (1999) Progesterone in conjunction with estradiol has neuroprotective effects in an animal model of neurodegeneration. *Pharmacol.Biochem.Behav.* **64,** 777-785.
Walsh DM *et al* (2002) Naturally secreted oligomers of amyloid beta protein potently inhibit hippocampal long-term potentiation in vivo. *Nature* **416,** 535-539.
Wang H, Tiedge H (2004) Translational control at the synapse. *Neuroscientist.* **10,** 456-466.
Wang JM, Irwin RW, Liu L, Chen S, Brinton RD (2007) Regeneration in a degenerating brain: potential of allopregnanolone as a neuroregenerative agent. *Curr.Alzheimer Res.* **4,** 510-517.

Wang JZ, Grundke-Iqbal I, Iqbal K (2007) Kinases and phosphatases and tau sites involved in Alzheimer neurofibrillary degeneration. *Eur.J.Neurosci.* **25,** 59-68.
Wang XP *et al* (2009) Conformation-dependent single-chain variable fragment antibodies specifically recognize beta-amyloid oligomers. *FEBS Lett.* **583,** 579-584.
Ward PP, Paz E, Conneely OM (2005) Multifunctional roles of lactoferrin: a critical overview. *Cell Mol. Life Sci.* **62,** 2540-2548.
Warner TT, Schapira AH (2003) Genetic and environmental factors in the cause of Parkinson's disease. *Ann.Neurol.* **53 Suppl 3,** S16-S23.
Webber KM *et al* (2005) The cell cycle in Alzheimer disease: a unique target for neuropharmacology. *Mech.Ageing Dev.* **126,** 1019-1025.
Webster MJ, O'Grady J, Kleinman JE, Weickert CS (2005) Glial fibrillary acidic protein mRNA levels in the cingulate cortex of individuals with depression, bipolar disorder and schizophrenia. *Neuroscience* **133,** 453-461.
Weidenhofer J, Scott RJ, Tooney PA (2008) Investigation of the expression of genes affecting cytomatrix active zone function in the amygdala in schizophrenia: Effects of antipsychotic drugs. *J.Psychiatr.Res.*
Weill-Engerer S *et al* (2002) Neurosteroid quantification in human brain regions: comparison between Alzheimer's and nondemented patients. *J.Clin.Endocrinol.Metab.* **87,** 5138-5143.
White KP, Rifkin SA, Hurban P, Hogness DS (1999) Microarray analysis of Drosophila development during metamorphosis. *Science* **286,** 2179-2184.
Wilhelmus MM, Otte-Holler I, Wesseling P, de Waal RM, Boelens WC, Verbeek MM (2006) Specific association of small heat shock proteins with the pathological hallmarks of Alzheimer's disease brains. *Neuropathol.Appl.Neurobiol.* **32,** 119-130.
Wilton DC, Munday KA, Skinner SJ, Akhtar M (1968) The biological conversion of 7-dehydrocholesterol into cholesterol and comments on the reduction of double bonds. *Biochem.J.* **106,** 803-810.
Winkler S *et al* (2007) alpha-Synuclein and Parkinson disease susceptibility. *Neurology* **69,** 1745-1750.
Wintermeyer P *et al* (2000) Mutation analysis and association studies of the UCHL1 gene in German Parkinson's disease patients. *Neuroreport* **11,** 2079-2082.
Wishart HA *et al* (2006) Increased brain activation during working memory in cognitively intact adults with the APOE epsilon4 allele. *Am.J.Psychiatry* **163,** 1603-1610.
Wolfinger RD *et al* (2001) Assessing gene significance from cDNA microarray expression data via mixed models. *J.Comput.Biol.* **8,** 625-637.
Wolozin B, Kellman W, Ruosseau P, Celesia GG, Siegel G (2000) Decreased prevalence of Alzheimer disease associated with 3-hydroxy-3-methyglutaryl coenzyme A reductase inhibitors. *Arch.Neurol.* **57,** 1439-1443.
Wood PL, Etienne P, Lal S, Gauthier S, Cajal S, Nair NP (1982) Reduced lumbar CSF somatostatin levels in Alzheimer's disease. *Life Sci.* **31,** 2073-2079.
Wu DC, Teismann P, Tieu K, Vila M, Jackson-Lewis V, Ischiropoulos H, Przedborski S (2003) NADPH oxidase mediates oxidative stress in the 1-methyl-4-phenyl-1,2,3,6-tetrahydropyridine model of Parkinson's disease. *Proc Natl Acad Sci U S A* **100,** 6145-6150.
Wu X, Dewey TG (2006) From microarray to biological networks: Analysis of gene expression profiles. *Methods Mol.Biol.* **316,** 35-48.
Xie J, Marusich MF, Souda P, Whitelegge J, Capaldi RA (2007) The mitochondrial inner membrane protein mitofilin exists as a complex with SAM50, metaxins 1 and 2, coiled-coil-helix coiled-coil-helix domain-containing protein 3 and 6 and DnaJC11. *FEBS Lett.* **581,** 3545-3549.
Xu HP, Tian N (2008) Glycine receptor-mediated synaptic transmission regulates the maturation of ganglion cell synaptic connectivity. *J.Comp Neurol.* **509,** 53-71.
Xu PT *et al* (2006) Differences in apolipoprotein E3/3 and E4/4 allele-specific gene expression in hippocampus in Alzheimer disease. *Neurobiol.Dis.* **21,** 256-275.
Yagi T, Hatefi Y (1987) Thiols in oxidative phosphorylation: thiols in the F0 of ATP synthase essential for ATPase activity. *Arch.Biochem.Biophys.* **254,** 102-109.
Yague JG, Munoz A, de Monasterio-Schrader P, Defelipe J, Garcia-Segura LM, Azcoitia I (2006) Aromatase expression in the human temporal cortex. *Neuroscience* **138,** 389-401.
Yankner BA, Lu T, Loerch P (2008) The aging brain. *Annu.Rev.Pathol.* **3,** 41-66.
Yao Y, Schroder J, Karlsson H (2008) Verification of proposed peripheral biomarkers in mononuclear cells of individuals with schizophrenia. *J.Psychiatr.Res.* **42,** 639-643.
Yassa MA, Verduzco G, Cristinzio C, Bassett SS (2008) Altered fMRI activation during mental rotation in those at genetic risk for Alzheimer disease. *Neurology* **70,** 1898-1904.
Yavich L, Jakala P, Tanila H (2006) Abnormal compartmentalization of norepinephrine in mouse dentate gyrus in alpha-synuclein knockout and A30P transgenic mice. *J.Neurochem.* **99,** 724-732.
Yavich L, Tanila H, Vepsalainen S, Jakala P (2004) Role of alpha-synuclein in presynaptic dopamine recruitment. *J.Neurosci.* **24,** 11165-11170.

Yi XN, Zheng LF, Zhang JW, Zhang LZ, Xu YZ, Luo G, Luo XG (2006) Dynamic changes in Robo2 and Slit1 expression in adult rat dorsal root ganglion and sciatic nerve after peripheral and central axonal injury. *Neurosci.Res.* **56,** 314-321.
Zaahl MG, Merryweather-Clarke AT, Kotze MJ, van der MS, Warnich L, Robson KJ (2005) Gene symbol: DCYTB/CYBRD1. Disease: primary iron overload. *Hum.Genet.* **118,** 549.
Zecca L, Youdim MB, Riederer P, Connor JR, Crichton RR (2004) Iron, brain ageing and neurodegenerative disorders. *Nat.Rev.Neurosci.* **5,** 863-873.
Zecca L, Zucca FA, Wilms H, Sulzer D (2003) Neuromelanin of the substantia nigra: a neuronal black hole with protective and toxic characteristics. *Trends Neurosci* **26,** 578-80.
Zhang B *et al* (2004) Retarded axonal transport of R406W mutant tau in transgenic mice with a neurodegenerative tauopathy. *J.Neurosci.* **24,** 4657-4667.
Zhang B, Zelhof AC (2002) Amphiphysins: raising the BAR for synaptic vesicle recycling and membrane dynamics. Bin-Amphiphysin-Rvsp. *Traffic.* **3,** 452-460.
Zhang Y, James M, Middleton FA, Davis RL (2005) Transcriptional analysis of multiple brain regions in Parkinson's disease supports the involvement of specific protein processing, energy metabolism, and signaling pathways, and suggests novel disease mechanisms. *Am J Med Genet B Neuropsychiatr.Genet* **137,** 5-16.
Zhang YW, Xu H (2007) Molecular and cellular mechanisms for Alzheimer's disease: understanding APP metabolism. *Curr.Mol.Med.* **7,** 687-696.
Zhang ZJ *et al* (2008) Lack of evidence for association of a UCH-L1 S18Y polymorphism with Parkinson's disease in a Han-Chinese population. *Neurosci.Lett.* **442,** 200-202.
Zhong N *et al* (2006) DJ-1 transcriptionally up-regulates the human tyrosine hydroxylase by inhibiting the sumoylation of pyrimidine tract-binding protein-associated splicing factor. *J.Biol.Chem.* **281,** 20940-20948.
Zhu X, Perry G, Moreira PI, Aliev G, Cash AD, Hirai K, Smith MA (2006) Mitochondrial abnormalities and oxidative imbalance in Alzheimer disease. *J.Alzheimers.Dis.* **9,** 147-153.
Zimprich A *et al* (2004) Mutations in LRRK2 cause autosomal-dominant parkinsonism with pleomorphic pathology. *Neuron* **44,** 601-607.
Zucca FA *et al* (2006) Neuromelanin and iron in human locus coeruleus and substantia nigra during aging: consequences for neuronal vulnerability. *J.Neural Transm.* **113,** 757-767.

Nederlandse samenvatting

De ziekte van Alzheimer (AD) en de ziekte van Parkinson (PD) zijn de twee meest voorkomende neurodegeneratieve ziekten. Het beloop van zowel AD als PD is progressief: patienten worden in de loop der jaren steeds zieker. Leeftijd is een belangrijke risicofactor voor deze ziekten. Dit, tezamen met de stijgende levensverwachting, zorgt ervoor dat AD en PD steeds meer mensen treft, en deze ziekten een steeds grotere belasting voor de samenleving worden. Grofweg 1 op de 100 mensen van 70 jaar en ouder heeft AD endit aantal stijgt echter dramatisch naarmate mensen ouder worden. Bij mensen van 85 jaar en ouder komt AD bij 1 op de 3 mensen voor. Op dit moment bestaan er geen effectieve behandelmethoden die de voortgang van deze slopende ziektes kunnen stoppen.

In de afgelopen 20 jaar is er veel vooruitgang geboekt in het identificeren van biologische processen die mogelijk zijn betrokken bij deze ziektes. Deze vooruitgang is voornamelijk toe te schrijven aan ontdekkingen vanuit de genetica: er is een aantal genmutaties gevonden die leiden tot zeldzame, erfelijke vormen van PD en AD. Verder zijn er toxines gevonden diePD-achtige veranderingen in de hersenen veroorzaken. De identificatie van deze genen en toxines heeft geleid tot het ontwikkelen van celkweekmodellen en diermodellen die het mogelijk maken bepaalde aspecten van PD en AD te bestuderen (zie **hoofdstuk 1**).

De nu bekende oorzakelijke genmutaties zijn echter zeer zeldzaam. Het overgrote deel (meer dan 95%) van de ziektegevallen van AD en PD zijn van 'sporadische oorsprong', wat betekent dat de genetische veranderingen niet op de klassieke manier overerven ('zit in de familie'). Ze zijn waarschijnlijk veroorzaakt worden door een combinatie van onbekende biologische en omgevingsfactoren. Een valide vraag is dus of de genetische en sporadische vormen wel direct met elkaar verband houden. Ofwel, zijn de oorzakelijke veranderingen in de genetische vormen van AD en PD ook direct oorzakelijk in de sporadische variant?

Het is nu duidelijk dat dit niet het geval is. De huidige theorie is dan ook dat PD en AD waarschijnlijk niet worden veroorzaakt door één duidelijke verandering in de hersenen van de patiënt. Het is veel aannemelijker dat een combinatie van verschillende factoren ten grondslag ligt aan het ziekteproces.

Een van de manieren waarop moleculair biologen ziekteprocessen bestuderen, is door het meten van veranderingen in genactiviteit . Tot voor kort was het slechts mogelijk de activiteit van enkele tot maximaal tientallen genen tegelijk te meten. Het menselijke genoom bevat ongeveer 20.000 verschillende genen, en het is onbekend welke van deze genen meer of minder actief zijn in AD of PD. Op de 'klassieke' moleculair biologische manier is het dus niet mogelijk om een totaalbeeld te krijgen van de moleculaire veranderingen die zijn geassocieerd met AD of PD.

Een recent ontwikkelde techniek maakt het wel mogelijk om de veranderingen in activiteit van heel veel genen in één keer te meten. Dit gebeurt met behulp van

microarrays, microscoopglaasjes waarop minuscule detectoren voor vrijwel alle 20.000 genen zitten. Dit totaalplaatje van de genactiviteit kan vervolgens inzicht geven in veranderingen in biologische processen in de hersenen van de patiënt. Daarom zijn microarrays bij uitstek geschikt voor het onderzoeken van complexe, multifactoriële ziekten zoals AD en PD.

De belangrijkste onderzoeksvraag waarop dit proefschrift een antwoord probeert te geven is dan ook: welke veranderingen in genactiviteit vinden er plaats in de hersenen van patiënten met AD of PD?

Wij zijn in het bijzonder geïnteresseerd in veranderingen die vroeg in het ziekteproces plaatsvinden, op een moment dat interventie door middel van medicatie in de toekomst nog kan voorkomen dat het ziekteproces van AD of PD zich door het gehele brein verspreidt. De toepassing van de zojuist beschreven microarray-techniek staat centraal in dit proefschrift. Het gebruik van menselijk hersenmateriaal is een uniek en essentieel aspect van het onderzoek, omdat celkweek- en diermodellen nooit een volledig beeld kunnen geven van de ziekte zoals die zich in de menselijke hersenen manifesteert.

In **hoofdstuk 3** beschrijven wij de veranderingen in genactiviteit door middel van microarray-analyse in de hersenen van PD-patiënten ten opzichte van donoren die niet lijden aan enige hersenziekte. Drie hersengebieden zijn onderzocht, te weten de substantia nigra, de nucleus caudatus en het putamen. Wij hebben gekozen voor de substantia nigra, omdat dit gebied het meest is aangedaan in PD: meer dan 80% van de zenuwcellen gaat verloren tijdens de ziekte. Deze afstervende zenuwcellen staan in contact met de nucleus caudatus en het putamen, en de huidige behandelingsmethode (het toedienen van L-dopa) is erop gericht het verlies van deze contacten te compenseren.

De resultaten van dit onderzoek laten zien dat er weinig veranderingen zijn waar te nemen in de nucleus caudatus en de putamen. Dit komt waarschijnlijk doordat de patiënten zijn behandeld met L-dopa, en doordat er geen zenuwcellen afsterven in deze hersengebieden.

In de substantia nigra daarentegen hebben wij een groep van 287 genen gevonden waarvan de activiteit significant veranderd was in PD. De meeste van deze genen zijn verminderd actief. Omdat wij specifiek gedeeltes van de substantia nigra hebben onderzocht waarbij de afname van zenuwcellen beperkt was, was de verminderde genactiviteit in de meeste gevallen niet toe te schrijven aan het verlies van zenuwcellen. Een uitgebreide analyse door middel van bio-informatica heeft aangetoond dat een gedeelte van de minder actieve genen betrokken is bij de overdracht van zenuwsignalen, de energievoorziening van de cel en het opruimen van kapotte eiwitten. Sommige van de door ons gemeten veranderingen zijn eerder beschreven in de literatuur, maar wij laten voor het eerst zien dat deze veranderingen al plaatsvinden voordat de zenuwcellen afsterven.

Ook hebben we een aantal niet eerder beschreven veranderingen in genactiviteit gevonden die wijzen op de afname van neurotrofe ondersteuning (het in stand houden van zenuwcellen door middel van groeistoffen) en veranderingen in signalen die de uitgroei van en contacten tussen zenuwcellen reguleert. Wij denken dat deze veranderingen een oorzakelijke bijdrage kunnen leveren aan het afsterven van zenuwcellen in PD. Namelijk, als zenuwcellen minder goed contact kunnen maken met elkaar en noodzakelijke groeistoffen verminderd aanwezig zijn, lopen deze cellen een verhoogd risico te sterven.

Hoofdstuk 4 beschrijft een alternatieve methode voor het analyseren van datasets die zijn gegenereerd door middel van twee-kleurenmicroarrays. Deze microarrays kenmerken zich doordat tegelijkertijd de genactiviteit wordt bepaald van twee monsters, waarvan er één groen en de ander rood fluorescerend gekleurd is. Als het groen gekleurde monster van een AD-patiënt komt, en het rood gekleurde monster van een gezonde oftewel controledonor, dan is de verhouding tussen het groene en rode signaal direct een maat voor de relatieve genactiviteit in AD ten opzichte van de controledonor. Deze twee-kleurenmicroarrays zijn dus bij uitstek geschikt voor de vergelijking van twee condities, zoals ziek en gezond. Verder zijn deze microarrays goed bestand tegen variatie die is veroorzaakt door verschillen tussen experimenten.

Een nadeel van de twee-kleurenmicroarrays is dat de vergelijking tussen meerdere condities veel moeilijker is. Er kunnen immers maar twee monsters tegelijkertijd worden gemeten. Wij hebben daarom onderzocht of de analyse van tweekleuren microarray data kan worden gedaan op de intensiteit van de afzonderlijke signalen, in plaats van op de ratio tussen het rode en groene signaal. Op deze manier worden de signalen onafhankelijk van elkaar behandeld, en kunnen alle gemeten monsters direct met elkaar worden vergeleken.

De resultaten van dit onderzoek laten zien dat de op intensiteit gebaseerde analyse inderdaad mogelijk is. Sterker nog, de reproduceerbaarheid van de resultaten, en de gevoeligheid voor veranderingen in genactiviteit verbetert wanneer er gebruik wordt gemaakt van een intensiteits-analyse. Dit geldt vooral wanneer er meerdere groepen met elkaar vergeleken moeten worden, en er veel variatie tussen de monsters is. Deze intensiteits-gebaseerde analyse hebben we toegepast in het microarray experiment in hoofdstuk 5.

In **hoofdstuk 5** beschrijven we, gebruik makend van microarray technologie, de veranderingen in genactiviteit gedurende de ontwikkeling van de ziekte van Alzheimer. De microscopische veranderingen die gepaard gaan met AD verspreiden zich via een vast patroon door de hersenen. Hierdoor is het mogelijk na de dood van de donor vast te stellen in welk stadium van de ziekte deze overleed. Deze stagering van het ziektebeeld staat ons ook in staat donoren die nog geen cognitieve afwijkingen vertoonden, op te delen in groepen met verschillende mate van AD pathologie. De verschillende stadia van AD werden voor het eerst beschreven door prof. H. Braak, en worden daarom ook wel aangeduid als de Braak stadia.

Wij hebben hiervan in ons onderzoek gebruikgemaakt voor het verzamelen van donoren. Voor elk van de 6 Braak stadia hebben we 7 donoren geselecteerd. Ook hebben we een groep van 7 donoren onderzocht die geen AD-geassocieerde pathologie vertoonden. Het hersengebied dat we hebben onderzocht is de prefrontale cortex, een gebied dat relatief laat is aangedaan in het ziekteproces. Dankzij deze aanpak waren wij in staat de genactiviteit van alle genen te volgen terwijl de ziekte zich ontwikkelde. Hierdoor konden wij onderscheid maken tussen vroege en dus mogelijk oorzakelijke veranderingen in genactiviteit, en late veranderingen in genactiviteit die mogelijk een gevolg zijn van de ziekte. Deze kennis kan van groot belang zijn bij het ontwikkelen van medicijnen die beschermen tegen het krijgen van AD, in plaats van medicatie die alleen symptomen bestrijdt.

Het belangrijkste resultaat van deze studie is de verhoogde activiteit van een grote groep genen in de allervroegste stadia van AD, net voordat de eerste microscopische veranderingen optreden in de prefrontale cortex. Het gaat onder meer om genen die betrokken zijn bij de signaaloverdracht tussen en de energievoorziening van zenuwcellen .

Wij denken dat deze veranderingen in genactiviteit een verhoogde activiteit van zenuwcellen vertegenwoordigen, als een compensatoire reactie op de allereerste, nog onbekende veranderingen in AD. Op het moment dat de met AD gepaard gaande typische microsopische veranderingen zichtbaar worden, vermindert de activiteit van deze groep genen sterk, om uiteindelijk in de laatste stadia van de ziekte nog verder af te nemen. Verder bevindt zich in deze groep een aantal genen die direct te maken hebben met de vorming en afbraak van de voornaamste component van één van de microscopische afwijkingen bij AD, de seniele plaque. Wij denken dan ook dat activiteitsveranderingen van juist deze genen, waarschijnlijk in combinatie met andere nog onbekende factoren, een oorzakelijke rol kunnen spelen bij het onwikkelen van de ziekte.

Ook al zijn de resultaten van microarray experimenten tegenwoordig zeer betrouwbaar, toch is onafhankelijke bevestiging van veranderingen in genactiviteit een belangrijke stap. Dit is des te meer het geval bij experimenten met menselijk weefsel, omdat die gepaard gaan met een grote variatie tussen individuen. In **hoofdstuk 6** combineren we daarom de resultaten van onze microarray studie uit hoofdstuk 5, en vier reeds gepubliceerde microarray-studies op humaan hersenmateriaal naar veranderingen in genactiviteit in het eindstadium van AD.

Deze 'meta'-analyse resulteerde in een lijst van 69 genen, waarvan een veranderde activiteit is gemeten in minimaal 3 van de 5 studies. Een aantal van deze genen speelt een rol in het handhaven van de calciumbalans of de energiehuishouding van zenuwcellen. Verder bevinden zich in deze lijst genen die op veranderingen duiden in het vermogen DNA-schade te repareren, de regulering van celdeling en de afbraak van cholesterol in de hersenen van AD patiënten. Deze resultaten geven aanleiding voor verder onderzoek naar de specifieke betrokkenheid van deze processen bij AD.

Het is bekend dat vrouwen een groter risico lopen op het ontwikkelen van AD, zelfs wanneer je corrigeert voor het feit dat vrouwen ouder worden dan mannen. Recent onderzoek suggereert dat geslachtshormonen ook geproduceerd kunnen worden door de hersenen, en dat geslachtshormonen zoals progesteron en estradiol betrokken zijn bij de algemene bescherming van zenuwcellen. Verder kunnen geslachtshormonen en afgeleiden daarvan de overdracht van zenuwsignalen veranderen, doordat ze de werking van receptoren (ontvangers van zenuwsignalen) beïnvloeden. Deze waarnemingen wijzen op een mogelijk verband tussen verschillen in geslachtshormonen en de vatbaarheid voor AD.

In **hoofdstuk 7** beschrijven we een systematische studie naar veranderingen in de aanmaak en afbraak van verschillende geslachtshormonen in AD, door het meten van genactiviteit en het aantonen van bijbehorende eiwitten in het hersenweefsel. De resultaten hiervan wijzen op een verhoging van de aanmaak van geslachtshormonen in vroege stadia van AD, wat waarschijnlijk een compensatoir mechanisme vertegenwoordigt dat zenuwcellen beschermt tegen AD-geassocieerde veranderingen.

In de algemene discussie van dit proefschrift (**hoofdstuk 8**) worden de experimenten, zoals beschreven in de voorgaande hoofdstukken, samengevat en bediscussieerd. We behandelen een aantal interessante observaties die verder onderzoek behoeven, zoals de interactie tussen variaties in het ApoE gen -de belangrijkste genetische risicofactor voor AD- en de veranderingen in genactiviteit in AD, de overeenkomsten en verschillen tussen normale veroudering en AD, en de rol van genetische variaties in signalen die de uitgroei van zenuwvezels uitgroei reguleren in PD.

Verder besteden wij aandacht aan de specifieke randvoorwaarden - zoals parameters die de kwaliteit van hersenweefsel beïnvloeden - die onontkoombaar gepaard gaan met onderzoek aan humaan postmortem hersenweefsel. En in het tweede gedeelte van de algemene discussie doen wij voorstellen voor vervolgonderzoek. Dit onderzoek moet zich volgens ons concentreren op de vraag wat de specifieke functionele betekenis is van de gevonden veranderingen in genactiviteit voor het ontstaan van PD en AD. Wij stellen een aantal bio-informatica, celkweek- en diermodelexperimenten voor die deze vraag verder moet beantwoorden. Momenteel zijn we zelf bezig met het uitvoeren van zulke experimenten.

Dankwoord

Joost en Dick, ik begin met jullie, en daar heb ik alle reden toe. Ten eerste wil ik jullie bedanken voor het vertrouwen dat jullie in mij hebben gesteld. Dat vertrouwen kwam al naar voren tijdens ons sollicitatiegesprek. Ik dacht: wat moeten die mensen nou met een scheikundestudent die zo goed als alleen maar ervaring heeft met computerwerk, en amper weet hoe hij een PCR moet inzetten. Jullie dachten: handig, zo'n jongen die weet hoe een computer werkt en hoe je met grote datasets om moet gaan. Dat pipetteren leren we hem hier wel. Met als resultaat dat, op de terugweg van ons tweede-rondegesprek, nog voordat ik de sleutel van mijn Nijmeegse appartement had omgedraaid, Joost mij de baan al had aangeboden.

Het vertrouwen uitte zich ook in de manier waarop jullie mij lieten werken. Hierbij kies ik met opzet voor het woord "lieten". Ik kreeg van jullie de ruimte om het werk zelf in te delen, zelf op zoek te gaan naar de juiste bio-informaticatools, zelf de beslissingen te nemen welke data-analyse het meest geschikt was voor mijn experimenten. Ik denk dat deze manier van begeleiden een zeer grote bijdrage heeft geleverd aan mijn opleiding tot "zelfstandig" onderzoeker. Dit betekent overigens niet dat jullie mij aan mijn lot hebben overgelaten. In tegendeel, naast onze regelmatige werkbesprekingen kon ik altijd binnenvallen met een vraag of opmerking. Veel dank voor dit alles, en ik ben blij dat we nog een aantal jaren mogen samenwerken.

Beste Chris, mijn promotor-op-afstand. Mede dankzij jouw interesse voor het werk op het toenmalige NIH is onze samenwerking tot stand gekomen. Tijdens onze besprekingen werden Joost, Dick en ik regelmatig geconfronteerd met de opmerking "zeer interessante genen die je daar bespreekt, maar zijn ze ook drugable?". Waarop wij, ruw uit onze academische gedachtengang getrokken, meestal geen antwoord hadden. Nu blijkt de vraag welke genen het meeste potentie hebben als aangrijpingspunt voor een geneesmiddel wel een moeilijke te zijn. Zo moeilijk, dat we daar nog maar eens 4 jaar op gaan broeden binnen onze voortgezette samenwerking, nu onder de TIPharma paraplu. Ik zou zeggen: wordt vervolgd! Jeroen en Pieter, dank voor alle discussies!

Beste Gideon, Anke, Unga en Rawien. Jullie expertise en pipet-skills hebben me erg geholpen op de momenten dat ik die nodig had. Heel veel dank voor jullie flexibiliteit en inzet! Hersenbankers Michiel, Afra en José, zonder jullie gezonde (en zieke) stel hersenen was ik nergens!

Beste Sasja, ik vond het erg leuk dat je mijn data interessant genoeg vond om een scriptie rond te bouwen. Je hebt met je meta-analyse een belangrijke bijdrage geleverd aan dit proefschrift, en ik ben ervan overtuigd dat hoofdstuk 6 nog een staartje krijgt. Veel succes met jouw eigen promotie bij Peter Heutink, we gaan elkaar zeker nog tegenkomen.

Dear Sabina, thank you very much for your outstanding work on characterizing the alterations in steroid pathways in AD. You've taken the microarray data to a next level, by measuring gene expression changes that are hard to detect on the microarray, and show that some of these alterations are indeed reflected on the protein level. I'm looking forward to our continuing collaboration!

Dear Asia and Kerstin. I'm very proud and honored that you chose to accept a PhD position in our TIPharma project, and that you are now working on elucidating the contribution of the genes described in this thesis to neurodegenerative events in AD and PD. I will do my utmost best to help you to reach the point where I'm at right now: writing my "dankwoord" (but don't take this too literally: no I will not fetch you coffee or tea every single day!).

Martijn, ik heb genoten van onze samenwerking maar vooral vriendschap. Onze gezamelijke grachtengordeltijd (Daft Punk, drie kwartier lang midden op de gracht dobberend je buitenboordmotor proberen te starten ten overstaan van een lachend terras) is voorbij. Gelukkig kan je ons blijkbaar niet missen, en kom je een dag per week hier rondhangen. Elske, ik vond het erg gezellig met jou op onze kamer, en heb veel van je geleerd! Heel veel succes in Cambridge! Tam: snacken, jeugdseries en gadgets zullen nooit meer hetzelfde zijn zonder jou. Je blijft een mysterie voor me: hoe kan zo'n klein ventje zoveel eten, én en passant in de aandacht staan van alle vrouwelijke studentes...

Ruben en Erich: jullie zijn de "senioren" van onze groep, maar jullie kennis is meer dan up-to-date. Het is altijd prettig om de dag te beginnen met een kopje koffie en als Statler-en-Waldorf-met-zijn-drieen (zie de muppetshow) de stand van zaken door te nemen.

Beste (oud)-collegas! Kasper, Matthew, Freddy, William, Bas, Paula, Floor, Joris, Fred, Harold, Nathalie, Jinte, Simone, Jeroen, Barbara, Jaqcueline en Karianne. Ontzettend veel dank voor jullie werkgerelateerde, maar vooral ook niet-werkgerelateerde bijdragen aan die gekke tijd die promotie heet. Ik mis de vrijdagmiddagborrels op de gang... Alle andere collega's van het NIN: heel erg bedankt!

Lieve pa en ma, jullie staan aan de basis van dit proefschrift door mij leergierig op te voeden. Dank jullie wel voor alle steun tijdens mijn middelbare schooltijd, mijn studie scheikunde, mijn promotie en voor wat nog komen gaat.

Allerliefste vrouw Remy. Ik ben bij jou beland. Sorry voor alle vrijdagavond-in-de-kroeg-heb-er-al-drie-op-wetenschapsverhalen van mij. Ik ga niet uitweiden over hoe belangrijk jij bent, bent geweest en zal zijn, want dan schrijf ik zo weer een boek vol. Dus ik beperk me tot het volgende: ik ben zó ontzettend blij dat jij er bent.

Curriculum vitae

Koen Bossers is op 30 juni 1977 geboren te Nijmegen. In 1995, na het behalen van zijn VWO-diploma op het Liemers College te Zevenaar, keerde hij terug naar Nijmegen als student Scheikunde aan de Radboud Universiteit Nijmegen. Koen specialiseerde zich in de richting van de biochemie, moleculaire biologie en bio-informatica. Zijn eerste stage vond plaats op het Centre for Molecular and Biomolecular Informatics aan dezelfde universiteit. Onder begeleiding van prof.dr. Gert Vriend deed hij onderzoek naar de drie-dimensionale configuraties van calcium-bindende sites in eiwitten. Koen deed zijn tweede stageproject bij het toenmalige Organon te Oss, op de afdelingen Bio-informatica en Chemische Informatica. Daar werkte hij onder meer aan computationele modellen die de interactie tussen nucleaire receptoren en hun liganden voorspellen (supervisie: dr. Paula van Noort en prof.dr. Jacob de Vlieg).

Na zijn afstuderen in 2003 begon Koen als promovendus onder begeleiding van prof.dr. Joost Verhaagen en prof.dr. Dick Swaab in het toenmalige Nederlands Instituut voor Hersenonderzoek – nu het Nederlands Instituut voor Neurowetenschappen genaamd - te Amsterdam. De resultaten van zijn onderzoek staan beschreven in dit proefschrift.

Momenteel is hij werkzaam als postdoctoraal onderzoeker binnen dezelfde vakgroep, waarbij hij samen met twee promovenda werkt aan de functionele karakterisering van de in dit proefschrift beschreven veranderingen. Koen woont samen met zijn vrouw Remy in Amsterdam.